



**FLORIDA A&M
UNIVERSITY-FLORIDA
STATE UNIVERSITY
UNIVERSITY OF NORTH
FLORIDA**

Feasibility Analysis of Real-time Intersection Data Collection and Processing Using Drones

Sponsor Award No.: BDV30-977-29

A Report Submitted to Florida Department of Transportation, Traffic Engineering and
Operations Office

Task 6: Final Report

Start Date: 08/31/2021; End Date: 09/30/2021

FDOT Project Manager: Alan El-Urfali,
State Traffic Services Program Manager, Traffic Engineering and Operations Office

Eren Erman Ozguven, Ph.D., Assistant Professor & Principal Investigator

E-mail: cozguven@eng.famu.fsu.edu / Phone: +1(850) 410-6146

Alican Karaer, M.Sc., Graduate Research Assistant

E-mail: akaraer@fsu.edu / Phone: +1(904) 236-2608

Mohammadreza Koloushani, M.Sc., Graduate Research Assistant

E-mail: mk18h@my.fsu.edu / Phone: +1(850) 300-1622

Ren Moses, Ph.D., PE, Professor & Co-Principal Investigator

E-mail: rmoses@eng.famu.fsu.edu / Phone +1(850) 410-6191

Maxim Dulebenets, Ph.D., PE, Assistant Professor & Co-Principal Investigator

E-mail: mdulebenets@eng.famu.fsu.edu / Phone: +1(850) 410-6621

Department of Civil & Environmental Engineering

Florida A&M University-Florida State University

Thobias Sando, Ph.D., P.E., PTOE, Professor & Co-Principal Investigator

E-mail: t.sando@unf.edu / Phone: +1(904) 620-1142

School of Engineering, University of North Florida

September 2021

DISCLAIMER

The opinions, findings, and conclusions expressed in this publication are those of the authors and not necessarily those of the State of Florida Department of Transportation.

METRIC CONVERSION CHART

U.S. UNITS TO METRIC (SI) UNITS

LENGTH

| SYMBOL | WHEN YOU KNOW | MULTIPLY BY | TO FIND | SYMBOL |
|-----------|---------------|-------------|-------------|-----------|
| in | inches | 25.4 | millimeters | mm |
| ft | feet | 0.305 | meters | m |
| yd | yards | 0.914 | meters | m |
| mi | miles | 1.61 | kilometers | km |

METRIC (SI) UNITS TO U.S. UNITS

LENGTH

| SYMBOL | WHEN YOU KNOW | MULTIPLY BY | TO FIND | SYMBOL |
|-----------|---------------|-------------|---------|-----------|
| mm | millimeters | 0.039 | inches | in |
| m | meters | 3.28 | feet | ft |
| m | meters | 1.09 | yards | yd |
| km | kilometers | 0.621 | miles | mi |

TECHNICAL REPORT DOCUMENTATION PAGE

| | | | |
|-------------------------------------------------------------------------------------------------------------------------------------------------------------------------------------------------------------------------------------------------------------------------------------------------------------------------------------------------------------------------------------------------------------------------------------------------------------------------------------------------------------------------------------------------------------------------------------------------------------------------------------------------------------------------------------------------------------------------------------------------------------------------------------------------------------------------------------------------------------------------------------------------------------------------------------------------------------------------------------------------------------------------------------------------------------------------------------------------------------------------------------------------------------------------------------------------------------------------------------------------------------------------------------------------------------------------------------------------------------------------------------------------------------------------------------------------------------------------------------------------------------------------------------------------------------------------------------------------------------------------------------------------------------------------------------------------------------------------------------------------------------------------------------------------------------------------------------------------------------------------------------------------------------------------------------------------------------------------------------------------------------------------------------------------------------------------------------------------------------------------------------------------------------------------------------------------------------------------------------------------------------------------------------------------------------------------------------------------------|------------------------------------------------------|--------------------------------------------------------------------------------------------------|-----------|
| 1. Report No. | 2. Government Accession No. | 3. Recipient's Catalog No. | |
| 4. Title and Subtitle Feasibility Analysis of Real-time Intersection Data Collection and Processing Using Drones | | 5. Report Date 09/31/2021 | |
| | | 6. Performing Organization Code 59-1961248 | |
| 7. Author(s) Eren Erman Ozguven, Alican Karaer, Mohammadreza Koloushani, Ren Moses, Maxim A. Dulebenets, Thobias Sando | | 8. Performing Organization Report No. 044187, 044518 | |
| 9. Performing Organization Name and Address Florida A&M University-Florida State University 2525 Pottsdamer Street Tallahassee, FL 32310-6046, USA | | 10. Work Unit No. (TRAIS) | |
| | | 11. Contract or Grant No. BDV30-977-29 | |
| 12. Sponsoring Agency Name and Address Florida Department of Transportation 605 Suwannee Street, Tallahassee, FL 32399 | | 13. Type of Report and Period Covered Final Report Period Covered: 10/15/2019 – 09/31/2021 | |
| | | 14. Sponsoring Agency Code | |
| 15. Supplementary Notes | | | |
| 16. Abstract Traditional data collection techniques at intersections are known to be time consuming and costly while handling the complexity associated with the heavy traffic volume and travel demand on today's roadways. Therefore, transportation agencies have been searching for more innovative, safer, and cheaper data collection solutions to have a faster and lower cost collection and analysis of traffic data to obtain traffic volume, speeds, queues, turning movements and conflict points (e.g., vehicle to vehicle, vehicle to pedestrian or bicycle, etc.) at intersections. One innovative solution is using drones in combination with computer vision applications. The overall goal of this project was to provide a feasibility analysis on the utilization of drones and computer vision applications to extract microscopic traffic data at intersections. Findings are expected to help the Florida Department of Transportation (FDOT) in integrating new technologies into their day-to-day data collection operations. Consistent with this goal, the following tasks have been completed as part of the project: (a) perform literature review and analyze state-of-the-practice to provide guidance and recommendations on legally and safely using drones with video/image processing techniques for the uniform traffic studies; (b) generate statewide crosswalk inventory using aerial images and artificial intelligence (AI2); (c) investigate the fatal pedestrian-involved crashes that occur at locations other than intersections in Florida and analyze their detailed crash reports; (d) design and conduct exercises with tethered drones to collect intersection data in the cities of Tallahassee and Jacksonville, Florida; and (e) perform a cost analysis comparing traditional methods with different drone-based traffic data collection techniques. Meeting these objectives led to appropriate guidelines and recommendations to FDOT in terms of evaluating and justifying the feasibility of using drones as safer and cheaper data collection alternatives while significantly improving intersection safety and operations. Results and recommendations of this research will also be used by the FDOT consultants who already perform traffic data collection on Florida's roadways. | | | |
| 17. Key Word Innovative traffic data collection; unmanned aerial vehicles (UAV); unmanned aerial systems (UAS); drones; computer vision; image processing | | 18. Distribution Statement No restrictions | |
| 19. Security Classif. (of this report) Unclassified | 20. Security Classif. (of this page) Unclassified | 21. No. of Pages 231 | 22. Price |

ACKNOWLEDGEMENTS

This project was sponsored by the State of Florida Department of Transportation (FDOT). The Principal Investigators would like to thank the FDOT Project Manager Alan El-Urfali and Javier Ponce from the FDOT Traffic Engineering and Operations Office for their valuable feedback throughout this project. The research team would like to thank the following devoted and motivated students, who played an active and critical role in this project: Alican Karaer, Mohammadreza Koloushani, Will Kaczmarek, and Luciano Lalika. We are very grateful for their time and energy they invested in the task. Alican Karaer, who is the student team leader, has shown exceptional skills in management and analysis.

EXECUTIVE SUMMARY

Traditional data collection techniques at intersections are known to be time consuming and costly while handling the complexity associated with the heavy traffic volume and travel demand on today's roadways. Therefore, transportation agencies have been searching for more innovative, safer, and cheaper data collection solutions to have a faster and lower cost collection and analysis of traffic data to obtain traffic volume, speeds, queues, turning movements and conflict points (e.g., vehicle to vehicle, vehicle to pedestrian or bicycle, etc.) at intersections. One innovative solution is using drones in combination with computer vision applications. However, there is still a wide gap in the literature with respect to the efficiency and feasibility of using drones for intersection data collection purposes, especially for longer periods of time during peak hours. To this end, there has not been a study on using the drones for real-time daily traffic collection and processing, and a study related to how this can benefit vehicles, pedestrians, and bicyclists. A significant challenge in evaluating the feasibility of using drones for daily traffic data collection is related to the evaluation of appropriate tools with the rationale and priority for each alternative to be used, developing options and recommendations, and conducting a pilot test at selected intersections. Although drones have been used for a variety of purposes such as bridge inspections by other states, the objectives of traffic data collection are totally different inherently.

The overall goal of this project was to provide a feasibility analysis on the utilization of drones and computer vision applications to extract microscopic traffic data at intersections. Findings are expected to help the Florida Department of Transportation (FDOT) in integrating new technologies into their day-to-day data collection operations. Consistent with this goal, the following tasks have been completed as part of the project: (a) perform a literature review and analyze state-of-the-practice to provide guidance and recommendations on legally and safely using drones with video and image processing techniques for the uniform traffic studies; (b) generate a statewide crosswalk inventory using aerial images and artificial intelligence (AI2); (c) investigate the fatal pedestrian-involved crashes that occur at locations other than intersections in Florida and analyze their detailed crash reports; (d) design and conduct exercises with tethered drones to collect intersection data in the cities of Tallahassee and Jacksonville, Florida; and (e) perform a cost analysis comparing traditional methods with different drone-based traffic data collection techniques. Meeting these objectives led to appropriate guidelines and recommendations to FDOT in terms of evaluating and justifying the feasibility of using drones as safer and cheaper data collection alternatives while significantly improving intersection safety and operations. Results and recommendations of this research will also be used by the FDOT consultants who already perform traffic data collection on Florida's roadways.

TABLE OF CONTENTS

| | |
|------------------------------------------------------------------------------------------------------------------------------------------|----------|
| DISCLAIMER | ii |
| METRIC CONVERSION CHART | iii |
| TECHNICAL REPORT DOCUMENTATION PAGE | iv |
| ACKNOWLEDGEMENTS | v |
| EXECUTIVE SUMMARY | vi |
| LIST OF FIGURES | x |
| LIST OF TABLES | xiv |
| 1. INTRODUCTION..... | 1 |
| 1.1. Study Objectives | 1 |
| 1.2. Report Structure | 2 |
| 2. TASK 1: CONDUCT A REVIEW OF LITERATURE AND PRACTICE TO IDENTIFY BEST IMPLEMENTATIONS, STRATEGIES AND OPERATIONAL BARRIERS..... | 3 |
| 2.1. Drone Types and Terminology | 3 |
| 2.2. Legislative Rules..... | 5 |
| 2.3. State-of-the-Practice and Literature Review..... | 9 |
| 2.3.1. State-of-the-Practice of UAS Utilization in Traffic Agencies..... | 9 |
| 2.3.2. Example Use Cases among DOTs | 13 |
| 2.3.3. Literature Review..... | 18 |
| 2.4. Desired Data Based on Manual on Uniform Traffic Control Devices (MUTCD) and Manual on Transportation Traffic Studies (MUTS)..... | 22 |
| 2.4.1. Roadway User Trajectories: <i>U_i, x, t</i> | 24 |
| 2.4.2. User Classification | 25 |
| 2.4.3. Geometric and Spatial Characteristics | 25 |
| 2.4.4. Speed..... | 25 |
| 2.4.5. Acceleration and Deceleration | 25 |
| 2.4.6. Approach Volume | 25 |
| 2.4.7. Vehicle Turning Movements | 26 |
| 2.4.8. Vulnerable User Turning Movements | 26 |
| 2.4.9. Gap Acceptance | 27 |
| 2.4.10. Queue Length, Delay, and Shockwave..... | 27 |
| 2.4.11. Fundamental Diagram..... | 29 |
| 2.4.12. Conflict Analysis | 29 |
| 2.5. Computer Vision Algorithms for Drone-based Traffic Data Extraction | 30 |

| | |
|---------------------------------------------------------------------------------------------------|-----------|
| 2.5.1. Preprocessing | 30 |
| 2.5.2. Object Detection and Tracking | 31 |
| 2.6. Challenges and Operational Barriers | 32 |
| 2.7. Market Analysis | 33 |
| 2.7.1. Vendor 1: Drone Operator | 34 |
| 2.7.2. Vendor 2: Video Analyzer | 34 |
| 2.8. Conclusions..... | 35 |
| 3. TASK 2: ROADWAY GEOMETRIC DATA EXTRACTION FROM VERY HIGH-RESOLUTION AERIAL IMAGES | 38 |
| 3.1. Task Description | 38 |
| 3.1.1. Why Crosswalks?..... | 38 |
| 3.2. Background on Roadway Feature Extraction from Imagery | 42 |
| 3.3. Automated Crosswalk Detection and Mapping | 45 |
| 3.3.1. Data Description | 45 |
| 3.3.2. Pre-processing..... | 46 |
| 3.3.3. YOLOv2 Crosswalks Detection Model | 49 |
| 3.3.4. Post-processing | 53 |
| 3.4. Case Studies and Results | 53 |
| 3.4.1. Case Study I: Overall Performance Evaluation Using the Ground Truth Data | 53 |
| 3.4.2. Case Study II: Performance Evaluation with Categorized Crosswalks | 57 |
| 3.5. Final Data Description | 63 |
| 3.6. Discussions and Recommendations..... | 64 |
| 4. TASK 3: CONDUCT A PILOT-DRONE TEST IN SELECTED INTERSECTIONS 65 | |
| 4.1. Background..... | 65 |
| 4.2. Exercise Design and Execution | 65 |
| 4.2.1. Introduction..... | 65 |
| 4.2.2. Purchased Service | 66 |
| 4.2.3. Exercise Locations | 69 |
| 4.2.4. Operational Steps and Challenges | 72 |
| 4.3. Conclusions..... | 77 |
| 5. TASK 4: PROPOSE GUIDELINES FOR USING DRONES TO COLLECT INTERSECTION TRAFFIC DATA..... | 78 |
| 5.1. Background | 78 |
| 5.2. Data Analysis Demonstration on the Obtained Trajectory Sample | 78 |
| 5.2.1. Exercise Background | 78 |

| | |
|-------------------------------------------------------------------------------------------------------------------------------------------------|------------|
| 5.2.2. Sample Trajectory Data and Classified Turning Movement Extraction..... | 78 |
| 5.2.3. Challenges on Georeferenced Trajectory Extraction from Drone Videos..... | 80 |
| 5.2.4. Proposed Data Collection and Analysis Framework | 80 |
| 5.3. Pedestrian Involved Crash Analysis | 84 |
| 5.3.1. Background..... | 84 |
| 5.3.2. Methodology..... | 85 |
| 5.3.3. Facts and Statistics..... | 90 |
| 5.3.4. Hotspot Counties..... | 96 |
| 5.3.5. Crashes in the Vicinity of a Left-Turn Lane..... | 109 |
| 5.3.6. Conclusions on Crash Analysis | 112 |
| 5.4. Comparative Cost Analysis and Recommendations on Drone-based Traffic Data Collection Analysis..... | 112 |
| 5.4.1. Summary of Previously Conducted Work Using Traditional Methods..... | 113 |
| 5.4.2. Comparative Cost Analysis..... | 113 |
| 5.4.3. Alternative Methods..... | 115 |
| 5.4.4. Cost per Intersection Estimates..... | 115 |
| 5.5. Recommendations for Consultants to Set a Drone Operation Team | 118 |
| 6. CONCLUSIONS | 120 |
| REFERENCES | 121 |
| APPENDIX A : Aerial Images of Locations where the Recorded 143 Pedestrian Fatality Crashes Occurred between 2011 and 2020 in Florida | 130 |
| APPENDIX B: Crash Diagrams for the Recorded 10 Pedestrian-involved Fatalities Occurred between 2011 and 2020 in Orange County, Florida | 209 |

LIST OF FIGURES

| | |
|-------------------------------------------------------------------------------------------------------------------------------------------------------------------------|----|
| FIGURE 2-1: COMMONLY USED UAS PLATFORMS | 4 |
| FIGURE 2-2: FDOT UAS BROCHURE | 6 |
| FIGURE 2-3: FAA WAIVER TREND ANALYSIS FOR OPERATIONS OVER (A) PEOPLE, AND (B) BEYOND THE VISUAL LINE OF SIGHT. | 7 |
| FIGURE 2-3: FAA WAIVER TREND ANALYSIS FOR OPERATIONS OVER (A) PEOPLE, AND (B) BEYOND THE VISUAL LINE OF SIGHT | 8 |
| FIGURE 2-4: SECTIONS FROM (A) NORTH CAROLINA AND (B) OHIO PRESENTATIONS IN THE FHWA PEER EXCHANGE (FHWA, 2018)..... | 9 |
| FIGURE 2-5: AASHTO 2018 SURVEY RESULTS ON UAS USE CASES BY STATE DOTs | 11 |
| FIGURE 2-6: UAS UTILIZATION OF STATE DOTs FROM 2016 TO 2019 | 12 |
| FIGURE 2-7: NUMBER OF STATE DOTs WHO HIRED PEOPLE SPECIFICALLY FOR UAS OPERATIONS | 12 |
| FIGURE 2-8: MDOT TRAFFIC MONITORING DEMONSTRATION THROUGH TETHERED BLIMP AT THE ITS WORLD CONGRESS IN SEPTEMBER 2014..... | 13 |
| FIGURE 2-9: MDOT TRAFFIC MONITORING SOFTWARE TO ANALYZE UAS-OBTAINED TRAFFIC SURVEILLANCE..... | 14 |
| FIGURE 2-10: TIME SPACE DIAGRAM IS GENERATED FROM THE UAS-EXTRACTED TRAJECTORIES . | 14 |
| FIGURE 2-11: TETHERED DRONE-CAPTURED LIVE VIDEO STREAMING OF A SIMULATED TOW FOR THE HOUSTON METRO AREA | 15 |
| FIGURE 2-12: OHIO DOT INVESTIGATING TETHERED DRONES FOR TRAFFIC MONITORING | 16 |
| FIGURE 2-13: SALT LAKE CITY, UTAH, DIVERGING DIAMOND INTERSECTION OBSERVATION WITH TETHERED DRONE | 17 |
| FIGURE 2-14: OREGON DOT DRIVING SIMULATION ENVIRONMENT FOR TESTING DRIVER DISTRACTION DUE TO DRONES..... | 18 |
| FIGURE 2-15: METADATA OF PUBLISHED WORK: NUMBER OF STUDIES (A) PER DATA INTEREST, (B) PER YEAR, (C) PER DRONE TYPE, AND (D) PER DATA GATHERING SPEED | 22 |
| FIGURE 2-16: PROJECT FLOW CHART AND DESIRED OUTPUTS..... | 24 |
| FIGURE 2-17: SHOCKWAVE AND QUEUE DISSIPATION FROM DRONE-OBTAINED TRAJECTORIES | 28 |
| FIGURE 2-18: PET AND RTTC CALCULATIONS ON XY SURFACE AND TIME ELEVATION (CHEN ET AL., 2017) | 29 |
| FIGURE 2-19: NUMBER OF STUDIES PER COMPUTER VISION ALGORITHMS (ML: MACHINE LEARNING, DL: DEEP LEARNING) | 30 |
| FIGURE 3-1: INITIAL PROJECTION FOR GEOMETRIC DATA FOR SINGLE INTERSECTIONS..... | 38 |
| FIGURE 3-2: (A) U.S. PEDESTRIAN FATALITIES: 1988-2019, (B) PERCENTAGE INCREASE IN NUMBER OF PEDESTRIAN AND ALL OTHER TYPES OF FATALITIES FROM 2009 TO 2018, AND (C) THE | |

| | |
|---------------------------------------------------------------------------------------------------------------------------------------------------------------------------------------------------------------------------------------------------------------------------------------------------------------------------------------------------------------------------------------------------------------------------------------------------------------------------------------------------|----|
| STATES WHERE MOST OF THE PEDESTRIAN FATALITIES OCCURRED IN THE FIRST HALF OF 2019 (RETTING & GHSA, 2020) | 39 |
| FIGURE 3-3: SAFETY BENEFITS OF PROPOSED COUNTERMEASURES (FHWA, 2020c) | 40 |
| FIGURE 3-4: PROCESS DIAGRAM FOR INSTALLATION OF PEDESTRIAN CROSSING COUNTERMEASURES (BLACKBURN ET AL., 2017) | 41 |
| FIGURE 3-5: CATEGORIZATION OF ROADWAY INVENTORY DATA COLLECTION (JALAYER ET AL., 2015) | 42 |
| FIGURE 3-6: PREPROCESSING APPROACH | 47 |
| FIGURE 3-7: AUTOMATED IMAGE MASKING MODEL USED IN THE FOURTH STEP OF PREPROCESSING | 48 |
| FIGURE 3-8: STATE PLANE COORDINATE SYSTEM (SPCS) ZONES IN FLORIDA. SOURCE: (FDOT, 2017) | 49 |
| FIGURE 3-9: DEVELOPED YOLOv2 CROSSWALK DETECTOR ACCURACY | 51 |
| FIGURE 3-10: CROSSWALK DETECTION WITH BOUNDING BOXES AND CONFIDENCE SCORES ON SINGLE IMAGES FROM LEON, ORANGE, AND SUMTER COUNTIES | 52 |
| FIGURE 3-11: CROSSWALK DETECTION AND MAPPING AT THE COUNTY LEVEL | 53 |
| FIGURE 3-12: MANUALLY LABELED GROUND TRUTH CROSSWALKS (GT) AND OSM CROSSWALKS IN THE STUDY AREA | 54 |
| FIGURE 3-13: AUTOMATED CROSSWALK DETECTION AND MAPPING RESULTS. (A AND B) TRUE POSITIVE (TP) DETECTION WITH 1:1 MATCHING, (C AND D) TP DETECTION WITH 1: ANY MATCHING, (E) FALSE POSITIVE (FP) DETECTION, (F) FALSE NEGATIVE (FN), UNDETECTED CROSSWALK, (G) DETECTION PROBLEMS DUE TO PEELED OFF MARKINGS AND RELATIVELY LONG PLACEMENT ON THOMASVILLE RD., TALLAHASSEE, FL. | 57 |
| FIGURE 3-14: GROUND TRUTH (GT) CROSSWALK POINTS AND THEIR CATEGORIZATION INTO THREE BINARY NODES | 59 |
| FIGURE 3-15: DISTANCE ANALYSIS FOR THE TARGET CATEGORIZATION IN THE STATEWIDE CROSSWALKS INVENTORY LIST. (A) S1 CROSSWALKS TO SIGNALIZED INTERSECTION POINTS, AND (B) PARALLEL CROSSWALKS TO THE ROADWAY CENTERLINES | 62 |
| FIGURE 3-16: ZONES FOR CATEGORIZING THE SIGNALIZED INTERSECTION, MIDBLOCK, AND DRIVE WAY CROSSWALKS | 63 |
| FIGURE 4-1: PICTURES FROM THE EXERCISE. (A) DRONE DJI M210/ RTK, (B) DJI M200 WITH ZENMUSE Z30 CAMERA ATTACHED AND TWO BATTERIES (ONE OF THEM IS ELISTAIR’S AIR MODULE FOR DJI M200/210), (C) LIGHT-T TETHER AND BS6500 GENERATOR, (D) INSIDE THE TRAILER WHERE THE AIRSPACE IS CONTINUOUSLY OBSERVED (TOP SCREENS) AND LIVE-FEED VIDEO IS LABELED WITH YOLO, (E) CRYSTAL SKY SCREEN ATTACHED TO THE MASTER DRONE CONTROLLER AND TETHER OBSERVATION SCREEN, AND (F) LABELED LIVE FEED VIDEO. | 68 |
| FIGURE 4-2: TALLAHASSEE LOCATION 1: APALACHEE PKWY. & MARCH RD. HOURS OF OPERATION: SUNDAY, MAR 14, 2021 BETWEEN 10:17 AM – 5:02 PM, AND TUESDAY, MARCH 16, 2021 BETWEEN 9:43 AM – 6:39 PM | 69 |

| | |
|-------------------------------------------------------------------------------------------------------------------------------------------------------|----|
| FIGURE 4-3: TALLAHASSEE LOCATION 2: US-231 & JACOB RD. (RCUT INTERSECTION). HOURS OF OPERATION: MONDAY, MAR 15, 2021, BETWEEN 7:28 AM – 7:47 PM | 70 |
| FIGURE 4-4: JACKSONVILLE LOCATION 1: US-90 (BEACH BLVD.) & LEON RD. HOURS OF OPERATION: THURSDAY, MAR 18, 2021, BETWEEN 6:46 AM – 8:05 AM..... | 70 |
| FIGURE 4-5: JACKSONVILLE LOCATION 2: SR-10 (ATLANTIC BLVD.) & LEON RD. HOURS OF OPERATION: FRIDAY, MAR 19, 2021, BETWEEN 6:49 AM – 8:38 PM..... | 71 |
| FIGURE 4-6: JACKSONVILLE LOCATION 3: US-301 & SR 228 (NORMANDY BLVD.). HOURS OF OPERATION: SATURDAY, MAR 20, 2021, BETWEEN 8:33 AM – 5:02 PM | 71 |
| FIGURE 4-7: FLIGHT CARD FOR THE TALLAHASSEE LOCATION 1 INDICATING THE PRIOR RISK ASSESSMENT | 73 |
| FIGURE 4-8: TETHER OPERATION PRE-TAKEOFF CHECKLIST | 74 |
| FIGURE 4-9: REAL-TIME VIDEO IMAGE PROCESSING SYSTEM CHECKLIST | 75 |
| FIGURE 5-1: SAMPLE TRAJECTORY DATA. (A) ORIGINALLY OBTAINED DATA POINTS. (B) PREPROCESSED AND CLUSTERED TRAJECTORY LINES | 79 |
| FIGURE 5-2: NUMBER OF CLASSIFIED ROAD USERS PER APPROACH | 79 |
| FIGURE 5-3: HOMOGRAPHY TRANSFORMATION OF THE VIDEO FRAMES USING THE INTERSECTION BOUNDARIES. | 80 |
| FIGURE 5-4: RECOMMENDED FRAMEWORK FOR REAL-TIME TRAJECTORY EXTRACTION..... | 82 |
| FIGURE 5-5: RECOMMENDED FRAMEWORK FOR AUTOMATED TMC EXTRACTION FROM TRAJECTORIES | 83 |
| FIGURE 5-6: DATA FILTRATION PROCESS BASED ON ROADWAY NETWORK DISTANCE | 87 |
| FIGURE 5-7: CRASH DISTRIBUTION BY YEAR | 90 |
| FIGURE 5-8: CRASH DISTRIBUTION BY DAY OF WEEK..... | 91 |
| FIGURE 5-9: ALCOHOL AND/OR DRUG INFLUENCE ON PEDESTRIAN-INVOLVED CRASHES | 91 |
| FIGURE 5-10: CRASH DISTRIBUTION BY LIGHT CONDITION..... | 92 |
| FIGURE 5-11: CRASH DISTRIBUTION BY WEATHER CONDITION..... | 92 |
| FIGURE 5-12: CRASH DISTRIBUTION BY CRASH LANE..... | 93 |
| FIGURE 5-13: CRASHES LABELED AS “SIDE OF ROADWAYS” (WRONGLY MAPPED IN THE MIDDLE OF THE ROADWAY). {CONTINUED WITH THE NEXT PAGE} | 93 |
| FIGURE 5-13: CRASHES LABELED AS “SIDE OF ROADWAYS” (WRONGLY MAPPED IN THE MIDDLE OF THE ROADWAY). {CONTINUED FROM THE PREVIOUS PAGE} | 94 |
| FIGURE 5-14: DISTANCE BETWEEN CRASHES AND NEAREST INTERSECTION | 95 |
| FIGURE 5-15: RELATIONSHIP BETWEEN THE HIGHEST LEVEL OF INJURY AND DISTANCE FROM THE NEAREST INTERSECTION..... | 95 |
| FIGURE 5-16: FATALITY PEDESTRIAN-INVOLVED CRASHES IN FLORIDA DURING 2011-2020 | 97 |
| FIGURE 5-17: PEDESTRIAN-INVOLVED CRASHES IN ORANGE COUNTY | 98 |

| | |
|---------------------------------------------------------------------------------------------------------------------------------|-----|
| FIGURE 5-18: ORANGE COUNTY – AREA (A) – ALOMA AVE..... | 99 |
| FIGURE 5-19: ORANGE COUNTY – AREA (B) | 99 |
| FIGURE 5-20 : ORANGE COUNTY – AREA (C)..... | 100 |
| FIGURE 5-21: ORANGE COUNTY – AREA (D)..... | 100 |
| FIGURE 5-22: ORANGE COUNTY – AREA (E) – WEST CENTRAL BLVD..... | 101 |
| FIGURE 5-23: ORANGE COUNTY – AREA (F) – EAST COLONIAL DR. | 101 |
| FIGURE 5-24: ORANGE COUNTY – AREA (G) – SOUTH SEMORAN BLVD..... | 102 |
| FIGURE 5-25: ORANGE COUNTY – AREA (H) – SOUTH ORANGE BLOSSOM AND WEST OAK RIDGE RD..... | 102 |
| FIGURE 5-26: ORANGE COUNTY – AREA (I) – INTERNATIONAL DR. | 103 |
| FIGURE 5-27: ORANGE COUNTY – AREA (J) – LANDSTREET RD. | 103 |
| FIGURE 5-28: PEDESTRIAN-INVOLVED CRASHES IN HILLSBOROUGH COUNTY | 104 |
| FIGURE 5-29: HILLSBOROUGH COUNTY - AREA (A) – EAST FLETCHER AVE., MAPLE DR. (AROUND USF CAMPUS), AND BRUCE B DOWNS BLVD..... | 104 |
| FIGURE 5-30: HILLSBOROUGH COUNTY – AREA (B) – BRANDON BLVD. | 105 |
| FIGURE 5-31: PEDESTRIAN-INVOLVED CRASHES IN PASCO COUNTY | 105 |
| FIGURE 5-32: PASCO COUNTY - AREA (A) – US-19 HIGHWAY AND LITTLE RD..... | 106 |
| FIGURE 5-33: PASCO COUNTY - AREA (B) – US-19 HIGHWAY | 106 |
| FIGURE 5-34: PASCO COUNTY - AREA (C) | 107 |
| FIGURE 5-35: PEDESTRIAN-INVOLVED CRASHES IN LEON COUNTY..... | 107 |
| FIGURE 5-36: LEON COUNTY - AREA (A) – TENNESSEE ST..... | 108 |
| FIGURE 5-37: FATALITY CRASHES IN FRONT BEACH RD.- PANAMA CITY - BAY COUNTY – SPEED LIMIT 30 MPH | 109 |
| FIGURE 5-38: ALTERNATIVES OF SIGNAL WARRANT ANALYSIS..... | 115 |

LIST OF TABLES

| | |
|-----------------------------------------------------------------------------------------------------------------------------------------------------------|-----|
| TABLE 2-1: COMMON ACRONYMS FOR DRONES | 3 |
| TABLE 2-2: APPLICATION CHARACTERISTICS OF DIFFERENT UAS DESIGNS..... | 4 |
| TABLE 2-3: BASIC AREAS OF CONCERN AT INTERSECTIONS AND SUGGESTED DATA SETS. SOURCE: MUTS (FLORIDA DEPARTMENT OF TRANSPORTATION, 2016) | 23 |
| TABLE 2-4: CONTACTED DRONE SERVICE PROVIDERS | 34 |
| TABLE 2-5: CONTACTED VISION-BASED TRAFFIC DATA COLLECTION COMPANIES..... | 35 |
| TABLE 3-1: CATEGORIZATION OF RELATED LITERATURE ON ROADWAY GEOMETRY EXTRACTION USING IMAGERY | 43 |
| TABLE 3-2: PERFORMANCE EVALUATION METRICS | 55 |
| TABLE 3-3: PROPOSED MODEL PERFORMANCE EVALUATION AND COMPARISON WITH OSM..... | 56 |
| TABLE 3-4: NUMBER OF GROUND TRUTH (GT) CROSSWALKS | 59 |
| TABLE 3-5: PERFORMANCE EVALUATION RESULTS ON CATEGORIZED CROSSWALKS..... | 60 |
| TABLE 3-6: STATEWIDE CROSSWALK INVENTORY WITH THE FINAL NUMBERS | 64 |
| TABLE 4-1: EXPECTED FINAL TRAJECTORY OUTPUT..... | 66 |
| TABLE 4-2: MAIN EQUIPMENT PROVIDED AND USED BY THE CONTRACTOR AND THEIR CURRENT PRICES..... | 67 |
| TABLE 4-3: DRONE TIME AND LOCATION TABLE WITH ASSOCIATED CHALLENGES | 76 |
| TABLE 5-1: PEDESTRIAN FATALITY CRASHES BY RELATED FACTORS, 2019, USA* | 84 |
| TABLE 5-2: CRASH LANE IDENTIFIER (NAME OF ATTRIBUTE: ACCLANE/CRASHLANE)..... | 86 |
| TABLE 5-3: PEDESTRIAN-INVOLVED CRASHES IN FLORIDA BY LOCATION AND CRASH LANE..... | 88 |
| TABLE 5-4: INJURY SEVERITY IDENTIFIER CODES (HIGHEST IN CRASH) (SOURCE: FDOT SAFETY OFFICE)..... | 88 |
| TABLE 5-5: PEDESTRIAN-INVOLVED CRASHES BY THE HIGHEST LEVEL OF INJURY..... | 89 |
| TABLE 5-6: LINEAR REGRESSION MODEL BETWEEN HIGHEST LEVEL OF INJURY AND DISTANCE FROM INTERSECTION | 96 |
| TABLE 5-7: FATAL PEDESTRIAN-INVOLVED CRASHES THAT OCCUR AT LOCATIONS THAT ARE NOT INTERSECTIONS AND UNDER THE DIRECT INFLUENCE OF LEFT TURN LANES..... | 111 |
| TABLE 5-8: SUMMARY OF PREVIOUS STUDIES CONDUCTED USING TRADITIONAL METHODS | 114 |
| TABLE 5-9: COMPARATIVE COST ANALYSIS BETWEEN THE TRADITIONAL METHOD AND DRONE- BASED METHODS TO CONDUCT A SIGNAL WARRANT STUDY IN FLORIDA | 118 |

1. INTRODUCTION

Traditional data collection techniques at intersections are known to be time consuming and costly while handling the complexity associated with the heavy traffic volume and travel demand on today's roadways. Therefore, transportation agencies have been searching for more innovative, safer, and cheaper data collection solutions to have a faster and lower cost collection and analysis of traffic data to obtain traffic volume, speeds, queues, turning movements and conflict points (e.g., vehicle to vehicle, vehicle to pedestrian or bicycle, etc.) at intersections. One such innovative solution is using unmanned aerial systems (UASs), also known as drones. Several states such as Michigan and Ohio have already implemented the use of drones for their daily operations, including traffic monitoring and management as well as incident scene data collection, and have reported satisfactory results with their implementation programs (Massachusetts DOT, 2016). Their experiences have shown that utilizing drones for data collection has demonstrated significant cost savings and offers substantial safety advantages while reducing accidents and mitigating congestion. The American Association of State Highway and Transportation Officials (AASHTO) conducted a survey in 2018. This survey revealed that drone-based data collection is four times faster compared to traditional methods, and it increases the productivity by three times (AASHTO, 2018b). Similarly, AASHTO's 2019 survey report indicated that UAS-based data collection for a bridge inspection was approximately four times less costly compared to manual data collection, without even considering the user delay cost associated with the manual collection process (AASHTO, 2019). However, there is still a wide gap in the literature with respect to the efficiency and feasibility of using drones for intersection data collection purposes, especially for longer periods of time during peak hours. To this end, there has not been a study on using the drones for real-time daily traffic collection and processing nor a study related to how this can benefit vehicles, pedestrians, and bicyclists.

Therefore, a significant challenge in evaluating the feasibility of using drones for daily traffic data collection is related to the evaluation of appropriate tools with the rationale and priority for each alternative to be used, developing options and recommendations, and conducting a pilot test at an intersection. Although drones have been used for a variety of purposes such as bridge inspections by other states, the objectives of traffic data collection are totally different inherently. As such, there is a need to conduct an extensive review of the literature and practice to (a) extract the vast amount of knowledge with respect to the drone implementations video/image processing techniques and other related data collection equipment and identify the operational barriers, (b) analyze the results of this search to identify best implementations, practices, and strategies, and (c) conduct a field exercise through a pilot drone study at selected intersections in Florida.

1.1. Study Objectives

The objectives of the study are as follows: (a) perform a literature review and analyze state-of-the-practice to provide guidance and recommendations on legally and safely using drones with video/image processing techniques for the uniform traffic studies; (b) generate statewide crosswalk inventory using AI2 (i.e., aerial images and artificial intelligence); (c) investigate the fatal pedestrian-involved crashes that occur at locations other than intersections in Florida and analyze their detailed crash reports; (d) design and conduct exercises with tethered drones to collect intersection data in the cities of Tallahassee and Jacksonville, Florida; and (e)

perform a cost analysis comparing traditional methods with different drone-based traffic data collection techniques.

1.2. Report Structure

The remainder of this report is structured in the following manner. After describing the research gaps based on the stated objectives in Chapter 1, Chapter 2 describes Task 1 Deliverable of this project, which includes the legal regulations on drone operations, state-of-the-practice, and literature review. Chapter 3 presents Task 2, where a statewide crosswalk inventory map was developed by implementing computer vision applications on high-resolution aerial images. Chapter 4 focuses on the drone-based video data collection and analysis as part of Task 3 and presents the pilot exercises conducted at selected intersections in Florida to obtain real-time traffic data for intersection control evaluation purposes. Describing the detailed findings of Task 4, Chapter 5 presents data analysis results and compares traditional methods with the drone-based traffic data collection performing a comparative cost analysis. Chapter 5 also includes a detailed evaluation of the fatal pedestrian-involved crashes that occur at locations that are not intersections. Chapter 6 presents the challenges faced and provides guidelines and recommendations for FDOT.

2. TASK 1: CONDUCT A REVIEW OF LITERATURE AND PRACTICE TO IDENTIFY BEST IMPLEMENTATIONS, STRATEGIES AND OPERATIONAL BARRIERS

Task 1 aimed to evaluate current state-of-the-practice and extract the vast amount of knowledge from the published work to help and guide this research project. Through an extensive literature review, this task evaluated the existing drone-focused traffic research, drone technologies, communication technologies, and video image processing software available in the market. This was followed by a discussion on the identification and extraction of the desired data that could be obtained from aerial videos to evaluate the mobility and safety performance of intersections. This was supported with a discussion on the up-to-date computer vision algorithms extracted from the literature review. This task also presented several challenges and operating barriers. The findings were also presented through the reviewed documentation and provided the preliminary steps of a framework for the pilot study, which will be conducted in Task 3 (Chapter 4 in this document).

2.1. Drone Types and Terminology

The use of drones dates back more than a century. The first pilotless flight, recorded in 1918, was performed to deliver explosive materials. This first unmanned aircraft was called “Kattering Bug”, and it was an early version of today’s cruise missiles (Kwasniak & Kerezman, 2017). After a long-term restricted use for military purposes only, drone technologies have become more available and affordable over the last two decades. Drones have been used for a variety of civil applications as well as for recreational purposes, with the advantages of maneuverability, flexibility, and large field-of-view. Being a fast-growing market with various new opportunities, there are several acronyms and abbreviations associated with describing drones, which are shown in Table 2-1. In this study, we will use the terms drones and Unmanned Aerial Systems (UASs) interchangeably. Also, note that tUAS abbreviation is used for tethered drones.

Table 2-1: Common acronyms for drones

| | |
|--------------|------------------------------------------------------|
| UAS: | Unmanned Aerial Systems, Unmanned Aircraft Systems |
| UAV: | Unmanned Aerial Vehicles, Unmanned Aircraft Vehicles |
| RPAS: | Remotely Piloted Aircraft Systems |
| UA: | Unmanned Aircrafts |
| sUAS: | Small Unmanned Aerial Vehicles |
| tUAS: | Tethered Drones |

Although there are many different designs, UASs can be categorized into fixed wing drones and multi-rotor drones. Figure 2-1 depicts the commonly used drone designs. Please note that tethered drones are multi-rotor drones mounted to a ground unit. An automated crane in the ground unit keeps the tether cable taut during the flight. Although it limits the maneuverability, tether cable also provides power. Therefore, tethered drones can provide persistent and long

duration surveillance. Table 2-2 presents the advantages and disadvantages of different designs as well as preferred area of applications for each type of drone design. The following section discusses the legislation rules needed to legally operate UASs in the U.S.



Figure 2-1: Commonly used UAS platforms

Table 2-2: Application Characteristics of different UAS designs

| | Fixed Wing | Rotorcraft | Tethered |
|------------------------------------|----------------------------------------------------------------------------------------------------------------------------------------|------------------------------------------------------------------------------------------------------------------------------|-----------------------------------------------------------------------------------------------------------------------------------------------------------------------|
| Major Advantages | <ul style="list-style-type: none"> • Longer flight endurance • Higher speed • Larger area of coverage | <ul style="list-style-type: none"> • Vertical take-off/landing • Hovering • Maneuverability | <ul style="list-style-type: none"> • Longer flight endurance • Vertical take-off/landing • Hovering • No risk for flaw away |
| Major Challenges | <ul style="list-style-type: none"> • Requires additional efforts for launching | <ul style="list-style-type: none"> • Limited flight endurance | <ul style="list-style-type: none"> • Limited Maneuverability |
| Preferred Areas of Interest | <ul style="list-style-type: none"> • Area Surveys • Long distance operations | <ul style="list-style-type: none"> • Structural Inspection • Confined Space | <ul style="list-style-type: none"> • Traffic Monitoring |
| Examples of Application | <ul style="list-style-type: none"> • Roadside mapping • Rail inspection | <ul style="list-style-type: none"> • Bridge inspection • Light pole inspection | <ul style="list-style-type: none"> • Intersection Analysis • Incident Monitoring • Back-up ITS element |

2.2. Legislative Rules

Federal Aviation Administration (FAA) regulates the operations and certifications of small UAS in the U.S. with Part 107 of 14 Code of Federal Regulations (CFR), which was released on August 29, 2016. This regulation fully covers only sUAS which weigh less than 55 lbs. (25 kg.) and more than 0.55 lbs. (1 g.). Part 107 still applies for other drone operations, but this is not sufficient. Every drone should also be registered in FAA databases and only sUAS can be registered online.

After receiving many questions about the use and operation of tethered UAS, FAA made a clear statement in the rules of Part 107 as follows: “...*the FAA notes that the definition of small UAS in this rule includes tethered powered small UAS.*” (p. 93). Therefore, tUAS operations are also regulated under FAA Part 107 as long as the sum of the total weights of flying platform and tether connection is less than 55 lbs. Drones heavier than 55 lbs. should be registered through a paper system and they may require additional licenses to operate.

Recently, regulations are updated by FAA with an additional remote identification requirement to assign a “digital license plate” for UAS. This has been incorporated to improve safety and security issues for the National Airspace System towards allowing more complex UAS operations. Based on these requirements, all drones must broadcast signals to all other aircrafts in the broadcasting distance. This signal includes information on the altitude, speed, and position of the UAS in addition to the UAS Remote Identification. Personal information is secured from the public by FAA; however, it may be shared with national and federal authorities if asked.

Other than recreational purposes, UASs cannot be operated without a remote pilot certificate/license. To get the license, each candidate should pass FAA’s aeronautical knowledge exam at one of available the test centers. Every two years, the license must be renewed by passing the current aeronautical knowledge exam. The exam costs \$150 as of December 2019. The regulation also clearly states that a sUAS must weigh less than 55 lbs. (25 kg) including its attached systems such as payload, tethered connection, or cargo package. sUAS should be registered on the FAA website (FAA, 2019b). Other than the weight limitations, the rules allow only day-light operations with the maximum altitude of 400 ft. (120 m). Also, visual line-of sight must be kept during the flight and the drone should not be allowed to fly above people. The regulation allows UAS operations over people when they are covered in buildings or stationary vehicles; however, operations over moving vehicles are not allowed since the UASs can distract drivers and lead to a serious traffic incident (Hurwitz et al., 2018).

UAS flights are not allowed near airports or over stadiums during major events. Although location limitations have been specified in the rules Part 107, the app “B4UFly” has been created by FAA. This app guides drone operators for airspace authorization before flying the drone. In February 2019, FAA announced that “B4UFly” will not be updated anymore so that the current version will continue to serve. Instead, FAA has partnered with Kittyhawk to provide real time authorization for drone users and active UASs tracking for the air traffic controllers through Low Altitude Authorization and Notification Capability (LAANC) (FAA & Kittyhawk, 2019; *LAANC Kittyhawk*, 2019). Once the user pins the flight location on the interactive map, the app creates a list of restrictions for a possible drone operation. Please refer to the following website for more information: knowbeforeyoufly.org (FAA, 2019a). This website is a great source for drone operators of any purpose. Figure 2-2 depicts a part of the Florida DOT UAS Brochure which

clearly summarizes the aforementioned FAA rules (Florida DOT, 2019). Some applications may specifically require operations over people or flights beyond the vision line of sight. In such cases, FAA may waive some rules by providing the Certificate of Authorization (COA) for those who can justify the waiver request. FAA has also conducted a waiver trend analysis since they have received numerous amounts of requests for such operations over people and beyond the vision line of sight. Figure 2-4 indicates the results for the waiver trend analysis. For more information about UAS regulations, please refer to the following FAA website: www.faa.gov/uas/ (FAA, 2019b).

Federal UAS Operator Laws & Guidance

The following federal laws and guidelines are provided for operators of UAS:

ALL UAS MUST BE REGISTERED WITH THE FAA!

Small UAS (those weighing more than 0.55 pounds but less than 55 pounds, including all attachments and payload, such as cameras) can be registered at: www.faa.gov/uas/registration

UAS weighing 55 pounds or more must be registered through a paper system. For more information, please visit: www.faa.gov/licenses_certificates/aircraft_certification/aircraft_registry/

5 MILES

Contact the airport or air traffic control tower before flying within five miles of an airport

LINE OF SIGHT

Operate UAS within visual sight at all times

400'

Operate UAS no higher than 400 feet and remain below surrounding obstacles

Do not fly near or over sensitive infrastructure (e.g., power stations, correctional facilities, public roadways, etc.)

Do not fly under the influence of alcohol or drugs

Must remain clear, and yield to all manned aircraft operations

Do not fly an UAS if it has not been registered with the FAA

Do not fly in adverse weather conditions such as high winds or reduced visibility

Figure 2-2: FDOT UAS brochure

(a)
Figure 2-3: FAA waiver trend analysis for operations over (a) people, and (b) beyond the visual line of sight. *Continued...*

| Beyond Visual Line of Sight (107.31) Waiver Trend Analysis | | | | |
|----------------------------------------------------------------------------------------------------------------------------------------------------------------------------------|---------------------------------------------------------------------------------------------------------------------------------------------------------------------------------------------------------------------------------------------------------------------------------------------------------------------------------------------------------------------------------------|-------------------------------------------------------------------------------------------------------------------------------------------------------------------------------------------------------------------------------------------------------------------------------------------------------------------------------------------------------------------------------------------------------------------------------------------------------------------------------------------------------------------------------------------------------------------------------------------------------------------------------------------------------------------|-------------------------------------------------------------------------------------------------------------------------------------------------------------------------------------------------------------------------------------------------------------------------|-----------------------------------------------------------------------------------------------------------------------------------------------------------------------------------------------------------------------------------------------------------------------------------------------------------------------------------------|
| Waiver Application Elements | Command and Control (C2) Link and Emitters Performance Capabilities | Detect-and-Avoid (DAA) Methods | Weather Tracking and Operational Limitations | Training Requirements for Pilots and Other Participating Persons |
| <p>Sufficient Information</p> <p>--</p> <p>Characteristics of the Beyond Visual Line of Sight (BVLOS) applications approved after requests for additional information</p> | <p>-States and demonstrates max range and envelope that C2 can operate in, taking into account geographic area, environment, and terrain</p> <p>-Provides a complete description of each emitter, including the Federal Communications Commission (FCC) grant of authorization and FCC ID number for each transmitter/emitter on the sUA and ground control station</p> | <p>-Detailed descriptions and procedures for risk mitigations to avoid collisions with aircraft (ex. Visual Observers, and technology)</p> | <p>-Details when weather reports will be gathered, what will be gathered, and where they will be taken from.</p> <p>-States weather limitations, such as small unmanned aircraft system (sUAS) manufacturer's limitations or wind speed</p> | <p>-Details and provides means for validating effectiveness of employee training and testing program.</p> <p>Example:</p> <p>-Lists out courses/subjects covered</p> <p>-Tests corrected to 100% and stored for easy retrieval later</p> |
| <p>Insufficient Information</p> <p>--</p> <p>Characteristics of the Beyond Visual Line of Sight (BVLOS) applications after requests for additional information</p> | <p>-C2 operational capabilities not evident</p> <p>-Not demonstrating C2 can operate at stated max range or stating the envelope. i.e. lacking data</p> <p>-Application did not include FCC grant of authorization or FCC identification number for each emitter on the small unmanned aircraft system (sUAs) and ground control station</p> | <p>-Detailed methods or procedures to see and avoid or detect and avoid participating or non-participating aircraft and non-participating persons/moving vehicles are not evident or adequately described</p> <p>Examples:</p> <p>-If used, a video feed alone may not be sufficient, because detection would be limited to the direction the camera is pointing (i.e. not 360 degree detection) and does not address avoidance.</p> <p>-If used, Automatic dependent surveillance - broadcast (ADS-B) In alone may not be sufficient because ADS-B In only provides data for cooperative traffic and does not address avoidance.</p> | <p>-Providing general, or no statements</p> <p>Examples:</p> <p>-‘We only fly on clear days’</p> <p>-‘Weather is to be of Visual Flight Rules in nature’</p> <p>- Multiple applications not addressing weather requirements</p> | <p>-Provision of a method of assuring all required persons participating in operation have knowledge in all aspects of BVLOS not evident</p> <p>-Not stating who will have the training, what the training will consist of, or a method of assuring all required persons have been successfully trained</p> |

(b)

Figure 2-4: FAA waiver trend analysis for operations over (a) people, and (b) beyond the visual line of sight.

2.3. State-of-the-Practice and Literature Review

This section evaluates the drone state of the practice used by state and federal traffic agencies. This will be supported with a discussion of the existing AASHTO surveys on UAS utilization among state DOTs. Published work in the literature will also be presented in order to discover relevant information that can help inform, shape, or guide to conduct this research project.

2.3.1. State-of-the-Practice of UAS Utilization in Traffic Agencies

National Cooperative Highway Research Program (NCHRP) commissioned Scan 17-01 in order to provide a knowledge base for beneficial innovation and information sharing among state and other transportation agencies (Snyder et al., 2018). Their report revealed the successful approaches for UAS implementations among different state DOTs. According to the report, successful programs of UAS implementations among nation's traffic agencies showed the following benefits:

- Increased safety or reduced liability
- Increased efficiency and productivity or reduced impact on the public
- Cost savings
- Environmental protection
- Higher quality end products

Federal Highway Administration (FHWA) organized a peer exchange to learn how certain state DOTs are utilizing UAS (FHWA, 2018). Several DOTs have presented their current UAS employment and use cases as part of this peer exchange. Figure 2-5 illustrates examples of such use cases from states of North Carolina and Ohio.

(a)

(b)

Figure 2-5: Sections from (a) North Carolina and (b) Ohio presentations in the FHWA peer exchange (FHWA, 2018)

Furthermore, a UAS Integration Pilot Program has been established according to an October 2017 presidential memorandum for the Secretary of Transportation directing the following: "... the Secretary of Transportation, in consultation with the Administrator of the

FAA, [to] establish a UAS Integration Pilot Program to test the further integration of UASs into the NAS in a select number of states, local, and tribal jurisdictions”. Published in the Federal Register on 8 November 2017 and consistent with the presidential memorandum, the U.S. DOT and FAA announced the formation of the UAS Integration Pilot Program (Snyder et al., 2018). Current leader participants are:

- Choctaw Nation of Oklahoma, Durant, OK
- City of San Diego, CA
- Innovation and Entrepreneurship Investment Authority, Herndon, VA
- Kansas Department of Transportation, Topeka, KS
- Memphis-Shelby County Airport Authority, Memphis, TN
- North Carolina Department of Transportation, Raleigh, NC
- North Dakota Department of Transportation, Bismarck, ND
- The City of Reno, NV
- University of Alaska-Fairbanks, Fairbanks, AK

2.3.1.1. **2016 Survey Findings** (AASHTO, 2016)

- 33 state DOTs are either already using or considering aerial drones for a range of possible cost-and time-saving tasks, including bridge inspections, and even helping allocate assets to clear vehicle crashes.
- 17 state DOTs have researched drones.
- 16 state DOTs are considering UAVs for certain tasks such as traffic incidents.

2.3.1.2. **2018 Survey Findings** (AASHTO, 2018b)

- 35 State DOTs are deploying drones to save lives, time, and money.
- 35 of 44 responding state departments of transportation (80%) are using unmanned aircraft systems (UAS), or drones, for a wide range of purposes.
- 20 state DOTs have incorporated drones into their daily operations (44%).
- Another 15 state DOTs are in the research phase - testing drones to determine how they can be utilized.
- All 20 of the state DOTs operating drones on a daily basis, are deploying them to gather photos and videos of highway construction projects.
- 14 state DOTs also reported that the use drones for surveying.

Please note that AASHTO 2018 survey was the only survey that provided details on the UAS use cases of state DOTs. Figure 2-6 summarizes UAS activities found in this 2018 AASHTO survey.

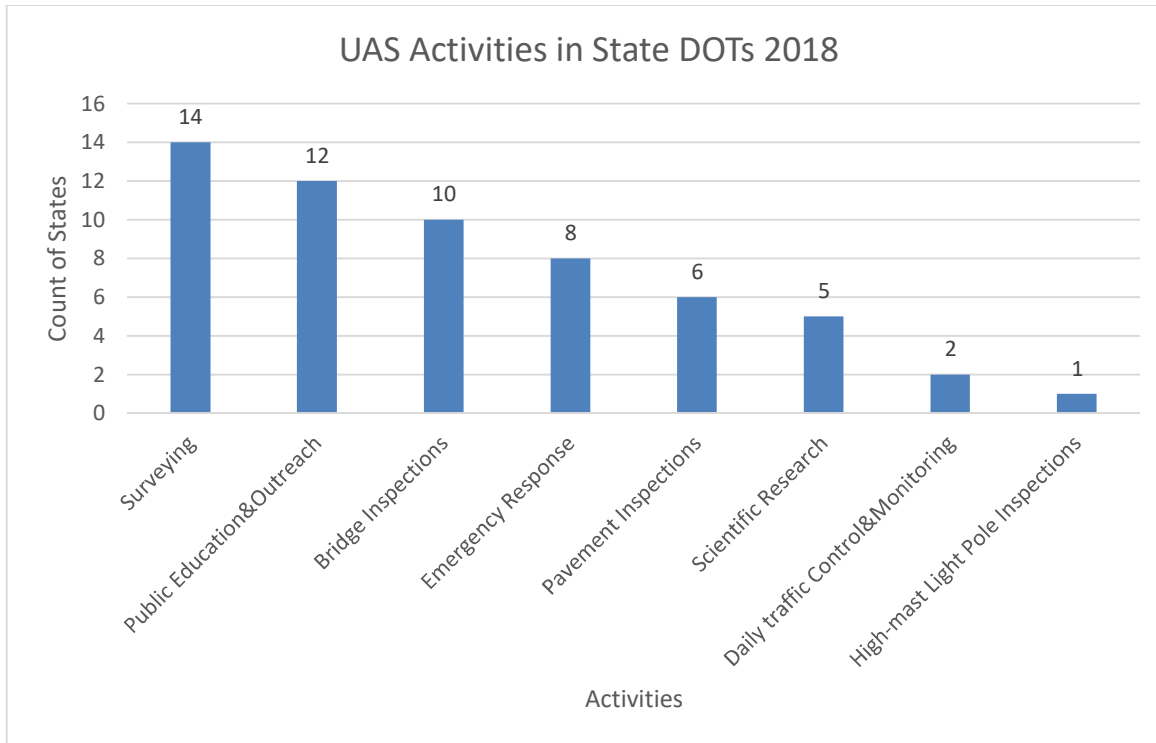


Figure 2-6: AASHTO 2018 survey results on UAS use cases by state DOTs

2.3.1.3. *2019 Survey Findings* (AASHTO, 2019)

- AASHTO finds that 49 of 50 states are using Unmanned Aerial Systems (UAS) or drone technologies for a variety of missions such as disaster and emergency response, infrastructure inspections, and avalanche control.
- Among those state DOTs, seven out of 10 have hired specialized staff, including highly skilled personnel to manage drone operations.
- 36 state DOTs reported having 279 FAA certified drone pilots on staff or approximately eight pilots per state.
- 36 out of 50 state DOTs or 72% are now funding centers or programs to operate drones. Note that this was 20 out of 44 state DOTs or 45% in AASHTO’s 2018 survey.
- 10 state DOTs have teamed up with academic organizations for training purposes.
- 24 state DOTs are conducting research in collaboration with an academic institution.
- 3 state DOTs are gathering real-world data through their participation in the FAA’s Integration Pilot Program, which allows them to fly drones beyond visual line of sight, at night, and over people – three things drone operators cannot do at this time without a special FAA waiver.
- 29 DOTs say drones help save money.

Figure 2-7 and Figure 2-8 compare the UAS utilization of state DOTs according to AASHTO surveys between 2016 and 2019. Figure 2-7 shows how the opinion of traffic agencies on utilizing drones changed in this 3-year span. Figure 2-8 indicates the number of state DOTs that have hired specified personnel for drone operations. According to the 2019 survey, there are 279 certified drone pilots hired by 36 state DOTs. Note that in 2016 there was no single personnel specified for UAS operations for all 50 state DOTs.

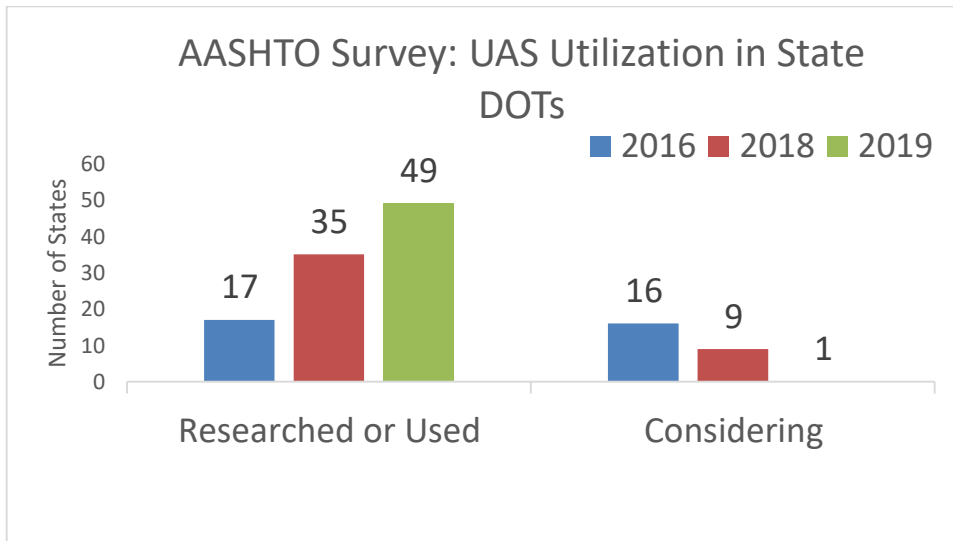


Figure 2-7: UAS utilization of state DOTs from 2016 to 2019

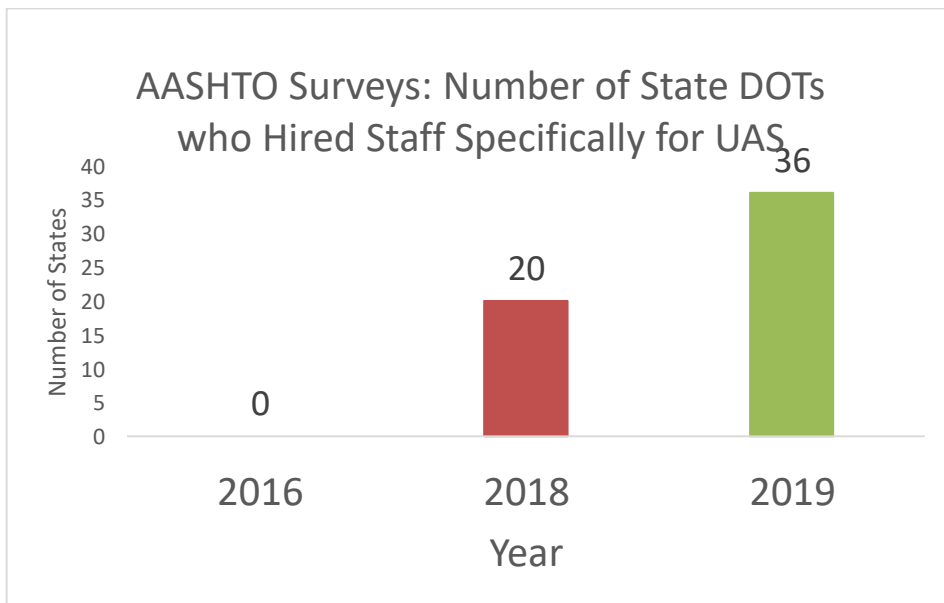


Figure 2-8: Number of state DOTs who hired people specifically for UAS operations

2.3.2. Example Use Cases among DOTs

2.3.2.1. *State of Michigan*

In the State of Michigan, Michigan DOT (MDOT) conducted a two-phase study to utilize drones for traffic monitoring purposes. In Phase 1, they used a tethered blimp to record an aerial video. Figure 2-9 indicates their demonstration at the ITS World Congress in Detroit, MI between September 2 and 11, 2014 (Brooks et al., 2014).

Figure 2-9: MDOT traffic monitoring demonstration through tethered blimp at the ITS World Congress in September 2014

In the second phase of the study, they used actual drones and created a semi-automatic traffic monitoring software using C++ and wxWidget Libraries in a Graphical User Interface (GUI). Figure 2-10 indicates the interface of their software (Brooks et al., 2018). They utilized Open Computer Vision (OpenCV) libraries for non-parametric algorithms to detect vehicles and roadways in a UAS video within 6 steps. At first, landmark annotation allowed the software convert pixels into coordinates. Second step required road annotation to specify the region of interest where vehicles would be detected. Third step, on the other hand, was related to the vehicle annotations and the training data for the machine learning and this is what makes the algorithm semi-automated. Next, the software generated the annotations for each frame and extracted outputs for the final step of traffic analysis and visualization. Although the software requires some manual labeling, their algorithm could overcome the UAS vibration issues. Besides, their documentation on extracting vehicle trajectories was very useful as they shared their code as an appendix. Figure 2-11 indicates the time space diagram generated in their software from the UAS obtained video.

Figure 2-10: MDOT traffic monitoring software to analyze UAS-obtained traffic surveillance

Figure 2-11: Time space diagram is generated from the UAS-extracted trajectories

2.3.2.2. *State of Texas*

Researchers from Texas A&M University conducted a two-phase study to demonstrate the real-time capabilities of UAS utilization for incident management. After providing an overall information about UAS utilization in traffic engineering, which constituted as the first step (Stevens, 2017), they utilized tethered drones and provided a real-time video footage demonstration of the selected highway in Houston, TX at the traffic management center (Stevens & Blackstock, 2017). Figure 2-12 indicates their demonstration in the Houston Metro area with a live video stream from a tethered drone capturing a simulated tow.

Figure 2-12: Tethered drone-captured live video streaming of a towing drill for the Houston metro area. Adapted from (Stevens & Blackstock, 2017)

2.3.2.3. *State of New Jersey*

New Jersey DOT (NJDOT) has applied for and won three FHWA grants to generate a fully operational UAS program to invest in new equipment and train employees (FHWA, 2018). For NJDOT to be selected for a UAS-involved project, the criteria is that the project must meet at least one of the following conditions: i) increase safety, ii) increase efficiency, iii) save time, and iv) save money. Their well know application is the high mast light pole inspection. They have inspected total 250 poles with drones more quickly and less expensive than other methods.

2.3.2.4. *State of Ohio*

Ohio DOT is currently conducting research for 11 critical UAS-involved missions with the University of Cincinnati. One of the missions in this project is traffic monitoring with tethered drones. The PI of the project, presented their progressive report in Ohio Transportation Engineering Conference on October 29-30, 2019 (Helmicki, 2019). The research team conducted a 400+ vendors market analysis and they bought 10 different UASs. For tethered drones, they have decided to buy a Hoverfly Power Tether and Yuneec Typhoon H drone with a 4 k. 12 MP. camera. Figure 2-13 indicates their equipment with which they conducted a test flight. Initial market search indicates that ground unit was approximately \$5,000. They found out that off-the-shelf software did not present real-time drone video solutions, or it was just prohibitive. Therefore, this analysis requires a critical algorithm that detects and tracks vehicles with a real-time video feed.

Figure 2-13: Ohio DOT investigating tethered drones for traffic monitoring

2.3.2.5. *State of Utah*

In Salt Lake City, Utah, a tUAS was utilized to analyze different signal phases on a diverging diamond interchange (Hainen et al., 2015). The study measured the vehicle arrivals on green with the event-based data and demonstrated these arrivals with signal state graphics on the videos recorded by a tethered drone. Figure 2-14, with the attached QR code that was linked to the video, are copied from the study to show their tUAS obtained video. Unfortunately, other than the maximum flight altitude (100 ft.), the details for the flight characteristics were not explained in detail within the study. The authors also did not clarify how they extracted data from tUAS-obtained video and technical details of tUASs. However, a 15-min section of recorded video for this study along with signal state graphics were published in Purdue University Research Repository (Hainen et al., 2014).

Figure 2-14: Salt Lake City, Utah, diverging diamond intersection observation with tethered drone

2.3.2.6. *State of Oregon*

Oregon DOT conducted a simulation-based study to evaluate the driver distraction due to drones. By using driving simulations, they tracked the eyes of the participants at the time when they saw a drone during the simulation. They found unsafe glances (>2 sec) at all three lateral offsets of the drone, 0 ft., 25 ft., and 50 ft., respectively (Hurwitz et al., 2018). Figure 2-15 indicates their simulation environment in two different lateral offset scenarios.

Figure 2-15: Oregon DOT driving simulation environment for testing driver distraction due to drones

These are all the relevant DOT applications with regards to traffic data collection with drones. The following section presents a detailed literature review.

2.3.3. Literature Review

As the previous section indicates, UASs utilization has become a prominent need for DOTs over the last few years and there is a certain need to use UASs for intersection performance evaluations. This section presents and elaborates on the published UAS-focused traffic engineering studies.

Several researchers have summarized the current research directions for the UASs-based traffic analyses around the world (Barmounakis et al., 2016; Kanistras et al., 2015; Khan et al.,

2017a; Puri, 2005). They stated that processing and analyzing the visual traffic data was one of the critical challenges associated with UASs. According to the literature, vision-based traffic analysis consists of two basic steps. The first step detects and tracks the vehicles towards providing data such as position, speeds, or classes of vehicles. The second step, on the other hand, analyzes the interaction between vehicles to perform tasks like turning movements, behavior prediction, conflict analysis, or gap acceptance by utilizing the outputs of the first step (Datondji et al., 2016). When it comes to the aerial vision, another step is required for vehicle detection because the movement is related to both camera and interest object itself. A study (Rodríguez-Canosa et al., 2012) calculated the movement of vehicles and the camera separately with four major modules: feature extraction, image registration, vehicle shape detection, and vehicle tracking. This was conducted in order to calculate vehicle trajectories and speeds. Some studies focused only on the roadway detection so that background can be extracted and the problem can be solved with basic optical flow algorithms (Z. Kim, 2005; Lin & Saripalli, 2012; Zhou et al., 2015). For example, a novel real-time approach was proposed in Kim (2005) for roadway detection learning from a single image. Although additional features such as ramps and overpasses decreased the accuracy of roadway detection, this study could be successfully applied to aerial vision-based navigation (Ke et al., 2017a; Z. Kim, 2005).

Although unmanned aircrafts have been used for high mobility to cover large areas, most of the studies utilized them just for “eye-in-the-sky” logic (Barmounakis et al., 2016; Kanistras et al., 2015). Therefore, stabilization of the camera is more beneficial than the mobility for some tasks such as intersection performance evaluation and speed, volume, and position extraction on a roadway segment (Aguilar & Angulo, 2014; Knoppers et al., 2012). In this regard, 3-axis gimbals, and hovering flights (i.e., no vibration or drifting) have been employed by many recent studies in order to stabilize the background. A study (E. J. Kim et al., 2019) extracted vehicle trajectories on congested traffic conditions by incorporating a machine learning-based computer vision algorithm and hovering ability of new generation drones. A four-step algorithm was implemented in (Ke et al., 2017a) for stable and unstable UAS videos in order to estimate the bidirectional flow characteristics such as speed and volume in real-time. The study reached a 96% accuracy for speed and 87% accuracy for the vehicle counts, regardless of the UAS movements.

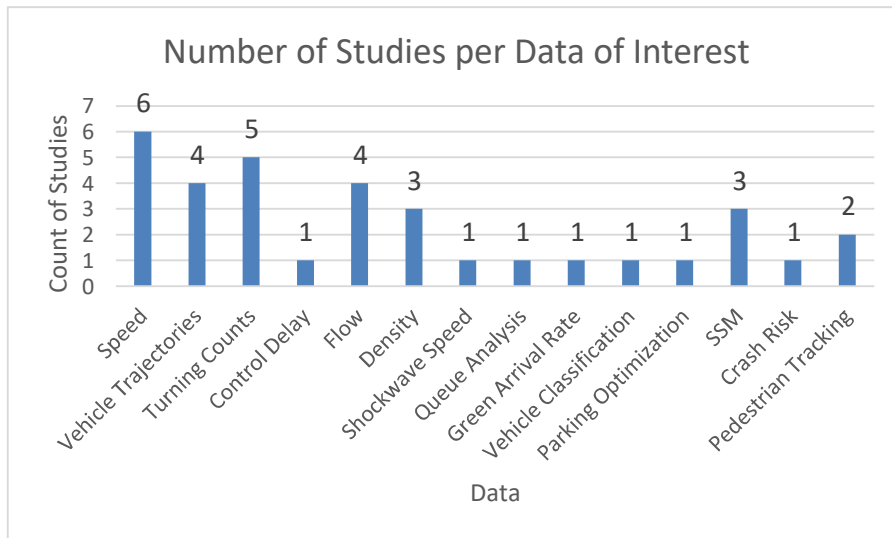
As vehicles can be detected and tracked in a sequence of frames obtained by UASs, the performance of intersection operations can also be evaluated by calculating the key measures such as delay (Pan et al., 2019), green arrival rate (Hainen et al., 2015), queue detection (Khan, Ectors, Bellemans, Janssens, et al., 2018), and origin-destination matrices (Braut et al., 2012; Coifman et al., 2006). These applications may require special time indexing for the frames and detection for stopped or reaccelerating vehicles. The dwelling time for each vehicle can be calculated with the time information of the frames at which a vehicle stopped and started to accelerate.

To sum up, UAS-based traffic monitoring requires a preprocessing step for background subtraction and geo-referencing to extract accurate vehicle trajectories and traffic flow parameters such as speed and volume. Nevertheless, there is a chicken-and-egg problem in accuracy calculations due to the lack of validation data. Some studies validated their results with randomly selected sample frames from the same UAS-recorded video that had been used for the actual analysis (Ke et al., 2017b; Niu et al., 2018). Some other studies used simulation results for

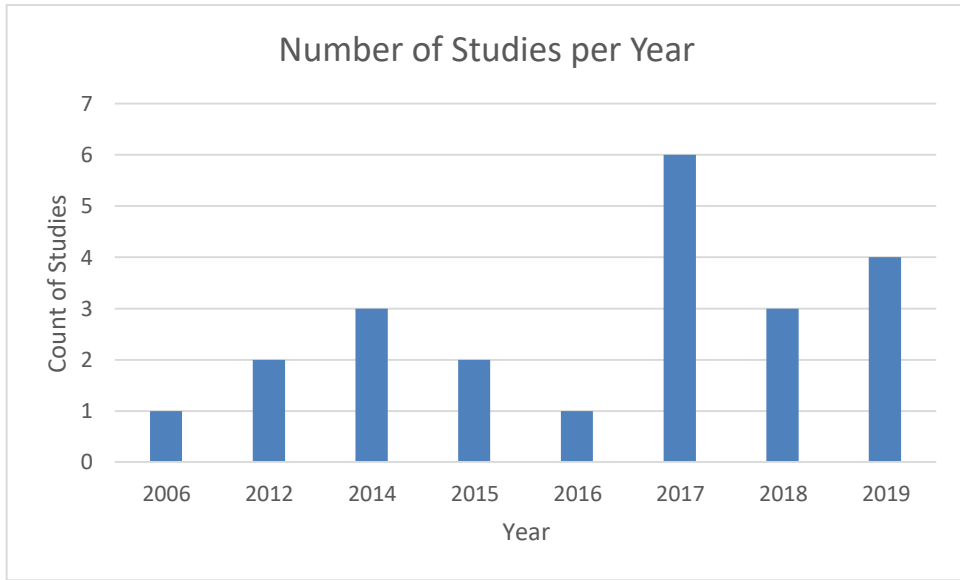
validating their UASs-based traffic analysis (Pan et al., 2019). After the validation, UASs acquired georeferenced images can be used for several tasks such as intersection performance evaluation, origin destination generation, and driver behavior observation.

Regarding tethered drone applications, researchers from Texas A&M Transportation Institute conducted a study for evaluating tUASs as a traffic incident management tool (Stevens & Blackstock, 2017). They have used tethered drones to broadcast live traffic video to the traffic management center. With two different demonstrations, researchers were able to show that tUAS could provide real-time traffic video streams to the traffic management center building in Houston, TX.

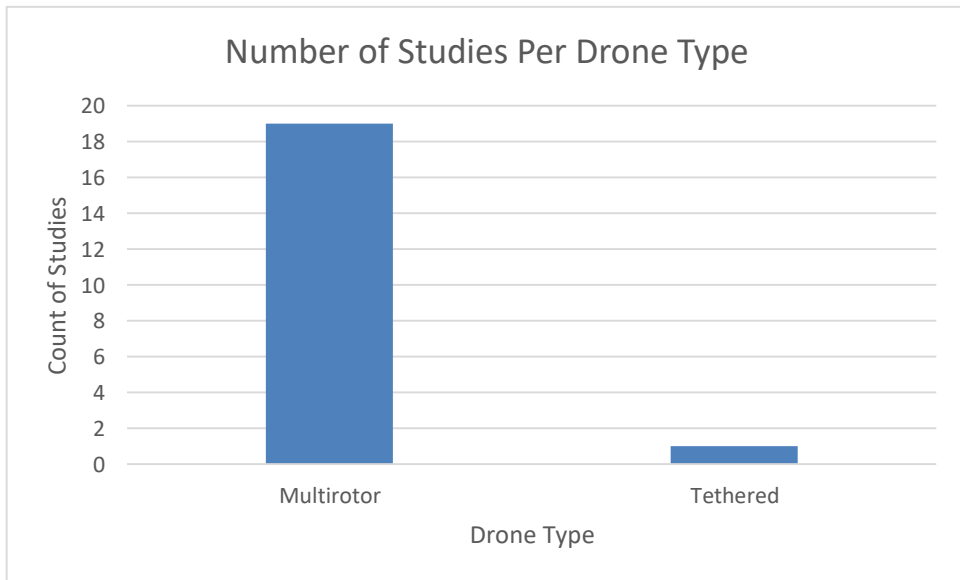
Figure 2-15 indicates the meta-data of the published work. Figure 2-15a indicates number of studies per data of interest, Figure 2-15b groups the studies by their year, Figure 2-15c demonstrates the drone types used in these published work, and Figure 2-15d depicts the performance of the video image processing algorithm used in the studies. Note that “applicable for real time” in Figure 2-16d indicates that the algorithm executes faster than 25 frame-per-second, which is the average recording speed by UAS-mouthed cameras.



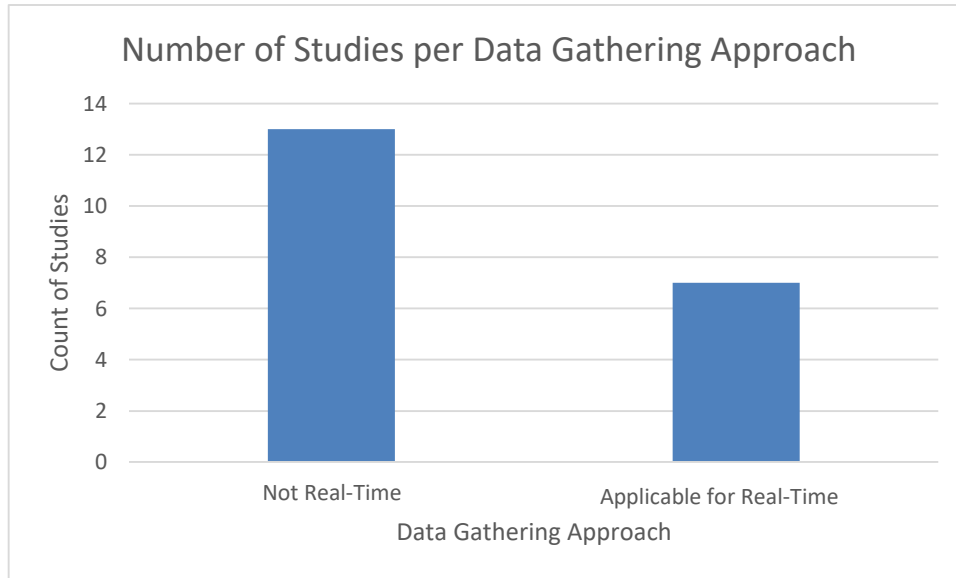
(a)



(b)



(c)



(d)

Figure 2-16: Metadata of published work: Number of studies (a) per data interest, (b) per year, (c) per drone type, and (d) per data gathering speed

2.4. Desired Data Based on Manual on Uniform Traffic Control Devices (MUTCD) and Manual on Transportation Traffic Studies (MUTS)

Federal Highway Administration (FHWA) and the United States Department of Transportation (U.S. DOT) issued the Manual on Uniform Traffic Control Devices (MUTCD) to specify the standards by which traffic signs, pavement markings and signals are designed, installed and used (FHWA et al., 2009). Although MUTCD provides top-down details for traffic control devices, it recommends the use of engineering judgement to conduct engineering studies to decide whether there is a need for an installment or a treatment of a traffic control device at a particular location. Subsequently, Manual on Transportation Traffic Studies (MUTS) provides minimum standards for conducting traffic engineering studies on the roadways under the jurisdiction of FDOT. MUTS was prepared by FDOT in 1978 through a grant from Governor’s Highway Safety Commission under the provisions of Federal Highway Safety Standards. The Manual has been updated periodically and currently serves as a guideline for compiling and analyzing data collected for traffic engineering study activities (FDOT Traffic Engineering & Operations Office, 2016). The desired data output is selected based on MUTS guidelines.

MUTS categorizes the basic areas of concern at intersections as vehicle problems, vulnerable user problems, and crashes. It should be noted that the problem under consideration might be related with multiple areas of concern. MUTS also provides guidance on data to be collected to determine the extent of these problems. Table 2-3 indicates the basic areas of concerns and the data set that may help to identify and analyze the problems at intersections.

Table 2-3: Basic areas of concern at intersections and suggested data sets. Source: MUTS (FDOT Traffic Engineering & Operations Office, 2016)

Basic Areas of Concern at Intersections

| | | <u>Vehicle Problems</u> | <u>Vulnerable User Problems</u> | <u>Crashes</u> |
|----------------------------|--|---------------------------------------------------------------------------|---------------------------------------------------------------------------------------------|----------------------------------------------------------------------------------------------------------|
| Suggested Data Sets | | <ul style="list-style-type: none"> • Volume | <ul style="list-style-type: none"> • Volume | <ul style="list-style-type: none"> • Collision Diagram, Geometric Design, Sight Distances |
| | | <ul style="list-style-type: none"> • Progressive Move | <ul style="list-style-type: none"> • Gap Study | <ul style="list-style-type: none"> • Conflict Analysis |
| | | <ul style="list-style-type: none"> • Travel time and Delay | <ul style="list-style-type: none"> • Distance to the Crosswalk | <ul style="list-style-type: none"> • Speed |
| | | | <ul style="list-style-type: none"> • Demographics Related with Walking speed | <ul style="list-style-type: none"> • Vulnerable User Volume |
| | | | | <ul style="list-style-type: none"> • Historical Data |
| | | <p>Can be obtained with UAS</p> | | |
| | | <p>Requires additional sources</p> | | |

Suggested data sets of Table 2-3 can be categorized as the first order data, dynamic data, and volume data so that more deterministic decisions can be made regarding the basic areas of concern. Figure 2-16 indicates the proposed flow chart of collecting these data sets in this project. The following sections explain each data product of the study with regards to MUTS guidelines.

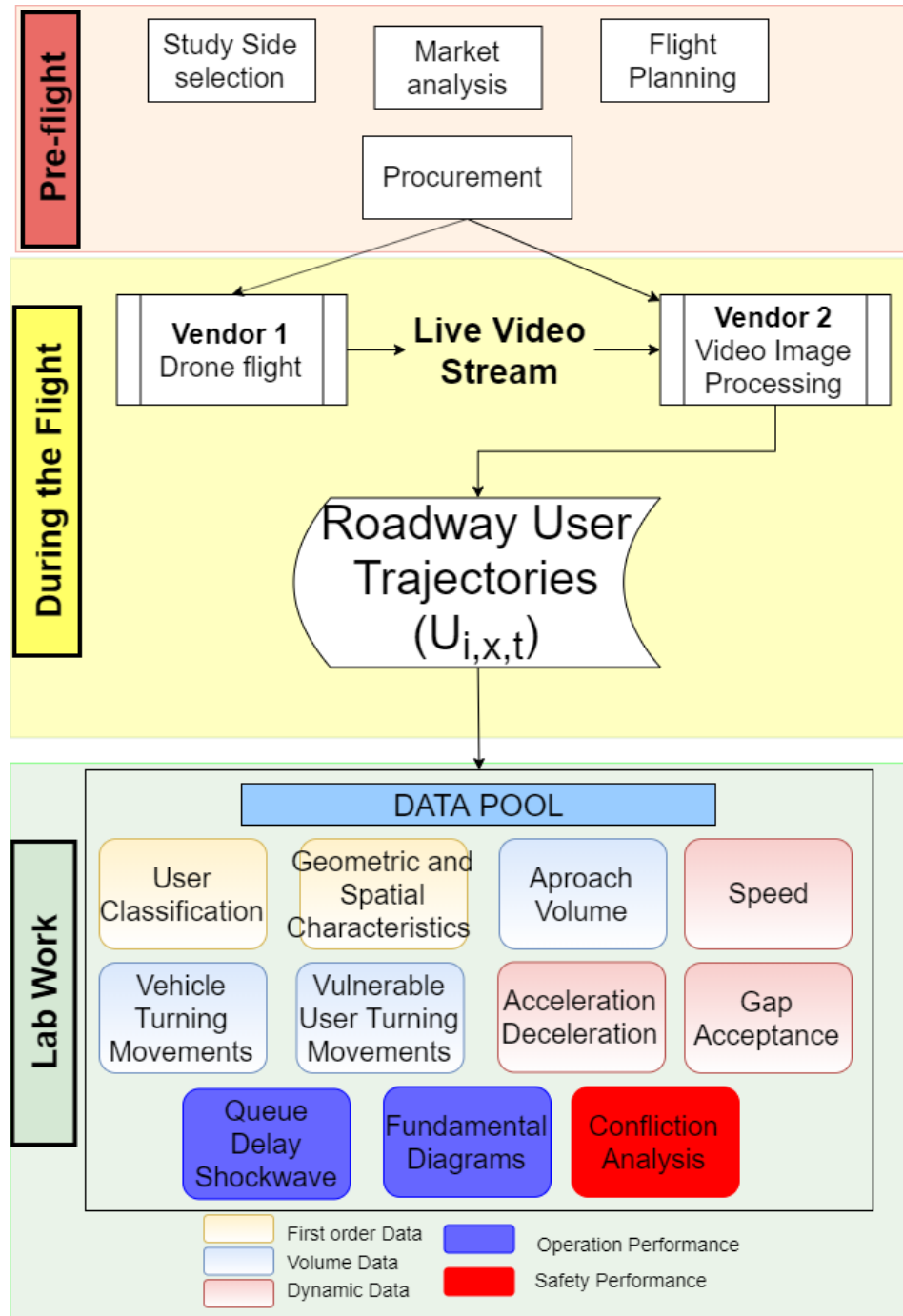


Figure 2-17: Project flow chart and desired outputs

2.4.1. Roadway User Trajectories: $U_{i,x,t}$

This data set constitutes as the main output of the flight operations. It specifies the position (x) of user i at time t . Based on the literature, trajectory data is found to be the best option to obtain UAS-based real-time traffic data. Also, it is promising for vision-based non-video traffic data. The main challenge is detecting objects with significantly different sizes such

as pedestrians and vehicles within the live stream video. However, for traffic analysis purposes, 0.1 second can be accepted as high-resolution data although 10 frame-per-second refers to a relatively high computational cost in image processing even with the advanced deep learning algorithms. In this regard, by sacrificing the computational speed of the standard image processing algorithm, a more sensitive algorithm can be built.

2.4.2. User Classification

This data set identifies the roadway users such as vehicles, pedestrians, bicyclists, motorcyclists, trucks, and buses. This data set can be obtained at the detection phase and should be included in the trajectory data set.

2.4.3. Geometric and Spatial Characteristics

This data set includes local characteristics about the intersection. These characteristics could be the type of intersection and type of control device used in the intersection as well as some of the signal warrant study inputs such as an approximation of the surrounding population, schools, and railroads in the proximity of the intersection. Also, distance to adjacent intersections can help identify progressive movement at the intersection. Beyond these critical local characteristics, a frame of the video obtained from the UAS that shows the intersection on top view can be used to determine number of lanes on each approach, exclusive left and right turning lanes, median width, shoulder width, and lane width. This one frame image can also provide intersection skewness and number of bus stops in the proximity of the intersection. Such data can be used to identify the crash modification factors as described in MUTS Chapter 5 Data collection for Safety Studies. Finally, this one frame can be used as a condition diagram as described in MUTS Chapter 6.

2.4.4. Speed

With the accurate trajectory data, speed can be calculated at each time step by using the current position and the position at one-time step before. By selecting certain positions, vehicle spot speed can also be collected without sampling as described in MUTS Chapter 12.

2.4.5. Acceleration and Deceleration

Similar to the speed, acceleration or deceleration can be calculated with the position differences at consecutive time steps.

2.4.6. Approach Volume

Approach volume simply indicates the number of vehicles approaching to intersection from a particular direction. It can be used in the warrant study if turning movements are too low. However, according to MUTS, turning movement counts may not be enough to determine the volume of the intersection because the vehicle can wait more than one cycle to leave the intersection on a saturated flow. In this regard, approaching volume should be collected for the vehicles stopping at the queue. As speed can easily be obtained from trajectory data set, those vehicles that stopped before reaching the intersection can be determined. Approach volume can also be used for estimating the Annual Average Daily Traffic (AADT), which is one of the key factors on crash frequency predictions.

One setback on extracting approach volumes with drone-based videos can be the limitation of field-of-view (FOV). If the queue extends the FOV, drone camera cannot capture

where the queue starts. Therefore, approaching volume cannot be calculated. This indicates that drone-based traffic analysis relies heavily on selected camera and the looking angle as well as the flying height. Tethered drones with a larger field-of-view can help solve this problem.

2.4.7. Vehicle Turning Movements

Turning movement counts refer to the amounts of vehicles passing the stop bar on each approach and can be used for making decisions regarding geometric design, sign and signal installation, signal timing, pavement marking, traffic circulation patterns, capacity analysis, parking and loading zones, and vehicle classification (FDOT Traffic Engineering & Operations Office, 2016).

Turning movement counts can be identified with relative changes on the x and y coordinates of the vehicles in the trajectories data set. Entry and exit gates can virtually be drawn on the video and turning movement data set can be automatically extracted from a recorded video. Turning movement counts should be extracted by populating the digital version of “Summary of Turning Movement Counts” form (FORM – 750 – 020 – 02) given in MUTS, 2016.

MUTS suggests manual and automated counting methods for counting the turning movements. Manual methods can be done in the field with tally sheets or laptops by directly populating the digital version of the form as well as watching a video recorded at the intersection. However, depending on the observation period and type of the intersection, manual counting may require significant manpower. Also, counting the turning movements at roundabouts, superstreets (R-CUTs), and Michigan U-Turn intersections require path-based counting and manual methods are limited with the human ability. License plate matching and origin-destination matrix sampling methods are also recommended in MUTS for path-based counts. However, those methods may also lead to high error and require extensive lab work.

In that sense, tethered drone-based traffic monitoring can easily be utilized to collect the turning movement counts by tracking the path of vehicles from their entry to exit on those intersections. MUTS also suggests embedded detectors for automated turning counts. Those detectors provide continuous data and are very useful for different purposes such as queue detection, embedded detectors cannot provide turning counts, and vulnerable user counts. MUTS also briefly discusses using image-video processing algorithms for automated turning movement counts at intersections. However, this requires more details. Based on the identified advantages and challenges of this feasibility analysis, the methods section of MUTS Chapter 4 Turning Movement Counts can be updated.

2.4.8. Vulnerable User Turning Movements

Similar to vehicle turning movements, crossing pedestrians and bicycles can be extracted from aerial video-based trajectories. Manual counting methods may also help collect demographic data such as age, sex or disability. These factors can help analyze pedestrian behavior; however, movement tracks cannot be acquired with a manual observation. Drone-obtained roadway user trajectories will allow the use of conflict analysis between vehicles to vehicles, vehicles to bicycles, and vehicles to pedestrians. A study recently identified surrogate safety measurements such as time-to-collision and post-encroachment time between right turning vehicles and pedestrians (P. Chen et al., 2017). Pedestrian tracking data can also be used on cross bar use and pedestrian speed analyses. Vulnerable user moving counts can be extracted by

populating the populated digital version of “Summary of Pedestrian and Bicycle Movements” form (FORM – 750 – 020 – 10) given in MUTS, 2016.

2.4.9. Gap Acceptance

Gap refers to the time difference between the rear end and the front bumper of two consecutive vehicles passing the same point in same direction. Critical gap indicates the minimum gap between two consecutive major street vehicles or a side street vehicle, or a pedestrian or group of pedestrians that cross the street.

Gap studies become more critical at the roundabout intersections since the capacity can be calculated using the gaps. Additional to the critical gap, follow up time is also another time value that indicates the time between two consecutive vehicles entering the circulating traffic in the same gap. These values can be extracted from drone obtained vehicle trajectories (Khan, Ectors, Bellemans, Ruichek, et al., 2018).

MUTS Chapter 8 examines the gap studies for critical gap analysis at two-way stop-controlled intersections. The chapter also provides insight for pedestrian-related critical gaps; however, no details were presented for roundabout gap studies. Drones can certainly be a good alternative for analyzing the capacity on roundabouts. Based on the results, gap studies part of MUTS can be updated. Further, a complete section can be dedicated for roundabout studies since MUTS does not specifically cover roundabouts.

2.4.10. Queue Length, Delay, and Shockwave

These data sets are the basic performance measurements for a signalized intersection. Queue length and queue dissipation can be calculated from the arrival and turning movement counts. Also, shockwave speed can be extracted by identifying the critical points on time space diagram of detected vehicles. Figure 2-18 indicates an example of shockwave analysis with trajectories obtained from an aerial video in Belgium (Khan, Ectors, Bellemans, Janssens, et al., 2018). Figure 2-18 also depicts the critical point identification combined with other detected vehicles, where accumulating waves and dissipating waves can be identified. Where these waves meet also leads to the queue dissipation time.

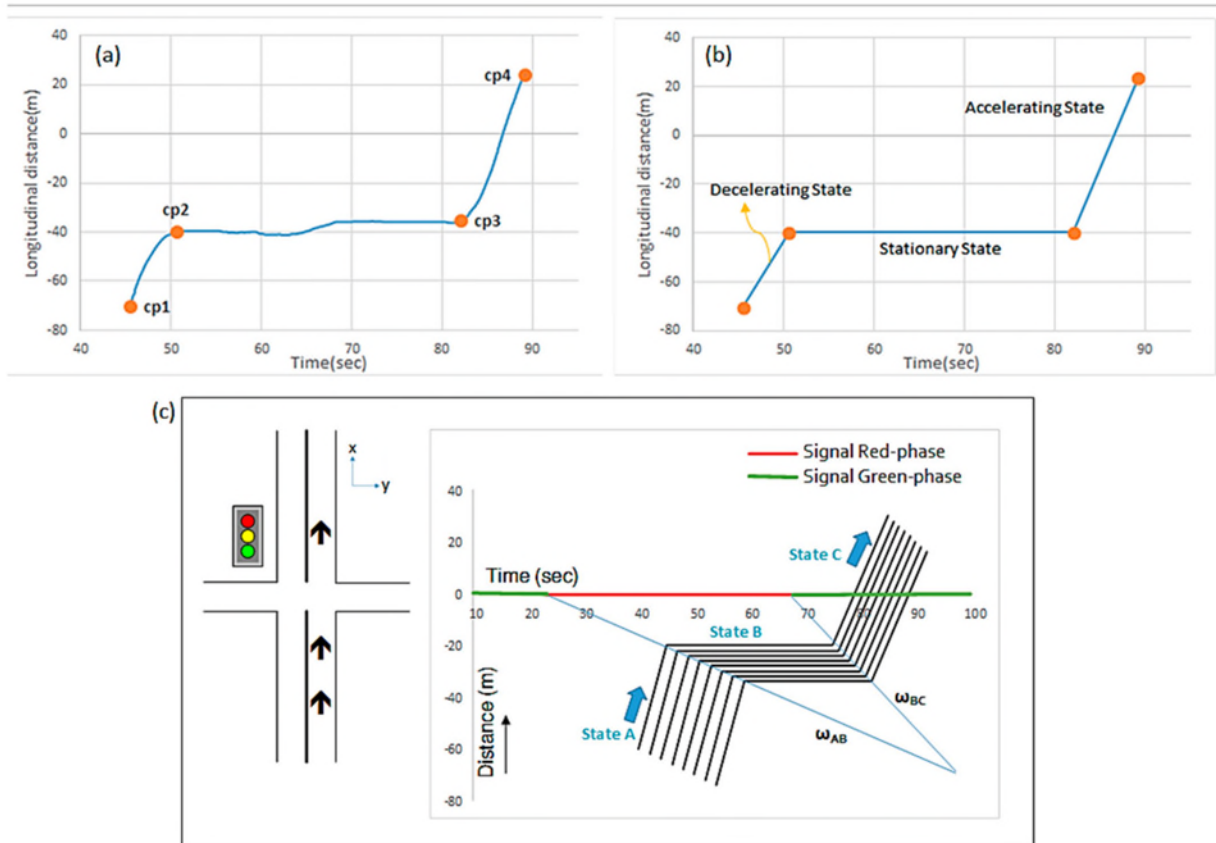


Figure 2-18: Shockwave and queue dissipation from drone-obtained trajectories

MUTS examines intersection delays in three different ways:

- Time in Queue Delay (TIQD) = the time difference between a vehicle stops at the intersection and the time it clears the intersection
- Control Delay = TIQD + deceleration and acceleration delay due to signal control
- Travel time delay = time difference between the vehicle could have reached to a point with its approaching speed as if there was no control device and the actual travel time passing through the intersection

Table 7-1 in MUTS 2016 indicates commonly used equipment for delay studies with their advantages and disadvantages. Particularly, manual, and electronic methods are counted for control delay study and floating car is counted for travel time delays. Although video method is listed as “much more labor in the office”, which is a disadvantage of electronic methods, TIQD and travel time delay can be extracted automatically from drone-obtained trajectories.

2.4.11. Fundamental Diagram

Fundamental diagrams depict the pair-wise relationship of flow ($q = \text{veh/h/lane}$), speed ($v = \text{mph}$), and density ($k = \text{veh/mi/lane}$). For a single lane approach, flow and density can be extracted from the time-space diagram. For example, in Figure 2-18 where we see a standardized time-space diagram with multi vehicles, a horizontal line crossing all the vehicles on the line can lead to flow, and vertical line can lead to density. Speed can be extracted directly from trajectory data. Fundamental diagrams are highly used for freeways.

2.4.12. Conflict Analysis

By using the trajectories from different users, some surrogate safety measures can be identified. As aforementioned, a pioneer work conducted a safety analysis on an intersection in China by using drone-obtained trajectories (P. Chen et al., 2017). They collected trajectories for vehicles and pedestrians as points. At the end, they analyzed the following parameters: post-encroachment time (PET) and relative time to collision (RTTC). PET can be defined as the time between a vehicle leaving the intersection and another one going in. RTTC, on the other hand, indicates the time between the first vehicle gets into a conflicted area and second one enters the same confliction area. Another reason for selecting these measures was that the authors only had trajectory data, which indicates that a single point represents the vehicles throughout the move. Instead of using time to collision, they used entry- and exit-based surrogate safety analysis. Figure 2-19 shows the PET and RTTC calculations.

Figure 2-19: PET and RTTC calculations on XY surface and time elevation (Chen et al., 2017)

The following section presents an evaluation of the computer vision algorithms in the context of drone-based video analysis.

2.5. Computer Vision Algorithms for Drone-based Traffic Data Extraction

UAS-based traffic data acquisition heavily relies on ‘detect-and-track’ logic. Once vehicles are detected, tracking algorithm can follow the objects in the following frames as long as the pixels have the same coordinates in subsequent frames. Hovering flight mode can significantly decrease the preprocessing effort since it leads to a more stable background. Traffic data extraction from moving flights, on the other hand, requires an additional preprocessing stage for each frame and re-detection of the vehicles. This is considered as a bottleneck for real-time data acquisition since tracking algorithm runs much faster than the detection algorithm (Biswas et al., 2019). This section examines the computer vision techniques required for preprocessing, object detection, and tracking separately. The section also evaluates these algorithms for obtaining the desired traffic data for intersection studies. Figure 2-20 indicates number of studies with a focus on the computer vision algorithms used. Please note that ML refers to machine learning and DL refers to deep learning.

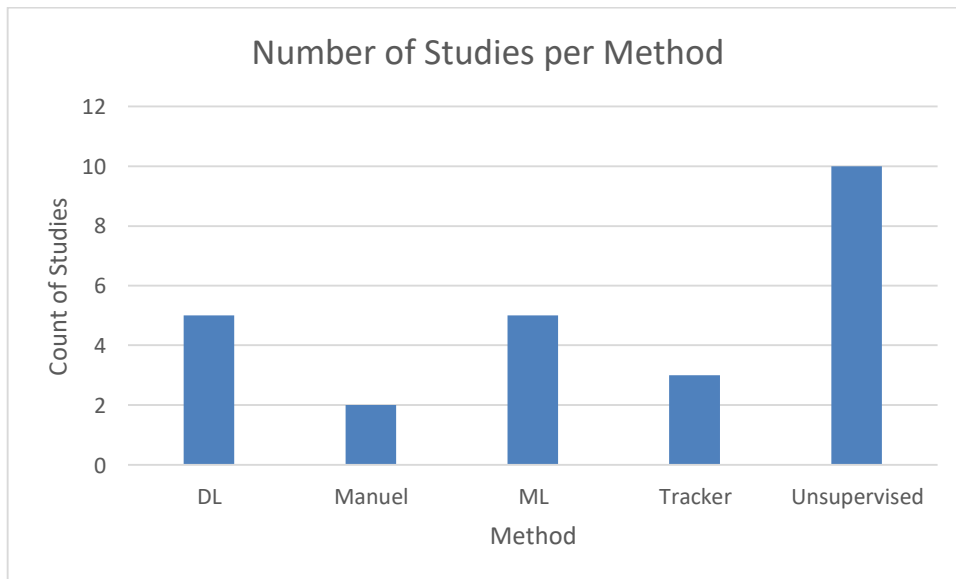


Figure 2-20: Number of studies per computer vision algorithms (ML: Machine Learning, DL: Deep Learning)

2.5.1. Preprocessing

Although hovering provides almost stable platforms, just a little shaking of a UAS may have significant influence on the vehicle trajectory extraction. Mathwork’s stabilization approach can be used to stabilize the video even in real-time applications. Geo-referencing, on the other hand, is mostly done by a Geographic Information System (GIS) software (Salvo et al., 2014). First, video images are turned into a mosaic raster so that 2D planar images can be calibrated into 3D real world coordinates. Random sample consensus (RANSAC) algorithm also provides a 2D to 3D transformation using a homography matrix. Those algorithms are fast enough so that they can be utilized in real-time applications (Khan et al., 2017b).

For stabilizing backgrounds, Kanade-Lucas-Tomasi (KLT) point tracker can be used to detect the predefined points in each frame for geo processing. However, it requires initial geo-referencing for the predefined points, and it could increase the computational cost. Structural Similarity Index Measurement (SSIM) is generally used to check the similarities between consequent frames. If the SSIM calculated is lower than the threshold value (0.5), feature-based image alignment (FBIA) can be used to align the frames (Biswas et al., 2019).

Tethered UASs (tUAS), with the advantages of extra stability compared to their non-tethered counterparts, can maintain a non-zero attitude while hovering in a constant speed (Nicoira et al., 2017). Therefore, tUASs can overcome the preprocessing step and fasten the traffic data acquisition from aerial images.

2.5.2. Object Detection and Tracking

Roadway user detection is the key component of the vision-based traffic analyses and methods can be categorized into point detection, machine learning, and deep learning algorithms. Most of the point detection and tracking algorithms, such as KLT point tracking or blob analysis, are unsupervised algorithms and can be applied rapidly without any training data set. These algorithms represent early stages of computer vision utilization in transportation as they can be found in vehicle detection and surveillance technologies used in 2000 (Mimbela, 2000). Also, they are easy to cluster with simple algorithms like k-means algorithm (Ke et al., 2015). Speed clustering of the interest points can be used for background subtraction as well (Ke et al., 2017b). However, these algorithms are very sensitive to the complexity of the image such as shadows, roadway facilities and adjacent vehicles. Their performance especially reduces in congested traffic conditions.

Most of the supervised vehicle detection algorithms come from the Viola-Jones face recognition algorithm (VJ) with hand crafted features (i.e., Haar, Histogram Oriented Gradients (HOG), or SIFT Local Binary Pattern) (Viola & Jones, 2005). Moreover, Integral Channel Features (ICF) (Dollár et al., 2012) and its improved version Aggregated Channel Features (ACF) (Appel et al., 2014) also originated from the VJ-based object detection algorithms. Basically, the cascade function in these algorithms needs to be trained with positive and negative images. Training data set consists of positive and negative images to emphasize what the interest object is and what is not. For example, in vehicle detection, positive images include vehicle(s) and negative ones include only the roadway with trees or other side features. The larger size of the training data set, the higher accuracy on the vehicle detection similar to the face recognition. When an object has all the features according to a running vehicle training set, it will be detected as a vehicle and a bounding box will be drawn around it (Xu et al., 2016). They can be used to detect vehicles in the congested traffic flow; however, there is still an overlapping problem. A study (E. J. Kim et al., 2019) used a 40% overlapping threshold for ACF-based vehicle detection. If the overlapping area is higher than 40 % of the total detected area, only the vehicle with higher detection score is retained. Haar like features and HOG were also used for pedestrian detection and tracking from UAS-obtained images (Ma et al., 2016).

More recently, deep learning-based convolutional neural networks (CNN) have shown an outstanding performance in object detection (T. Tang et al., 2017; Vattapparamban et al., 2016; Xie et al., 2018; Xu et al., 2017). These algorithms have been improved with region-based CNN (R-CNN) (Girshick et al., 2012), Fast R-CNN (Girshick, 2015), and finally with Faster R-CNN

(Ren et al., 2017). CNN algorithm basically extracts region proposals as candidate locations for the objects followed by the computation of the CNN features. Faster R-CNN improves the performance by using a Region Proposal Network (RPN) additional to the object detection network. A recent study (E. J. Kim et al., 2019) proposed a detailed comparison on the vehicle detection and tracking performances of deep learning (faster R-CNN) and machine learning algorithms (ACF). Their findings indicated that faster R-CNN outperforms ACF. Therefore, the algorithm to run the analysis should be selected carefully. Depending on the purpose of the analysis, output of the vehicle detection and tracking algorithms can be speed, volume, or vehicle trajectories. Unlike point tracking algorithms, vehicle detection algorithms can classify vehicles as well.

2.6. Challenges and Operational Barriers

Ch1. One of the biggest challenges on drone operations is the weather dependency. For example, rain during the work can ruin the whole data collection operation. UASs are weather dependent and Remote Pilot in Command (RPIC) should continuously check the weather and wind. FAA Part 107 regulations do not provide a threshold for the wind speed since there are a variety of aircraft models under these rules. Please note that tethered drones are more sensitive to the wind speeds since the surface exposed to the wind is much larger and it causes extra pull on the tether.

Ch2. Aerial footage arises numerous privacy issues. In Florida and many other states, UASs cannot capture and fly on privately owned lands without written consent.

Ch3. Safe and legal UAS operations are the major priority. Remote Pilot in Command (RPIC) must inform FAA regarding every injury crash and higher than \$500 property damage crash. One of the biggest concerns for UAS operations is a drone's fall on people or vehicles causing severe incidents. To avoid this, some of the drone companies developed parachutes. There are available automated altitude observing systems that enable UASs to release parachutes. Tethered drones have more reliable expectations in this aspect since the ground units can retrieve the UAS through an automated crane control.

Ch4. Just like any emerging technology, UASs rely heavily on wireless communications. Although Federal Communication Commission has standardized all types of wireless communication to enhance safety, the biggest problem of emerging technologies is the cybersecurity. Researchers (Vattapparamban et al., 2016) have evaluated the impacts of drones on future smart cities considering cyber-attacks. They have performed UAS hacking through the wireless communication with off the shelf, ready to use software. Nowadays, drone manufacturing companies and communication technology leaders have focused on more secure operation of drones since secure wireless control/communication is critical.

Ch5. Beyond general operation challenges, UAS based video-image processing has its own problems. Rapid advancement on computer vision technology has enhanced the power of image processing. Today, people trust this technology to secure their privacy like in the case of those new generation iPhones. In the transportation field, vision-based traffic monitoring dates back to 1990s. However, when it comes to the aerial videos, the problem gets more challenging since there is a six more degree of freedom that is related to the movement of the camera.

Ch6. Although mobility is one of the biggest advances for drones, they have been used in the context of eye-in-the-sky logic. In some cases, stability is more beneficial than the mobility to stabilize the background. There are some algorithms that can align the subsequent frames before

detect-and-track algorithms; however, they increase the computational cost. It is expected that tethered drones will increase the performance of the gimbal and provide more stable video footages.

Ch7. The performance of vision-based detection and tracking algorithms depends on the density of the object to be determined. Therefore, vehicle, bicycle, motorcycle, and pedestrian detection in congested conditions may have a lack of accuracy. Machine learning and deep learning algorithms can overcome this problem as they are trained with positive and negative images of the objects. However, this may become a bottleneck on real time data extraction. For example, (E. J. Kim et al., 2019) specifically focused on vehicle trajectory extraction in saturated flows by comparing machine learning algorithms with deep learning algorithms. They found that machine learning algorithms process one frame of the video in 1.15 seconds whereas deep learning algorithms analyzed a frame of the video within a 0.65 second speed. Real-time data extraction requires the algorithm to extract data in 0.04 seconds, assuming the camera records and broadcasts the video in 25 frames per second.

Ch8. Another problem is the visibility disruptions due to light. As the performance of UAS-based traffic monitoring rely heavily on a clear video footage, the study can be disrupted by occlusion, due to clouds or foggy weather. Although drones bring some solutions for this, they are still sensitive to daylight conditions. There is no study in the literature testing drones during night for traffic monitoring; however, a drone company named DataFromSky has published a video on their YouTube channel to indicate their algorithm can handle nighttime videos as well.

Ch9. Object detection algorithms are very sensitive to the size of objects, especially when it comes to detection speed. This also plays an important role on the performance of object detection and tracking. Therefore, tracking vehicles and pedestrians at the same time is a big challenge since their sizes as well as their speeds vary. Beyond this variation, object detection algorithms struggle when it comes to the crowded or “close proximity” objects. Therefore, vehicle detection during congestion is a big challenge that have been tackled several times (E. J. Kim et al., 2019).

Ch10. When drone services and video image processing services are provided from different vendors, this requires extra configuration steps between vendors so that their software and hardware can be compatible.

Ch11. Another challenge will be locating the tethered drone ground unit since the operation will require a certain clear distance and a vertical connection should be kept taut. Elistair adopted 300 ft. protection zone when they demonstrated the traffic monitoring ability of their tethered model (Elistair, 2019). Where to locate the unit is also critical since it may require additional permissions from the owner of the location if it is not part of the right-of-way.

2.7. Market Analysis

This chapter presents a preliminary market analysis for drone operating and video analyzing vendors to be contracted for this research project. In general, the drone operating vendor will manage the flight and provide the live stream video for a predefined period of time at a predefined location. Video analyzing vendor, on the other hand, will use this live stream video as an input of their video image processing algorithm. The product of their analysis will be the

roadway user trajectories. This section of the report elaborates the performed preliminary market analysis separately for selecting the best providers.

2.7.1. Vendor 1: Drone Operator

Vendor 1 will be contracted to provide a live stream video through operating their own tethered drone and camera equipment. Therefore, a preliminary market analysis is conducted to determine the potential vendors among commercial drone service providers. Vendor 1 will be responsible for:

- Providing safe and legal flights with a tethered UAS for a minimum of 12 hours (given the day light availability, including both AM and PM peak hours as well as the mid-day off-peak hours).
- Providing a live stream video that can incorporate with the video processing algorithm.
- Safely storing the video considering the privacy and cybersecurity issues.

Through this preliminary market analysis, the research team has already contacted ten companies, which are known to be commercial drone-obtained service providers. Table 2-4 indicates these companies and the conversation history. The research team will continue meeting with these companies in Task 2 and Task 3 before the proposal and vendor selection process.

Table 2-4: Contacted drone service providers

| Companies | Inquiry Date | Response Date | Headquarters |
|-------------------------------|--------------|---------------|-------------------|
| ArchAerial | 12.04.2019 | | Houston, TX |
| Hoverfly | 12.04.2019 | | Orlando, FL |
| Drone Aviation Corp | 11.04.2019 | 11.15.2019 | Jacksonville, FL |
| South East Drone Technologies | 12.04.2019 | 12.04.2019 | Tallahassee, FL |
| Vedair Drone Services | 12.04.2019 | 12.04.2019 | Jacksonville, FL |
| Orlando Aerial Videos | 12.04.2019 | 12.04.2019 | Orlando, FL |
| CellAntenna Wireless | 12.04.2019 | | Coral Springs, FL |
| Dronegenuity | 12.04.2019 | | Hudson, MA |
| Flyworx | 12.04.2019 | | Atlanta, GA |
| Drone Base | 11.29.2019 | | Santa Monica, CA |
| Elistair | 10.20.2019 | 10.20.2019 | France |

2.7.2. Vendor 2: Video Analyzer

Vendor 2 will be contracted to extract real-time or near real-time roadway user trajectories. Thus, a preliminary market analysis is conducted to determine the potential vendors among the existing vision-based traffic data providers. Vendor 2 will be responsible for:

- Providing an algorithm that successfully analyzes the live stream video.

- Detection, classification and tracking of roadway users with reasonable accuracy (Such roadway users can be vehicles, pedestrians, motorcycles, bicycles, trucks and buses).
- Safely storing the video for visualization purposes considering the privacy and cybersecurity issues.

Based on this preliminary market analysis, the research team has already contacted seven different video analytics companies that have already served other traffic agencies by building custom video image processing algorithms. Table 2-5 indicates these companies and the conversation history. The research team will continue meeting with these companies in Task 2 and Task 3 before the proposal and vendor selection process.

Among these companies, DataFromSky, a Czech Republic-based traffic data provider, is one of the leaders in the vision-based traffic data extraction market. Once the user uploads the video into their cloud system, the system analyzes the video and sends back a log file that includes trajectories and user classification. The user can further analyze the trajectories in their license free “viewer” software without being connected to the internet. The Viewer software lets the user set different configuration such as entry and exit gates to extract more data. Viewer is also a great visualization tool that allows the user create speed heat maps or conflict projections. Trafficvision, on the other hand, promotes real-time incident alerts to traffic management centers by leveraging their static camera network. Their system can provide non-video traffic data within the detection level such as counting vehicles. Miovision is also a well-known traffic data provider that has been utilized many traffic agencies.

Table 2-5: Contacted vision-based traffic data collection companies

| Companies | Inquiry Date | Response Date | Web address |
|------------------------------------|---------------------|----------------------|-----------------------------------------------------------------------------------------------|
| DataFromSky | 10.22.2019 | 10.24.2019 | https://datafromsky.com/ |
| Miovision | 12.04.2019 | 12.05.2019 | https://miovision.com/ |
| CountingCars | 11.04.2019 | 11.15.2019 | https://www.countingcars.com/ |
| IntuVision | 12.04.2019 | 12.06.2019 | https://www.intuvisiontech.com/#traffic |
| Tri-State Traffic (TST) | 12.04.2019 | | http://www.tstdata.com/index.html |
| TrafficVision | 12.04.2019 | | http://www.trafficvision.com/ |
| Goodvision | 12.05.2019 | 12.05.2019 | https://goodvisionlive.com/ |
| Transoft | 12.05.2019 | | https://www.transoftsolutions.com/ |
| Traffic Data Inc (Spack Solutions) | 12.04.2019 | | http://trafficdatainc.com/ |

2.8. Conclusions

The following conclusions are made as a result of Task 1:

- A thorough review of the literature and practice indicates that tUASs are promising tools for automated traffic data extraction at intersections. To the authors' knowledge, there are no studies that have utilized tUASs for long-duration data collection and real-time analysis for traffic operations and safety purposes.
- tUAS-obtained traffic data can be used for variety of purposes in order to improve traffic performance or safety at intersections.
- Using the findings of this study, MUTS can be updated as explained in Section 5. Particularly, the methods sections regarding the turning movement counts and pedestrian movement counts can be updated with the proposed UAS-based data collection. Also, MUTS gap studies chapter (Chapter 8) do not cover critical gaps on roundabouts. Drones may be used to collect data on roundabouts and MUTS can have a new chapter for roundabouts.
- Other intersections such as RCUTs and Michigan U-turns can also be studied with tethered drones with the large field of view provided.
- Based on the needs of FDOT, a web-based data sharing platform such as the one created by Montana DOT, can be developed (Montana DOT, 2018). They do not have tethered drones, and their video image processing is limited to flight endurance.
- There is keen interest for utilizing UAS in a variety of purposes from state governments. UAS Integration Pilot Program is the best example since it brings state DOTs, investment authorities, other government agencies, cities, and universities all together with the order from the president.
- Traffic agencies also have been utilizing this technology in many aspects such as bridge inspection, precise agriculture, pavement checking, and highlighting potholes to name a few.
- Aerial vision-based traffic monitoring is currently emerging rapidly compared to utilizing drones for other aforementioned services such as bridge inspections.
- Computer vision is currently in its golden era. People trust this technology to secure their privacy like in the case of those new generation iPhones.
- UAS-based traffic monitoring has a high potential to provide extensive data that can be used on operations as well as the safety aspects of transportation.
- Flight endurance issue of UAS has already been tackled with tethered drone cables that significantly decrease the mobility of the drone; however, it provides stability. For traffic monitoring, stability is more valuable since the video is captured with a large field of view.
- FHWA have different grant programs for state DOTs to support UAS utilizations by state DOTs. New Jersey have started their UAS initiative through this grant from FHWA (FHWA, 2018).
- Drones have been used on intersections for safety purposes and provided very valuable information in (Papadoulis et al., 2019). Aerial videos enabled researchers to find conflict analysis between pedestrian and vehicles. Although they did not collect the video with tethered drones, this work is a pioneer on UAS utilization for safety.

- Another study collected a detailed intersection operation study with UAS-collected videos (Khan, Ectors, Bellemans, Janssens, et al., 2018). Based on this study, researchers have found the queue dissipation time, accumulation and dissipation shock wave speeds, density, flow, and speed, and their pairwise relationship as fundamental diagrams.
- Findings indicate that UASs are promising solutions to obtain data accurately and in a non-intrusive manner.

3. TASK 2: ROADWAY GEOMETRIC DATA EXTRACTION FROM VERY HIGH-RESOLUTION AERIAL IMAGES

3.1. Task Description

Following the proposed execution plan and projected data pool creation, an additional and more urgent task identified was to extract the roadway geometric and spatial data from aerial images, which led to Task 2 of this project. Initially, as shown Figure 3-1, projected roadway geometry data were similar to the data requirements of MUTS and Highway Safety Manual (AASHTO, 2010). However, these geometric data for a single intersection could be easily collected from online visualization sources (i.e., Google Maps). As such, the main objective of this task was to create a statewide crosswalk map especially due to the fact that pedestrian safety concerns have been arising in the state and nation. In addition, this task explores the capabilities of computer vision techniques to extract statewide roadway geometry data from high-resolution aerial images.

In this task, an automated crosswalk detection and mapping model was developed and three case studies were conducted in order to evaluate the efficacy of the developed model. Also, variety of data including shape files, preprocessed images, csv files with coordinates were provided along with this task deliverable.

Figure 3-1: Initial projection for geometric data for single intersections

3.1.1. Why Crosswalks?

The number of pedestrian fatalities in the U.S. increased by 53% from 2009 to 2018 (i.e., from 4,109 deaths in 2009 to 6,283 deaths in 2018) (Retting & GHSA, 2020). This increase was quite sharp as the increase was only 35% from 2008 to 2017 (Retting & GHSA, 2019). The annual number of pedestrian fatalities in the U.S. between 1988 and 2019 are illustrated in Figure 3-2a. Note that number of pedestrian fatalities in 2019 (6,590*) was projected from the preliminary data and historical trends. However, actual numbers from 2018 clearly shows the highest pedestrian fatalities since 1990, accounting for 17% of all the traffic deaths, which was

the highest since 1982 (Retting & GHSA, 2020). When it is compared with the 2% increase on all other type of fatal crashes (Figure 3-2b), pedestrian safety seems to be extremely alarming in the U.S. and the State of Florida, which is among the five states with the highest pedestrian fatalities (Figure 3-2c).

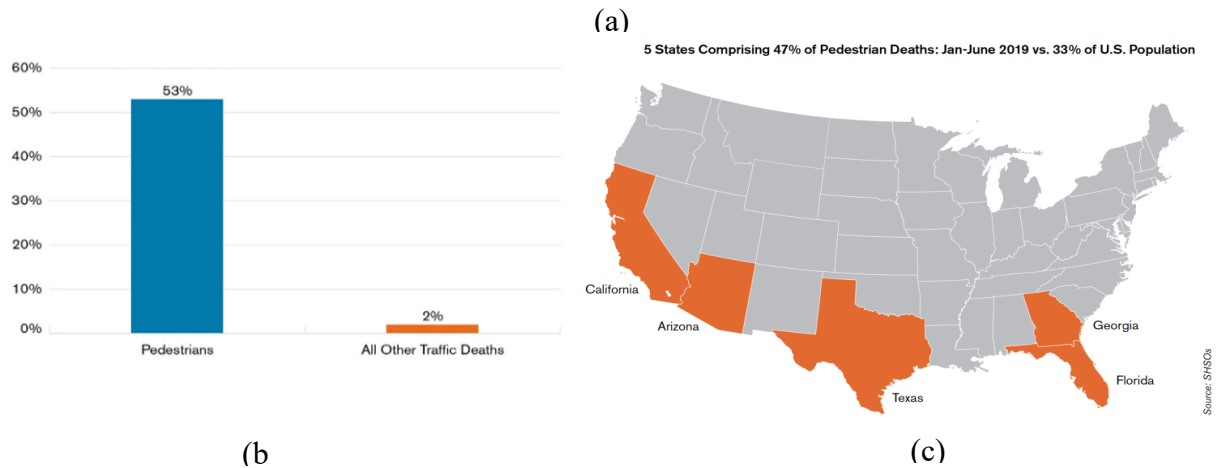


Figure 3-2: (a) U.S. pedestrian fatalities: 1988-2019, (b) percentage increase in number of pedestrian and all other types of fatalities from 2009 to 2018, and (c) the states where most of the pedestrian fatalities occurred in the first half of 2019 (Retting & GHSA, 2020)

In order to help address this national safety problem, FHWA has enacted Every Day Counts (EDC) initiative on Safe Transportation for Every Pedestrian (STEP) (FHWA, 2020a). Within this initiative, it was observed that 72% of pedestrian fatalities occurred away from intersections (i.e., midblock crosswalks) and approximately 26% occurred at intersection crosswalks where motor vehicles were given more priorities compared to pedestrians. Therefore, seven pedestrian safety countermeasures, so-called “spectacular seven”, were developed to guide state DOTs and other transportation agencies to improve safety on the crosswalks where this national safety issue predominantly occurs (FHWA, 2020c). FHWA’s YouTube channel has provided a playlist to explain the working principles of each countermeasure with short clips (FHWA, 2020b). Basically, these seven countermeasures are:

- Rectangular Rapid Flashing Beacons (RRFB): Flashing LED lights that can be actuated by the users or with automated detection on midblock or uncontrolled crosswalks.
- Leading Pedestrian Intervals (LPIs): Reduces pedestrian vehicle conflicts and increase yielding on signalized intersections allowing pedestrians walk 3-4 s before vehicles.
- Crosswalk Visibility Enhancements: Enhancing signage, lighting, and markings helps drivers to detect pedestrians.
- Raised Crosswalks: Reduces vehicle speed, increase visibility and calms traffic.
- Pedestrian Crossing/Refuge Island: Provides a safer place to stop at the median, especially useful for pedestrians with limited mobility.
- Pedestrian Hybrid Beacons (PHBs): As an intermediate option between a full pedestrian signal and a flashing beacon, PHBs are useful for multilane roads with high speed and volume.
- Road Diets: Decreasing number of driving lanes, road diets can reduce vehicle speed and create space for refuge islands and bike lanes.

Initial studies on these countermeasures indicated tremendous safety benefits as shown in Figure 3-3 with the potential reduction on pedestrian crashes (FHWA, 2020c).

Potential Reduction in Pedestrian Crashes

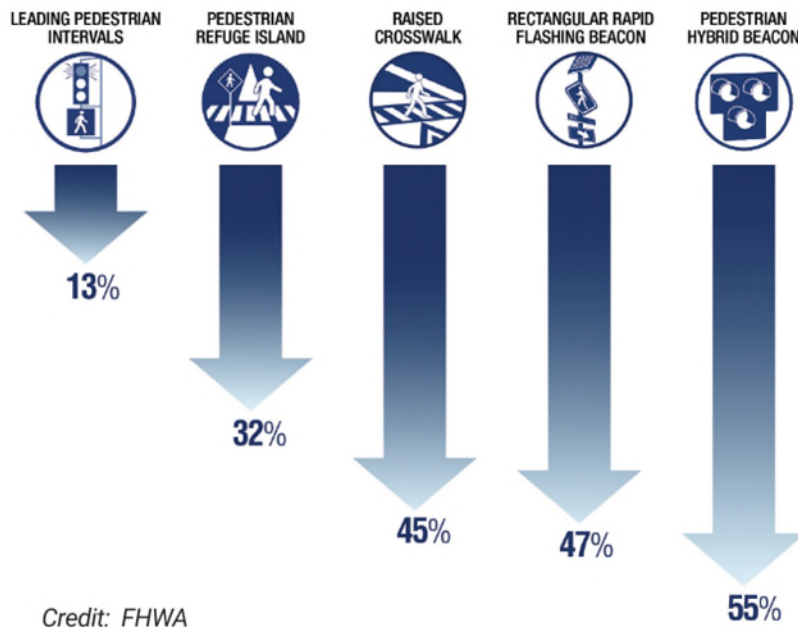


Figure 3-3: Safety benefits of proposed countermeasures (FHWA, 2020c)

Furthermore, FHWA provides guidelines for the agencies to describe a comprehensive decision-making process for the installation of pedestrian crossing countermeasures (Blackburn

et al., 2017). In this guide, FHWA leads the agency to follow a 6-step process as shown in Figure 3-4.

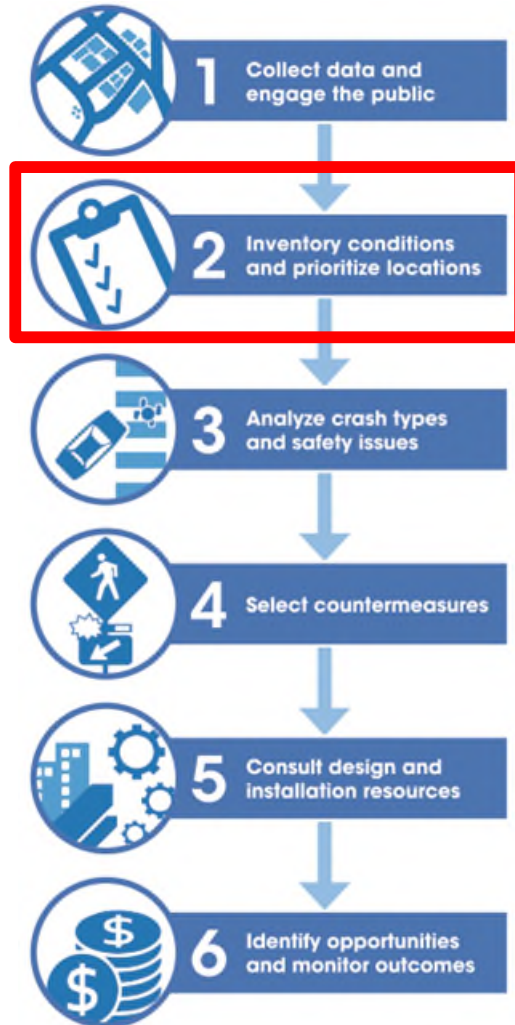


Figure 3-4: Process diagram for installation of pedestrian crossing countermeasures (Blackburn et al., 2017)

Task 2 of this project focuses on the second step of FHWA’s guidelines where a crosswalk inventory list is requested with a detailed categorization focusing on the midblock and signalized intersection crosswalks. As aforementioned, Florida is among the five pedestrian crash prone states in the U.S. where higher number of pedestrian fatalities were observed compared to other states Therefore, following these guidelines and creating such a crosswalk inventory list is essential for FDOT.

Since this project heavily involves computer vision techniques in conjunction with drones and the roadway geometry data is a part of the projected traffic data to be extracted, Task 2 is devoted to (a) create a statewide crosswalk map from aerial high-resolution images, and (b) evaluate the capabilities of computer vision techniques for roadway feature extraction purposes.

3.2. Background on Roadway Feature Extraction from Imagery

Rapid advancement on computer vision technology enables traffic agencies to save money and time in various aspects of data collection. In the past, image processing has been considered a time-consuming and error-prone approach for road inventory recording. Recent significant improvements on computational power and image pattern recognition algorithms have created new opportunities to detect and map roadway features from imagery data. For example, a study (Wu & Tsai, 2006) used selected image frames from a video recorded by the camera mounted on a vehicle (street view) to update 118,000 mile centerlines of road inventory data for Georgia DOT. They successfully performed this task in days, which could have taken years with manual desktop observations. Another study (Jalayer et al., 2015) evaluated the remote sensing technologies for the extraction of roadway geometry data required for Highway Safety Manual (AASHTO, 2010) implementations. The projected geometry data set in this project (Figure 3-1) also stemmed from the Highway Safety Manual. They provided a simple categorization of the roadway inventory collection methods (illustrated in Figure 3-5). More importantly, a satisfaction survey among the state DOTs from the same study indicated that the collection of geometry data with aerial and satellite images happened to be more satisfactory than field observations in terms of equipment cost, data accuracy, crew safety, data collection cost and data collection time. On the other hand, field observations were found to be more satisfactory in terms of data completeness and data reduction time. However, it is highly possible that these results have changed in the last six years with the advancement on the computing power and the processing methods of imagery data.

Figure 3-5: Categorization of roadway inventory data collection (Jalayer et al., 2015)

In this study, existing literature on roadway geometry data extraction using computer vision techniques were categorized based on the imagery data source and extracted data type. Table 3-1 indicates the categorized studies found in the literature. Note that there are several other roadway geometry data types (e.g., slope, trees, and traffic sign/control devices) that should be included for a full inventory list. However, those data types are outside the scope of this study.

Table 3-1: Categorization of related literature on roadway geometry extraction using imagery

| Extracted Data | Imagery Data Source | | | |
|----------------------------------|--------------------------------------------------------------------------------------------------------------------------------------|----------------------------------------------------------------------------------------------------------------------------------------------------------------------------------------|---------------------------------------------------------------------------------|------------------------------------------------------------------------------------------------------------------------------------------------------------------------------------|
| | Satellite | Aerial | LIDAR | Street View |
| Roadway Extraction | <ul style="list-style-type: none"> • (K. Sun et al., 2019) • (Ye et al., 2017) • (Dai et al., 2019) | | | |
| Lane Marking Segmentation | <ul style="list-style-type: none"> • (Zang et al., 2017) | <ul style="list-style-type: none"> • (Fischer et al., 2018) • (Azimi et al., 2019) • (L. Tang et al., 2014) | | <ul style="list-style-type: none"> • (Wu & Tsai, 2006) |
| Intersection Detection | <ul style="list-style-type: none"> • (Dai et al., 2020) | | | <ul style="list-style-type: none"> • (Tümen & Ergen, 2020) |
| Crosswalk Detection | | <ul style="list-style-type: none"> • (Koester et al., 2016) • (Berriel, Lopes, et al., 2017) • (Kurath et al., 2017) • (Y. Sun et al., 2016) | <ul style="list-style-type: none"> • (Liang & Urtasun, 2018) | <ul style="list-style-type: none"> • (Haider et al., 2019) • (Z. S. Chen & Zhang, 2018) • (Fan et al., 2020) • (X. Liu et al., 2017) |

The roadway extraction method involves the semantic segmentation of the entire roadway segment, where the pixels that fell onto roadways are classified and visualized with the value of 1 (white) and all other pixels are classified and visualized with the value of 0 (black). Using multispectral images (near-infrared or more bands additional to the RGB bands) helped increase the accuracy and disregard the vegetation around roadways (Ye et al., 2017) although panchromatic (single band, black and white) satellite images have also been used on roadway extraction and intersection detection (K. Sun et al., 2019). Regardless of the number of bands, satellite-based road geometry data collection requires very high-resolution images (<1 m/pixel), which cannot be acquired freely. GeoEye-1 (0.41 m/pixel), GF2 (0.8 m/pixel), IKONOS (1 m/pixel), QuickBird (0.61 m/pixel) SV-1 (0.5 m/pixel), Pleiades (0.5 m/pixel) and WorldView-1

(0.46 m/pixel) are some commercial satellites commonly used for roadway geometry extraction purposes in varying studies such as (Dai et al., 2019, 2020; K. Sun et al., 2019).

Lane marking segmentation works similarly to the roadway extraction; however, in this case, not the entire roadway but only the pixels that fall onto the lane markings are classified as 1 and others, including the roadway pavement, are classified as 0. This method is commonly used to generate high definition (HD) maps where all roadway features including dashed lines and turning arrow pavement markings are extracted from imagery into the map format (Fischer et al., 2018). Additionally, aerial images from FDOT (FDOT Surveying and Mapping Office, 2020) were used to extract the number of lanes in six different street segments in Miami (L. Tang et al., 2014). Lane marking segmentation has also been used as the starting point for some crosswalk detection studies (Z. S. Chen & Zhang, 2018). Although it is commonly performed to analyze the street view for these purposes, lane marking segmentation is also crucial for several advanced driver assistance systems (ADAS) such as lane keeping assistance, lane advisory, and even for the automated driving (Azimi et al., 2019; Fischer et al., 2018) as well as for the safety of people with vision limitations. Some roadway geometric data can be extracted with lane marking segmentation; however, the inference of vehicles and occlusion by trees and shadows significantly affect the accuracy, and thus, lane marking segmentation requires very high-resolution images.

Intersection detection has been performed on extracted roadways with ball-shaped detections (Dai et al., 2020) and vanishing point identification (Tümen & Ergen, 2020). Vanishing point is commonly used on street level studies, and it refers to the point where the roadway and all line features along the roadway become a point on the horizon line. Crosswalk detection studies have also used vanishing point at the street level analysis, even for multiple crosswalk detections in the single frame (Fan et al., 2020). On the other hand, OpenStreetMap (OSM) crosswalk data have been commonly used for developing crosswalk detection models and testing them (Berriel, Lopes, et al., 2017). Moreover, Kurath et al. (2017) developed a model to automatically detect crosswalks and update the OSM database if the detected crosswalks were not already available in the system. OSM is a very good, if incomplete, free data source for geocoded data.

On the other hand, reconstruction and full boundary drawing of the crosswalks have been performed by using multiple sensor technologies such as LIDAR and aerial imagery in Liang & Urtasun (2018). Drawing the entire crosswalk is important specifically for people with vision limitations (Haider et al., 2019; Y. Sun et al., 2016). Additionally, the performance of the crosswalk detection models has been tested on the crosswalks with different lighting and pavement conditions by (Z. S. Chen & Zhang, 2018). Although the sample size was very limited (50), no impact was found due to the lighting conditions (100% detection of 40); however, obscuration (80% of 10) and peeled-off markings (0% of 2) have significantly affected the performance. Also, a crosswalk detection model was used for defilement and impairment analysis as crosswalk pavement markings are prone to be peeled off by the continuous traffic (X. Liu et al., 2017). They used street view images to classify seriously impaired or partially impaired crosswalks and clear crosswalks, reaching an average of 87.7% and 85% precision, respectively.

Despite the variation and high accuracy achieved in the presented crosswalk detection studies, a large-scale analysis to develop a statewide crosswalk inventory is still missing in the

literature. Most of the studies tested their model in a single aerial image with less than 100 crosswalks. This study, with the objective of generating a crosswalk inventory list for the entire state of Florida, is one of a kind to the best of authors' knowledge. Additionally, most of the cited studies have only performed detection of the crosswalks from the specified imagery source; however, maps of detected crosswalks have been the data formats required for the extracted roadway geometry data to be archived and used again for different purposes such as pedestrian safety analysis. Finally, several studies were able to detect only zebra crosswalks (Berriel, Lopes, et al., 2017; Z. S. Chen & Zhang, 2018; Koester et al., 2016). However, crosswalk markings vary in Florida. All in all, the developed model should perform not only detection but also mapping of the crosswalks for the entire state while identifying both zebra and non-zebra crosswalks.

3.3. Automated Crosswalk Detection and Mapping

3.3.1. Data Description

3.3.1.1. *Image Data*

Florida Department of Transportation (FDOT) Surveying and Mapping Office maintains an aerial photography archive. These georeferenced images of all 67 counties of the State of Florida are stored for multiple years and well-indexed with the file names consisting of three letter county code, the year recorded and the tile number. FDOT provides public access to this archive through the Aerial Photography Look-Up System (APLUS) (FDOT Surveying and Mapping Office, 2020). In this platform, a limited number of images can be downloaded online, whereas large datasets, covering an entire county or even the state, can only be acquired by request followed by mailing or providing an external driver with adequate available storage space.

For this study, the most recent images (as of December 2019) were extracted for every county of Florida, with a total size of 1.2 TB. Note that these images are considered to have very high-resolution. Although the exact resolution varies depending on the county, most of the images are in the 0.5 ft./pixel (~0.15 m/pixel) resolution with a size of 10,000 x 10,000, and 3-band (RGB) image format. Also, the images are available in MrSID format where it can be projected on a map using a Geographical Information Systems (GIS) software such as ArcGIS.

3.3.1.2. *Vector Data*

Florida Department of Transportation (FDOT) Transportation Data and Analytics Office provides a variety of GIS data. These data have been categorized into the four major classes: (a) designated roadway data, (b) roadway characteristics data, (c) traffic data, and (d) bicycle and pedestrian data. Each class has multiple shape files including but not limited to interstate centerlines, roadway surface widths, annual average daily traffic, separated bike lanes, number of through lanes, resting areas, signalized intersection points, truck traffic volumes, and weigh-in-motion locations. These rich datasets and their detailed descriptions (metadata) can be found in (FDOT Transportation Data and Analytics Office, 2020) where each shape file can be downloaded individually or as a bulk within a geodatabase file.

This study focused on the crosswalks located on the state highway system roadways (ON System Roads) as well as those located on the county- or city-controlled roadways (OFF System Roads). For this purpose, interstates were excluded from the ON System Roads shapefile and OFF System Roads shapefile was merged to combine all centerlines. In addition, signalized intersection points were used to categorize the detected crosswalks. Note that the GIS data

provided by (FDOT Transportation Data and Analytics Office, 2020) can help obtain several geometric data required for the mobility and safety performance evaluations except the crosswalk locations. As aforementioned, the major purpose of this study is to develop a statewide crosswalk inventory that also includes a categorization of midblock and signalized intersections for FDOT.

3.3.1.3. *OpenStreetMap (OSM) Data*

OpenStreetMap (OSM) is a well-known, crowd-sourced, and free digital map database of the entire world (OpenStreetMap, 2020a). All types of vector data, including but not limited to roadway centerlines, building footprints, grocery store locations, bike lanes, restaurants, signalized or stop sign-controlled roadway intersections, city or county borderlines with demographics, and many others can be acquired with their associated key and tag pairs and imported into a GIS software. In this study, the key and tag pair “highway=footway” was used to extract the sidewalk line features and “highway=crossing” to extract the crosswalk point features from the OSM database for the entire state. This has been performed by using an out-of-the-bag toolbox named Get OSM Data from (Klinger, 2020) in ArcGIS Pro. Note that the OSM platform is not a completed data source as it works based on volunteering. Therefore, the sidewalks and the crosswalks that have already been uploaded by the OSM users were only extracted and used for validation of our crosswalk detection model in the Case Study III given below. On the other hand, the completeness of the OSM data set was tested with manually labeled complete data set of Leon County ON System Roads crosswalks in the Case Study I.

OSM was developed in London, UK back in early 2000s. Although this platform has initially gained popularity in places where governments do not provide free spatial data, the platform has grown rapidly with bulk uploads of publicly available data sources such as TIGER lines in the U.S. Today, there are more than 6M users that actively update and edit geocoded data in this platform (OpenStreetMap, 2020c). Generally, OSM works in style that is very similar to the Wikipedia in which the users upload and edit the geospatial data, which is often called Volunteering Geographic Information (VGI) (Quinn & Dutton, 2020). These volunteering efforts constitute a social event known as “mapping parties” where a group of people gather and walk, bike, or drive through with GPS devices. Later, these recorded GPS tracts are uploaded to a central lab where data are entered with associated tags. The mapping party events around the world are quite often as announced in the main page of the OSM platform (OpenStreetMap, 2020a). Although uploading GPS tracks is still useful, many OSM users enter the data by tracing aerial images or through the Overpass API nowadays (Application Programming Interface) (OpenStreetMap, 2020b).

Although it is not complete and categorized, it is important to note that crosswalk locations around the world are available in OSM and have been used in many studies for developing and testing a crosswalk detection model (Berriel, Lopes, et al., 2017; Berriel, Rossi, et al., 2017; Kurath et al., 2017). Furthermore, the purpose of providing free map data based on OSM is also acknowledged by the U.S. DOT agencies; thus, it is highly recommended to initiate an OSM study for analyzing the further benefits.

3.3.2. Pre-processing

Preprocessing is a required step due to the size of the data and the complexity of the object detection process. Broadly, our approach selects and excludes the images that does not intersect with a roadway centerline and then masks out the pixels that are not covered by a buffer

zone around the roadway centerlines. In this way, the number of images was reduced from ~90K to ~30K and the features outside the area of interest (100 ft. around ON- and OFF-System Roads) were ignored by the model.

Details of the preprocessing approach are visualized in Figure 3-6. Initially, all images from all counties (approximately ~90K) were imported into a mosaic dataset within the ArcGIS Pro software. Mosaic datasets were used to manage and display multiple geocoded images (ESRI, 2020). Also, mosaic datasets allow one to make location-based image tile selections with intersections of other geocoded vector data. For example, individual images, that include a part of roadway centerline, were selected, and extracted to create a subset collection of the images (approximately ~30K). Furthermore, the model-builder interface of ArcGIS Pro was employed to develop an automated image masking tool. As indicated in Figure 3-7, the tool iterates through the images in a folder, masks each image based on the 100-ft buffer around the roadway centerlines, and converts masked images into JPG format for the object detection algorithm.

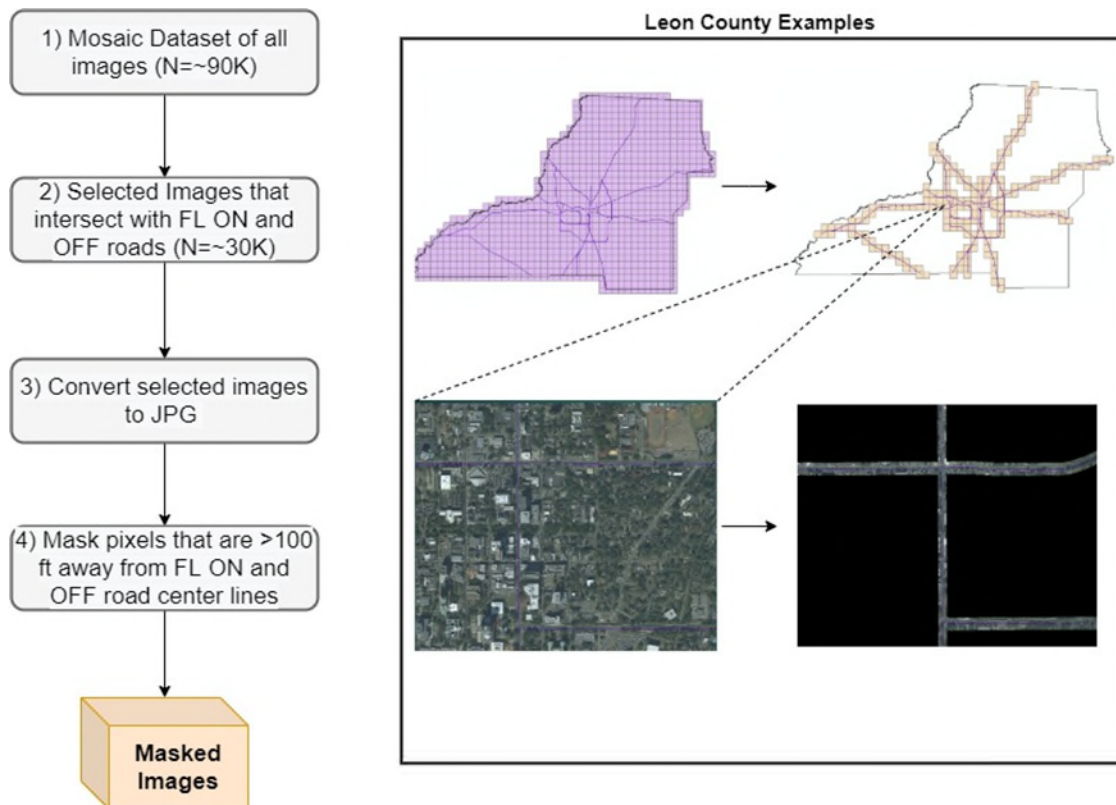


Figure 3-6: Preprocessing approach

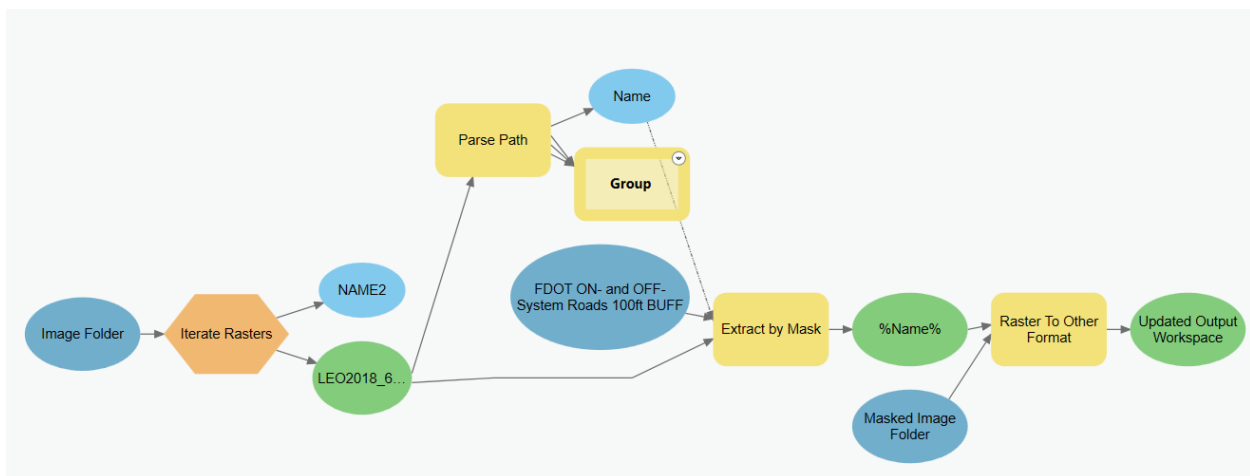


Figure 3-7: Automated image masking model used in the fourth step of preprocessing

Finally, a metadata table was generated to indicate the exact coordinates of each image. Note that object detection algorithms can only identify which pixels in the given image cover the object (e.g., a crosswalk in this study). Therefore, exact location of each pixel of masked images must be known to be able to map the detected crosswalks. Fortunately, the aerial images in the APLUS Archive are well indexed by their name and precisely projected in the State Plan Coordinate System (SPCS), which converts the angular-based coordinate system (Latitude and Longitude) to a Cartesian system with the linear unit of U.S. Surveying feet. In Florida, 67 counties are categorized into 3 different SPCS zones (SPCF83_903 N_FL, SPCF83_902 W_FL, SPCF83_901 E_FL) as shown in Figure 3-8. Although the resolution and size of the images vary within some counties (i.e., Miami-Dade), the exact corner locations of each image can be extracted in feet once the images are displayed in a mosaic dataset within their associated SPCF zone. Eventually, a metadata table was generated with the original name of the images, their SPCF zone, and the corner coordinates within the associated SPCS. By reading this table and using the size information, object detection model rescales the image if necessary and calculates the coordinates of the detected crosswalks instantly.

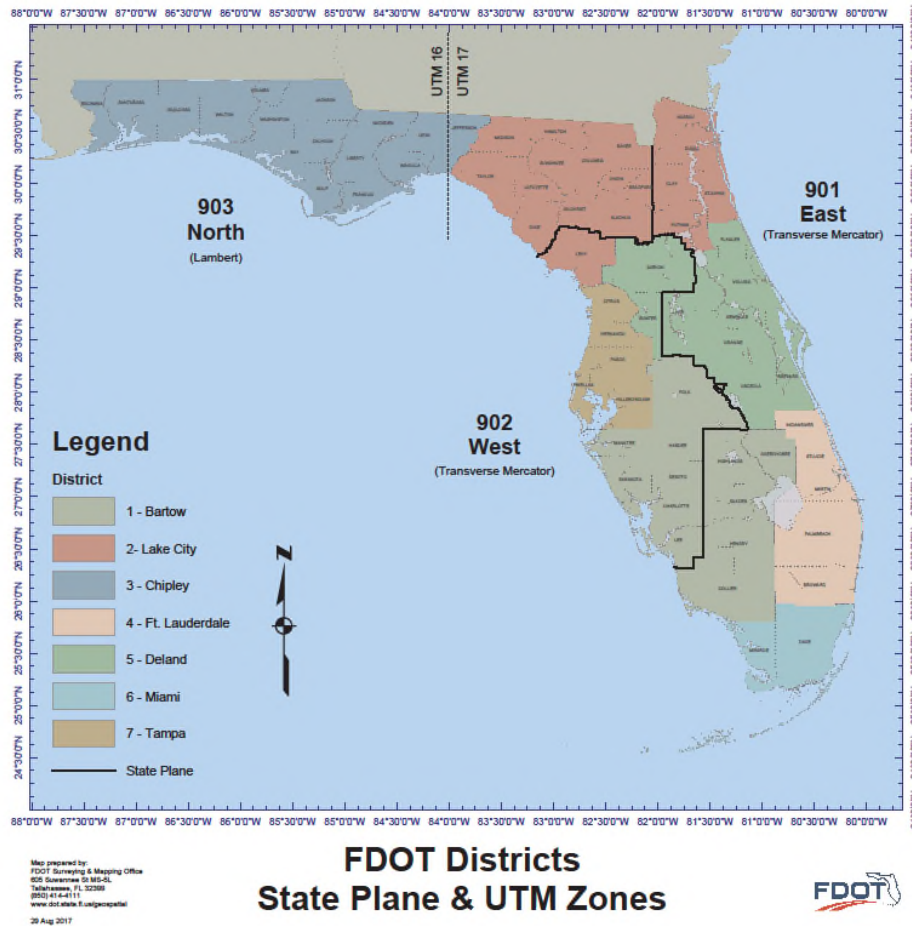


Figure 3-8: State plane coordinate system (SPCS) zones in Florida. Source: (FDOT, 2017)

3.3.3. YOLOv2 Crosswalks Detection Model

You Only Look Once (YOLO) is a neural network model mostly used for real-time object detection purposes. The main advantage of YOLO compared to other object detection models like Region-based Convolutional Neural Network (R-CNN) or Faster R-CNN is its speed. That is, YOLO is 1000x and 100x faster than both R-CNN and Faster R-CNN architectures, respectively (Redmon, 2020). This is mainly because the other object detection models run hundreds of network evaluations on a single image. They also work as classifiers of the candidate regions and detect the object(s) based on the classification probability of those regions. The YOLO model, on the other hand, can search for the entire image with a single network evaluation and make predictions informed by the global context of the image. YOLO object detection algorithm was first published in 2016 (Redmon et al., 2016), the speed and accuracy was enhanced in the second version (YOLOv2) (Redmon & Farhadi, 2016), and the multi-scale predictions was improved in the third version (YOLOv3) (Redmon & Farhadi, 2018). Recently, YOLOv4 (Bochkovskiy et al., 2020) and YOLOv5 (Jocher, 2020) was published. Since there is not a scale problem present in our dataset and due to its ease of applicability with the available sources, YOLOv2 was employed in this study.

3.3.3.1. *Crosswalk Detector*

The model was trained using manually labeled 4,658 ON and OFF-road crosswalks in MATLAB v. 2020a, which was supported with Deep-Learning Toolbox and GPU enhancements when the hardware was available. The locations of training crosswalks were mined from the OpenStreetMap crosswalk data set and labeled with manually drawn bounding boxes on the masked images by using the Image Labeler interface of MATLAB. Although most of the training data consisted of the crosswalks from Alachua (1,360), Duval (756), and Miami-Dade (669) counties, crosswalks from 28 counties were included. For a fair performance evaluation in the case studies, Leon, Orange, and Sumter County crosswalks were not included in the training data set. In this way, a county from each SPCS zone was included in the case studies with moderate, high, and low population densities, respectively.

This crosswalk detection network model was trained using 25 anchor boxes and ADAM optimizer (Kingma & Ba, 2014), which is commonly used in training deep learning algorithms to optimize the learning rate. The number of anchor boxes was automatically calculated with the k-means algorithm from the training data to represent the prior knowledge on the target bounding boxes. Additionally, 30 epochs and 128 batch sizes were adopted on the training with the L2 Regularization value of 0.0004.

The performance of the detection model was evaluated with a 15% split of the test dataset. That is, a randomly chosen set of 698 crosswalks was not used in the training but utilized in order to test the accuracy of the model. A default 50% overlap between the label and the detection bounding boxes was accepted as a true prediction. Subsequently, precision was calculated as the true prediction rate among all the predictions and recall was calculated as the true prediction rate among the original labels. Figure 3-9 indicates the precision-recall curve, which is a commonly used measure of success for classifiers. The area under this curve was calculated as the average precision and it spans between 0 and 1. The value 1 indicates a perfect classifier with 100% match. Based on the resulting value of 0.95, we can conclude that the developed detector is performing quite well.

Figure 3-9: Developed YOLOv2 crosswalk detector accuracy

3.3.3.2. *Mapping Crosswalks*

The crosswalk detector was first applied on single images. As shown in Figure 3-10, the detector successfully draws bounding boxes around crosswalks with the confidence score of the detection. To prevent false positives, the default value of minimum 0.5 confidence score was adopted as the threshold and more than 20% overlapping between two bounding boxes was prevented to avoid multiple detections.

The detector was trained with 1,000 x 1,000 sub-images with a 0.5 ft. pixel resolution. Therefore, the detection was performed sliding this sub-image window with a step size of 900 pixels on original images (10,000 x 10,000). If the given image had different size or resolution, it was rescaled and parsed with black pixels to have similar properties. With the sliding window, an overlap of 100 pixels was provided for each sub image on X and Y axis which helps detect crosswalks on the edges. However, the main reason for the sub image is to skip non-roadway areas in the full-size image. If the sub-image consisted mostly of black or white pixels, that sub-image was ignored by the detector as it refers to a region outside 100 ft. surrounding the roadway centerlines (i.e., masked out area in the preprocessing). Also, using large images is not practical in object detection algorithms as the computation cost increases exponentially.

Since the detector performed quite well on single images, the mapping process was performed at the county level. This process is summarized in Figure 3-11. First, based on the image names matching with the user input of 3-letter county code, the images in the masked images folder were selected and iterated to the detector. Then, the spatial information of the image was extracted from the metadata table in order to calculate the coordinates of the bounding boxes in that image. Once all images were passed to the detector, an output file was generated including all the crosswalks coordinates in that county. Additionally, confidence

scores, and the image names on which the crosswalk were detected are included in the output file. This file was used as an XY table to map crosswalks.










| Image Name | Examples of crosswalk detection from single images | | |
|----------------|-------------------------------------------------------------------------------------------------------------------------------------|--------------------------------------------------------------------------------------------------------------------------------------|---------------------------------------------------------------------------------------------------------------------------------------|
| LEO2018_649377 |  <p>LEO2018_649377_PG.jpg Part 6-7 (row-col)</p> |  <p>LEO2018_649377_PG.jpg Part 2-7 (row-col)</p> |  <p>LEO2018_649377_PG.jpg Part 7-10 (row-col)</p> |
| ORA2019_258372 |  <p>ORA2019_258372_PG.jpg Part 5-2 (row-col)</p> |  <p>ORA2019_258372_PG.jpg Part 5-8 (row-col)</p> |  <p>ORA2019_258372_PG.jpg Part 5-8 (row-col)</p> |
| SUM2017_451133 |  <p>SUM2017_451133_PG.jpg Part 5-5 (row-col)</p> |  <p>SUM2017_451133_PG.jpg Part 9-7 (row-col)</p> |  <p>SUM2017_451133_PG.jpg Part 6-1 (row-col)</p> |

Figure 3-10: Crosswalk detection with bounding boxes and confidence scores on single images from Leon, Orange, and Sumter counties

Figure 3-11: Crosswalk detection and mapping at the county level

3.3.4. Post-processing

Post-processing step cleans the duplicate detections due to the overlapping distance on sliding windows. Additionally, it separates ON road and OFF road crosswalks. No further categorization was performed on the OFF road crosswalks; however, ON roads detections were used for performance evaluation and further categorization in order to have a complete list that can serve as the statewide crosswalk inventory list.

Cleaning the duplicate points was performed by integrating the detection points, which were less than 5 ft. from each other. Then, X and Y coordinates were calculated and added to the attribute table. Finally, the records with duplicating X and Y coordinate fields were cleaned. This process used a 5-ft minimum distance between each crosswalk and all performance evaluations and further categorizations were performed following this rule.

3.4. Case Studies and Results

3.4.1. Case Study I: Overall Performance Evaluation Using the Ground Truth Data

3.4.1.1. *Experimental Design*

The first case study evaluated the performance of the model with a focus on both correctness and completeness and compared the findings with OpenStreetMap (OSM) data. For a proof of concept, a complete, manually placed Ground Truth (GT) dataset was generated in Leon County ON System Roads. A total of 1,272 GT points was placed on each visible crosswalk by using the masked images as the background. Figure 3-12 illustrates the GT dataset and OSM crosswalks in the study area. Note that OSM dataset missed all the crosswalks on the West Pensacola St. illustrated in Figure 3-12c and yet included crosswalks without visible pavement marking as illustrated in Figure 3-12b. This is mainly because some of the line features are missed as OSM crosswalks are mostly located at the intersection of roadway line features and footway line features. Including a broader dataset and missing all the crosswalks in a location can be considered as the tradeoffs of the Volunteered Geographic Information (VGI) concept.

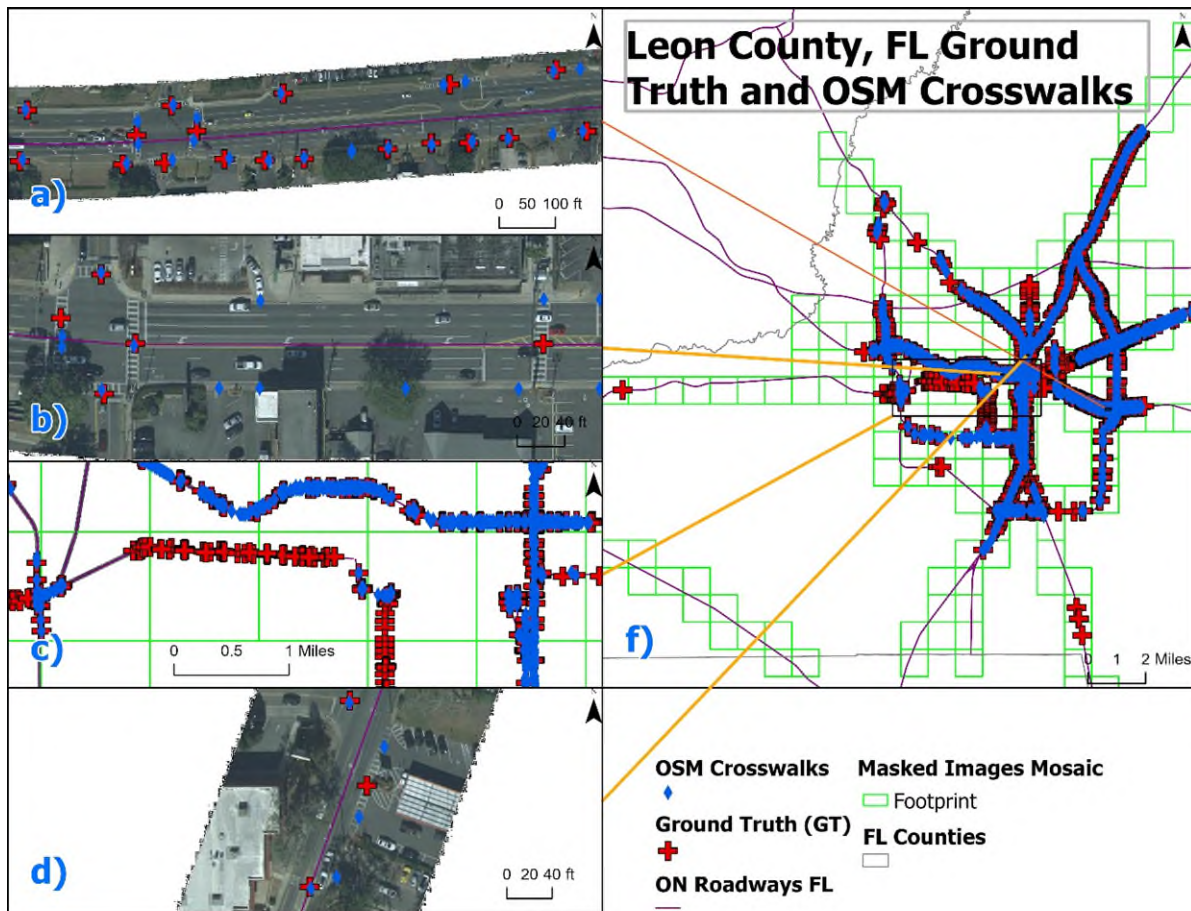


Figure 3-12: Manually labeled ground truth crosswalks (GT) and OSM crosswalks in the study area

As aforementioned, the proposed model has detected ON and OFF-road crosswalks in Florida with a minimum of 0.4 confidence score and these were mapped as points. For this case study, the model detected crosswalks (M) within the Leon County on ON Roads, which were extracted. A similar location-based selection approach was applied on the OSM crosswalks. Since the GT, M, and OSM are all points, the performance of the proposed model was evaluated by checking the 30 ft. surrounding of those points (i.e., detection proximity). In order to determine the 30 ft. radius for the detection proximity and the 0.4 confidence threshold for M crosswalks, sensitivity analyses were conducted with different values, but the results are not presented in this report to focus on the actual findings.

Completeness (precision), correctness (recall), and quality (Intersection Over Union) were used to evaluate the performance of proposed model. These metrics are commonly used for performance evaluation of the similar models (Dai et al., 2020; K. Sun et al., 2019) since they were first used in (Wiedemann et al., 1998) and (Wiedemann & Ebner, 2000) for roadway extraction purposes. Details of these metrics are presented in Table 3-2. The following are determination rules required to calculate the performance evaluation metrics shown in Table 3-2.

- False Negative (FN): # of GT crosswalks with no M crosswalk in 30 ft. radius
- False Positive (FP): # of M crosswalks with no GT crosswalk in 30 ft. radius

- GT: Number of GT crosswalks
- M: Number of Model detected crosswalks

Table 3-2: Performance evaluation metrics

| Metric | Formula | Description |
|---------------------|-----------------------------------|----------------------------------------------------------------------------------------------------|
| Completeness | $\frac{GT - FN}{GT} * 100\%$ | True detection rate among GT crosswalks (recall) |
| Correctness | $\frac{M - FP}{M} * 100\%$ | True detection rate among M crosswalks (precision) |
| Quality | $\frac{GT - FN}{GT + FP} * 100\%$ | True detection among M crosswalks plus the undetected GT crosswalks (Intersection over Union: IoU) |

The main objective of this case study was to evaluate the quality of the predictions made by the proposed model and compare it with the OSM dataset, another available source for crosswalks. After examining both correctness (precision) and completeness (recall) performance of the model with a complete dataset, completeness performance can be evaluated on categorized crosswalks.

3.4.1.2. **Results**

Performance evaluation results are presented in Table 3-3 and several examples are illustrated in Figure 3-13. Overall results indicate that the model have successfully detected 85.9% of the GT crosswalks (Figure 3-13(a, b, c, and d)) whereas OSM data could only detect 77.8%. Figure 3-13(a) illustrates this where a GT was detected by the model but not included in the OSM dataset. On the contrary, most of the undetected crosswalks (FN), are included in the OSM data set as shown in Figure 3-13(f and g). In addition, it is proven that the proposed model can perform precise estimates as the correctness is 88.7%. This indicates that the model does not generate many false positives and GT crosswalks are eventually detected. Instead, FP is relatively low, and an example is depicted in Figure 3-13(e). However, the correctness is quite low for the OSM dataset. This is expected as it includes crosswalks that are not visible on the aerial images. Some of those crosswalks can be seen in Figure 3-13(b) where they are counted as FP for the OSM dataset.

Note that almost all the undetected crosswalks are covered in the OSM data set. For example, one of the undetected crosswalks in Figure 3-13(g) is a midblock crosswalk on the Thomasville Rd., Tallahassee and it is included in the OSM data set. The reason for the crosswalk is missed in the model could be the peeled off pavement markings and the reason for OSM covers this crosswalk is that the existing footway line and roadway centerline intersect somewhere on that crosswalk. This is a good example of the benefits of the Volunteered

Geographic Information (VGI). Some users upload the data into the system and some other users process that data and create new data, despite missing all of the crosswalks in certain locations.

Regardless, the developed model performs quite well, and it has high potential to not only create a state-wide crosswalk inventory but also to complete the OSM crosswalks in the future. In addition, the detection problems on peeled off crosswalks are commonly addressed challenges in the related literature. In this regard, crosswalks with a low detection confidence score or no detection can be utilized to determine the crosswalks that need visibility improvements and/or routine maintenance.

Note that the conceptualization of this performance evaluation allows multiple matches because some adjacent GT crosswalks were detected as a single M crosswalk, and vice versa. This can be seen in Figure 3-13(c and d). However, for the point detection performance evaluation, the GT crosswalk was still detected although there were multiple M crosswalks (max record is 3) in the 30 ft. vicinity, which clearly shows the sensitivity for detection assignment.

Table 3-3: Proposed model performance evaluation and comparison with OSM

| Ground Truth (GT) (n=1,272) | Model (M) (n=1,316) | OSM (n=2,312) |
|--------------------------------|------------------------|------------------|
| TP | 1,092 | 989 |
| FN | 180 | 283 |
| FP | 149 | 1,208 |
| Completeness | 85.9% | 77.8% |
| Correctness | 88.7% | 52.2% |
| Quality | 76.9% | 39.8% |

Figure 3-13: Automated crosswalk detection and mapping results. (a and b) true positive (TP) detection with 1:1 matching, (c and d) TP detection with 1: any matching, (e) false positive (FP) detection, (f) false negative (FN), undetected crosswalk, (g) detection problems due to peeled off markings and relatively long placement on Thomasville Rd., Tallahassee, FL.

Visual observations indicate that most of the missed crosswalks were on the side of the roadways. Also, the visual patterns on signalized intersection crosswalks appeared to be much more detectable than the crosswalks outside roadways. Therefore, categorizing GT crosswalks and checking the completeness of the proposed model can be a fairer performance evaluation.

3.4.2. Case Study II: Performance Evaluation with Categorized Crosswalks

3.4.2.1. *Experimental Design*

The purpose of this case study was to evaluate performance of the model against the crosswalks with different importance levels and marking patterns. To perform such an evaluation, the GT data used in the first case study were further classified into three different binary nodes (S, C, and Z) as illustrated in Figure 3-14 and Table 3-4. Additionally, this case

study also performed a sensitivity analysis on the final classification of the statewide crosswalk inventory.

Node (S) separates the signalized intersection crosswalks (S_1) and non-intersection crosswalks (S_0) as illustrated with square and circle shaped points in the Figure 3-14, respectively. 52% of the total crosswalks are signalized intersection crosswalks on Leon County ON System Roads. On the other hand, node (C) separates crosswalks where pedestrians cross an ON Road (C_1) and the crosswalks that are parallel to the ON Roads (C_0) as symbolized with red and blue colored points in the Figure 3-14, respectively. Only 27% of the total crosswalks are crossing (perpendicular) Leon County ON System Roads as shown in Table 3-4. Finally, node (Z) separates the crosswalks with strip pavement markings (zebra crosswalks) (Z_1) and the crosswalks marked with only two parallel lines (non-zebra crosswalks) (Z_0). They are symbolized with black strips and solid colors in the Figure 3-14, respectively and only 17% of the total crosswalks have zebra markings on Leon County ON System Roads as shown in Table 3-4. These binary nodes helped evaluate the performance of the model on the different importance levels of the crosswalks. For example, missing a crosswalk which is not crossing the roadway and not around signalized intersections (S_0C_0) can be more tolerable than missing other crosswalks. Also, as mentioned in the literature review section, the proposed model may perform differently on zebra and non-zebra crosswalks.

More importantly, this categorization of the crosswalks can lead to the target categorization of the crosswalks as follows: (a) signalized intersection, (b) midblock crosswalks, and (c) driveway crosswalks. Particularly, the threshold distance from the signalized intersection point can be determined to extract signalized intersection crosswalks (S_1). Then, another threshold distance from the roadway centerlines can help separate driveway (S_0C_0) and midblock crosswalks (S_0C_1) on the remaining crosswalks. Those threshold distances can be used in order to finalize the statewide crosswalk inventory list.

Figure 3-14: Ground truth (GT) crosswalk points and their categorization into three binary nodes

Table 3-4: Number of ground truth (GT) crosswalks

| <i>Crosswalk Types</i> | Code | # of Ground Truth (GT) Crosswalks in Leon |
|-----------------------------|----------------|--------------------------------------------------|
| Signalized Intersection | S ₁ | 665 (52%) |
| Non-Signalized Intersection | S ₀ | 607 |
| Crossing the ON Roads | C ₁ | 352 (27%) |
| Parallel to the ON Roads | C ₀ | 920 |
| Strips-Zebra | Z ₁ | 223 (17%) |
| Solid-No zebra | Z ₀ | 1,049 |
| TOTAL | | 1,272 |

3.4.2.2. Results

Table 3-5 indicates the performance evaluation results on the categorized crosswalks. We observe that the model performed much better on the C1 and S1 crosswalks. This is probably because of the variation on the crosswalk markings especially outside the roadways. These

crosswalks can be extracted from the images with a different method of masking in the preprocessing part such as roadway detection instead of using the 100-ft buffer zone around centerlines.

On the other hand, the detection performance on zebra and non-zebra crosswalks is balanced, and this proves that the developed model can perform well on both types of pavement markings. Note that object detection algorithms can only detect the introduced patterns in the training data set; therefore, the similarity of crosswalk markings plays a significant role on the performance of the proposed model. Therefore, occlusion by cars, especially white cars, significantly increases the FP and FN of the model. Also, auxiliary turning lane crosswalks with relatively smaller shapes become harder to detect. However, the overall results confirm that the proposed model is suitable for creating a crosswalk inventory map.

Table 3-5: Performance evaluation results on categorized crosswalks

| <i>Crosswalk Types</i> | Code | # of GT | # of Not-Detected GT | Completeness |
|-------------------------------|----------------|----------------|-----------------------------|---------------------|
| Signalized Intersection | S ₁ | 665 (52%) | 40 | 0.925 |
| Non-Signalized Intersection | S ₀ | 607 | 139 | 0.771 |
| Crossing the ON Roads | C ₁ | 352 (27%) | 12 | 0.966 |
| Parallel to the ON Roads | C ₀ | 920 | 167 | 0.818 |
| Strips-Zebra | Z ₁ | 223 (17%) | 34 | 0.848 |
| Solid-No zebra | Z ₀ | 1049 | 145 | 0.862 |
| TOTAL | | 1,272 | 179 | 0.859 |

3.4.2.3. *Target Crosswalk Categorization Rules*

Figure 3-15(a) indicates that the signalized intersection crosswalks in the GT data set have less than 213 ft. to the nearest signalized intersections on average. Based on this result, a 200-ft zone around the signalized intersection points was defined as the signalized intersection crosswalk zone. Any crosswalk detected and mapped in this zone was assigned to the signalized class in the statewide crosswalk inventory list. In the GT dataset, there were only a few S1 crosswalks outside of this zone; however, they were located on the auxiliary turning lanes, and these crosswalks were classified as driveway crosswalks.

Figure 3-15(b) indicates that the crosswalks parallel to the ON roads (C0) are within 15 ft. or more to the roadway centerlines. Based on these rules, a 10-ft buffer zone around roadway centerlines was defined as a midblock zone, and any crosswalk outside the signaled intersection zone but inside the midblock zone was defined as a midblock crosswalk. The detections outside of both zones were used to identify driveway crosswalks. Illustrations of the zones and categorized crosswalks are presented in Figure 3-16.

According to this classification method, there are three midblock crosswalks in Leon County: (1) Blountstown Hwy (illustrated in Figure 3-16), (2) S. Adams St. (Capital Cascades Trail) (3) Thomasville Rd. (Midtown Tallahassee). Note that there are crosswalks controlled with pedestrian actuated signals (i.e., W. Tennessee crosswalks in Figure 3-13), but these signals are

also included as part of the signalized intersections. Therefore, they are listed as signalized intersection crosswalks in the dataset. This is similar to the definition of the midblock crosswalks provided by FHWA in (Blackburn et al., 2017). The proposed model has detected two of these midblock crosswalks and missed the second one due to the peeling pavement markings as illustrated on Figure 3-13(g).

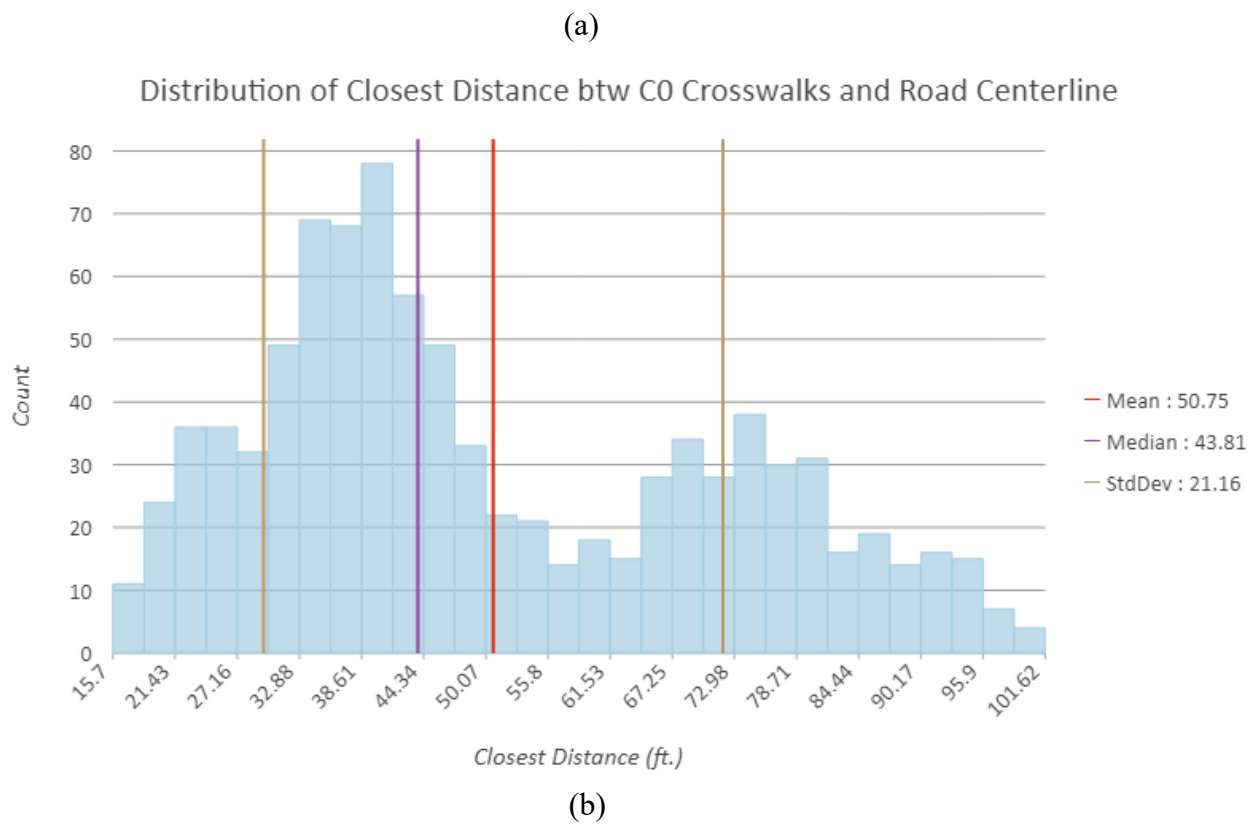


Figure 3-15: Distance analysis for the target categorization in the statewide crosswalks inventory list. (a) S1 crosswalks to signalized intersection points, and (b) parallel crosswalks to the roadway centerlines

Figure 3-16: Zones for categorizing the signalized intersection, midblock, and drive way crosswalks

3.5. Final Data Description

In this study, a deep learning- and GIS-based model was described, and its performance was evaluated while detecting the crosswalks. This automated crosswalk detection and mapping model can detect and map 86% of the crosswalks within a 30 ft. distance and there is a 88% precision on its detections. Additionally, a sensitivity analysis was conducted to categorize the detected crosswalks in order to obtain a more accurate statewide crosswalk inventory list. The final numbers of this list are illustrated in Table 3-6.

Note that the crosswalks were mapped based on the State Plan Coordinate System Zones. There are three different zones in Florida as shown in Table 3-6 and three different shape files are provided to fulfill the requirements of Task 2. In each shapefile, an attribute with the name “Class” indicates whether a crosswalk is a i) OFF road crosswalk, ii) Signalized intersection ON road crosswalk, iii) Midblock ON road crosswalk, and iv) Driveway ON road crosswalk.

These three shapefiles can serve as the crosswalk inventory list for FDOT in order to enhance the pedestrian safety throughout the state.

Table 3-6: Statewide crosswalk inventory with the final numbers

| <i>FL SPCS Zones</i> | OFF Road Crosswalks | ON Road Crosswalks | | | | Total |
|----------------------|---------------------|--------------------|------------|-----------------|---------------|----------------|
| | | Total | Midblock | Signalized Int. | Driveway | |
| <i>North (903)</i> | 12,234 | 7,733 | 287 | 2,243 | 5,203 | 19,967 |
| <i>West (902)</i> | 27,657 | 14,875 | 156 | 7,724 | 6,995 | 42,532 |
| <i>East (901)</i> | 61,078 | 35,794 | 418 | 18,246 | 17,130 | 96,872 |
| Total | 100,969 | 58,402 | 861 | 28,213 | 29,328 | 159,371 |

3.6. Discussions and Recommendations

This task aimed to develop an automated signalized intersection geometric data extraction algorithm based on high-resolution images in order to identify crosswalks. This is an innovative solution that employs the computer vision technology to potentially replace traditional manual inventory, which is labor intensive and prone to errors. Using high resolution images, the developed algorithm can extract key intersection geometrics such as pedestrian crossings (crosswalks and midblock crosswalks) that can be recognized from images. The findings of Task 2 will help FDOT obtain cost savings by eliminating a need for a manual inventory process and improved intersection data quality by eliminating errors due to manual data input.

There are several important limitations and future recommendations based on the findings of this task:

- Roadway data extraction from imagery is clearly critical for transportation agencies and can provide many benefits. For example, roadway extraction and lane marking segmentation can lead to lane/shoulder/median width inventory for intersections without significant obstructions.
- OSM a promising source and provides free geocoded data, which matches with FDOT's data policy. A study for analyzing the full benefits of OSM can be considered by FDOT.
- Defilement analysis can help identify which crosswalks need maintenance and visual improvements (X. Liu et al., 2017).
- Aerial images cannot be used to detect the crosswalks underneath trees.
- Regardless of the accuracy on the object detection part, geometry data collection requires mapping. Fortunately, this study uses free georectified aerial images maintained by FDOT.
- Roadway centerlines create problems on masking and midblock detection. A better methodology can be developed to mask the images and/or to determine the signalized intersection zones and midblock zones.

4. TASK 3: CONDUCT A PILOT-DRONE TEST IN SELECTED INTERSECTIONS

4.1. Background

With a focus on the feasibility analysis for drone-based traffic data collection, the research team has conducted field exercises with a third-party drone service provider. This chapter presents the details on the purchased services and details of the exercises. In addition to a written report, a hard disk drive including all the recorded videos are submitted to FDOT to fulfill the requirements of the Task 3.

4.2. Exercise Design and Execution

4.2.1. Introduction

With respect to the challenges and lessons learned from the literature review and best practices provided in Task 1, a series of exercises was conducted at five different locations in Florida (two in Tallahassee and three in Jacksonville) between March 13, 2021 and March 21, 2021. To conduct this exercise with a professional UAS service provider, a request for quote was announced and handled through Florida State University Procurement Services. In this request, the scope of their work was explained as follows:

- The vendor must comply with all of the federal and state laws to legally operate an unmanned aircraft and record aerial video over selected intersections.
- The vendor must provide 13 to 15 hours of continuous drone footage over each intersection and broadcast this footage in real-time (or near real-time) to a ground computer station where traffic data such as road user classification and trajectories, traffic volume, queue lengths, speeds, accelerations, turning movements and conflict points can be extracted.
- The vendor will provide HD quality video recordings of all legs of the intersections, to potentially share with FDOT Districts, and have it available for public outreach in Florida.
- Tethered drones are preferred to acquire continuous recordings, and these videos should include both AM and PM traffic as well as the mid-day traffic.
- The vendor should also conduct real-time video image analysis and processing to detect the road users (i.e., car, truck, bus, pedestrian, bicyclist) and track them in the subsequent frames to provide coordinates of those road users in every 0.1 second (or lower) as road user trajectories.
- While the road user trajectories are objected as the main output of this task, additional traffic data such as turning movement count or speed extractions without trajectories shall be used for the feasibility evaluation. An example trajectory is given in Table 4-1.
- The accuracy of any extracted data will be tested by using the raw video records.
- The vendor must protect the safety and privacy of the traveling public.

Table 4-1: Expected final trajectory output.

| Object ID | User Type | Time Stamp (hh:mm:ss.ss) | Position X (US. Surveying ft.) | Position Y (US. Surveying ft.) |
|------------------|------------------|-------------------------------------|-------------------------------------------|-------------------------------------------|
| 1 | Car | 00:00:10.00 | XXX.xxxxxx | YYY.yyyyyy |
| 1 | Car | 00:00:10.10 | XXX.xxxxxx | YYY.yyyyyy |
| 1 | Car | 00:00:10.20 | XXX.xxxxxx | YYY.yyyyyy |
| 2 | Pedestrian | 00:00:11.40 | XXX.xxxxxx | YYY.yyyyyy |
| 2 | Pedestrian | 00:00:11.50 | XXX.xxxxxx | YYY.yyyyyy |
| 2 | Pedestrian | 00:00:12.00 | XXX.xxxxxx | YYY.yyyyyy |
| 3 | Truck | 00:00:11.50 | XXX.xxxxxx | YYY.yyyyyy |
| 3 | Truck | 00:00:12.00 | XXX.xxxxxx | YYY.yyyyyy |
| 3 | Truck | 00:00:12.10 | XXX.xxxxxx | YYY.yyyyyy |
| 3 | Truck | 00:00:12.20 | XXX.xxxxxx | YYY.yyyyyy |
| 4 | Bicyclist | 00:00:12.00 | XXX.xxxxxx | YYY.yyyyyy |
| 4 | Bicyclist | 00:00:12.10 | XXX.xxxxxx | YYY.yyyyyy |
| 5 | Bus | 00:00:11.50 | XXX.xxxxxx | YYY.yyyyyy |
| 5 | Bus | 00:00:12.00 | XXX.xxxxxx | YYY.yyyyyy |
| 5 | Bus | 00:00:12.10 | XXX.xxxxxx | YYY.yyyyyy |
| . | . | . | . | . |
| . | . | . | . | . |
| n-1 | Car | 14:58:28.10 | XXX.xxxxxx | YYY.yyyyyy |
| n | Pedestrian | 14:59:42.10 | XXX.xxxxxx | YYY.yyyyyy |
| n | Pedestrian | 14:59:42.20 | XXX.xxxxxx | YYY.yyyyyy |
| n | Pedestrian | 14:59:42.30 | XXX.xxxxxx | YYY.yyyyyy |

Finally, a contract was signed with Sinclair Community College, National UAS Training and Certification Center from Ohio, USA. The contractor has also teamed up with Simlat Inc. to conduct the required video image processing tasks.

4.2.2. Purchased Service

The contractor provided four certified drone pilots for a total of 11 workdays between Friday, March 12 and Tuesday, March 23, 2021. This operation team left Ohio on Friday, March 12, 2021 morning and drove all the way to Florida. After two days of travel, drone exercises started in Tallahassee on Sunday, March 14, 2021 and continued on the following days of Monday and Tuesday. After the travel to Jacksonville on Wednesday, March 17, 2021, exercises

were conducted in Jacksonville on Thursday, March 17, 2021 and for the following days of Friday and Saturday. Note that the contractor travelled from Ohio with all the required equipment loaded on two trucks and a trailer. The equipment list, with their brand and model information, is presented in Table 4-2 including their current prices. Some items from this list as well as the drone exercise operations is illustrated in Figure 4-1.

Table 4-2: Main equipment provided and used by the contractor and their current prices.

| <i>Equipment</i> | <i>Brand / Model</i> | <i>Price</i> |
|------------------------------------------|--------------------------------------|--------------|
| <i>Drone #1</i> | DJI M200 | \$4,500 |
| <i>Drone #2</i> | DJI M210/RTK | \$6,500 |
| <i>Camera #1</i> | DJI Zenmuse Z30 | \$3,000 |
| <i>Camera #2 (backup)</i> | DJI Zenmuse X4S | \$600 |
| <i>Drone Controller Screen</i> | DJI Crystal Sky | \$500 |
| <i>Tether</i> | Elistair Light-T | \$6,600 |
| <i>Drone Battery matched with tether</i> | Elistair air module for DJI M200/210 | \$3,700 |
| <i>Generator for tether</i> | BS 6500 | \$800 |

For all drone operations, the maximum altitude was kept between 100 ft. and 120 ft. due to the tether cable restrictions. In addition, no operation was conducted when wind speed exceeded 20 knots (23 mph) due to the 800-W pull force limitation on the tether. The reason is that, when high wind is experienced, it swings the tether and creates extra pulling power.

Additionally, after every 2.5 hours of flight time, the drone was taken down and the team switched to the other drone to continue traffic monitoring. This was done mainly due to the controller battery limitation. The crystal sky controller screen battery life is approximately 2.5 hours and losing connection during the flight may even cause an unfavorable incident. Also, it was claimed that the just like most of the other drones, DJI M Series was made to fly a maximum of 30 minutes. If it was kept longer on the air, some problems such as losing the camera and/or gimbal control and malfunctioning of a critical flight control equipment might have occurred.

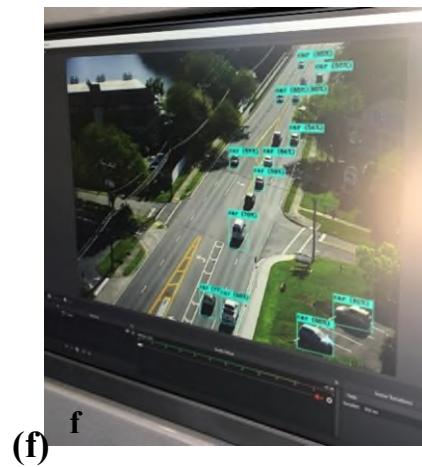


Figure 4-1: Pictures from the exercise. (a) Drone DJI M210/ RTK, (b) DJI M200 with Zenmuse Z30 camera attached and two batteries (one of them is Elistair's Air Module for DJI M200/210), (c) Light-T Tether and BS6500 generator, (d) inside the trailer where the airspace is continuously observed (top screens) and live-feed video is labeled with YOLO, (e) Crystal sky screen attached to the master drone controller and tether observation screen, and (f) labeled live feed video.

4.2.3. Exercise Locations

The study sites were selected from the intersections where a recent signal warrant study or any other type of analysis was conducted with traditional methods. Signal warrant study is the common method to conduct an engineering analysis that aims to determine whether a signal control is required on an uncontrolled or stop-sign controlled intersections. This process requires extensive field data collection such as 8-hour vehicular traffic volume, speed (if posted speed limit is not used as the reference speed), 4-hour vehicular traffic volume, peak hour, pedestrian volume. Therefore, a cost benefit analysis in the Task 4 deliverable of this project attempted to compare the costs associated with warrant studies conducted with traditional methods and the drone-based data collection.

Another constraint in terms of determining the study site was the air space classification since a Low Altitude Authorization and Notification Capability (LAANC) certification is required for operations nearby airports. Since obtaining this certification is time consuming, the research team avoided intersections closer to airports to conduct this exercise. The aerial images of the exercise locations with their coordinates and operation hours are presented in Figure 4-2, Figure 4-3, Figure 4-4, Figure 4-5, and Figure 4-6.



Figure 4-2: Tallahassee Location 1: Apalachee Pkwy. & March Rd. Hours of operation: Sunday, March 14, 2021 between 10:17 AM – 5:02 PM, and Tuesday, March 16, 2021 between 9:43 AM – 6:39 PM



Figure 4-3: Tallahassee Location 2: US-231 & Jacob Rd. (RCUT intersection). Hours of operation: Monday, March 15, 2021, between 7:28 AM – 7:47 PM



Figure 4-4: Jacksonville Location 1: US-90 (Beach Blvd.) & Leon Rd. Hours of operation: Thursday, March 18, 2021, between 6:46 AM – 8:05 AM



Figure 4-5: Jacksonville Location 2: SR-10 (Atlantic Blvd.) & Leon Rd. Hours of operation: Friday, March 19, 2021, between 6:49 AM – 8:38 PM



Figure 4-6: Jacksonville Location 3: US-301 & SR 228 (Normandy Blvd.). Hours of operation: Saturday, March 20, 2021, between 8:33 AM – 5:02 PM

4.2.4. Operational Steps and Challenges

As aforementioned, the contractor was responsible for abiding with all federal and state rules to operate drones legally and safely and securing the safety of their pilots and equipment. Therefore, the contractor conducted a risk assessment study for each pre-determined location. As an example, Figure 4-7 indicates the risk assessment document for the Tallahassee Location 1 study area on Apalachee Parkway.

Additionally, two supplementary checklists were strictly followed by the drone operation team. The first checklist, illustrated in Figure 4-8, was prepared by the Tether supplier Elistair to provide secure operations with tether attachments to DJI M series drones. Before every drone took off and after each one landed, the steps guided the drone pilots. The second checklist, illustrated in Figure 4-9, was prepared by the video image processing partner SIMLAT to initiate the object detection and labeling the road users on the live drone video feed. After every takeoff, the steps were followed by the drone operation team to transfer the live drone video into the computer in the trailer and run the pre-built YOLO algorithm on this video. Finally, three types of video recordings were obtained: a) YOLO labeled raw video, b) unlabeled raw video, and c) higher quality recorded video.

The step-by-step execution of the exercise for each takeoff is conducted as follows:

- 1) Start before 8 AM (10 AM for weekends) with two drone pilots.
- 2) Secure location to park and determine safe distancing and flying conditions.
- 3) Test camera (primary: ZENMUSE 30), controller, and other equipment prepared for takeoff with the tether operation checklist (Figure 4-8).
- 4) Test the live stream on the main and secondary controllers.
- 5) Initiate video image processing and start recording according to the checklist (Figure 4-9).
- 6) Lift off the drone to altitude between 100 ft. and 125 ft. and find the best field of view.
- 7) Continuously watch the camera, for other aircrafts, weather-related issues, and the tether-related variables (e.g., force, temperature).
- 8) Land on after 2 to 2.5 hours.
- 9) Change the battery on the controller and crystal sky.
- 10) Charge batteries and start from the step #3 with the other drone.

After 1 PM, drone pilots changed shifts and operation continued until sunset (around 8 PM) (6 PM for Weekends). Finally, the challenges faced during the exercise are presented in Table 4-3 for each study location.

| Flight Test Card | | | | | | |
|------------------------------------------------------------------------------------------------------------------------------------------------------------------------------------------------------------|-----------------------------------------|--------------------------------|--------------------------------------------------------------------------------------------|--------------------------------------------|------------------------|-----------|
| Date | 03/18/2021-03/20/2021 | Fuel Load | 100 % | Backup Batteries Brought (#) | 6 sets | |
| | | | | Generator (Y/N) | Yes | |
| Location | US-27 at March Road Tallahassee Florida | Joker | 80 % | Wind Limits (Launch/Recovery) | | |
| Aircraft + Registration Number | DJI M200 Wilkos FA3KHK4MXR | Bingo | 70 % | Max Crosswind: | Max Headwind/Tailwind: | Max Gust: |
| | | | | 27 mph | 27 mph | 30 mph |
| Payload | DJI Zenmuse 30x | | | | | |
| Crew Position | Call Sign | Name | Max Precipitation: 10 mm/h | | | |
| Air Vehicle Ops Part 107 RP | Moe | Alexander Catalan Drew Clawson | Visibility: 500 ft vertical and 2,000 horizontal seperation | | | |
| Visual Observer VO - Primary | Curly | Charles Reed Sam Heckel | Max Winds Aloft: 27 mph | | | |
| VO - Documents | Larry | SEE ALL | Temperature Limits: -4 F / 113 F | | | |
| EMERGENCY CONTACTS: | | | | FREQUENCIES: | | |
| <ul style="list-style-type: none"> Medical Emergency: 911 PIC/Officer: Charles Reed / Sam Heckel / Alexander Catalan / Drew Clawson Flight Authority (Boss): Charles Reed | | | | Hand Controller: 2.4 & 5.8 Commbox: N/A | | |
| Notes: | | | | | | |
| Teather Limitaitions: Power: Max 1200 W Length of Cable: 70 M Max Wind: Same as Aircraft (Use Caution) Max Flight Time: 4 Hours Weather: IPx64 | | | | | | |
| FLIGHT LIMITATIONS | | | | | | |
| Flight Operation - LIMITS: | | | UAS System - LIMITS: | | | |
| <ul style="list-style-type: none"> Maximum Altitude: 400 ft AGL Max Airspeed: 100 mph Max Absolute wind speed: 30 mph Min Altitude Over Participants: N/A | | | <ul style="list-style-type: none"> Aircraft velocity never exceed: 51.4 mph | | | |

Flight Test Card

Page 1 of 3



Figure 4-7: Flight card for the Tallahassee Location 1 indicating the prior risk assessment

Using the M200/M210 Air Module

The M200/M210 Air Module replaces the left-hand battery on the drone, and powers the aircraft continuously from the ground source through an Elistair tethering station, Ligh-T or Safe-T. The paracord lanyard should be affixed to the drone to provide an anchor point for the mechanical connector on the micro tether. To ensure a solid electrical connection, use the screw to secure the micro-tether connector (1) to the bolt on the module.

Pre-take-off checks

1. Turn ON the power supply to the SAFE-T or LIGH-T, ensure power to the tether is OFF.
2. Plug a fully charged battery in to the M200/M210 (Minimum 90% charged).
3. Plug the air module into the left-hand battery port on the drone.
4. Connect the tether to the module (1) and attach the cable using the screw fitting and mechanical attachment on the tether.
5. Power ON the output to the tether (Power Arming ON and Power switch ON for the SAFE-T and Power Arming ON for the LIGH-T)
 - a. After 3 seconds, the LED (2) should be blinking red and green.
6. Power ON the M200/M210.
 - a. After 10 seconds, the LED should be blinking red.
7. Power OFF the M200/M210.
 - a. After 10 seconds, the LED should be blinking red and green.
8. Power ON the M200/M210 again.
 - a. After 10 seconds, the LED should be blinking green slowly (1 blink per 0.5 second) (CAUTION: if the LED is a solid green or red, DO NOT take off, the module is not correctly initialized).
9. On the DJI Go app, select the Aircraft Battery page by touching the battery indicator at the upper right corner of the screen.

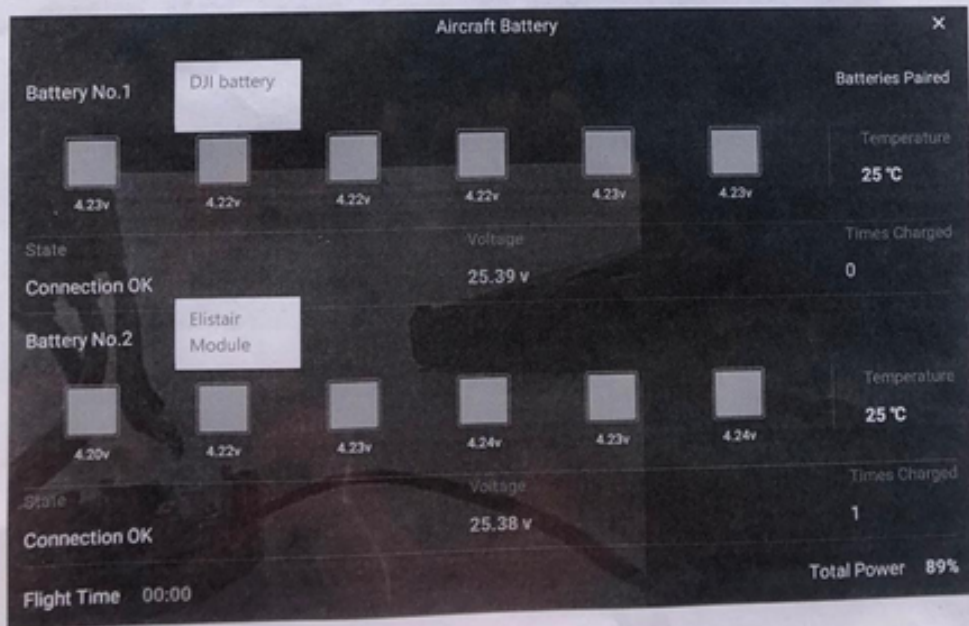


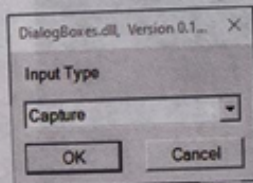
Figure 4-8: Tether operation pre-takeoff checklist

YOLO SETUP

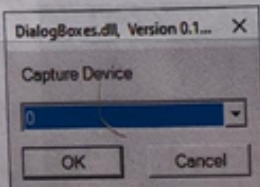
1. Power on computer using the button & switch combo below the bottom-left monitor. Push and hold the button until it beeps, wait 10 seconds, then push and hold the switch. The computer will then power on. Picture
2. Login to the PC. Password is "Simlat2015"
3. Power on laptop and place directly next to black shelves Ensure power is available.
4. If internet is required, connect both computers to the Verizon hotspot over WIFI.
5. Connect "YOTOCAP" Capture Card into left-most USB port on the PC Station.
6. Connect "MAGWELL" Capture Card into one of the USB ports on the right of the laptop
7. Connect the HDMI Splitter power cable into one of the USB ports in the right of the laptop. Place the Splitter on the black shelves.
8. Connect a HDMI cable between each capture card and a HDMI-Output on the Splitter (2x)
9. Connect a HDMI cable between the DJI Remote Controller and the HDMI-Input on the Splitter.
10. Ensure that the DJI is properly set up per relevant documentation.
11. Launch YOLO (Bottom left screen)



12. Select "Capture" and click OK



13. Select Capture Device "0" and click OK



JUSTBASICS

Made in Mexico
11017

Figure 4-9: Real-time video image processing system checklist

Table 4-3: Drone time and location table with associated challenges

| Date | Location | Major Road | Minor Road | Start Time | End Time | Duration | Challenges Faced |
|--------------------------|--------------------------------|-------------------------|--------------------|-------------------|-----------------|-----------------|------------------------------------------------------------------------------------------------------------------------------------------------------------------------------------------------------------------------------------------------------------------------------------------------------------------------------------------------------------------------------------------------------------------------------------------------------------------------------------------------------------------------------------------|
| Sunday, March 14, 2021 | Tallahassee 1 | Apalachee Pkwy. (US-27) | March Rd. | 10:17 AM | 5:02 PM | 6 h 45 m | <ul style="list-style-type: none"> The cemetery property was used without advance permit. Field of view was very limited from 120 ft maximum altitude. Total ~500 ft. length of major road was fit in the frame. (~250 ft. per approach) |
| Monday, March 15, 2021 | Tallahassee 2 | US- 231 | Jacob Rd. | 07:28 AM | 7:47 PM | 12 h 19 m | <ul style="list-style-type: none"> RCUT intersection did not fit on the frame. Each U-turn was recorded separately. Tether gave alert due to high temperature around 11 AM. Generator was mislocated to blow heat air on tether. Generator was relocated and no flight for ~15 m. A small plane was close by around 4 PM without any signal. Drone was taken to a lower altitude for safety. Lost camera and gimbal control around 5 PM and changed to the second camera. No flight for ~30 m. |
| Tuesday, March 16, 2021 | Tallahassee 1 | Apalachee Pkwy. (US-27) | March Rd. | 9:43 AM | 6:39 PM | 8 h 56 m | <ul style="list-style-type: none"> Cemetery management did not want us to use their property (turf). Agreement was done to use the large green area just by the cemetery fences and US 27. Morning peak has been missed. After some rain showers, operation was ended ~1 hour early. |
| Thursday, March 18, 2021 | Jacksonville 1 | Beach Blvd. (US-90) | Leon Rd. | 06:46 AM | 08:05 AM | 1 h 19 m | <ul style="list-style-type: none"> High wind speed blocked almost the entire day of operation. Several alert from the other aircrafts (i.e., plane) flying very high altitude. |
| Friday, March 19, 2021 | Jacksonville 2 | Atlantic Blvd. (SR-10) | River Hills Cir. E | 06:49 AM | 7:38 PM | 12 h 49 m | <ul style="list-style-type: none"> Very urban area, several cars stopped by to check and chitchat. One car almost hit the tether and generator. YOLO had problems with dense number of objects. |
| Saturday, March 20, 2021 | Jacksonville 3 | US-301 | Normandy Blvd. | 08:33 AM | 5:02 PM | 10 h 29 m | <ul style="list-style-type: none"> A swarm of eagles was present on the air and one of them wanted to attack the drone. ~15 m low altitude flight for safety. Short rain showers for three times between 2 PM and 5 PM. All equipment was carried in the cabinet until the rain has stopped. The operation continued afterwards No flight for a total of ~1 h and stopped the exercise earlier. |

4.3. Conclusions

Based on the conducted exercise and the challenges faced, following conclusions and future works are provided:

- The field work was very successful, and the drone pilots were very experienced.
- Trajectory extraction, or so-called multi-object tracking, is a very time-consuming task and warrants further research.
- We have three types of videos, namely the raw video (drone live footage recorded as is), the labeled video (raw video was labeled with YOLO and recorded in real time), and the high-resolution video (recorded on SD Card in drone during the flight) for more than 50 hours of aerial traffic surveillance from different altitudes and angles.
- This data set can be used for several research tasks such as multi-object tracking and extracting automated traffic performance metrics from the obtained trajectories.

5. TASK 4: PROPOSE GUIDELINES FOR USING DRONES TO COLLECT INTERSECTION TRAFFIC DATA

5.1. Background

Following up with the conclusions of Chapter 4, this chapter presents the results for drone-based data collection and analysis, a detailed fatal pedestrian-involved crash analysis and a comparative cost analysis, as part of the Task 4 Deliverable Report of this project. A sample of trajectories was acquired from the data analysis vendor and is presented in Section 2 of this chapter. In addition to the drone exercises, a pedestrian-involved crash analysis was carried out evaluating the spatial and statistical distributions of pedestrian-involved crashes in Florida between 2011 and 2020. The results of this safety assessment are presented in Section 3. Additionally, a comparative cost analysis was conducted comparing traditional methods with the proposed drone-based methodologies (Section 4). Finally, guidelines and recommendations for future drone-based traffic data collection are presented in Section 5.

5.2. Data Analysis Demonstration on the Obtained Trajectory Sample

After completing the drone exercises, the vendor provided sample trajectory data for 140 minutes of drone-captured video recorded at the Apalachee Pkwy. and March Rd. intersection. A 20-minute portion of these videos will be presented in this section. Firstly, this part of the study provides background information on the conducted experiment before demonstrating the recently obtained trajectory sample data.

5.2.1. Exercise Background

The research team signed a contract with Sinclair Community College National UAS Training and Certification Center from Ohio, USA, to operate tethered drones legally and safely to conduct the proposed exercises while providing the trajectory data. The contractor also teamed up with Simlat Inc. to conduct the required video image processing tasks.

5.2.2. Sample Trajectory Data and Classified Turning Movement Extraction

The sample data were provided for the Tallahassee Location 1 using the recordings on Tuesday, March 16, 2021, covering 20 minutes between 9:50 AM and 10:10 AM. The video source of the data can be accessed from the previously submitted external drive (Day 3 Mar16Tue Tallahassee Location 1>SD Card (Z30)>DJ_0001.mp4). Because the beginning of the video includes take-off scenes where no useful data can be extracted, the trajectories were provided starting from the seventh minute of the video.

Similar to the example trajectory format provided to the vendor before the experiments, the sample data included data points, road user classes, and trajectory IDs in addition to the latitudes, longitudes, and the State Plan Coordinate System (SPCS) coordinates. In total, 36,806 data points were extracted in this sample data, referring to 619 trajectories with 30 frame per second resolution. This original format with the trajectory points was preprocessed by the research team, converting points to the trajectory lines, and clustering those lines into each approach of the intersection. The results are demonstrated in Figure 5-1. The research team has analyzed these data to provide approach counts, which can be seen in Figure 5-1(b). In addition, the number of road user classes per approach is illustrated in Figure 5-2.

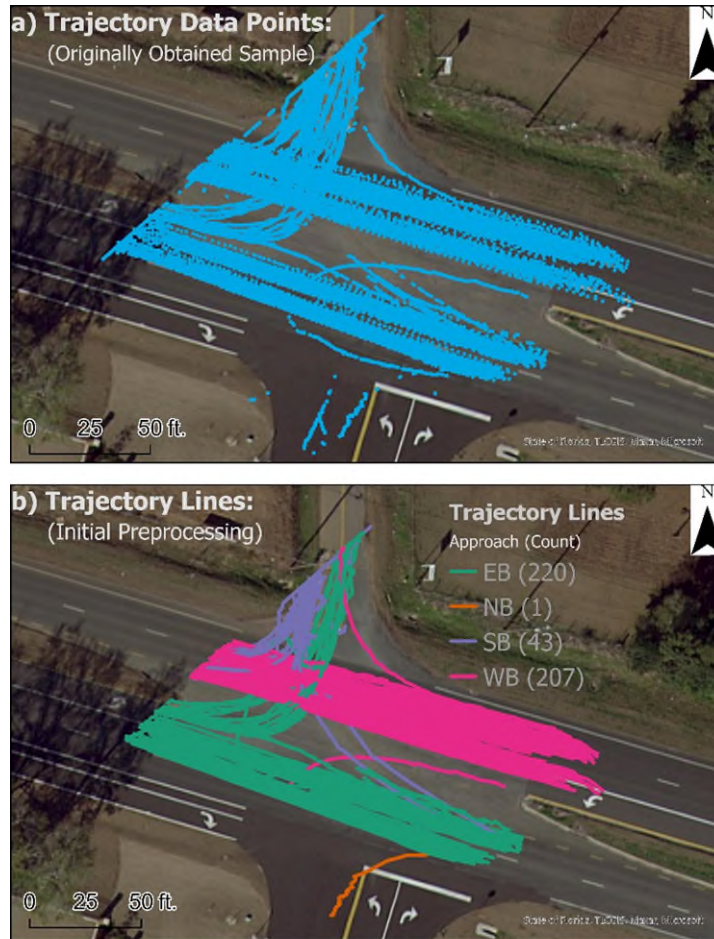


Figure 5-1: Sample trajectory data. (a) originally obtained data points. (b) preprocessed and clustered trajectory lines

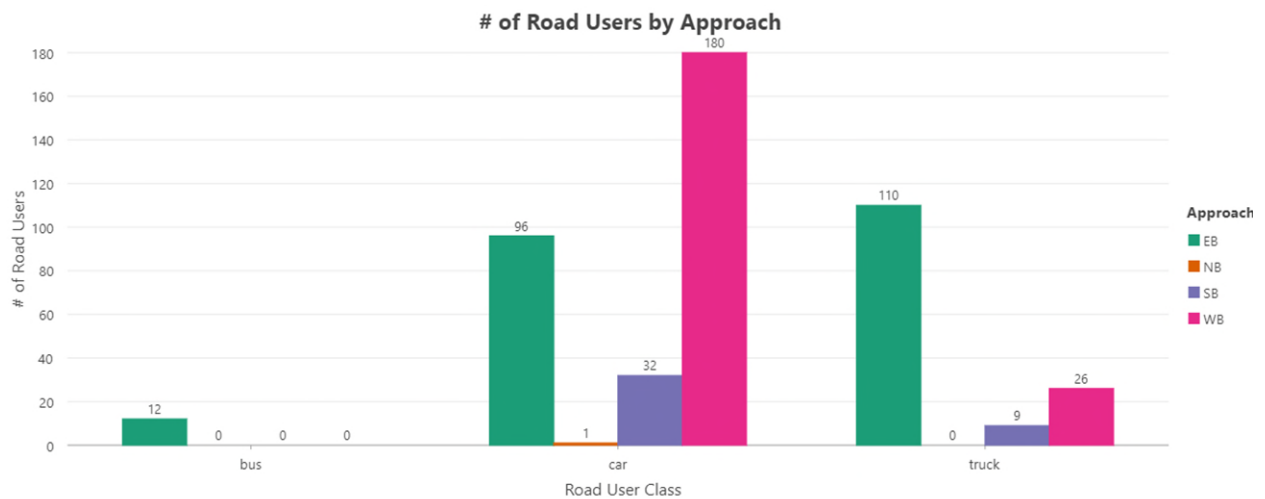


Figure 5-2: Number of classified road users per approach

5.2.3. Challenges on Georeferenced Trajectory Extraction from Drone Videos

All in all, the sample data demonstrates the capabilities of drone-based microscopic traffic data extraction. Although there are total of 50 hours video data, the vendor was able to process only 140 minutes in two months of timeframe. The research team and the data analyzing vendor has been in communication to identify the challenges faced to extract trajectories.

According to the video-image processing vendor the main challenges can be identified as:

- 1) Intersection not in the field of view: All the irrelevant frames needed to be cleaned out from the video. This includes the take off at the beginning, drafting or turning during the video, and landing at the end.
- 2) Unsteady video stream: This is the main challenge on drone-based video-processing task since the camera is not stable and even a slight replacement on the frame alignment causes big problem for the automated trajectory extraction system.
- 3) Lack of camera parameters and telemetry data: This is another challenge so far since the original plan of the vendor was to use the camera-related telemetry data for georeferencing video frames and any vehicle in those frames. However, the recorded telemetry data (i.e., the log files) did not include any camera-related information such as zoom level, look angle, and gimbal position.

Currently, the data analysis vendor uses computer vision techniques to overcome these challenges. For example, homography transformation is used to project frame coordinate system to actual SPCS by tracking the landmarks or boundaries of the intersection. Figure 5-3 indicates an example of this transformation.

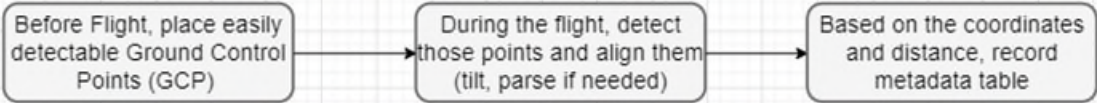
Figure 5-3: Homography transformation of the video frames using the intersection boundaries.

5.2.4. Proposed Data Collection and Analysis Framework

Drone-based traffic data collection requires a full collaboration with the traffic engineers, drone operators and video-image processing professionals because the whole process is fully connected. A system including these three domains can be set with a high fixed cost, but it can

operate with a very low maintenance cost and potentially higher accuracy than traditional methods while reducing the personal injury risks on the field. Including these three domains, a framework is recommended to extract road user trajectories from drone videos in real-time. The foundation of this framework, as presented in Figure 5-4, is on the metadata generation for each frame of the video. This allows one to exclude frames that are not focusing on the intersection so that georeferencing can be done seamlessly. Also, another framework is presented in Figure 5-5 to extract trajectories automatically from the trajectories. This framework requires three inputs, namely trajectory, time interval to aggregate counts, and gate coordinates, to provide Origin-Destination (O-D) matrix shaped turning movement counts (TMC) for each of the entrance and exit gates.

1) Align every video frame in real time



| Frame # | Start x Coordinates in SPCS | Start y Coordinates in SPCS | Resolution (Actual distance/# of pixels) | Camera Look Angle |
|---------|-----------------------------|-----------------------------|------------------------------------------|-------------------|
| Frame_0 | | | | |
| Frame_1 | | | | |

2) Run object tracking using aligned frames

One algorithm should be developed in advance by retraining an existing algorithm to robust detection on aerial images and present accuracy

```

Frame #: 102
Tracker ID: 1, Class: person, BBox Coords (xmin, ymin, xmax, ymax): (101, 41, 670, 464)
Tracker ID: 2, Class: cell phone, BBox Coords (xmin, ymin, xmax, ymax): (168, 219, 384, 414)
FPS: 1.26
  
```

3) Convert Pixel Coordinates to SPCS using Metadata

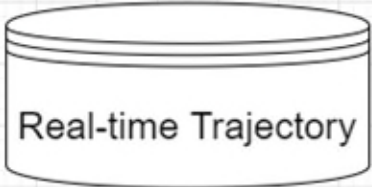
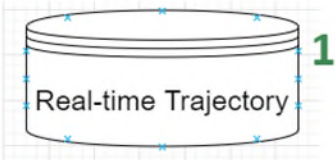


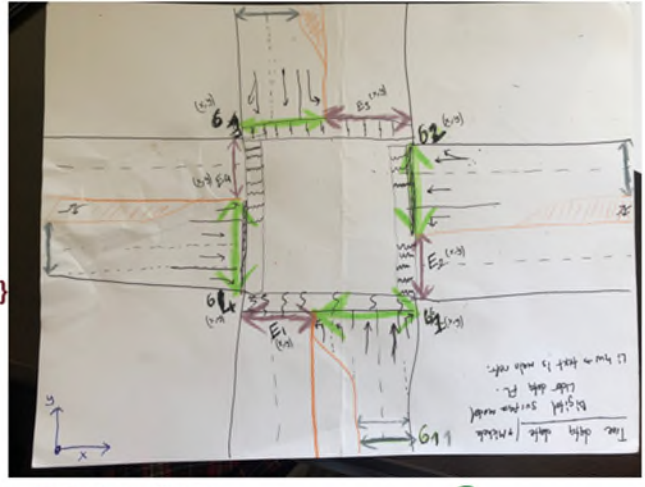
Figure 5-4: Recommended framework for real-time trajectory extraction

Inputs:



- Track ID
- User Type: {Car, Truck, Bike, Ped}
- SpaceTimeDictionary:
 - {'time1': (X1,Y1), 'time2': (X2,Y2),
.
}

User Input for Time interval 2



- Gate Coordinates: 3
 - {'Ent1': (StartXent1, StartYent1, EndXent1, EndYent1),
 - 'Ent2': (StartXent2, StartYent2, EndXent2, EndYent2),
 - 'Ext1': (StartXext1, StartYext1, EndXext1, EndYext1),
 - 'Ext2': (StartXext2, StartYext2, EndXext2, EndYext2),
 -}

Outputs

- O-D shaped Matrix for each user type indicating number of road user in the desired time interval

| | Ext1 | Ext2 | Ext3 | Ext4 |
|------|------|------|------|------|
| Ent1 | | | | |
| Ent2 | | | | |
| Ent3 | | | | |
| Ent4 | | | | |

↓
Populate MUTS Forms

Figure 5-5: Recommended framework for automated TMC extraction from trajectories

5.3. Pedestrian Involved Crash Analysis

This chapter provides a more detailed analysis on the pedestrian safety issues considering the provided crosswalk inventory.

5.3.1. Background

Pedestrians are among the most vulnerable road users due to the lack of protective equipment such as airbags, and seat belts. They also possess some distinctive characteristics, including slow walking speed, which increases the risk of getting involved in severe injury crashes particularly when crossing or walking along roadways. Safety design criteria and guidance (AASHTO, 2018a) should integrate their needs and focus on constructing sidewalks and other pedestrian facilities to prevent them from crashes. Note that design criteria could not necessarily guarantee pedestrian-involved crash occurrences (Alver et al., 2021)

Based on the National Highway Transportation Safety Administration (NHTSA) Traffic Safety Facts (NHTSA, 2018), pedestrians accounted for nearly 17% of traffic fatalities nationally in 2018. Fatality Analysis Reporting System (FARS) also revealed that 4,483 out of 6,205 fatal pedestrian-involved crashes occurred at locations that were not intersections in 2019, which was associated with 72.2% of them (NHTSA, 2019). Pedestrian-involved crashes mostly occurred due to the following reasons: a) failing to yield to pedestrians, b) improper crossing, and c) visibility. The contributing factors are listed in Table 5-1.

Table 5-1: Pedestrian fatality crashes by related factors, 2019, USA*

| Factors | Number | Percent |
|-----------------------------------------------------------|--------------|----------|
| Failure to yield right of way | 3,017 | 48.6 |
| Improper crossing of roadway or intersection | 1,185 | 19.1 |
| In roadway improperly (standing, lying, working, playing) | 921 | 14.8 |
| Not visible (dark clothing, no lighting, etc.) | 856 | 13.8 |
| Under the influence of alcohol, drugs, or medication | 562 | 9.1 |
| Wrong-way walking | 437 | 7.0 |
| Inattentive (talking, eating, etc.) | 245 | 3.9 |
| Failure to obey traffic signs, signals, or officer | 238 | 3.8 |
| Traveling on prohibited traffic ways | 149 | 2.4 |
| Other factors | 826 | 13.5 |
| Unknown | 1,035 | 16.7 |
| TOTAL | 6,205 | - |

*Source: FARS 2019 ARF

There are quite a few latent and hidden contributing factors that may increase the probability of crash risk among this vulnerable group such as land use, demographic parameters, and driver behavior at the time of crashes. In order to evaluate the contribution of these factors, there is a need to identify hotspot locations first. Therefore, the main objective of this analysis is to propose a spatial methodology to identify high-risk locations. As such, we focused on pedestrian-involved fatality crashes that occurred far away from intersections in this work. The objectives of this research for the Florida Department of Transportation (FDOT) include the following: a) identify high-risk locations regardless of the amount of number of crashes, b)

overlay drone output on hotspot location shapefiles to extract more detailed spatial contributing attributes, and c) evaluate hidden reasons behind pedestrian-involved crash occurrences.

5.3.2. Methodology

Conventional hotspot identification methods could not provide accurate results in case there is not enough data (i.e., crash occurrences) as inputs for these statistical methods. Based on zero-vision strategies applied in the crash analysis field, we acknowledge that each single fatal crash enables us to identify potential high-risk locations. This requires urgent attention to improve pedestrian safety and prevent crash occurrences. This research focused on pedestrians who intend to cross the minor roadways at driveways, crossing the major roadways at locations far away from intersections, or walking along the roadways. The following sections describe the process utilized to categorize pedestrian-involved crashes based on their distance from the nearest intersection, crash lane, and level of injury.

5.3.2.1. *Crash Data*

Pedestrian crash data is composed of points dispersed along with the roadway network and each point represents a crash with the associated information and attributes. This dataset was obtained from the Crash Analysis Reporting (CAR) online database for 10 years between 2011 and 2020. Roadway network and center of intersection location data, on the other hand, were obtained from FDOT Transportation Data & Analytics Office (TDA) database (TDA, 2021).

5.3.2.2. *Crash Data Filtration*

This analysis focuses on crashes that occurred far away from intersections, which we will name as “not at intersections”. Not at intersection crashes represent the ones that did not occur around the intersections and therefore not under the influence of intersection presence. In the State of Florida, a distance of 250 feet, measured from the center of the intersection, is set as the default value for “influenced by intersection” crashes. In order to separate not at intersection crashes from the original dataset, we mapped crash points based on their associated longitude and latitude coordinates provided as two attributes in the dataset. It is worth mentioning that crashes that occurred in parking lots did not contain coordinates (unmapped crashes) and we had to remove them from the original dataset. Next, we calculated the distances between crash locations and the nearest intersections using the network analyst built-in toolbox in ArcGIS. A 250 ft. threshold was used to split the dataset into “not at intersection” and “at intersection” crashes. Also, a certain type of crashes, namely scooter-involved crashes did not involve any pedestrian and therefore were removed from the dataset. Moreover, we used the crash lane attribute to identify crashes that occurred on driveways, crosswalks, or side of roadways based on what was given in Table 5-2. Additionally, Figure 5-6 illustrates the process of data filtration.

Table 5-2: Crash lane identifier (Name of attribute: ACCLANE/CRASHLANE)

| Lane Identifier Code | description |
|-----------------------------|---------------------------------------------------------|
| 1 | 1st thru lane from center |
| 2 | 2nd thru lane from center |
| 3 | 3rd thru lane from center |
| 4 | 4th thru lane from center |
| 5 | 5th thru lane from center |
| 6 | 6th thru lane from center |
| 7 | 7th thru lane from center |
| 8 | 8th thru lane from center |
| 9 | 9th thru lane from center |
| A | acceleration/merge lane |
| B | toll booth plaza |
| C | pedestrian impact in the crosswalk |
| D | crash in a driveway |
| E | ran off end of road at T |
| H | island area |
| K | service/access road |
| L | left-turn only lane |
| M | median or middle of intersection |
| P | parking lane (designated parking) |
| R | right-turn only lane |
| S | side of roadway/shoulder/off-road/emergency lane |
| T | continuous left turn lane, accessible both directions |
| U | unknown |
| V | bicycle travel lane |
| X | on a ramp |

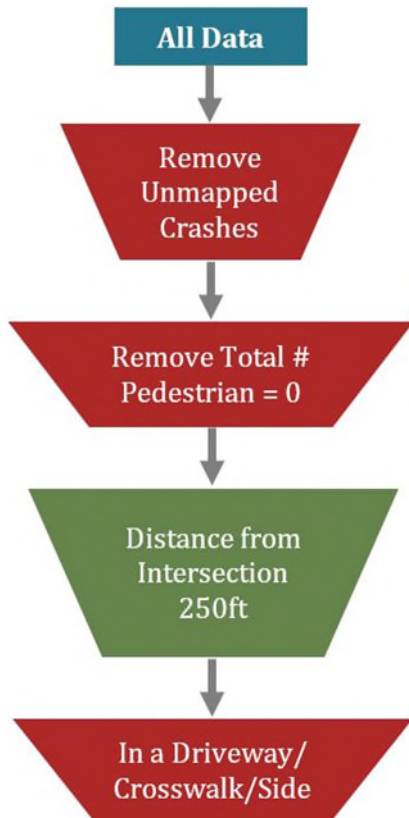


Figure 5-6: Data filtration process based on roadway network distance

The final output of the filtration process, shown in Figure 5-6, is presented in Table 5-3. On average, 18% of not at intersection crashes that occurred during the time of the study, were on driveways, mid-block crosswalks, or side of roadways. Previous studies concluded that crosswalks are mostly equipped with features that facilitate them for pedestrians (Høye & Lareshyn, 2019; Patella et al., 2020); however, aforementioned locations do not. Although several researchers developed countermeasures (e.g., the beacon, rapid-flash beacon, and shared-lane markings) to improve the safety of pedestrian crossings, the statistics reveal that there is still a need for further analysis and attention to decrease crash occurrences around driveways, mid-block crosswalks, and side of roadways.

The data extracted from the CAR online database contains an attribute that enables us to categorize crash data based on the highest level of injury. This information is initially converted from the incoming report data but may be changed during the Safety Office’s crash location processing. The single-digit code indicates the highest injury severity due to the crash. Table 5-4 listed the identifier codes in the order of severity from lowest to highest.

Table 5-3: Pedestrian-involved crashes in Florida by location and crash lane

| Year | Pedestrian-Involved Crash | | | | |
|--------------|---------------------------|---------------------|-----|-----------------------------|-----|
| | Total | Not at Intersection | | Driveway - Crosswalk - Side | |
| 2011 | 5356 | 984 | 18% | 73 | 7% |
| 2012 | 6047 | 1083 | 18% | 131 | 12% |
| 2013 | 6093 | 1032 | 17% | 311 | 30% |
| 2014 | 6422 | 1149 | 18% | 289 | 25% |
| 2015 | 7382 | 1325 | 18% | 302 | 23% |
| 2016 | 4897 | 956 | 20% | 204 | 21% |
| 2017 | 4925 | 967 | 20% | 226 | 23% |
| 2018 | 5933 | 1036 | 17% | 206 | 20% |
| 2019 | 5192 | 763 | 15% | 57 | 7% |
| 2020 | 3827 | 575 | 15% | 32 | 6% |
| TOTAL | 56074 | 9870 | | 1831 | |

Table 5-4: Injury Severity identifier codes (highest in crash) (Source: FDOT Safety Office)

| Severity Identifier Code | Description |
|--------------------------|---------------------------|
| 0 | not coded/ unknown |
| 1 | None |
| 2 | Possible injury |
| 3 | non-incapacitating injury |
| 4 | Incapacitating injury |
| 5 | fatal (within 30 days) |
| 6 | non-traffic fatality |

Using the identifier codes, we categorized the pedestrian-involved crashes that occurred far away from Intersections (250 ft.), on mid-block crosswalks, driveways, side of roadways, and shoulders into their associated highest level of injury (see Table 5-5). To highlight the importance of the objective of the study, we focused on fatal crashes and created a new subset from the previously generated data based on the highest level of injury (highlighted in red in Table 5-5). The current subset contains 143 points that present the location of fatal pedestrian-involved crashes that occurred far away from intersections (i.e., crosswalks, driveways, or side of roadways) between 2011 to 2020 in Florida. In the following section, some characteristics associated with this certain group of crashes were investigated in detail.

Table 5-5: Pedestrian-involved crashes by the highest level of injury

| Code | Description | Highest Injury Severity | | | | | | | | | | Total |
|------|---------------------------|-------------------------|------|------|------|------|------|------|------|------|------|-------------|
| | | 2011 | 2012 | 2013 | 2014 | 2015 | 2016 | 2017 | 2018 | 2019 | 2020 | |
| 0 | Not Coded/Unknown | 0 | 0 | 0 | 0 | 0 | 0 | 0 | 0 | 0 | 1 | 1 |
| 1 | No Injury | 12 | 18 | 53 | 54 | 49 | 13 | 21 | 15 | 2 | 3 | 240 |
| 2 | Possible Injury | 18 | 43 | 81 | 85 | 92 | 61 | 52 | 64 | 15 | 3 | 514 |
| 3 | Non-incapacitating Injury | 24 | 47 | 115 | 89 | 103 | 70 | 86 | 69 | 15 | 4 | 622 |
| 4 | Incapacitating Injury | 13 | 14 | 46 | 40 | 41 | 37 | 52 | 38 | 12 | 10 | 303 |
| 5 | Fatality (within 30 days) | 6 | 9 | 12 | 20 | 17 | 21 | 14 | 20 | 13 | 11 | 143 |
| 6 | Non-traffic Fatality | 0 | 0 | 4 | 1 | 0 | 2 | 1 | 0 | 0 | 0 | 8 |
| | Injury code 3 & 4 & 5 | 43 | 70 | 173 | 149 | 161 | 128 | 152 | 127 | 40 | 25 | 1068 |
| | Injury code 4 & 5 | 19 | 23 | 58 | 60 | 58 | 58 | 66 | 58 | 25 | 21 | 446 |
| | Injury code 5 | 6 | 9 | 12 | 20 | 17 | 21 | 14 | 20 | 13 | 11 | 143 |

5.3.3. Facts and Statistics

In this section, we focused on fatality pedestrian-involved crashes that occurred on crosswalks, driveway, or side of roadways from 2011 to 2020 in Florida and create the following bar plots to illustrate the distribution of these crashes based on various attributes. Figure 5-7 shows a significant increasing trend during the period of 2011-2014, and after the sharp incline in 2014, there is an almost uniform distribution until 2018. It is also worth mentioning that the decrease after 2018 was mainly due to fact that crashes that occurred after this certain year are still being updated in the CAR database. Therefore, this decreasing trend may not reliable enough as of now.

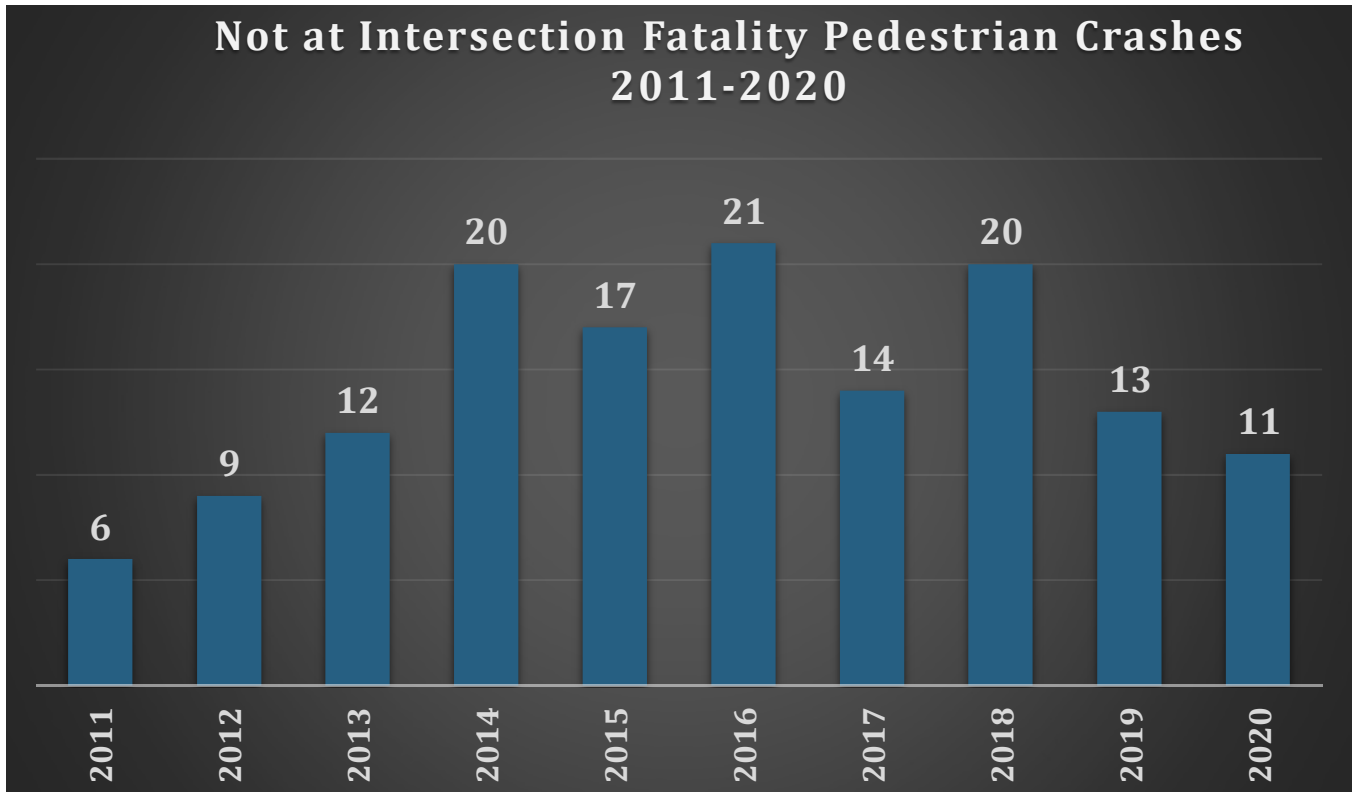


Figure 5-7: Crash distribution by year

We also investigated the crash distribution by the day of week and created the bar plot for the results (See Figure 5-8). No certain pattern was detected even when we categorized them based on weekdays and weekends. Moreover, Figure 5-9 illustrates that most of the fatal pedestrian-involved crashes did not occur under the influence of alcohol and/or drug influence, which is more common during weekend crashes (J. Liu et al., 2019; Pour-Rouholamin & Zhou, 2016). Thus, it could be concluded that pedestrian-involved crashes would be expected to occur on each day of a week. Light condition is also among the factors that was not highly correlated with the probability of this certain type of crash (See Figure 5-10). Assessing weather conditions associated with these crashes, on the other hand, reveals a significant contribution of clear weather conditions on increasing the probability of crashes (See Figure 5-11). This indicates that drivers and pedestrians both are more cautious during adverse weather conditions, as expected based on previous research works (Shaon, Qin, Chen, & Zhang, 2018).

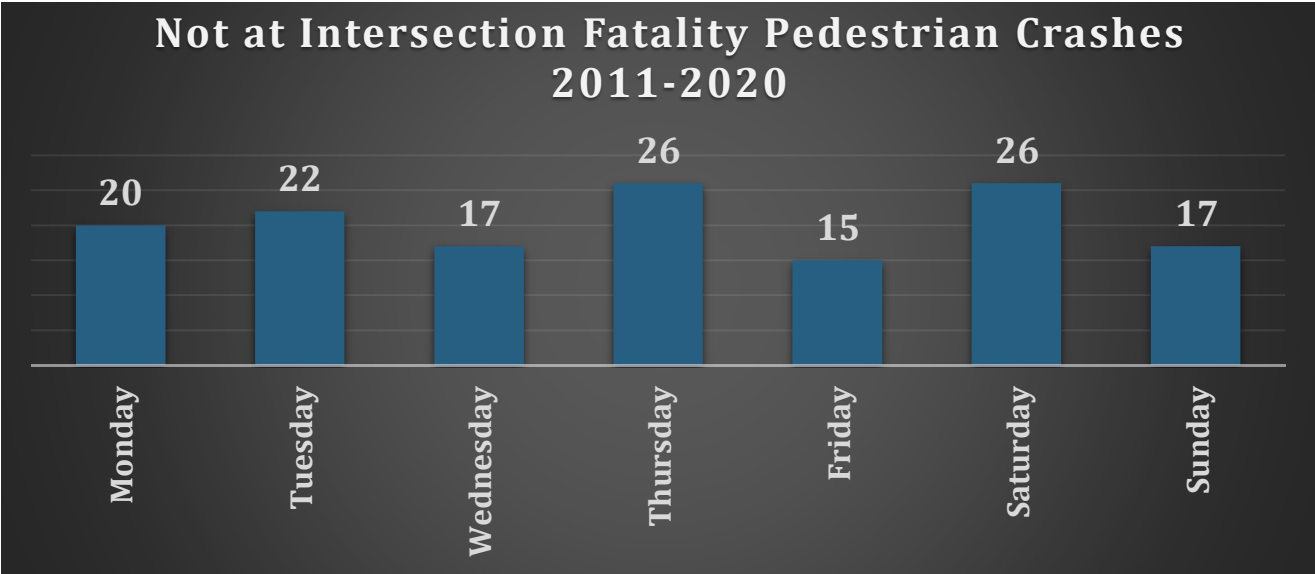


Figure 5-8: Crash distribution by day of week

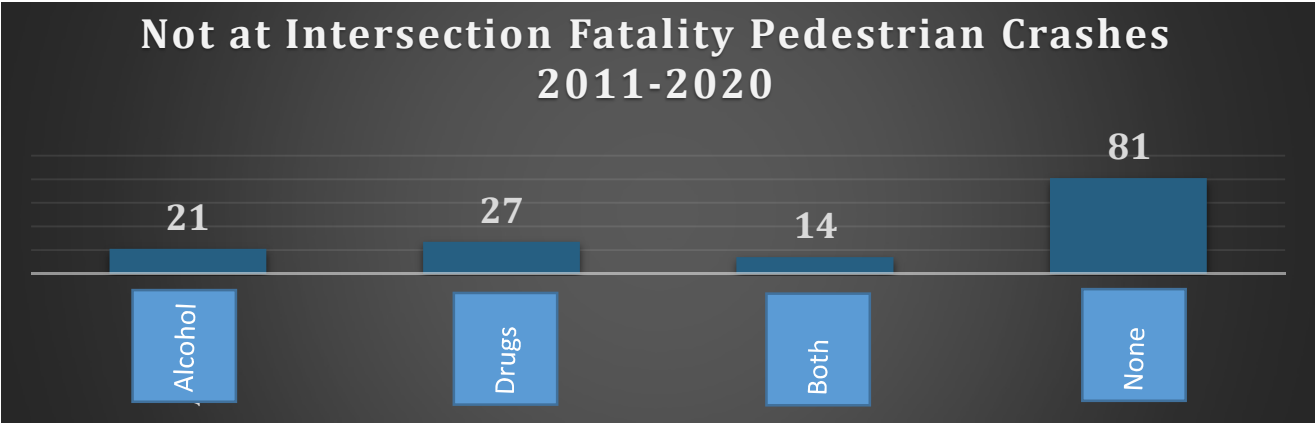


Figure 5-9: Alcohol and/or drug influence on pedestrian-involved crashes

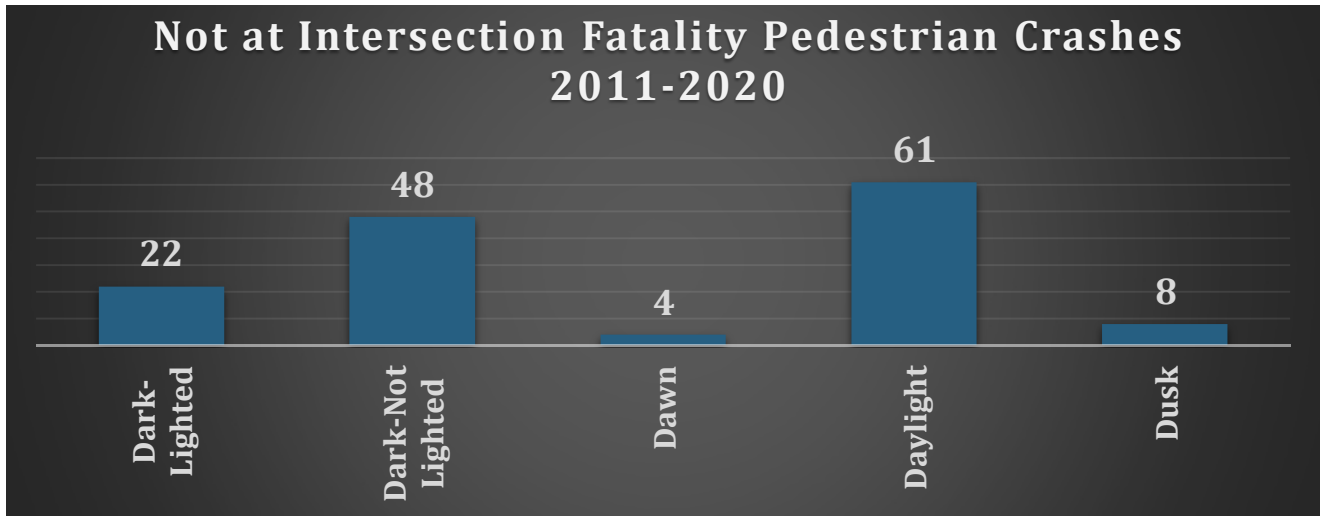


Figure 5-10: Crash distribution by light condition

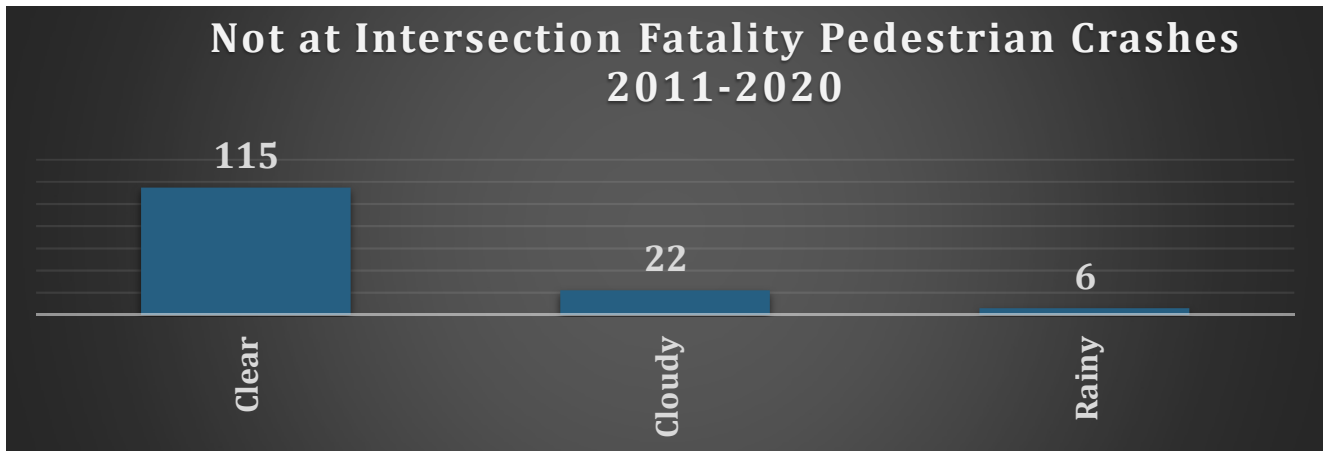


Figure 5-11: Crash distribution by weather condition

These distribution assessments are followed by a statistical spatial analysis approach that enables us to evaluate the contribution of crash lanes and crash locations based on their distance from the center of the nearest intersections. Figure 5-12 illustrates that the significant percentage (76.2%) of fatal pedestrian-involved crashes occurred on side of roadways and shoulders. We also explored the exact crash locations that occurred on side of roadways and identified that most of them were in the middle of the roadways or median lanes instead of the side of roadways or shoulders. Figure 5-14 shows some examples of these crashes that were wrongly mapped as they were in the middle of the roadways. In order to make sure that these crashes occurred on side of roadways, we need to go through the long format of the crash reports and check the narrative descriptions or the attributes associated with pedestrian action at the time of crashes. In this way, we would find if the pedestrian were walking along the roadway or crossing the segment and could categorize them as “on side of roadway” or “on main lanes”, respectively.



Figure 5-12: Crash distribution by crash lane

Figure 5-13: Crashes labeled as “side of roadways” (wrongly mapped in the middle of the roadway). {Continued with the next page}

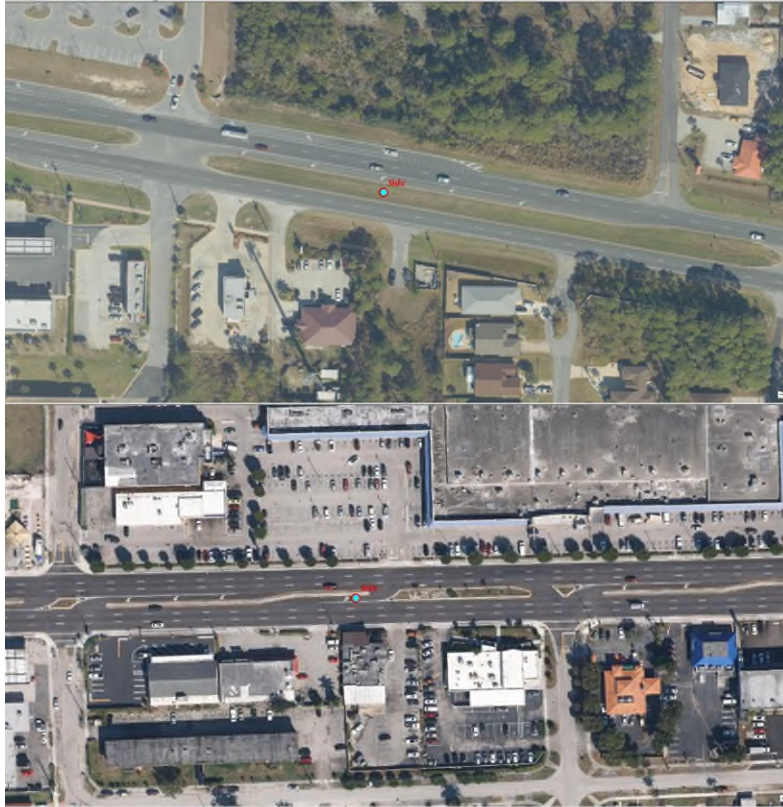


Figure 5-14: Crashes labeled as “side of roadways” (wrongly mapped in the middle of the roadway). {Continued from the previous page}

Next, a network analysis method has been performed to calculate the distances between fatal pedestrian-involved crashes and the nearest intersection center. Based on Figure 5-15, the crash frequencies seem to be skewed to right which denotes that the mean (average) distances are lower than the median value. This indicates that crashes that were not under the influence of intersection presence also still tended to occur closer to the intersections. Regardless of higher crash frequency near intersections, statistical analysis reveals there is a positive correlation between the above-mentioned distance and the highest level of injury. The black dash-line shown in Figure 5-16 has a slight positive slope that indicates getting far away from intersections would increase the probability of crash occurrences with a higher injury severity.

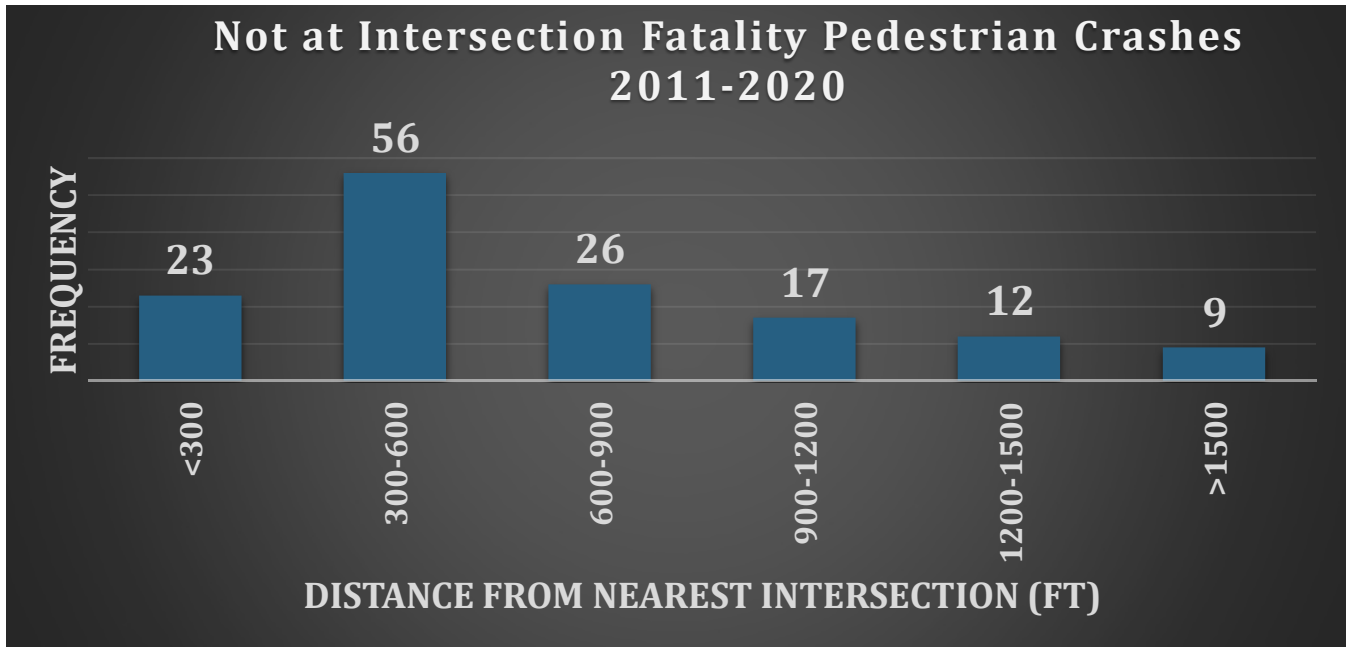


Figure 5-15: Distance between crashes and nearest intersection

Figure 5-16: Relationship between the highest level of injury and distance from the nearest intersection

The results of the linear regression model are provided in Table 5-6. In the table, the estimated coefficient shows the positive or negative contribution of the predictor variable, which is, the distance between the crash location and nearest intersection, on the response variable, the highest level of injury. Standard Errors, estimate the standard deviation of the coefficients in the model. That is, it measures the precision of the model. Also, p-values reveal the significance level of the predictor variable on the response variable, and this value has been used to examine whether a predictor variable has significance at the 90% or higher on the linear regression model.

Table 5-6: Linear regression model between highest level of injury and distance from intersection

| Variables | Estimated Coefficient | Standard Error | P-value | 90% Level of Significance |
|------------------------------------|------------------------------|-----------------------|----------------|----------------------------------|
| (Intercept) | 2.732e+00 | 3.671e-02 | <2e-16 | ✓ |
| Distance from Nearest Intersection | 8.591e-05 | 3.771e-05 | 0.0228 | ✓ |

Number of observations: 143; p-value: 0.02285; Multiple R-squared: 0.002829
Highest Level of Injury ~ Distance from Nearest Intersection

5.3.4. Hotspot Counties

In this section, we intended to identify hotspot locations where fatal pedestrian-involved crashes occurred the most. This will determine if there is any statistically significant clustering in the spatial pattern of the data. Crash point features can be analyzed using the point counts option; however, there are only 143 fatal pedestrian-involved crashes in the State of Florida. Thus, conventional hotspot identification methods could not provide accurate outputs and result in over/underestimations (Wang et al., 2021). Therefore, we calculated the number of crashes that occurred within each county and ranked them in descending order. Based on Figure 5-17, Orange, Hillsborough, and Pasco are among the counties with a significant number of crashes of this certain type. In addition to these three counties, we also explored Leon County due to the high rate of fatality pedestrian-involved crashes with regards to its low population.

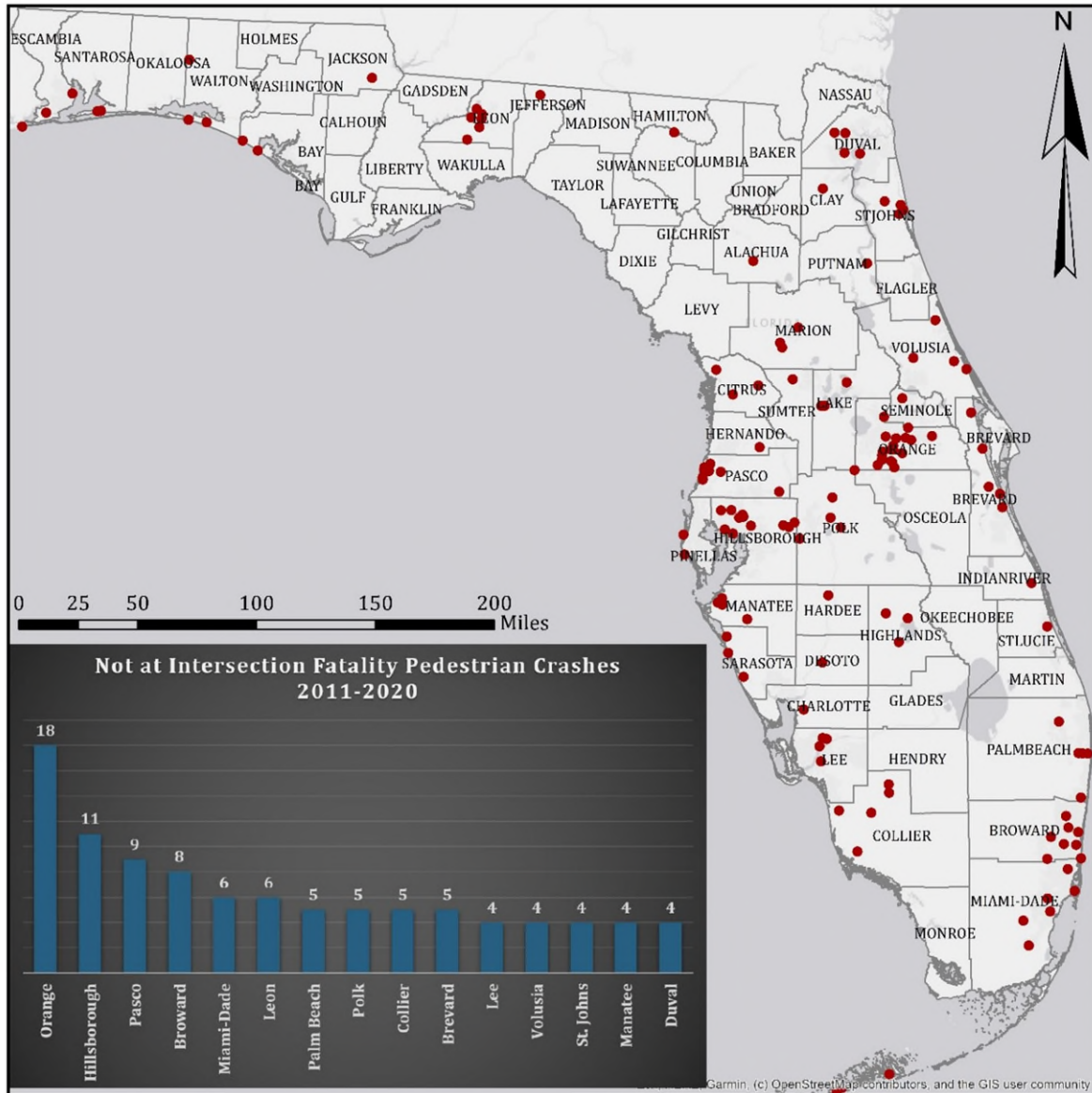


Figure 5-17: Fatality pedestrian-involved crashes in Florida during 2011-2020

To identify the roadway corridors that need urgent countermeasures to improve pedestrian safety, there is a need to explore the hotspot counties at a micro-level. There are 143 pedestrian-involved fatal crashes between 2011 and 2020 in Florida and detailed screenshots for crash are provided in the APPENDIX A. The following figures illustrate the pedestrian-involved crashes that occurred between 2011 and 2020 in each of these three counties. In each figure, the legend contains the number of crashes by crash lane. Moreover, crash points are symbolized based on their highest level of injury: a) red for fatal, b) black for incapacitating, and c) blue for incapacitating pedestrian-involved crashes. Detailed investigation of the crash locations revealed that, pedestrians mostly prefer the segments around turning left lanes to cross the roadways regardless of wider lane width. Presumably, pedestrians suppose that drivers may decrease their speed and be more cautious in these areas. Also, drivers may be more distracted while changing

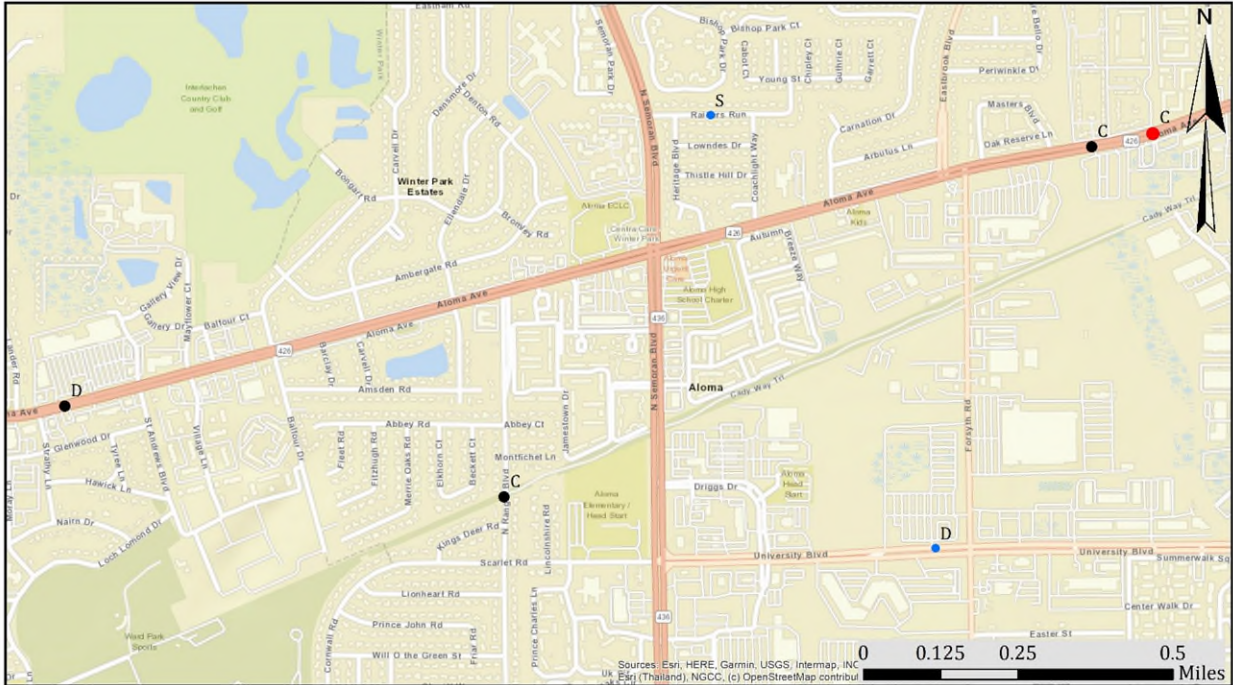


Figure 5-19: Orange County – Area (A) – Aloma Ave.

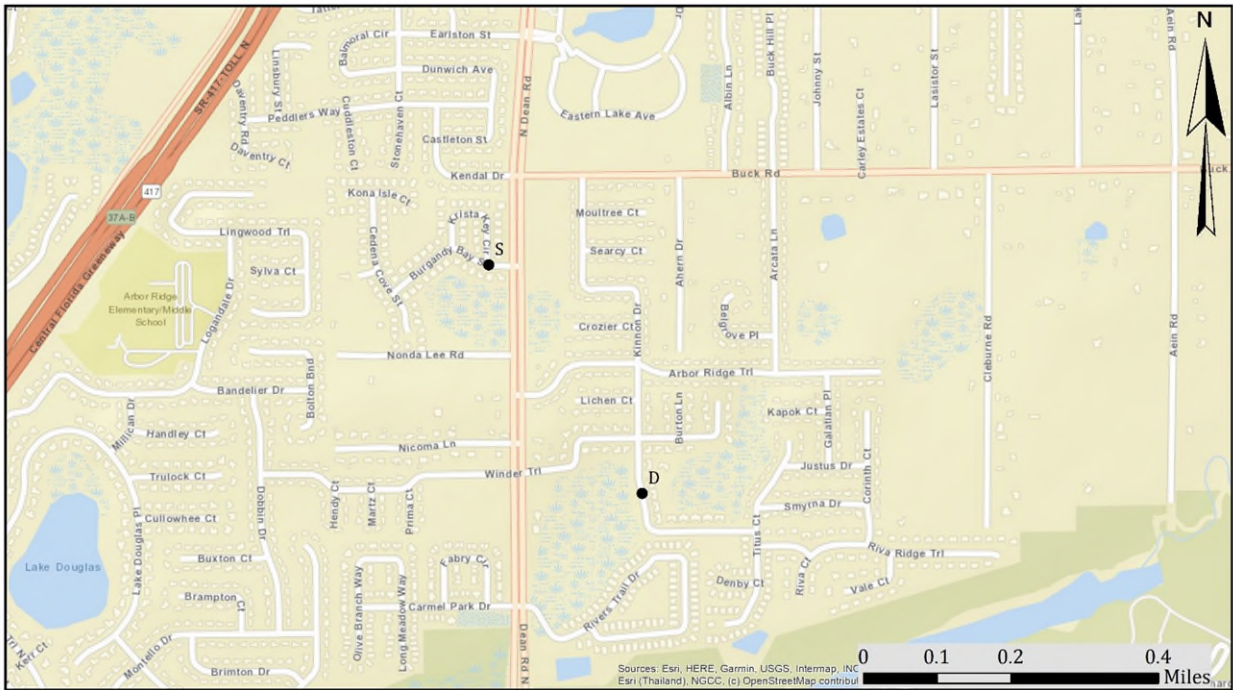


Figure 5-20: Orange County – Area (B)

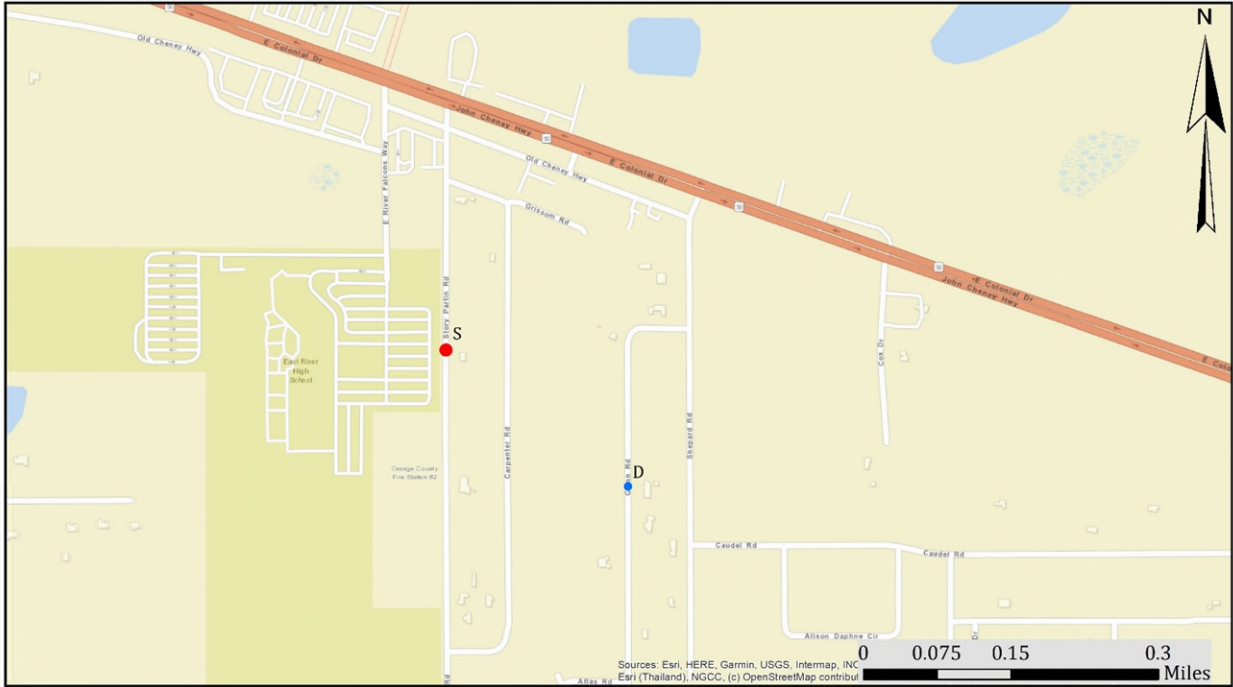


Figure 5-21 : Orange County – Area (C)

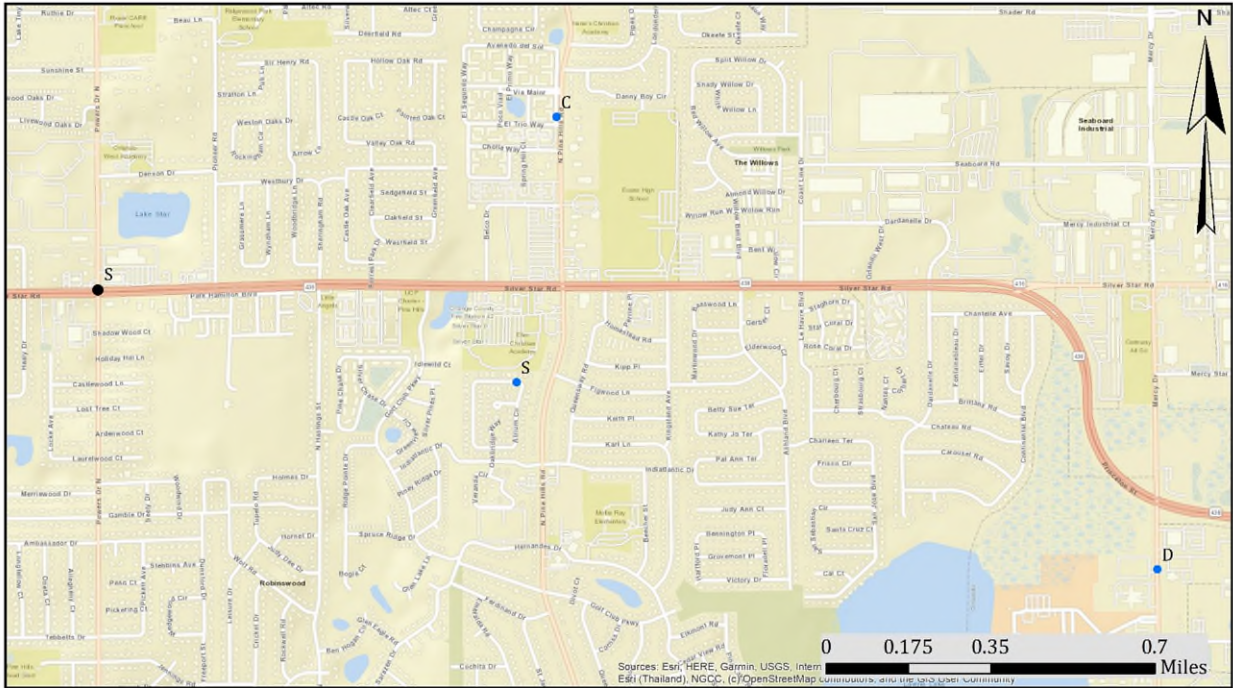


Figure 5-22: Orange County – Area (D)

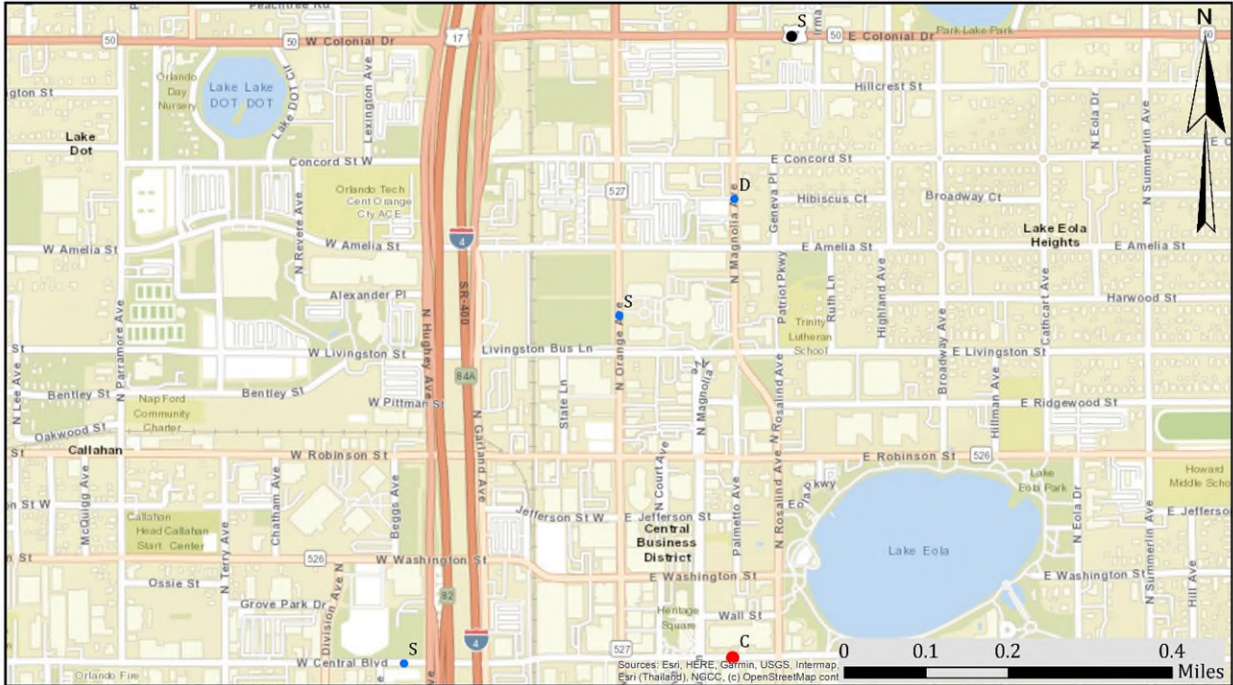


Figure 5-23: Orange County – Area (E) – West Central Blvd.

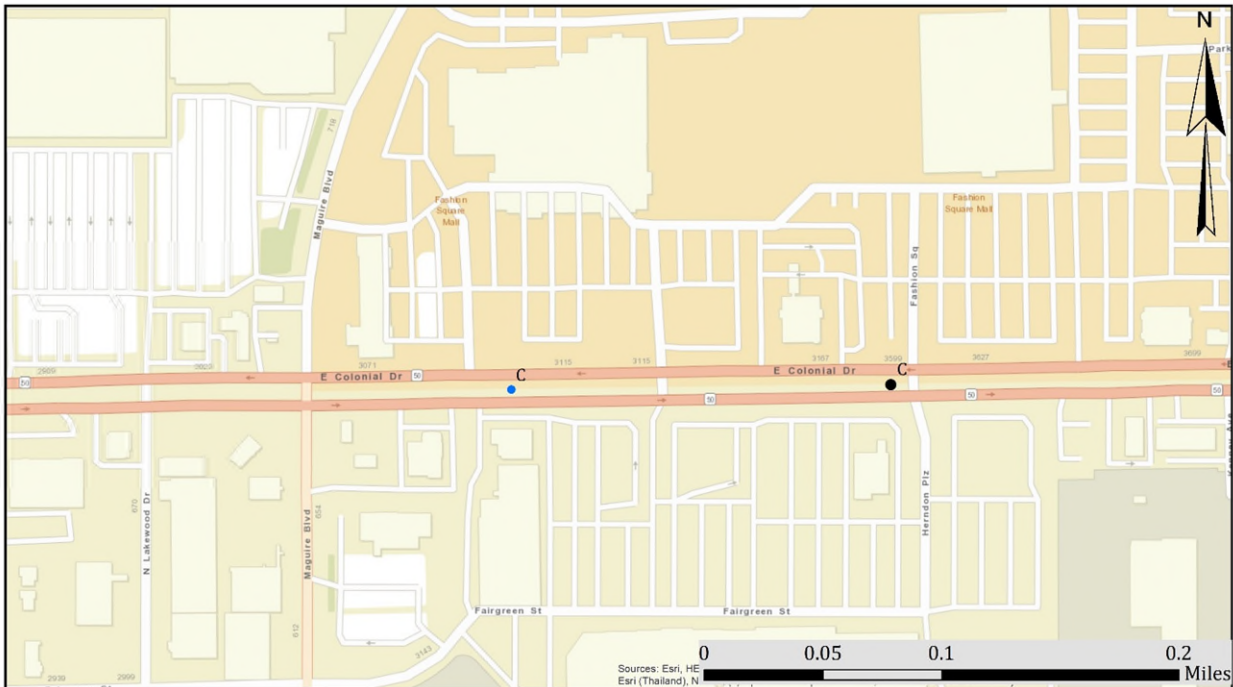


Figure 5-24: Orange County – Area (F) – East Colonial Dr.

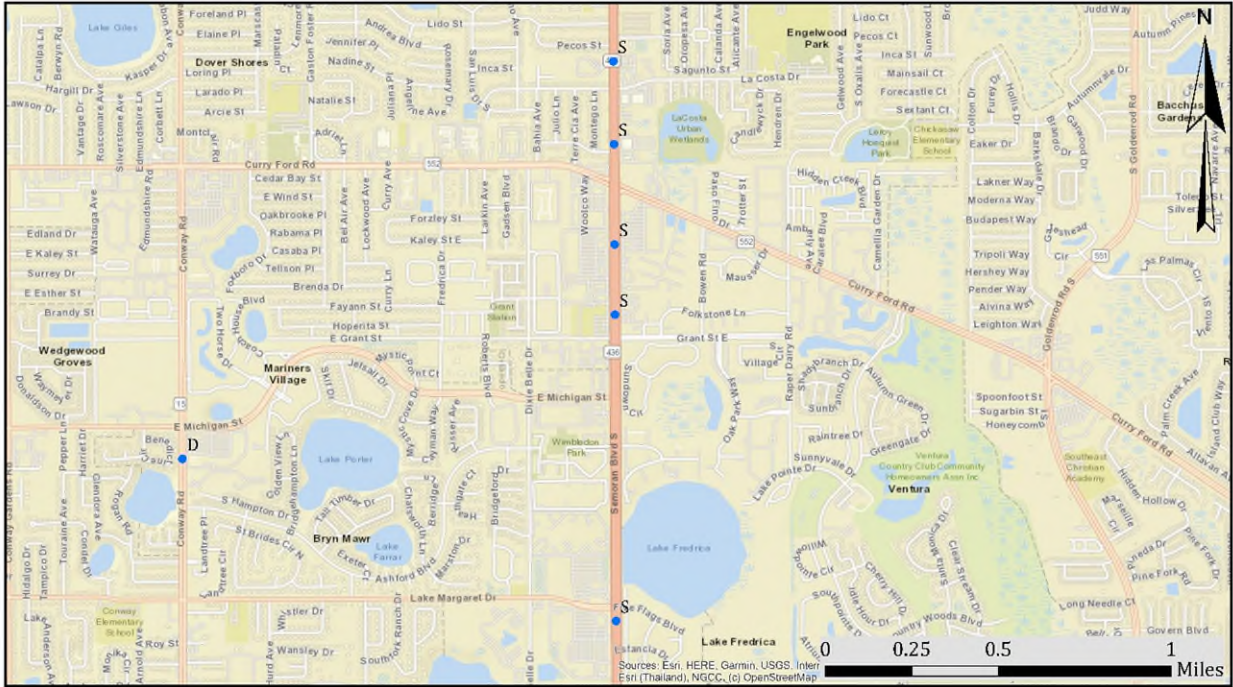


Figure 5-25: Orange County – Area (G) – South Semoran Blvd.

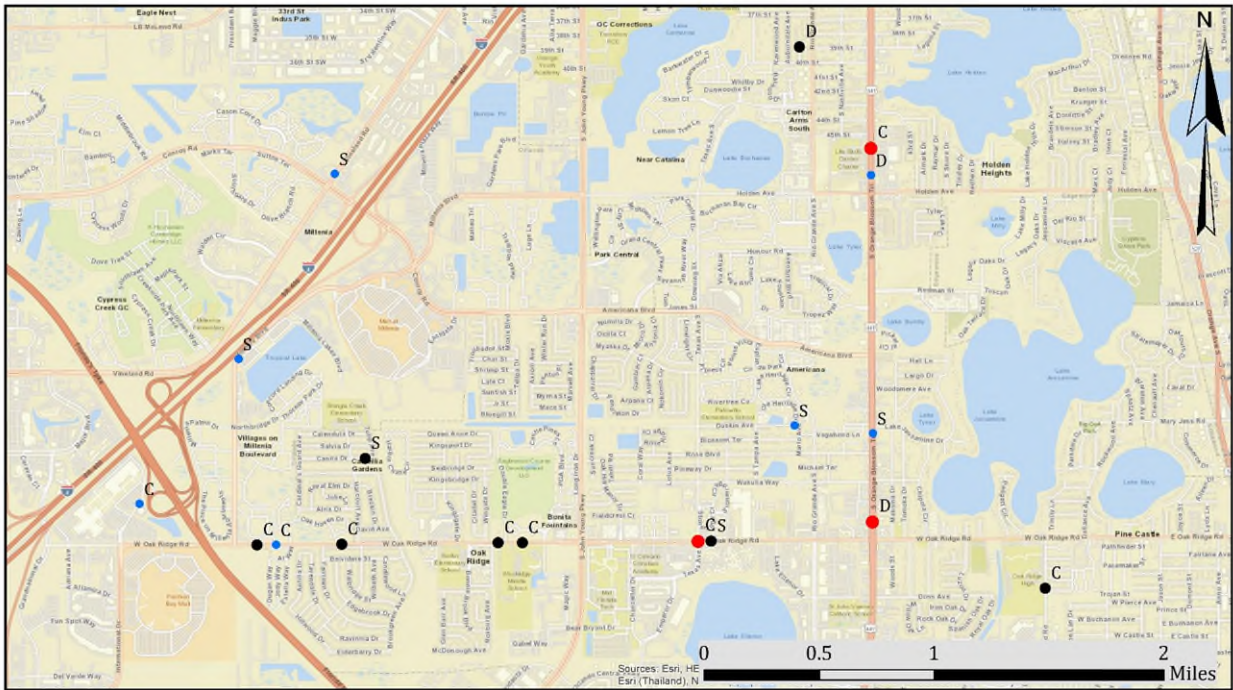


Figure 5-26: Orange County – Area (H) – South Orange Blossom and West Oak Ridge Rd

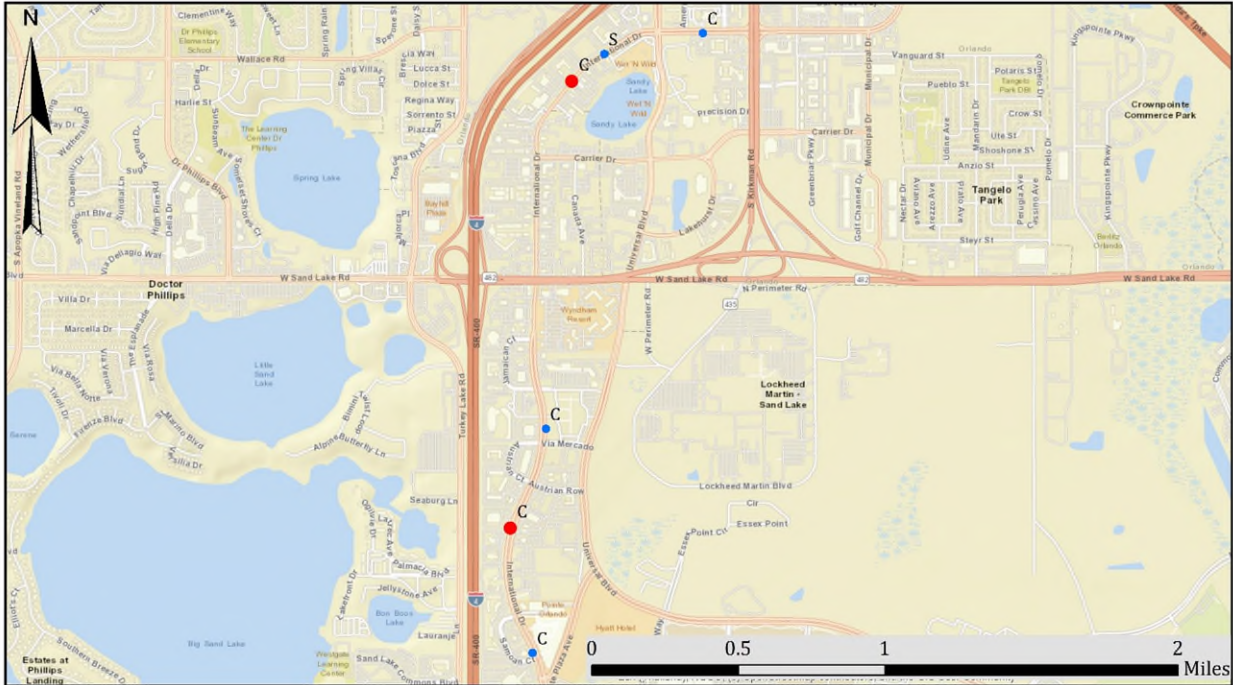


Figure 5-27: Orange County – Area (I) – International Dr.

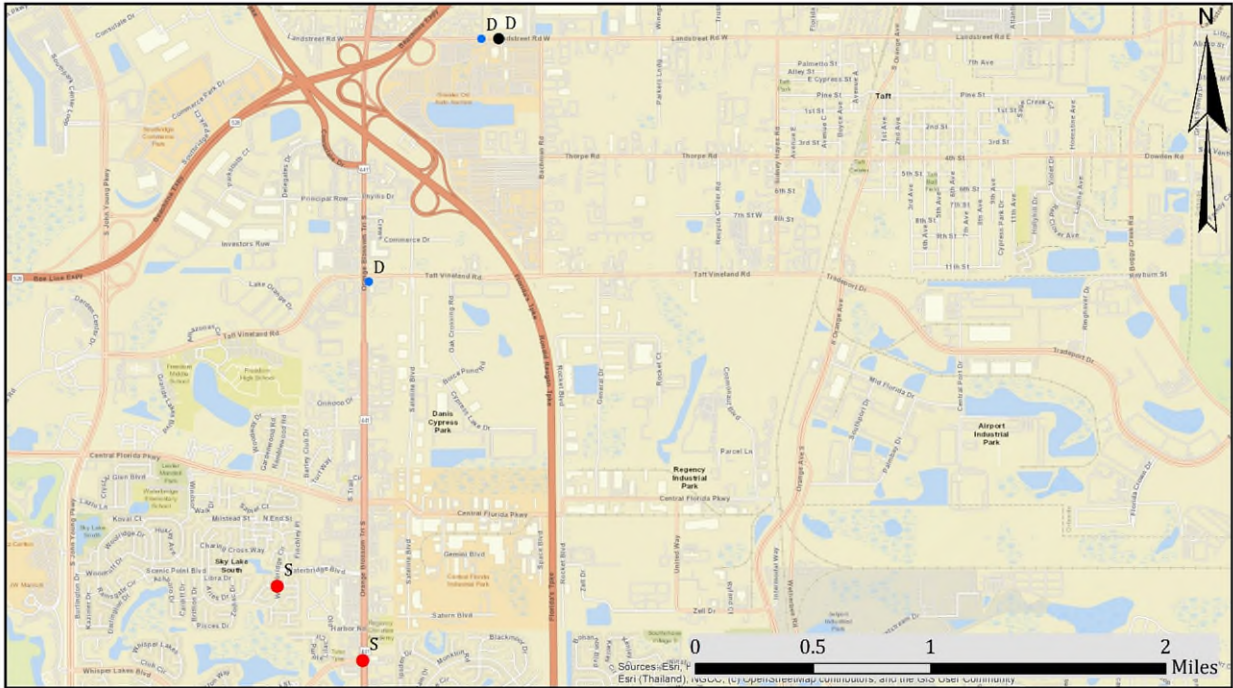


Figure 5-28: Orange County – Area (J) – Landstreet Rd.

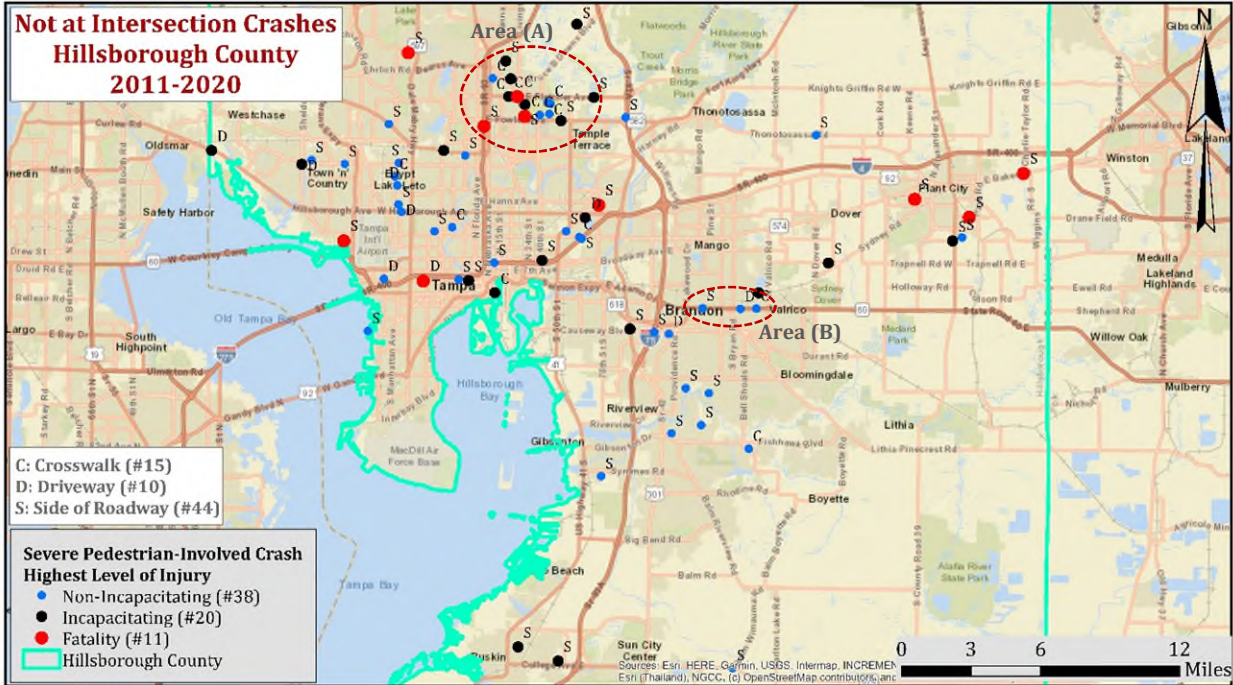


Figure 5-29: Pedestrian-involved crashes in Hillsborough County

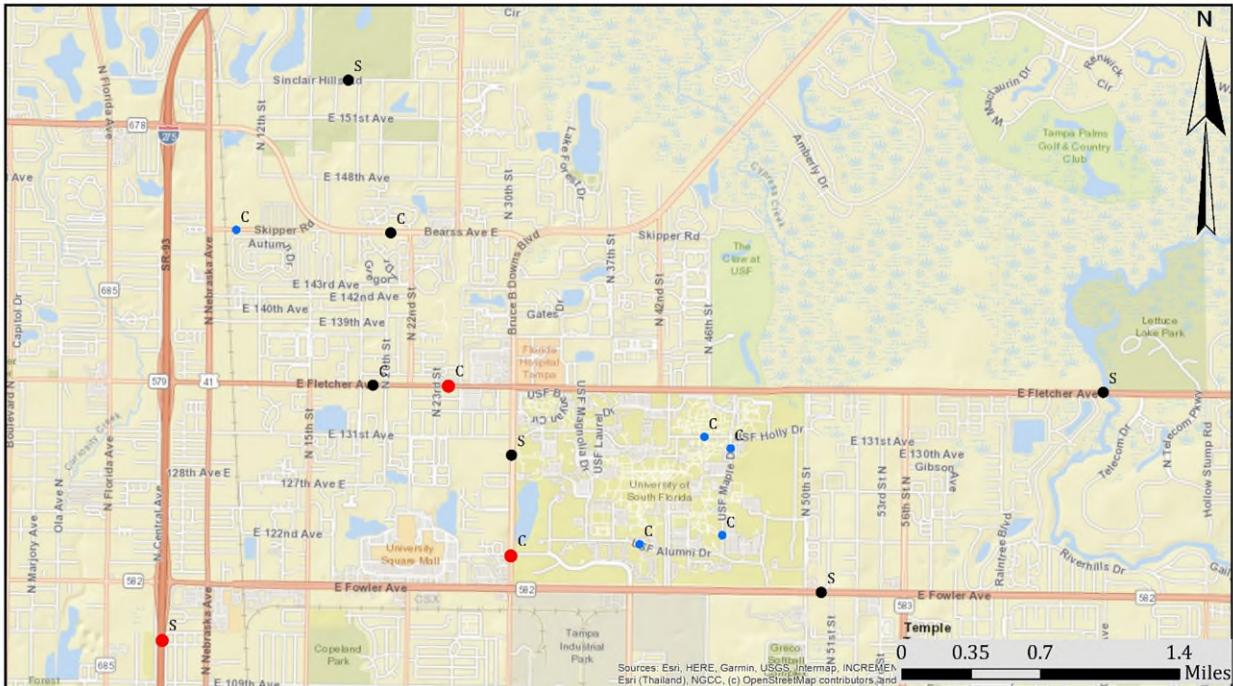


Figure 5-30: Hillsborough County - Area (A) – East Fletcher Ave., Maple Dr. (Around USF campus), and Bruce B Downs Blvd

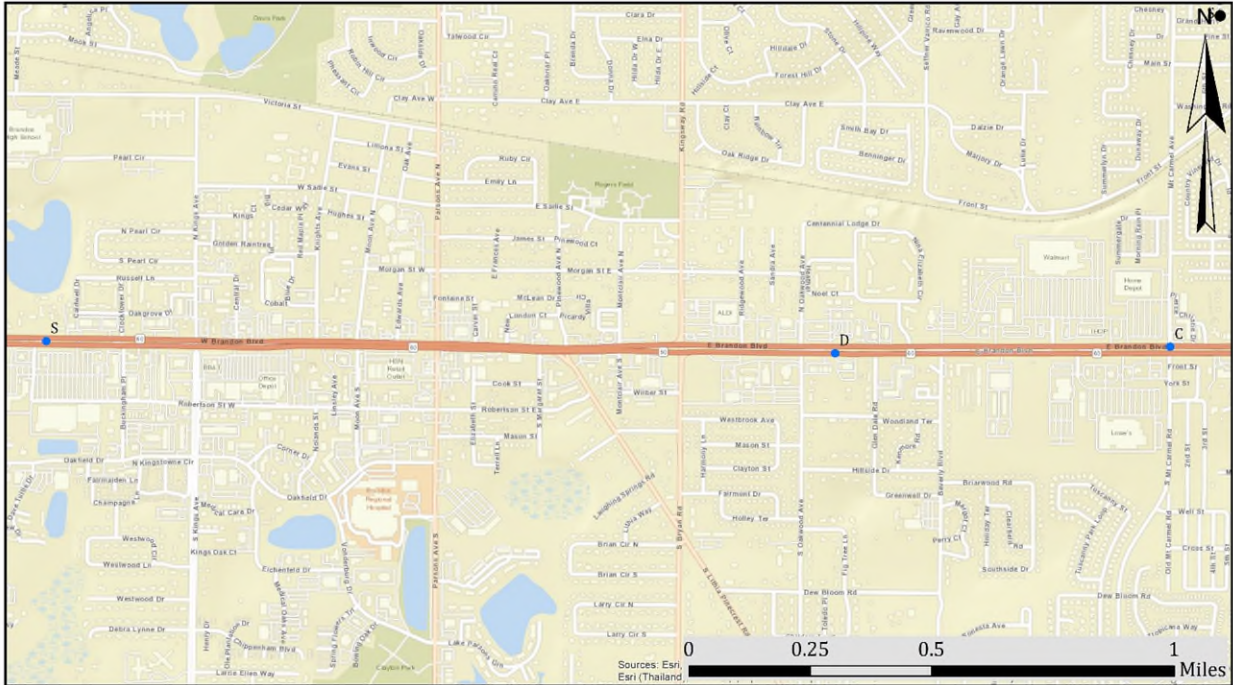


Figure 5-31: Hillsborough County – Area (B) – Brandon Blvd.

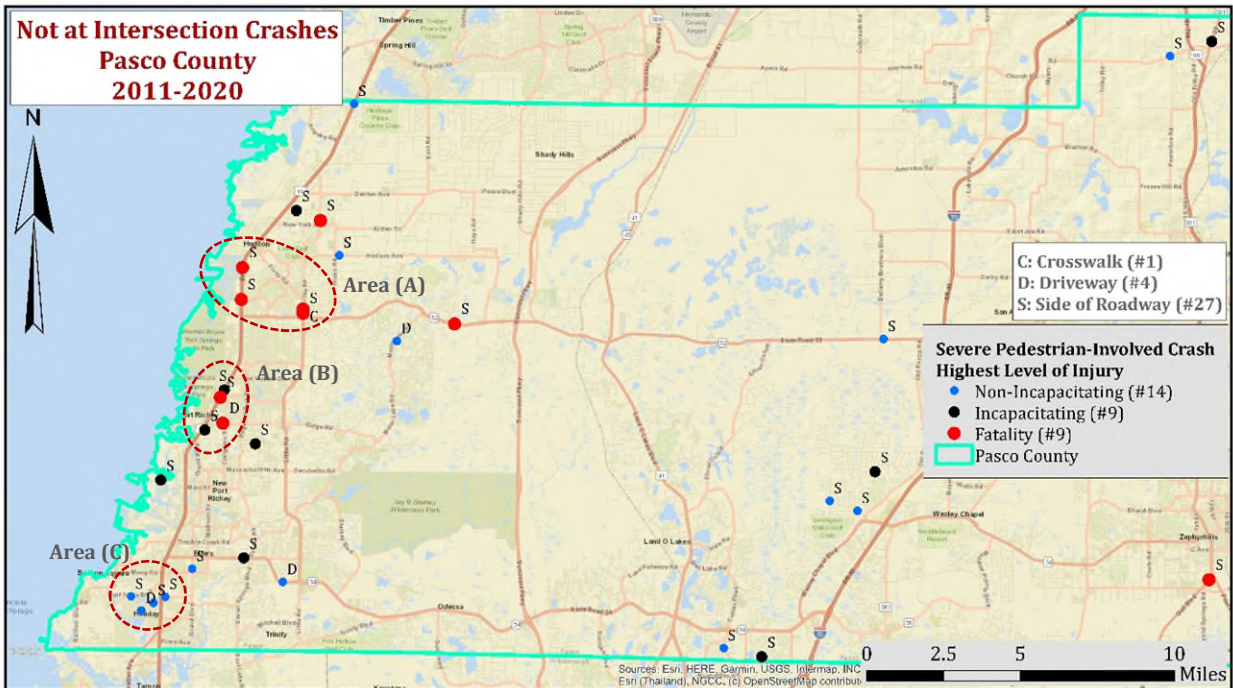


Figure 5-32: Pedestrian-involved crashes in Pasco County

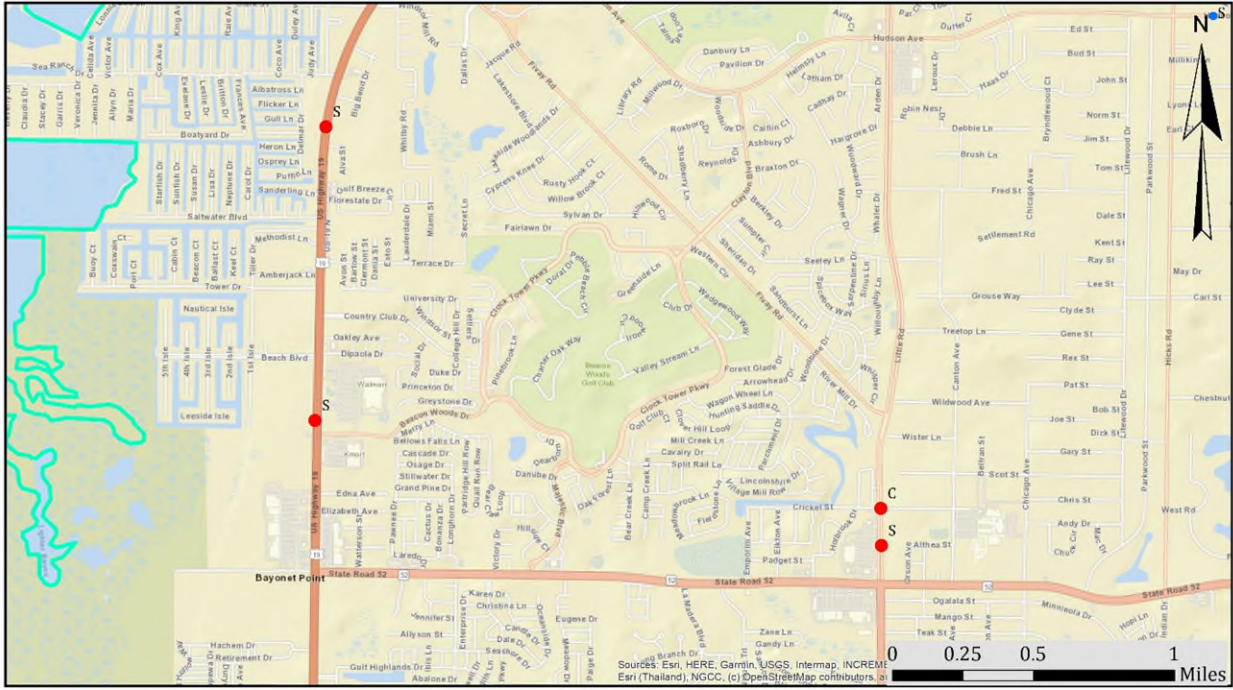


Figure 5-33: Pasco County - Area (A) – US-19 Highway and Little Rd

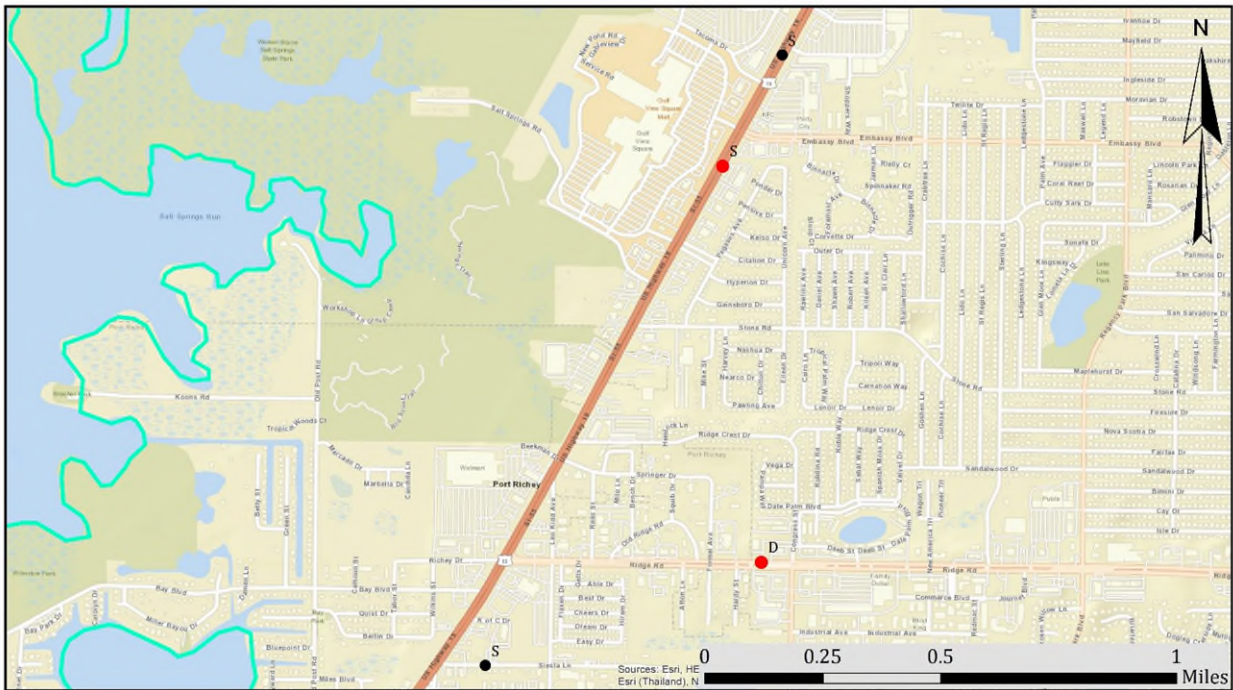


Figure 5-34: Pasco County - Area (B) – US-19 Highway

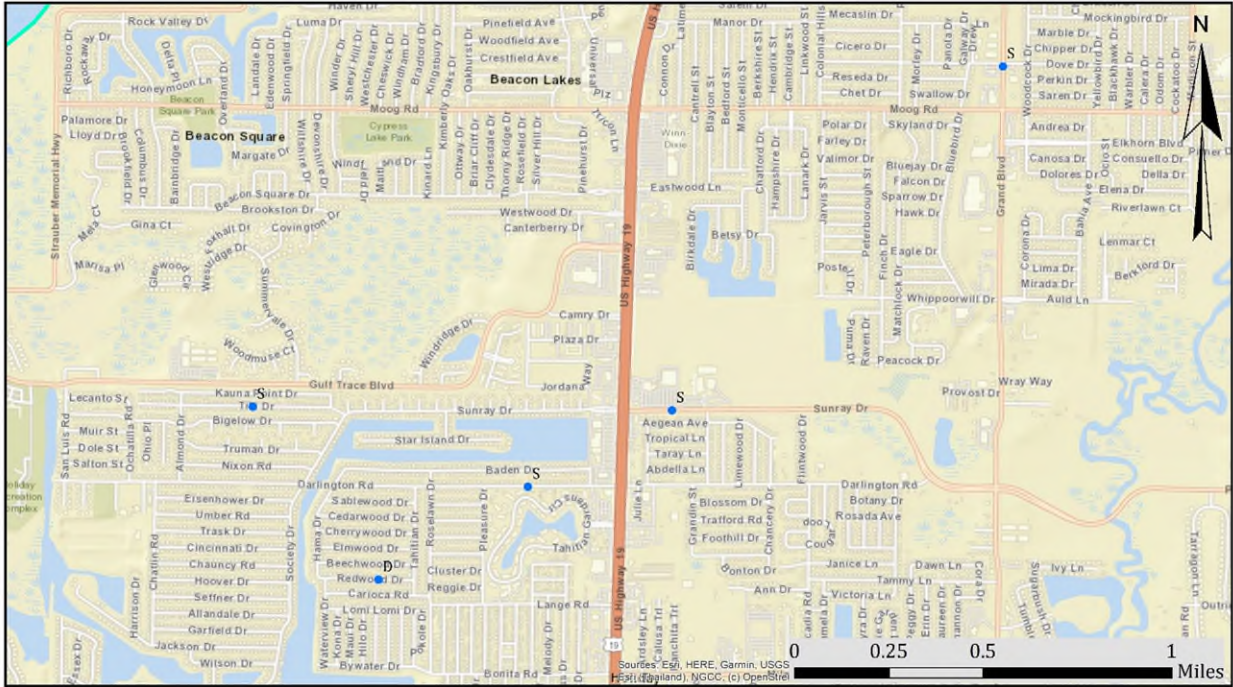


Figure 5-35: Pasco County - Area (C)

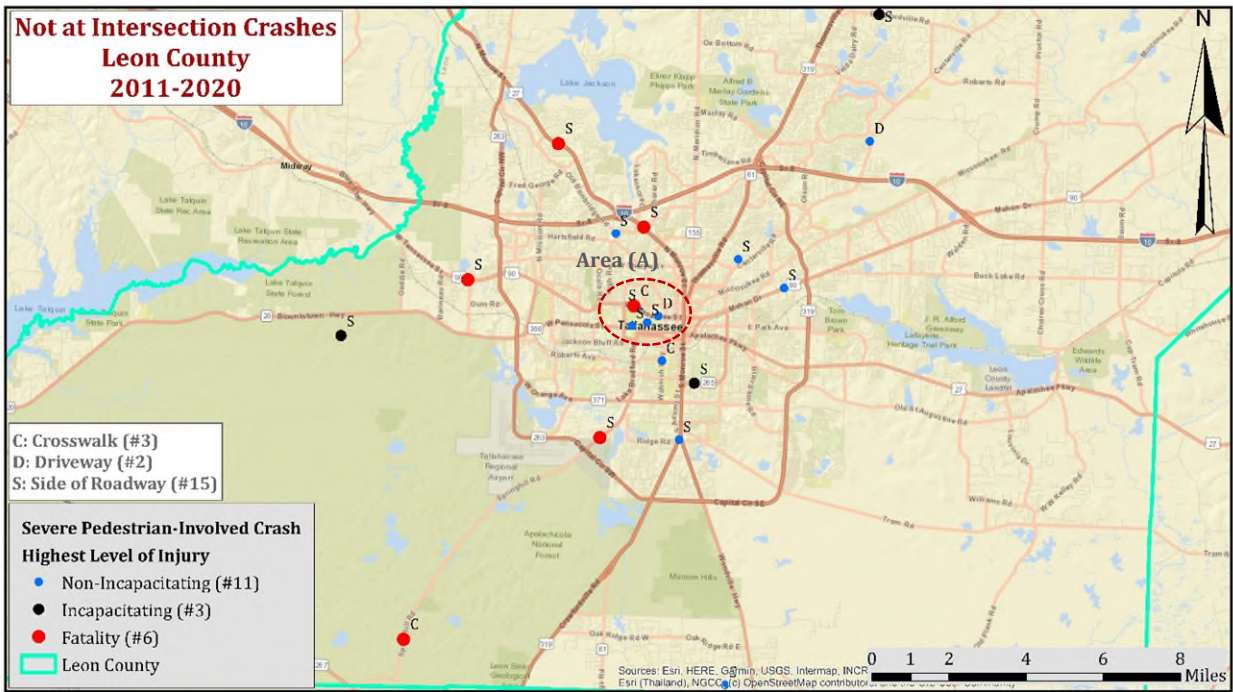


Figure 5-36: Pedestrian-involved crashes in Leon County

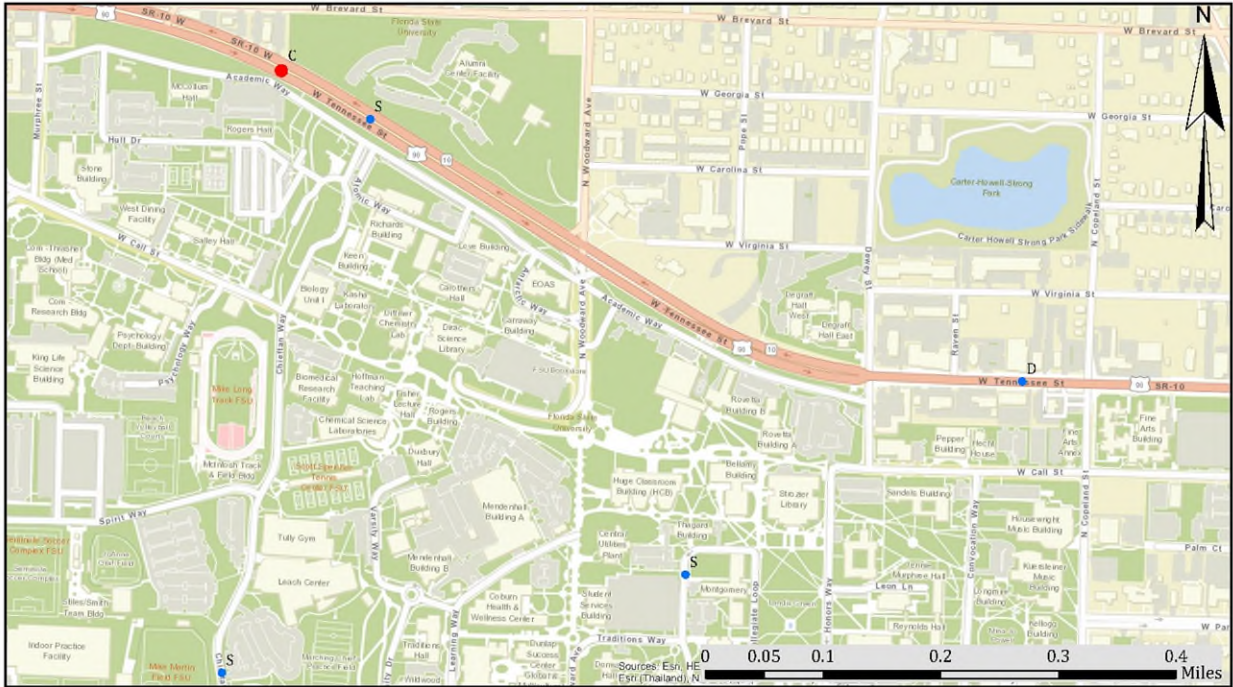


Figure 5-37: Leon County - Area (A) – Tennessee St.

Figure 5-38: Fatality crashes in Front Beach rd.- Panama City - Bay County – Speed limit 30 mph

5.3.5. Crashes in the Vicinity of a Left-Turn Lane

In this section, we intended to assess the contribution of turning left lane presence on occurrence of fatal pedestrian-involved crashes that occurred not at intersection. Our assumption is as follows: Pedestrians expect drivers to reduce their speed and yield the crosswalk to them when crossing the travel lane. In order to do so, we first examine the long format of the crash reports' narratives to assure that the pedestrian was attempting to cross the travel lane in the vicinity of turning left lanes. Therefore, we removed the crashes where pedestrians were walking along the side of roadways. After careful examination of the crash reports, we identified that 51

fatal pedestrian-involved crashes occurred in the vicinity of left turn lanes out of 143, and only 10 of them were directly influenced by the left turn lane presence. Remaining crashes mostly occurred on the side of roadways. With such a low number, there was not way to develop a statistical model that would evaluate the contributing factors to these crash occurrences. Table 5-7 shows more details for these crashes.

Table 5-7: Fatal pedestrian-involved crashes that occur at locations that are not intersections and under the direct influence of left turn lanes

| Year | County | Time | Light Condition | Weather Condition | On Crosswalk | Day of Week | Hit and Run | Drug/Alcohol Influence | | Age | | Gender | |
|------|---------------|-------|--------------------|-------------------|--------------|-----------------|-------------|------------------------|------------|--------|------------|--------|------------|
| | | | | | | | | Driver | Pedestrian | Driver | Pedestrian | Driver | Pedestrian |
| 2011 | Bay | 20:59 | Dark - Not Lighted | Clear | NO | Tuesday | NO | NO | NO | 43 | 43 | Male | Female |
| 2014 | Orange | 21:59 | Dark - Lighted | Clear | NO | Sunday | NO | NO | NO | 41 | 29 | Male | Female |
| 2015 | Brevard | 18:04 | Dark - Not Lighted | Cloudy | YES | Wednesday | NO | NO | NO | 68 | 48 | Male | Female |
| 2016 | Orange | 19:58 | Dark - Lighted | Clear | YES | Thursday | NO | NO | NO | 35 | 60 | Male | Male |
| 2016 | Orange | 8:21 | Daylight | Clear | YES | Sunday | NO | NO | NO | 22 | 59 | Female | Male |
| 2016 | Bay | 2:15 | Dark - Lighted | Clear | YES | Saturday | YES | NA | NO | NA | 51 | Na | Female |
| 2017 | Orange | 23:50 | Dark - Lighted | Clear | YES | Friday | NO | NO | NO | 46 | 66 | Female | Female |
| 2017 | Hillsborough | 7:08 | Daylight | Clear | YES | Saturday | YES | NO | NO | 23 | 70 | Male | Male |
| 2019 | Pasco | 21:02 | Dark - Not Lighted | Clear | NO | Saturday | NO | NO | NO | 62 | 55 | Male | Male |
| 2019 | Bay | 20:20 | Dark - Lighted | Clear | YES | Saturday | YES | NA | NO | NA | 46 | Na | Female |

Based on Table 5-7, Orange County appears to be still among the counties with the highest number of crashes of this type. Among these 10 crashes, 6 occurred during the weekend. In addition, visibility seems to be a significant factor since it increases the probability of occurrence of this type of crash. Based on the careful examination of the narratives and what was mentioned by the independent witnesses, the victims of these crashes were expecting the driver to stop and yield the crosswalk to them and continued walking on the crosswalk. However, drivers could not control their vehicle and hit the pedestrians. In some other cases, the vehicle in the inner lane stopped and yielded the crosswalk to the pedestrian, but the other vehicle in the outer lane continued to travel directly toward the pedestrian. This was mainly due to insufficient sight distance. The detailed crash diagrams for these 10 crashes are provided in the APPENDIX B.

5.3.6. Conclusions on Crash Analysis

Based on the conducted experiment and the challenges faced, the following conclusions are provided:

- Conventional statistical methods could not identify hotspot locations due to the low number of crashes.
- Although the pedestrian-involved crashes labeled as “crosswalks” were not exactly located on them, the distances were less than 50 ft.
- Turning left lanes are among the locations with a significant number of pedestrian-involved fatal crashes and therefore require more attention.
- As part of Task 4, we proposed a method to categorize crashes into “at intersection” and “not at the intersection” based on their associated roadway network distance from the center of intersections; however, a discontinuity in the roadway network shapefile results in the wrong detection in some cases.
- Careful evaluation of crash reports’ narratives reveals that despite the limited number of crashes that occurred under the direct influence of left turning movement, the pedestrians may still expect drivers to be more cautious and reduce their speed in order to yield the crosswalk to them. It could be also concluded that, the authorities may need to add more safety features to accommodate pedestrians with a safe route to cross in addition to facilitating a section of a roadway as a crosswalk. These safety features include beacons, flashing lights, speed humps, and pavement markings to inform the drivers of the possible presence of pedestrians ahead.

5.4. Comparative Cost Analysis and Recommendations on Drone-based Traffic Data Collection Analysis

This part of the study provides a cost-based comparison between the traditional methods and drone-based traffic data collection with tethered and untethered alternatives. First, previously performed work using the traditional methods were summarized. Second, a comparative cost

analysis was carried out with a focus on a) the fixed and work-hours, and b) potential software development that uses the trajectory data as input and populates the MUTS forms automatically.

5.4.1. Summary of Previously Conducted Work Using Traditional Methods

Previously conducted studies in the study locations are all related with signal warrant study and intersection control strategy evaluation. This process may require a 12 hours-long data collection and make the traditional methods compatible with the prolonged flight time capability of tethered drones. Details of the previously conducted studies are presented in Table 5-8 with the contractor company, field collected data and available cost of the work to FDOT.

As it can be seen from the previous studies, the main data collected from the field is the Turning Movement Counts (TMC). For example, signal warrant studies (performed on the locations of Tallahassee 1, Jacksonville 1, and Jacksonville 2) are the most common methods to conduct an engineering analysis to determine whether a signal control is required on an uncontrolled or stop-sign controlled intersection. This process requires extensive field data collection such as 8-hour vehicular traffic volume, speed (if posted speed limit is not used as the reference speed), 4-hour vehicular traffic volume, peak hour volume, and pedestrian volume. Therefore, the comparative cost analysis was based on the idea of extracting the TMCs using traditional methods versus drone-based traffic data collection.

5.4.2. Comparative Cost Analysis

This part of the study compares the costs associated with conducting a signal warrant analysis on a Florida intersection with different methods, namely drone-based alternatives and the traditional method. The cost estimates were calculated based on 8 hours of traffic count data (Warrant #1 requirements) and it was assumed that no further field data collection was required to sign and seal the final signal warrant study report. The 8 hours of the data collection was envisioned to be 3 hours for each AM and PM peaks and 2 hours for the midday peak (i.e., lunch time). The exact times can be determined by the traffic engineer using the previous volume counts on the major roadway of the studied intersection.

Table 5-8: Summary of previous studies conducted using traditional methods

| Study Location | Report Date | Contractor | Summary | Field Collected Data | Total Cost |
|--------------------------------|--------------|-------------------|-----------------------------------------------------------------------------------------------------------------------------------------------------------------------------------------------------------------------------------------------------------------------------------------------------------------------------------------------------------------------------------------------------------------------------------------------------------------------|---------------------------------------------------------------------------------------------------------------------------|-------------|
| Tallahassee 1 | Jan 8, 2021 | Roark Engineering | <ul style="list-style-type: none"> • 2019 data from an FDOT count station located half mile away used for background traffic. • Peak hours: 7:00-8:00 AM and 5:00-6:00 PM • TMC were collected only for peak hours. • No warrant were met to justify a signal installation | <ul style="list-style-type: none"> • 2 hours of turning movement counts (TMC) | - |
| Tallahassee 2 | Nov 5, 2018 | HNTB | <ul style="list-style-type: none"> • FDOT Intersection Control Evaluation (ICE) toolset were used • Safety Performance Evaluation and Benefit Cost analysis were carried out. • RCUT installation was found the most beneficial control strategy due to the angle crashes | <ul style="list-style-type: none"> • No field data collection (Mostly historical crash data are used) | - |
| Jacksonville 1 | Jan 26, 2021 | Peters & Yaffee | <ul style="list-style-type: none"> • Various analyses were conducted including access management, 5-year work program, crash history, field review for 1 h, TMC for 12 h, delay analysis, synchro analysis. • Warrants 1,2, and 3 met but there are intersections in the proximity (access management not met) • Recommended to prevent NB and SB left turns and additional volume of U turns were studied for closest intersections | <ul style="list-style-type: none"> • 12 hours of TMC • Delay study • 1 hour field review | \$10,703.09 |
| Jacksonville 2 | Jan 12, 2021 | Peters & Yaffee | <ul style="list-style-type: none"> • Various analyses were conducted including access management, 5-year work program, crash history, field review for 1 h, TMC for 12 h, delay analysis. • No warrant has met. | <ul style="list-style-type: none"> • 12 hours of TMC • Delay study • 1 hour field review | \$7,615.78 |
| Jacksonville 3 | Jul 17, 2019 | HNTB | <ul style="list-style-type: none"> • FDOT Intersection Control Evaluation (ICE) toolset were used. • Safety Performance Evaluation and Benefit Cost analysis were carried out. • RCUT installation was found the most beneficial control strategy due to the angle crashes. • Two-Way Stop control strategy is recommended based on the benefit cost analysis. | <ul style="list-style-type: none"> • No field data collection (Mostly historical crash data are used) | \$23,286.36 |

5.4.3. Alternative Methods

To include the financial aspect of the feasibility analysis of drone-based traffic data collection, three different alternative methods were compared in terms of the monetary cost per intersection. Figure 5-39 depicts these alternatives with their simplified cost items. Alternative 1 represents the base option referring to the traditional methods. Alternative 2 includes a tethered drone with 10 hours of flight endurance powered with a tether cable with the assumption of optimal weather conditions. Alternative 3, on the other hand, includes a more complex flight operation where two untethered drones are facilitated with overlapping flights times in the last 5 minutes of each flight.

Figure 5-39: Alternatives of signal warrant analysis

5.4.4. Cost per Intersection Estimates

For the Alternative 1 (Traditional Methods), the cost per intersection is extracted from the previous studies. \$9,000 per intersection is calculated as the approximate average of the 2 previous signal warrant studies. On the other hand, for Alternative 2 and 3, the fixed cost for equipment, the fixed cost for coding (programs for data collection and analysis) should be converted into a per intersection cost. Additionally, work-hours and the engineering cost to sign and seal the final report should be calculated.

5.4.4.1. *Drone Equipment Fixed Cost per Intersection*

As mentioned in Chapter 2, the cost of drones has exponentially decreased in the last decade. For example, DJI Phantom drones have been commonly used in traffic monitoring studies (Barmounakis & Geroliminis, 2020) and they cost approximately \$1,500 with a built in gimbal and high-resolution camera as well as smart screen control with first person view options. On the other hand, tethered drones are relatively new technologies; thus, they require more precise and costly equipment. Elistair is a leading brand for supplying tethers and associated drones. Their approximate price for an Orion model drone, Safe-T model tether and other necessary equipment is approximately \$30,000.

Drone life expectancy is an ongoing research in robotic and aviation fields; however, 800 hours of total flight time is recommended for an untethered drone in the ‘ask drone u’ podcast (which is a well-known platform among drone operators to learn from others’ experience)

(DroneU, 2021). This flight time is calculated considering the certain equipment such as propeller, gimbal, or folding parts. Therefore, 800 hours of total flight time can be extended by changing those parts, which costs considerably lower than investing on a brand-new drone. However, since we consider the worst-case scenario in this study, 800 hours of flight time is considered as the life time of an untethered drone. For the tethered drone, 1,000 h total flight time is considered as the life expectancy since tethered drones are designed to fly for hours as the continuous power supply is provided. With this life expectancy, the equipment fixed cost per intersection can be calculated as:

Alternative 2:

- Total cost for the equipment = ~\$30,000
- Tethered drone life expectancy = 1,000 h
- 8 h flight time per intersection

$$\frac{1,000}{8} = 125 \text{ intersections}$$

$$\frac{\$30,000}{125} = \$240 \text{ per intersections}$$

Alternative 3:

- Total cost for the equipment = ~\$3,000
- Tethered drone life expectancy = 800 h
- 4 h flight time per drone per intersection

$$\frac{800}{4} = 200 \text{ intersections}$$

$$\frac{\$3,000}{200} = \$15 \text{ per intersections}$$

5.4.4.2. Work-hour Cost per Intersection

According to the available databases in Florida, the average hourly wage for a trained drone pilot is \$40. Also, compared to operating two drones with partially overlapping times, a tethered drone can be operated with a single set up without having the need to land during a 3-hour flight. Therefore, one trained drone pilot for Alternative 2 is needed whereas two trained drone pilots are considered for Alternative 3. The costs can be calculated as:

Alternative 2:

$$\$40 * 8h = \$320 \text{ per intersection}$$

Alternative 3:

$$2 * \$40 * 8h = \$640 \text{ per intersection}$$

5.4.4.3. *Software Fixed Cost Per Intersection*

Both drone alternatives are assumed to be using the proposed frameworks for real-time trajectory extraction and automated turning movement count (TMC) calculation presented in Figure 5-4 and Figure 5-5, respectively. Note that once these programs are created with a desired accuracy, they can be used for an indefinite period. However, we envision that, with the current technology speed, a 5-year lifetime would be logical. After five years, the programs can be reevaluated or improved with better technology.

Additionally, it was assumed that five signal warrant study per month would be a logical number for the entire state of Florida based on expert knowledge. This would sum up to 300 intersections in the 5-year lifetime of the generated programs.

Finally, a rough cost estimate to develop these programs are presented using the \$27 average hourly wage for a programmer in Florida. The software cost estimates are based on the book of *Estimating Software Costs: Bringing Realism to Estimating* (Jones, 2007). According to this book, there is a rule of thumb to estimate the cost of a software based on the concept of Line of Code (LOC). The cost estimate calculates the monthly effort based on the LOC metrics and creates monthly function points based on these efforts. Cost estimates can be presented as:

Video to Trajectory:

- 100 – 1,000 Line of Code = 6 months = 1,040 work-hours of a programmer
 $1040 h * \$27 = \$28,080$
- Cost of AI Model development, Interface Design, Testing, Integration
 $= \$150,000$

Total cost = ~180,000

Trajectory to TMC:

- 100 – 1,000 Line of Code = 3 months = 520 work-hours of a programmer
 $520 h * \$27 = \$14,040$
- Cost of Interface Design, Testing, Integration
 $= \$100,000$

Total cost = ~120,000

5 Warrant Study per month for 5 years = 300 intersections

$$\$180,000 + \$120,000 = \$300,000$$

$$\frac{\$300,000}{300} = \$1,000 \text{ per intersection}$$

Finally, all estimated costs are presented in Table 5-9 with the addition of an engineering cost of, which generally constitutes to the 17% to 20% of the total cost. The engineering cost includes the sealing and signing of the final warrant study report according to the FDOT requirements. According to the Table 5-9, both tethered and untethered alternatives are more than 4.5 times cheaper than the traditional methods to conduct a warrant study on a Florida

intersection. Additionally, tethered drone alternative costs approximately \$100 less than the untethered option despite a significant difference on equipment prices.

Table 5-9: Comparative cost analysis between the traditional method and drone-based methods to conduct a signal warrant study in Florida

| Cost Categories | Unit Cost Value per Intersection | | |
|------------------------------------|----------------------------------|----------------|-------------------|
| | Traditional Methods | Tethered Drone | Untethered drones |
| Equipment Cost per Intersection | - | \$240 | \$15 |
| Coding Cost per Intersection | - | \$1000 | \$1000 |
| Work-hour Cost per Intersection | - | \$320 | \$640 |
| Engineering Cost | - | \$300 | \$300 |
| Total cost per intersection | \$9,000 | \$1,860 | \$1,955 |
| Comparative ratio | | 4.83 | 4.60 |

5.5. Recommendations for Consultants to Set a Drone Operation Team

Based on the comparative cost analysis using the worst-case scenario, drone-based traffic data collection and analysis indicate a significant financial advantage compared to the traditional methods. In order to take benefit of this advantage, following steps are recommended for consultants to have drone-based traffic data component in their efforts:

- Invest on the proposed drone equipment
- Set a team with:
 - 2 drone pilots
 - 4 programmers
 - 2 administrator staff
 - 1 manager
- Drone pilots are not necessarily to be expert since hovering the aircraft on air is not a complex job. However, they need to have the remote pilot license which requires to pass an FAA exam that costs \$150. The license should be renewed every 2 years. In addition, an experience is still required to trust the expensive equipment in the field. As a rule of

thumb, 20 hours to 50 hours of flight time experience is needed for the drone pilots given the type of drone.

- Among the four programmers, Programmer 1 can deal with the AI models to train and test neural networks and provide the ready to use detector/tracker with a clear explanation of the performance/accuracy. Programmer 2 must know how to deal with the image data as AI models are very sensitive to the input image properties. Programmer 3 can perform road user trajectory mining to extract end data for traffic operations. Programmer 4 can develop tools to populate the MUTS forms automatically.
- Two administrator staff can help with logistics and housekeeping.
- The manager should be somebody who can oversee all the work performed and communicate with the traffic engineer who seals and signs the final report.
- Note that this drone-based traffic data collection can help not only TMC and warrant studies, but any required work shown in MUTS can be performed such as roundabout gap acceptance, delay, vulnerable user analysis, conflict study, and fundamental diagrams.
- Collected microscopic traffic data can be used for traffic simulation calibration and driving behavior analysis.
- In addition, the team can focus on other source of imagery data to provide land use and control device inventory information similar to the work that was performed in Chapter 3.

6. CONCLUSIONS

The overall goal of this project was to provide a feasibility analysis on the utilization of drones and computer vision applications to extract microscopic traffic data at intersections. Findings are expected to help Florida Department of Transportation (FDOT) in integrating new technologies into their day-to-day data collection operations. Consistent with this goal, the following tasks have been completed as part of the project: (a) perform a literature review and analyze state-of-the-practice to provide guidance and recommendations on legally and safely using drones with video/image processing techniques for the uniform traffic studies; (b) generate statewide crosswalk inventory using aerial images and artificial intelligence (AI2); (c) investigate the fatal pedestrian-involved crashes that occur at locations other than intersections in Florida and analyze their detailed crash reports; (d) design and conduct exercises with tethered drones to collect intersection data in the cities of Tallahassee and Jacksonville, Florida; and (e) perform a cost analysis comparing traditional methods with different drone-based traffic data collection techniques.

Meeting these objectives led to appropriate guidelines and recommendations to FDOT in terms of evaluating and justifying the feasibility of using drones as safer and cheaper data collection alternatives while significantly improving intersection safety and operations. Both tethered and untethered alternatives are more than 4.5 times cheaper than the traditional methods to conduct a warrant study on a Florida intersection. Additionally, tethered drone alternative costs approximately \$100 less than the untethered option despite a significant difference on equipment prices. Results and recommendations of this research will also be used by the FDOT consultants who already perform traffic data collection on Florida's roadways.

An automated crosswalk detection and mapping model was also developed, and three case studies were conducted in order to evaluate the efficacy of the developed model. The model performed with an accuracy of more than 85%. The developed model performs quite well, and it has high not only created a state-wide crosswalk inventory but it can also complete the OSM crosswalks in the future. In addition, the detection problems on peeled off crosswalks are commonly addressed challenges in the related literature. In this regard, crosswalks with a low detection confidence score or no detection can be utilized to determine the crosswalks that need visibility improvements and/or routine maintenance.

Left turn lanes are among the locations with a significant number of pedestrian-involved fatal crashes and therefore require more attention. Careful evaluation of crash reports' narratives reveals that despite the limited number of crashes that occurred under the direct influence of left turning movement, the pedestrians may still expect drivers to be more cautious and reduce their speed in order to yield the crosswalk to them.

REFERENCES

- AASHTO. (2010). *Highway Safety Manual* (1st ed.). Washington D.C.: American Association of State Highway and and Transportation Officials. <http://www.highwaysafetymanual.org/>
- AASHTO. (2016). *Survey 2016: State DOTs Using Drones to Improve Safety, Collect Data and Cut Costs*. American Association of State Highway and and Transportation Officials. <http://asphaltmagazine.com/wp-content/uploads/2016/05/Dronesss.pdf>
- AASHTO. (2018a). *A policy on geometric design of highways and streets* (7th ed.). Washington D.C.: American Association of State Highway and Transportation Officials.
- AASHTO. (2018b). *Survey 2018: Most State DOTs Now Deploying or Testing Aerial Drones for Regular Use*. American Association of State Highway and and Transportation Officials. <https://indd.adobe.com/view/12579497-56a5-4d8a-b8fe-e48c95630c99>
- AASHTO. (2019). *Survey 2019 Finds State DOTs Hiring Next-Gen Workforce to Run Drone Operations*. American Association of State Highway and and Transportation Officials. <https://aviation.transportation.org/wp-content/uploads/sites/8/2019/05/2019-Drones-Press-release.pdf>
- Aguilar, W. G., & Angulo, C. (2014). Robust video stabilization based on motion intention for low-cost micro aerial vehicles. *2014 IEEE 11th International Multi-Conference on Systems, Signals & Devices (SSD14), Barcelona, Spain*, 1–6. <https://doi.org/10.1109/SSD.2014.6808863>
- Alver, Y., Onelcin, P., Cicekli, A., & Abdel-Aty, M. (2021). Evaluation of pedestrian critical gap and crossing speed at midblock crossing using image processing. *Accident Analysis and Prevention*, *156*(April), 106127. <https://doi.org/10.1016/j.aap.2021.106127>
- Appel, R., Belongie, S., Perona, P., & Doll, P. (2014). Fast Feature Pyramids for Object Detection. *IEEE Transactions on Pattern Analysis and Machine Intelligence*, *36*, 1532–1545. <https://doi.org/10.1109/TPAMI.2014.2300479>
- Azimi, S. M., Fischer, P., Korner, M., & Reinartz, P. (2019). Aerial LaneNet: Lane-Marking Semantic Segmentation in Aerial Imagery Using Wavelet-Enhanced Cost-Sensitive Symmetric Fully Convolutional Neural Networks. *IEEE Transactions on Geoscience and Remote Sensing*, *57*(5), 2920–2938. <https://doi.org/10.1109/TGRS.2018.2878510>
- Barmponakis, E., & Geroliminis, N. (2020). On the new era of urban traffic monitoring with massive drone data: The pNEUMA large-scale field experiment. *Transportation Research Part C: Emerging Technologies*, *111*(October 2019), 50–71. <https://doi.org/10.1016/j.trc.2019.11.023>
- Barmponakis, E., Vlahogianni, E. I., & Golias, J. C. (2016). Unmanned Aerial Aircraft Systems for transportation engineering: Current practice and future challenges. *International Journal of Transportation Science and Technology*, *5*(3), 111–122. <https://doi.org/10.1016/j.ijtst.2017.02.001>
- Berriel, R. F., Lopes, A. T., De Souza, A. F., & Oliveira-Santos, T. (2017). Deep Learning-Based Large-Scale Automatic Satellite Crosswalk Classification. *IEEE Geoscience and Remote Sensing Letters*, *14*(9), 1513–1517. <https://doi.org/10.1109/LGRS.2017.2719863>

- Berriel, R. F., Rossi, F. S., de Souza, A. F., & Oliveira-Santos, T. (2017). Automatic large-scale data acquisition via crowdsourcing for crosswalk classification: A deep learning approach. *Computers and Graphics (Pergamon)*, 68, 32–42. <https://doi.org/10.1016/j.cag.2017.08.004>
- Biswas, D., Su, H., Wang, C., & Stevanovic, A. (2019). Speed Estimation of Multiple Moving Objects from a Moving UAV Platform. *ISPRS International Journal of Geo-Information*, 8(6), 259. <https://doi.org/10.3390/ijgi8060259>
- Blackburn, L., Zegeer, C., Brookshire, K., & FHWA. (2017). *Guide for Improving Pedestrian Safety at Uncontrolled Crossing Locations* (FHWA-SA-17-072; Issue July).
- Bochkovskiy, A., Wang, C.-Y., & Liao, H.-Y. M. (2020). YOLOv4: Optimal Speed and Accuracy of Object Detection. *ArXiv*. <http://arxiv.org/abs/2004.10934>
- Braut, V., Culjak, M., Vukotic, V., Segvic, S., Sevrovic, M., & Gold, H. (2012). Estimating OD matrices at intersections in airborne video - A pilot study. *MIPRO, 2012 Proceedings of the 35th International Convention*, 977–982.
- Brooks, C., Dobson, R., David, B. M., Dean, D., Oommen, T., Escobar-Wolf, R., Havens, T. C., Ahlborn, T. M., Hart, B., Cook, S. J., & Clover, A. D. (2014). *Evaluating the use of unmanned aerial vehicles for transportation purposes* (RC-1616). https://www.michigan.gov/documents/mdot/RC1616_Part_A_488515_7.pdf
- Brooks, C., Dobson, R., David, B. M., Oommen, T., Zhang, K., Mukherjee, A., Havens, T. C., Ahborn, T., Escobar-Wolf, R., Bhat, C. R., Zhao, S., Lyu, Q., Marion, N., Cook, S. J., & Clover, A. D. (2018). *Implementation of Unmanned Aerial Vehicles (UAVs) for Assessment of Transportation Infrastructure – Phase II* (SPR-1674). https://www.michigan.gov/documents/mdot/SPR-1674_FinalReport_revised_631648_7.pdf
- Chen, P., Zeng, W., Yu, G., & Wang, Y. (2017). Surrogate Safety Analysis of Pedestrian-Vehicle Conflict at Intersections Using Unmanned Aerial Vehicle Videos. *Journal of Advanced Transportation*, 2017.
- Chen, Z. S., & Zhang, D. F. (2018). An Effective Detection Algorithm of Zebra-Crossing. In *Lecture Notes in Electrical Engineering* (Vol. 482, pp. 809–816). Springer Singapore. https://doi.org/10.1007/978-981-10-7986-3_81
- Coifman, B., McCord, M., Mishalani, R. G., Iswalt, M., & Ji, Y. (2006). Roadway traffic monitoring from an unmanned aerial vehicle. *IEEE Proceedings - Intelligent Transport Systems*, 153(1), 11. <https://doi.org/10.1049/ip-its:20055014>
- Dai, J., Wang, Y., Li, W., & Zuo, Y. (2020). Automatic Method for Extraction of Complex Road Intersection Points From High-Resolution Remote Sensing Images Based on Fuzzy Inference. *IEEE Access*, 8, 39212–39224. <https://doi.org/10.1109/ACCESS.2020.2974974>
- Dai, J., Zhu, T., Zhang, Y., Ma, R., & Li, W. (2019). Lane-level road extraction from high-resolution optical satellite images. *Remote Sensing*, 11(22). <https://doi.org/10.3390/rs11222672>
- Datondji, S. R. E., Dupuis, Y., Subirats, P., & Vasseur, P. (2016). A Survey of Vision-Based Traffic Monitoring of Road Intersections. *IEEE Transactions on Intelligent Transportation Systems*, 17(10), 2681–2698. <https://doi.org/10.1109/TITS.2016.2530146>
- Dollár, P., Wojek, C., Schiele, B., & Perona, P. (2012). Pedestrian detection: An evaluation of

- the state of the art. *IEEE Transactions on Pattern Analysis and Machine Intelligence*, 34(4), 743–761. <https://doi.org/10.1109/TPAMI.2011.155>
- DroneU. (2021). *What is My Drone Life Expectancy*. <https://www.thedroneu.com/adu-0704-life-expectancy-drone/>
- Elistair. (2019). *A busy roundabout in Lyon with Safe-T*. Elistair. <https://elistair.com/wp-content/uploads/2017/01/Use-Case-Road-Traffic-Monitoring-at-roundabout-in-Lyon-with-Safe-T-tethered-drone-station.pdf>
- ESRI. (2020). *Mosaic datasets*. ArcGIS Pro Help. <https://pro.arcgis.com/en/pro-app/help/data/imagery/mosaic-datasets.htm>
- FAA. (2019a). *knowbeforeyoufly.org*. <http://knowbeforeyoufly.org/>
- FAA. (2019b). *Unmanned Aircraft Systems (UAS)*. www.faa.gov/uas/
- FAA, & Kittyhawk. (2019). *B4UFLY Mobile App*. https://www.faa.gov/uas/recreational_fliers/where_can_i_fly/b4ufly/
- Fan, Y., Sun, Z., & Zhao, G. (2020). A Coarse-to-Fine Framework for Multiple Pedestrian Crossing Detection. *Sensors*, 20(15), 4144. <https://doi.org/10.3390/s20154144>
- FDOT. (2017). *FDOT Districts and State Plane & UTM Zones*. https://fdotwww.blob.core.windows.net/sitefinity/docs/default-source/geospatial/maps/zones-districts.pdf?sfvrsn=7ff7afe8_4
- FDOT Surveying and Mapping Office. (2020). *Aerial Photography Look-Up System (APLUS)*. <https://fdotewp1.dot.state.fl.us/AerialPhotoLookUpSystem/>
- FDOT Traffic Engineering & Operations Office. (2016). *Manual on Uniform Traffic Studies* (No. 750-020-007-d). <https://www.fdot.gov/traffic/trafficservices/studies/muts/muts.shtm>
- FDOT Transportation Data and Analytics Office. (2020). *Geographic Information System (GIS)*. <https://www.fdot.gov/statistics/gis>
- FHWA. (2018). *Use of Unmanned Aerial Systems (UAS) by State DOTs February 27, 2018 Peer Exchange* (FHWA-HIF-18-060). <https://www.fhwa.dot.gov/uas/peer/2018peer.pdf>
- FHWA. (2020a). *Safe Transportation for Every Pedestrian (STEP)*. https://www.fhwa.dot.gov/innovation/everydaycounts/edc_5/step2.cfm
- FHWA. (2020b). *Safe Transportation for Every Pedestrian (STEP)*. https://www.youtube.com/playlist?list=PL5_sm9g9d4T314Co020jzSf022naHKwox
- FHWA. (2020c, June). Taking STEPs to Boost Pedestrian Safety. *Innovator*, 78, 4–5. https://www.fhwa.dot.gov/innovation/innovator/issue78/img/Innovator_Issue78_MayJune20.pdf
- FHWA, ITE, AASHTO, ATSSA, & IMSA. (2009). *Manual on Uniform Traffic Control Devices* (2009th ed.). <http://scholar.google.com/scholar?hl=en&btnG=Search&q=intitle:No+Title#0%5Cnhttp://scholar.google.com/scholar?hl=en&btnG=Search&q=intitle:Manual+on+Uniform+Traffic+Control+Devices#0>
- Fischer, P., Azimi, S. M., Roschlaub, R., & Krauß, T. (2018). Towards HD maps from aerial

- imagery: Robust lane marking segmentation using country-scale imagery. *ISPRS International Journal of Geo-Information*, 7(12), 1–14. <https://doi.org/10.3390/ijgi7120458>
- Florida DOT. (2019). *Florida DOT UAS Brochure*. Florida DOT. <http://www.florida-aviation-database.com/library/filedownload.aspx?guid=5c60d4b8-45de-409a-b1dd-d07ea80177b8>
- Girshick, R. (2015). Fast R-CNN. *Proceedings of the IEEE International Conference on Computer Vision, 2015 Inter*, 1440–1448. <https://doi.org/10.1109/ICCV.2015.169>
- Girshick, R., Donahue, J., Darrell, T., Berkeley, U. C., & Malik, J. (2012). (r-cnn) Rich feature hierarchies for accurate object detection and semantic segmentation. *2014 IEEE Conference on Computer Vision and Pattern Recognition*, 2–9. <https://doi.org/10.1109/CVPR.2014.81>
- Haider, M. M., Hoque, M. R., Khaliluzzaman, M., & Hassan, M. M. (2019). Zebra Crosswalk Region Detection and Localization Based on Deep Convolutional Neural Network. *2019 IEEE International Conference on Robotics, Automation, Artificial-Intelligence and Internet-of-Things (RAAICON)*, 93–97. <https://doi.org/10.1109/RAAICON48939.2019.41>
- Hainen, A., Stevens, A. L., Day, C. M., Li, H., Mackey, J., Luker, M., Taylor, M., Sturdevant, J. R., & Bullock, D. M. (2015). Performance Measures for Optimizing Diverging Interchanges and Outcome Assessment with Drone Video. *Transportation Research Record: Journal of the Transportation Research Board*, 2487(1), 31–43. <https://doi.org/10.3141/2487-03>
- Hainen, A., Stevens, A., Li, H., & Bullock, D. (2014). Three-Phase Operations at a Diverging Diamond Interchange Using an Unmanned Aerial Vehicle (UAV) Camera. *Purdue University Research Repository*. <https://doi.org/doi:10.4231/R7C24TC4>
- Helmicki, A. J. (2019). *In Support of ODOT Operations Research Team*. Ohio DOT. <http://www.dot.state.oh.us/engineering/OTEC/2017Presentations/65/Helmicki-65.pdf>
- Høye, A., & Laureshyn, A. (2019). SeeMe at the crosswalk: Before-after study of a pedestrian crosswalk warning system. *Transportation Research Part F: Traffic Psychology and Behaviour*, 60, 723–733. <https://doi.org/10.1016/j.trf.2018.11.003>
- Hurwitz, D., Olsen, M., & Barlow, Z. (2018). Driving Distraction Due to Drones. In *Oregon Department of Transportation* (FHWA-OR-RD-18-12). <https://doi.org/FHWA-OR-RD-18-12>
- Jalayer, M., Gong, J., Zhou, H., & Grinter, M. (2015). Evaluation of Remote Sensing Technologies for Collecting Roadside Feature Data to Support Highway Safety Manual Implementation. *Journal of Transportation Safety and Security*, 7(4), 345–357. <https://doi.org/10.1080/19439962.2014.976691>
- Jocher, G. (2020). *YOLOv5*. <https://models.roboflow.com/object-detection/yolov5>
- Jones, C. (2007). *Estimating Software Costs: Bringing Realism to Estimating*. <http://www.amazon.com/Estimating-Software-Costs-Bringing-Realism/dp/0071483004>
- Kanistras, K., Martins, G., Rutherford, M. J., & Valavanis, K. P. (2015). Survey of unmanned aerial vehicles (uavs) for traffic monitoring. *Handbook of Unmanned Aerial Vehicles, February 2015*, 2643–2666. https://doi.org/10.1007/978-90-481-9707-1_122
- Ke, R., Kim, S., Li, Z., & Wang, Y. (2015). Motion-vector clustering for traffic speed detection from UAV video. *2015 IEEE 1st International Smart Cities Conference, ISC2 2015*, 1–5.

<https://doi.org/10.1109/ISC2.2015.7366230>

- Ke, R., Li, Z., Kim, S., Ash, J., Cui, Z., & Wang, Y. (2017a). Real-Time Bidirectional Traffic Flow Parameter Estimation from Aerial Videos. *IEEE Transactions on Intelligent Transportation Systems*, 18(4), 890–901. <https://doi.org/10.1109/TITS.2016.2595526>
- Ke, R., Li, Z., Kim, S., Ash, J., Cui, Z., & Wang, Y. (2017b). Real-Time Bidirectional Traffic Flow Parameter Estimation from Aerial Videos. *IEEE Transactions on Intelligent Transportation Systems*, 18(4), 890–901. <https://doi.org/10.1109/TITS.2016.2595526>
- Khan, M. A., Ectors, W., Bellemans, T., Janssens, D., & Wets, G. (2017a). UAV-Based Traffic Analysis: A Universal Guiding Framework Based on Literature Survey. *Transportation Research Procedia*, 22(2016), 541–550. <https://doi.org/10.1016/j.trpro.2017.03.043>
- Khan, M. A., Ectors, W., Bellemans, T., Janssens, D., & Wets, G. (2017b). Unmanned Aerial Vehicle-Based Traffic Analysis: Methodological Framework for Automated Multivehicle Trajectory Extraction. *Transportation Research Record: Journal of the Transportation Research Board*, 2626(1), 25–33. <https://doi.org/10.3141/2626-04>
- Khan, M. A., Ectors, W., Bellemans, T., Janssens, D., & Wets, G. (2018). Unmanned aerial vehicle-based traffic analysis: A case study for shockwave identification and flow parameters estimation at signalized intersections. *Remote Sensing*, 10(3). <https://doi.org/10.3390/rs10030458>
- Khan, M. A., Ectors, W., Bellemans, T., Ruichek, Y., Yasar, A. U. H., Janssens, D., & Wets, G. (2018). Unmanned Aerial Vehicle-based Traffic Analysis: A Case Study to Analyze Traffic Streams at Urban Roundabouts. *Procedia Computer Science*, 130, 636–643. <https://doi.org/10.1016/j.procs.2018.04.114>
- Kim, E. J., Park, H.-C., Ham, S.-W., Kho, S.-Y., & Kim, D.-K. (2019). Extracting Vehicle Trajectories Using Unmanned Aerial Vehicles in Congested Traffic Conditions. *Journal of Advanced Transportation*, 2019, 1–16. <https://doi.org/10.1155/2019/9060797>
- Kim, Z. (2005). Realtime Road Detection by Learning from One Example. *2005 Seventh IEEE Workshops on Applications of Computer Vision (WACV/MOTION'05) - Volume 1*, 455–460. <https://doi.org/10.1109/ACVMOT.2005.99>
- Kingma, D. P., & Ba, J. (2014). *Adam: A Method for Stochastic Optimization*. <http://arxiv.org/abs/1412.6980>
- Klinger, R. (2020). *Get OSM Data-An ArcGIS Toolbox*. Github. <https://github.com/riccardoklinger/OSMquery>
- Knoppers, P., van Lint, H., & Hoogendoorn, S. (2012). Automatic Stabilization of Aerial Traffic Images. *Transportation Research Board 91st Annual Meeting*, 1–13.
- Koester, D., Lunt, B., & Stiefelhagen, R. (2016). Zebra Crossing Detection from Aerial Imagery Across Countries. In *Lecture Notes in Computer Science (including subseries Lecture Notes in Artificial Intelligence and Lecture Notes in Bioinformatics)* (Vol. 9759, pp. 27–34). https://doi.org/10.1007/978-3-319-41267-2_5
- Kurath, S., Das Gupta, R., & Keller, S. (2017). OSMDeepOD - Object Detection on Orthophotos with and for VGI. *GI Forum*, 1(2), 173–188. https://doi.org/10.1553/giscience2017_02_s173

- Kwasniak, A., & Kerezman, A. (2017). Drones in Transportation Engineering: a Discussion of Current Drone Rules, Equipment, And Applications. *ITE Journal*, 40–43. https://mydigitalpublication.com/publication/?i=380807&article_id=2701568&view=article_Browser#%7B%22issue_id%22:380807,%22page%22:40%7D
- LAANC Kittyhawk. (2019). Kittyhawk. <https://kittyhawk.io/feature/laanc/>
- Liang, J., & Urtasun, R. (2018). End-to-End Deep Structured Models for Drawing Crosswalks. In *Lecture Notes in Computer Science (including subseries Lecture Notes in Artificial Intelligence and Lecture Notes in Bioinformatics): Vol. 11216 LNCS* (pp. 407–423). https://doi.org/10.1007/978-3-030-01258-8_25
- Lin, Y., & Saripalli, S. (2012). Road detection from aerial imagery. *Proceedings - IEEE International Conference on Robotics and Automation*, 3588–3593. <https://doi.org/10.1109/ICRA.2012.6225112>
- Liu, J., Hainen, A., Li, X., Nie, Q., & Nambisan, S. (2019). Pedestrian injury severity in motor vehicle crashes: An integrated spatio-temporal modeling approach. *Accident Analysis & Prevention*, 132, 105272. <https://doi.org/10.1016/j.aap.2019.105272>
- Liu, X., Zhang, Y., & Li, Q. (2017). AUTOMATIC PEDESTRIAN CROSSING DETECTION AND IMPAIRMENT ANALYSIS BASED ON MOBILE MAPPING SYSTEM. *ISPRS Annals of Photogrammetry, Remote Sensing and Spatial Information Sciences, IV-2/W4(2W4)*, 251–258. <https://doi.org/10.5194/isprs-annals-IV-2-W4-251-2017>
- Ma, Y., Wu, X., Yu, G., Xu, Y., & Wang, Y. (2016). Pedestrian detection and tracking from low-resolution unmanned aerial vehicle thermal imagery. *Sensors (Switzerland)*, 16(4). <https://doi.org/10.3390/s16040446>
- Massachusetts DOT. (2016). *The State of the Practice of UAS Systems in Transportation* (Issue December). <https://rosap.nrl.bts.gov/view/dot/35033>
- Mimbela, L. E. Y. (2000). A Summary of Vehicle Detection and Surveillance Technologies used in IN INTELLIGENT TRANSPORTATION SYSTEMS PREPARED BY : *Image (Rochester, N.Y.)*.
- Montana DOT. (2018). *Drone Library for Transportation*. National Transportation Library. <https://doi.org/https://transportation.libguides.com/uav/home>
- NHTSA. (2018). *Traffic Safety Facts 2018: A Compilation of Motor Vehicle Crash Data*. National Highway Traffic Safety Administration. <https://crashstats.nhtsa.dot.gov/Api/Public/Publication/812981>
- NHTSA. (2019). *Fatality Analysis Reporting System (FARS)*. National Highway Traffic Safety Administration. <https://www-fars.nhtsa.dot.gov/Main/index.aspx>
- Nicotra, M. M., Naldi, R., & Garone, E. (2017). Nonlinear control of a tethered UAV: The taut cable case. *Automatica*, 78, 174–184. <https://doi.org/10.1016/j.automatica.2016.12.018>
- Niu, H., González-Prelcic, N., & Heath, R. W. (2018). A UAV-Based Traffic Monitoring System - Invited Paper. *IEEE Vehicular Technology Conference, 2018-June*, 1–5. <https://doi.org/10.1109/VTCSpring.2018.8417546>
- OpenStreetMap. (2020a). *Wiki-Main Page*. https://wiki.openstreetmap.org/wiki/Main_Page

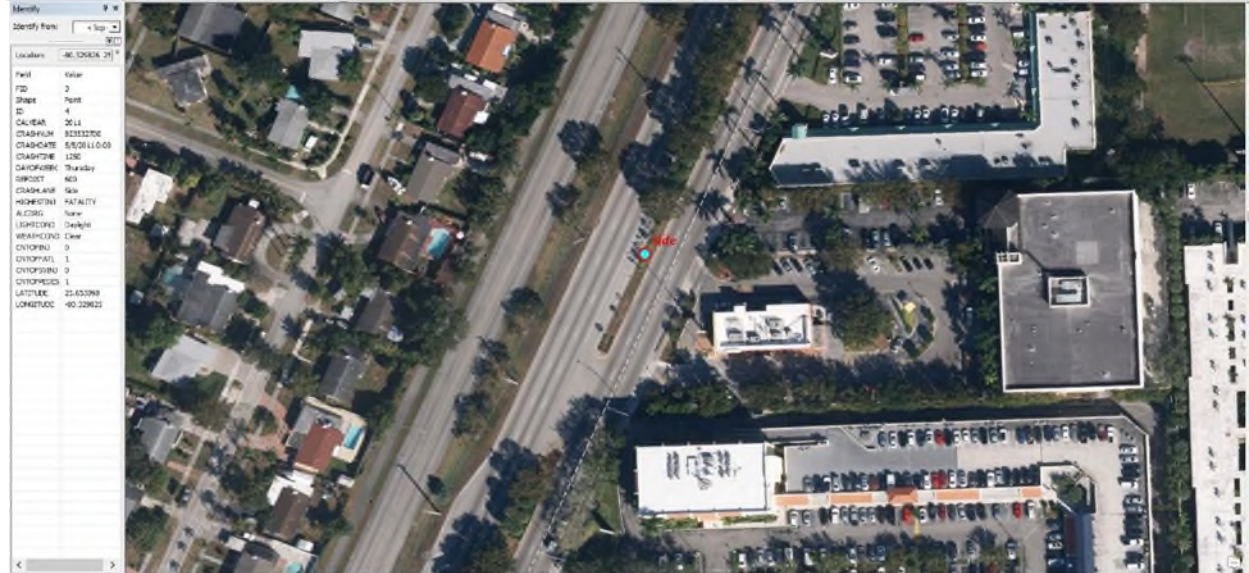
- OpenStreetMap. (2020b). *Wiki-Overpass API*.
https://wiki.openstreetmap.org/wiki/Overpass_API
- OpenStreetMap. (2020c). *Wiki-Stats*. <https://wiki.openstreetmap.org/wiki/Stats>
- Pan, P., Xue, C., & Zhou, H. (2019). Video Analytics for Estimating Control Delays at Signalized Intersections Based on Videos Collected by Unmanned Aerial Vehicles. *Proceedings of the TRB 2019 Annual Meeting*. <http://amonline.trb.org/68387-trb-1.4353651/t0005-1.4505752/1297-1.4506426/19-01667-1.4506515/19-01667-1.4506516>
- Papadoulis, A., Quddus, M., & Imprialou, M. (2019). Evaluating the safety impact of connected and autonomous vehicles on motorways. *Accident Analysis and Prevention, 124*(January), 12–22. <https://doi.org/10.1016/j.aap.2018.12.019>
- Patella, S. M., Sportiello, S., Carrese, S., Bella, F., & Asdrubali, F. (2020). The Effect of a LED Lighting Crosswalk on Pedestrian Safety: Some Experimental Results. *Safety, 6*(2), 20. <https://doi.org/10.3390/safety6020020>
- Pour-Rouholamin, M., & Zhou, H. (2016). Investigating the risk factors associated with pedestrian injury severity in Illinois. *Journal of Safety Research, 57*, 9–17. <https://doi.org/10.1016/j.jsr.2016.03.004>
- Puri, A. (2005). A Survey of Unmanned Aerial Vehicles (UAV) for Traffic Surveillance. *Technical Paper*, 1–29. papers2://publication/uuid/6D241E9E-AF0D-42BF-B87C-668CCD166527
- Quinn, S., & Dutton, J. A. (2020). *OpenStreetMap and its use as open data*. E-Education Institute, College of Earth and Mineral Sciences, The Pennsylvania State University. <https://www.e-education.psu.edu/geog585/node/738>
- Redmon, J. (2020). *YOLO: Real-Time Object Detection*. <https://pjreddie.com/darknet/yolo/>
- Redmon, J., Divvala, S., Girshick, R., & Farhadi, A. (2016). You only look once: Unified, real-time object detection. *Proceedings of the IEEE Computer Society Conference on Computer Vision and Pattern Recognition, 2016-Decem*, 779–788. <https://doi.org/10.1109/CVPR.2016.91>
- Redmon, J., & Farhadi, A. (2016). YOLO9000: Better, Faster, Stronger. *2017 IEEE Conference on Computer Vision and Pattern Recognition (CVPR), 2017-Janua*, 6517–6525. <https://doi.org/10.1109/CVPR.2017.690>
- Redmon, J., & Farhadi, A. (2018). YOLOv3: An Incremental Improvement. *ArXiv*. <http://arxiv.org/abs/1804.02767>
- Ren, S., He, K., Girshick, R., & Sun, J. (2017). Faster R-CNN: Towards Real-Time Object Detection with Region Proposal Networks. *IEEE Transactions on Pattern Analysis and Machine Intelligence, 39*(6), 1137–1149. <https://doi.org/10.1109/TPAMI.2016.2577031>
- Retting, R., & GHSA. (2019). *Pedestrian Traffic Fatalities by State: 2018 Preliminary Data*. <https://www.ghsa.org/resources/Pedestrians19>
- Retting, R., & GHSA. (2020). *Pedestrian Traffic Fatalities by State: 2019 Preliminary Data. In February 2020*. <https://www.ghsa.org/resources/Pedestrians20>
- Rodríguez-Canosa, G. R., Thomas, S., del Cerro, J., Barrientos, A., & MacDonald, B. (2012). A

- real-time method to detect and track moving objects (DATMO) from unmanned aerial vehicles (UAVs) using a single camera. *Remote Sensing*, 4(4), 1090–1111. <https://doi.org/10.3390/rs40401090>
- Salvo, G., Caruso, L., & Scordo, A. (2014). Gap acceptance analysis in an urban intersection through a video acquired by an UAV. *Recent Advances in Civil Engineering and Mechanics*, 199–205.
- Snyder, P., Waller, Z., Wheeler, P., Tootle, A., Milton, J., Larue, T., Gray, J., Gill, S., Frederick, G., Cook, S., & Banks, E. (2018). *Successful Approaches for the Use of Unmanned Aerial System By* (NCHRP Project 20-68A, Scan 17-01). http://onlinepubs.trb.org/onlinepubs/nchrp/docs/NCHRP20-68A_17-01.pdf
- Stevens, C. (2017). Concept of Operations and Policy Implications for Unmanned Aircraft Systems Use for Traffic Incident Management (UAS-TIM). In *Texas A&M Transportation Institute* (PRC 15-69F). <https://doi.org/PRC 15-69F>
- Stevens, C., & Blackstock, T. (2017). Demonstration of Unmanned Aircraft Systems Use for Traffic Incident Management (UAS-TIM) Final Report Demonstration of Unmanned Aircraft Systems Use for Traffic Incident Management (UAS-TIM). *Texas A&M Transportation Institute*. <https://doi.org/PRC 17-69 F>
- Sun, K., Zhang, J., & Zhang, Y. (2019). Roads and intersections extraction from high-resolution remote sensing imagery based on tensor voting under big data environment. *Wireless Communications and Mobile Computing*, 2019. <https://doi.org/10.1155/2019/6513418>
- Sun, Y., Zhang, F., Gao, Y., & Huang, X. (2016). Extraction and Reconstruction of Zebra Crossings from High Resolution Aerial Images. *ISPRS International Journal of Geo-Information*, 5(8), 127. <https://doi.org/10.3390/ijgi5080127>
- Tang, L., Gan, A., & Alluri, P. (2014). Automatic extraction of number of lanes from georectified aerial images. *Transportation Research Record*, 2460(1), 86–96. <https://doi.org/10.3141/2460-10>
- Tang, T., Zhou, S., Deng, Z., Zou, H., & Lei, L. (2017). Vehicle detection in aerial images based on region convolutional neural networks and hard negative example mining. *Sensors (Switzerland)*, 17(2). <https://doi.org/10.3390/s17020336>
- Tümen, V., & Ergen, B. (2020). Intersections and crosswalk detection using deep learning and image processing techniques. *Physica A: Statistical Mechanics and Its Applications*, 543, 123510. <https://doi.org/10.1016/j.physa.2019.123510>
- Vattapparamban, E., Güvenç, I., Yurekli, A. I., Akkaya, K., & Uluğağaç, S. (2016). Drones for smart cities: Issues in cybersecurity, privacy, and public safety. *2016 International Wireless Communications and Mobile Computing Conference, IWCMC 2016*, 216–221. <https://doi.org/10.1109/IWCMC.2016.7577060>
- Viola, P., & Jones, M. (2005). *Rapid object detection using a boosted cascade of simple features*. July 2014, I-511–I-518. <https://doi.org/10.1109/cvpr.2001.990517>
- Wang, X., Pei, Y., Yang, M., & Yuan, J. (2021). Meso-level hotspot identification for suburban arterials. *Accident Analysis & Prevention*, 156, 106148. <https://doi.org/10.1016/j.aap.2021.106148>

- Wiedemann, C., & Ebner, H. (2000). Automatic completion and evaluation of road networks. *International Archives of the Photogrammetry, Remote Sensing and Spatial Information Sciences - ISPRS Archives*, 33, 979–986.
- Wiedemann, C., Heipke, C., Mayer, H., & Jamet, O. (1998). *Empirical Evaluation Of Automatically Extracted Road Axes*.
<http://citeseerx.ist.psu.edu/viewdoc/summary?doi=10.1.1.57.5701>
- Wu, J., & Tsai, Y. (James). (2006). Enhanced Roadway Geometry Data Collection Using an Effective Video Log Image-Processing Algorithm. *Transportation Research Record: Journal of the Transportation Research Board*, 133–140. <https://doi.org/10.3141/1972-18>
- Xie, X., Yang, W., Cao, G., Yang, J., Zhao, Z., Chen, S., Liao, Q., & Shi, G. (2018). Real-Time Vehicle Detection from UAV Imagery. *2018 IEEE 4th International Conference on Multimedia Big Data, BigMM 2018*, 1–5. <https://doi.org/10.1109/BigMM.2018.8499466>
- Xu, Y., Yu, G., Wang, Y., Wu, X., & Ma, Y. (2016). A hybrid vehicle detection method based on viola-jones and HOG + SVM from UAV images. *Sensors (Switzerland)*, 16(8).
<https://doi.org/10.3390/s16081325>
- Xu, Y., Yu, G., Wang, Y., Wu, X., & Ma, Y. (2017). Car detection from low-altitude UAV imagery with the faster R-CNN. *Journal of Advanced Transportation*, 2017.
<https://doi.org/10.1155/2017/2823617>
- Ye, Q. Z., Wu, P., & Zhang, M. L. (2017). Research on automatic highway extraction technology based on spectral information of remote sensing images. *Journal of Information Hiding and Multimedia Signal Processing*, 8(2), 368–380.
- Zang, A., Xu, R., Li, Z., & Doria, D. (2017). Lane boundary extraction from satellite imagery. *Proceedings of the 1st ACM SIGSPATIAL Workshop on High-Precision Maps and Intelligent Applications for Autonomous Vehicles - AutonomousGIS '17*, 1–8.
<https://doi.org/10.1145/3149092.3149093>
- Zhou, H., Kong, H., Wei, L., Creighton, D., & Nahavandi, S. (2015). Efficient road detection and tracking for unmanned aerial vehicle. *IEEE Transactions on Intelligent Transportation Systems*, 16(1), 297–309. <https://doi.org/10.1109/TITS.2014.2331353>

APPENDIX A : Aerial Images of Locations where the Recorded 143 Pedestrian Fatality Crashes Occurred between 2011 and 2020 in Florida

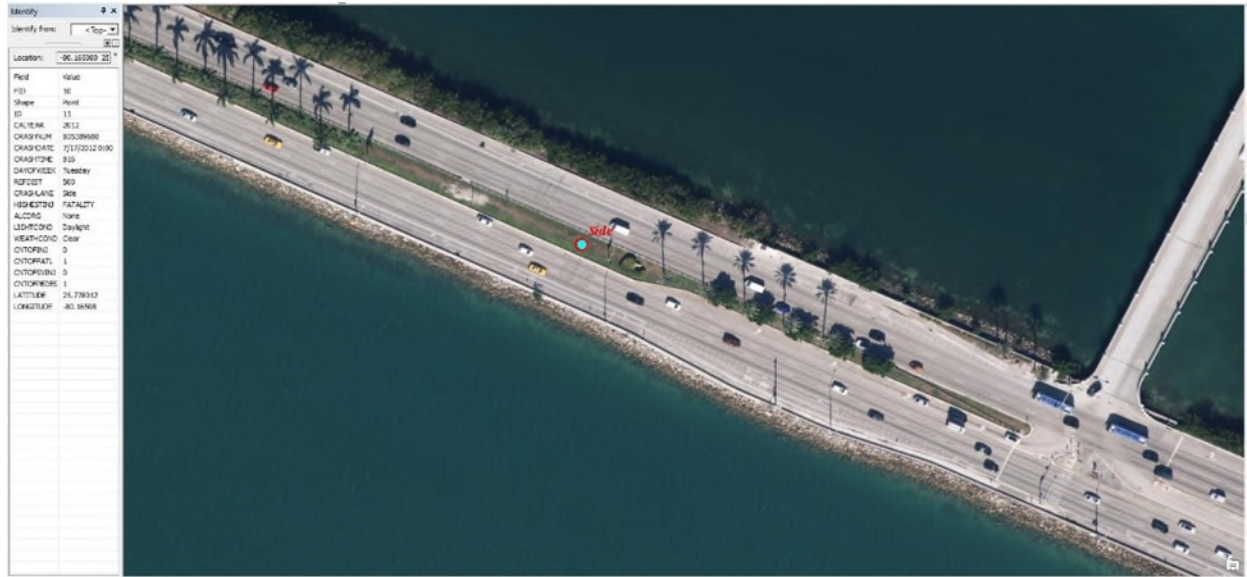




































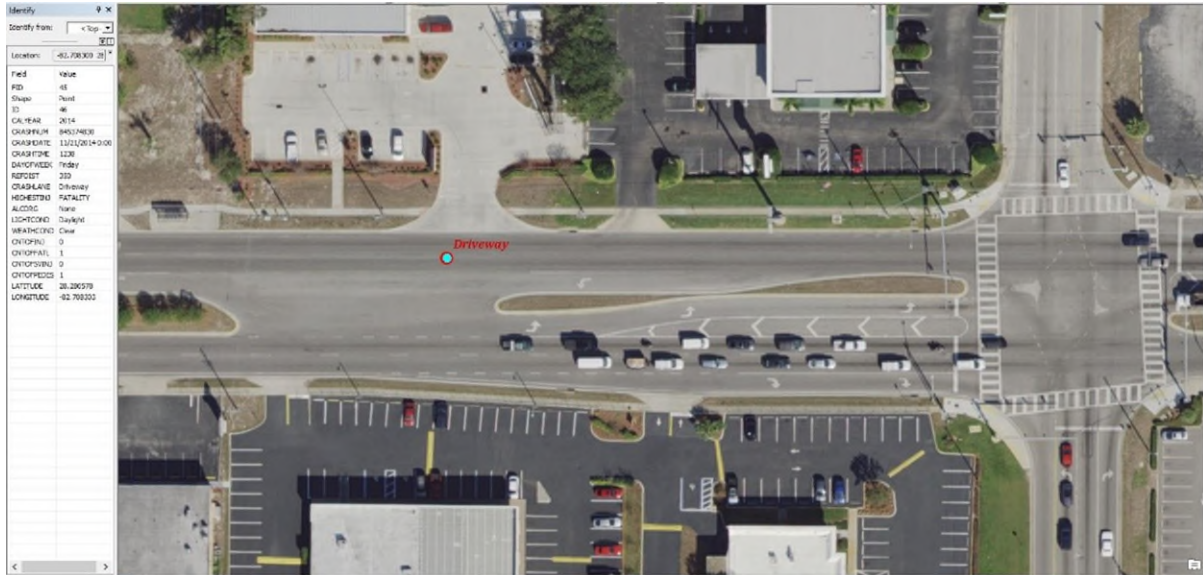












Identify

Identify from: < Top

Locations: -82.70000 28

| Field | Value |
|------------|-----------------|
| FID | 46 |
| Shape | Point |
| ID | 46 |
| CALYEAR | 2014 |
| CRASHNUM | 88034828 |
| CRASHDATE | 12/21/2014 0:00 |
| CRASHTIME | 12:00 |
| DAYOFFWEEK | Friday |
| REPORT | 200 |
| CRASHLANE | Driveway |
| HIGHWAY | FATALITY |
| AUDISC | None |
| LIGHTCOND | Dark/Not Lit |
| WEATHCOND | Clear |
| ONTOPRD | 0 |
| ONTOPFAT | 1 |
| ONTOPSRU | 0 |
| ONTOPRES | 1 |
| LATITUDE | 28.206579 |
| LONGITUDE | -82.700000 |

Identify

Identify from: < Top

Locations: -80.644702 28

| Field | Value |
|------------|-----------------|
| FID | 46 |
| Shape | Point |
| ID | 47 |
| CALYEAR | 2014 |
| CRASHNUM | 84768200 |
| CRASHDATE | 10/10/2014 0:00 |
| CRASHTIME | 2:00 |
| DAYOFFWEEK | Saturday |
| REPORT | 400 |
| CRASHLANE | Cross Walk |
| HIGHWAY | FATALITY |
| AUDISC | None |
| LIGHTCOND | Dark/Not Lit |
| WEATHCOND | Clear |
| ONTOPRD | 0 |
| ONTOPFAT | 1 |
| ONTOPSRU | 0 |
| ONTOPRES | 1 |
| LATITUDE | 28.121815 |
| LONGITUDE | -80.644702 |

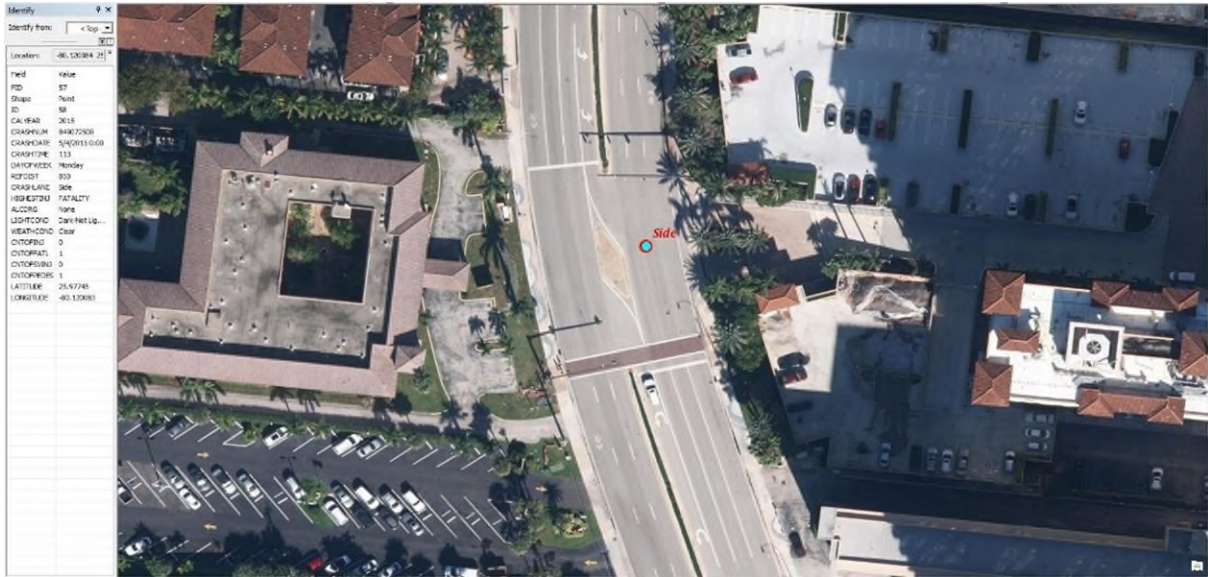








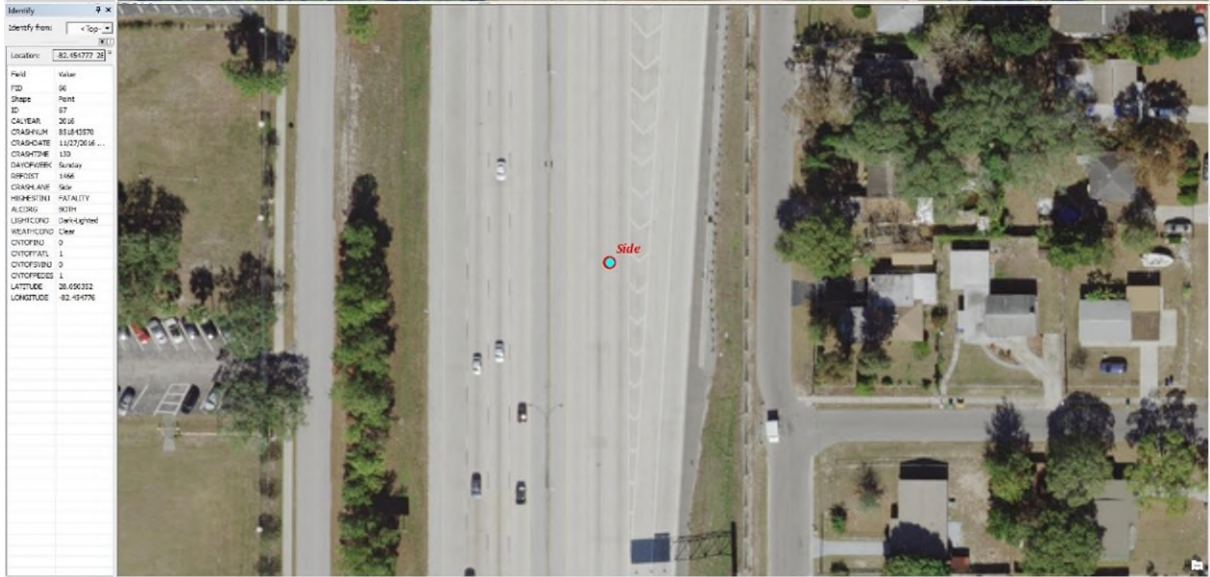












Identify 9 X

Identify from: < Top

Locators: 82.315468 28

| Field | Value |
|------------|---------------|
| FID | 87 |
| Shape | Point |
| ID | 88 |
| CALYEAR | 2016 |
| CSAPNUM | 88223488 |
| CSAPDATE | 4/1/2014 0:00 |
| CRASHTIME | 14:48 |
| DAYOFFENSE | Friday |
| REPORT | 1384 |
| CRASHLANE | 306 |
| REARSTRI | FATALITY |
| ADDRESS | None |
| LIGHTCOND | Daylight |
| WEATHCOND | Clear |
| ONTOPRD | 2 |
| ONTOPFAT | 1 |
| ONTOPDND | 2 |
| ONTOPPECS | 4 |
| LATITUDE | 28.181658 |
| LONGITUDE | 82.315468 |

Identify 9 X

Identify from: < Top

Locators: 87.517914 30

| Field | Value |
|------------|----------------|
| FID | 88 |
| Shape | Point |
| ID | 88 |
| CALYEAR | 2016 |
| CSAPNUM | 88241288 |
| CSAPDATE | 5/14/2016 6:00 |
| CRASHTIME | 11:00 |
| DAYOFFENSE | Saturday |
| REPORT | 209 |
| CRASHLANE | Cross Walk |
| REARSTRI | FATALITY |
| ADDRESS | None |
| LIGHTCOND | Daylight |
| WEATHCOND | Clear |
| ONTOPRD | 0 |
| ONTOPFAT | 1 |
| ONTOPDND | 0 |
| ONTOPPECS | 1 |
| LATITUDE | 30.231669 |
| LONGITUDE | 87.517914 |





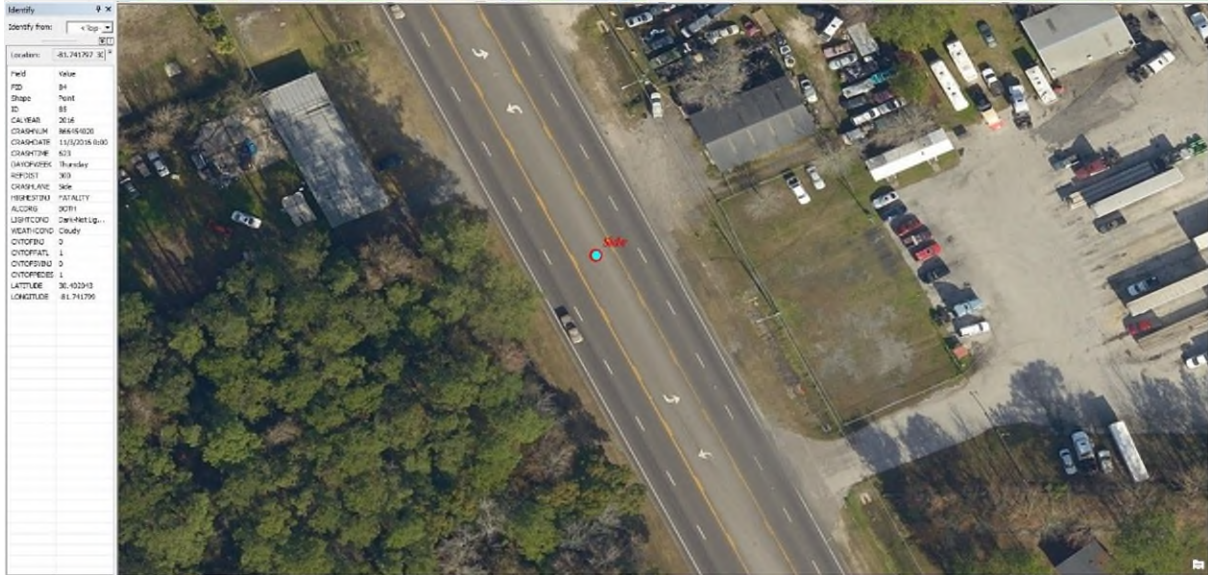


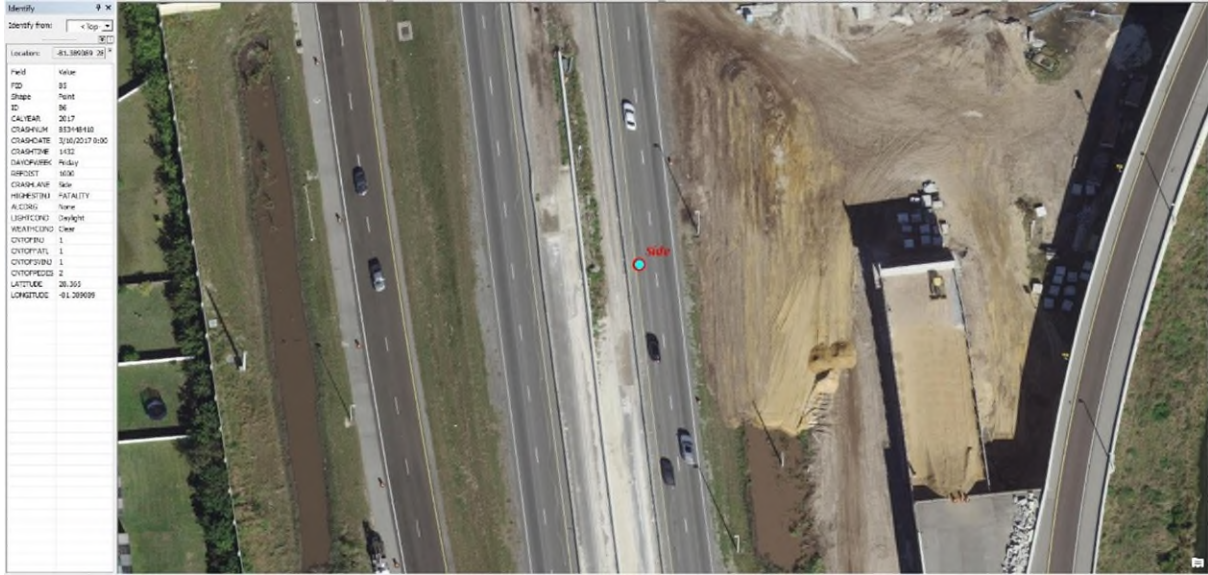






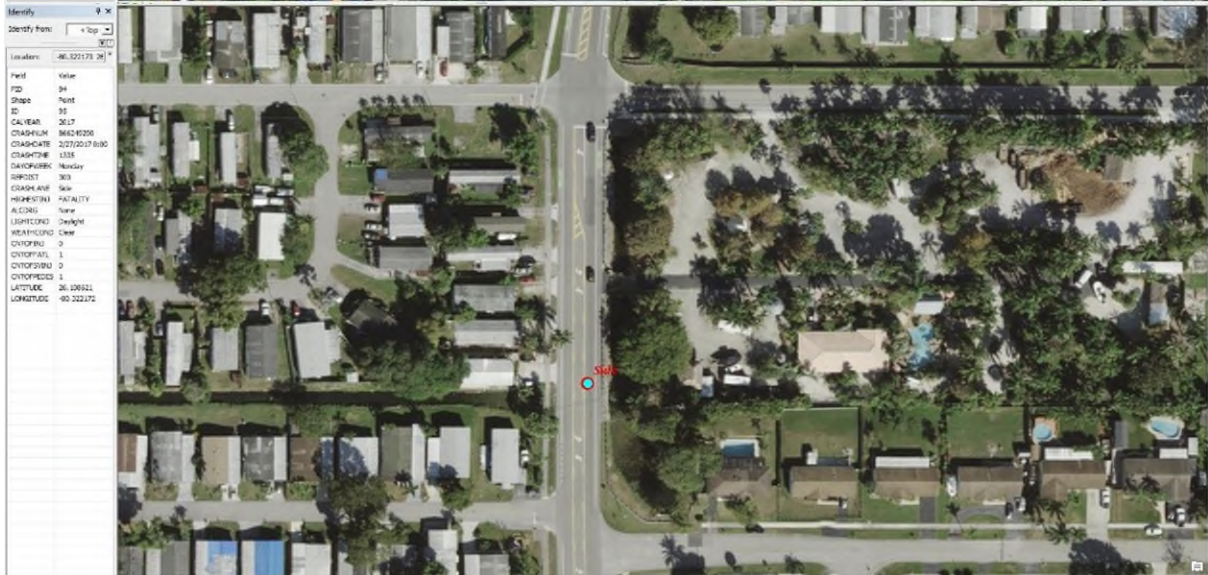














Identify from:

Location:

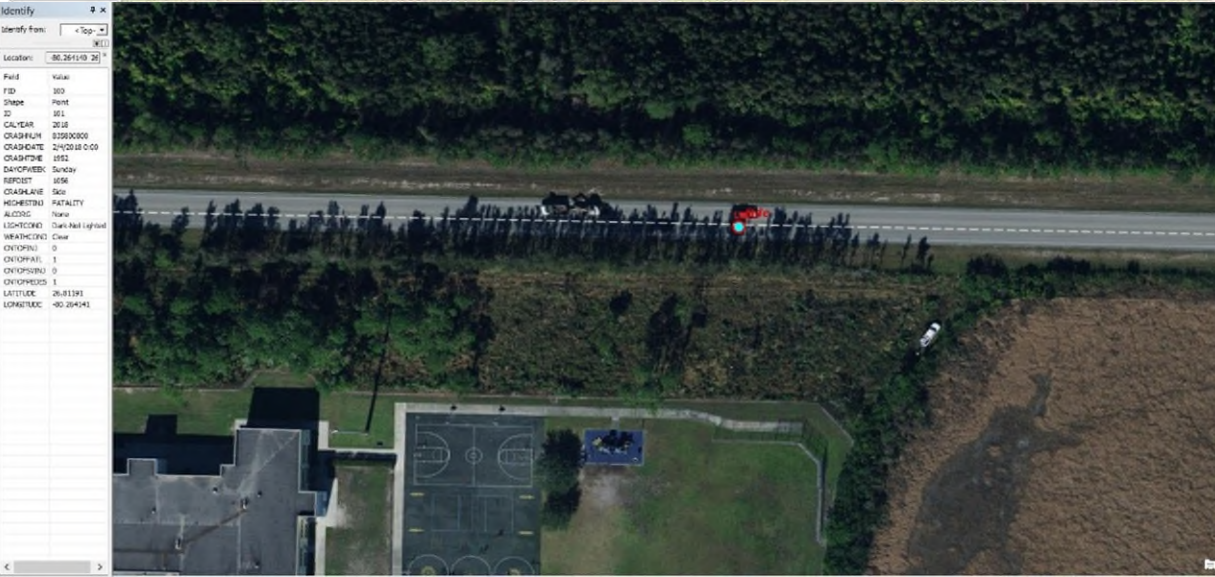
| Field | Value |
|-----------|----------------|
| FID | 95 |
| Shape | Point |
| ID | 96 |
| CALYEAR | 2017 |
| CRASHLINE | 86132316 |
| CRASHDATE | 6/24/2017 6:00 |
| CRASHTIME | 7:08 |
| DRIVERSEX | Suburban |
| WFOFID | 330 |
| CRASHLANE | Cross Walk |
| HOVRESTRI | FATALITY |
| ALCOH | None |
| LIGHTCOND | Daylight |
| WEATHCOND | Clear |
| OUTPTNO | 0 |
| OUTPTFAL | 1 |
| OUTPTSDU | 0 |
| OUTPTPRES | 1 |
| LATITUDE | 28.08027 |
| LONGITUDE | 82.4514 |

Identify from:

Location:

| Field | Value |
|-----------|------------------|
| FID | 95 |
| Shape | Point |
| ID | 97 |
| CALYEAR | 2017 |
| CRASHLINE | 87116080 |
| CRASHDATE | 10/12/2017 11:00 |
| CRASHTIME | 8:00 |
| DRIVERSEX | Tuesday |
| WFOFID | 400 |
| CRASHLANE | Driveway |
| HOVRESTRI | FATALITY |
| ALCOH | None |
| LIGHTCOND | Daylight |
| WEATHCOND | Clear |
| OUTPTNO | 0 |
| OUTPTFAL | 1 |
| OUTPTSDU | 0 |
| OUTPTPRES | 1 |
| LATITUDE | 28.47860 |
| LONGITUDE | -81.39651 |





Identify

Identify from: < Top

Location: 84.33756 30

| | |
|-----------|---------------|
| Field | Value |
| FID | 101 |
| Shape | Point |
| ID | 101 |
| CALYEAR | 2018 |
| CRASHNUM | 85542890 |
| CRASHDATE | 2/4/2018 9:00 |
| CRASHTIME | 1:17 |
| DAYOFWEEK | Sunday |
| REPORT | 856 |
| CRASHLANE | Side |
| HIGHWAY | FATALITY |
| ALCOH | Drugs |
| WEATHCOND | Overcast |
| CYTOFNU | 0 |
| CYTOFAC1 | 1 |
| CYTOFSDNU | 0 |
| CYTOFREES | 1 |
| LATITUDE | 30.56945 |
| LONGITUDE | -84.33753 |

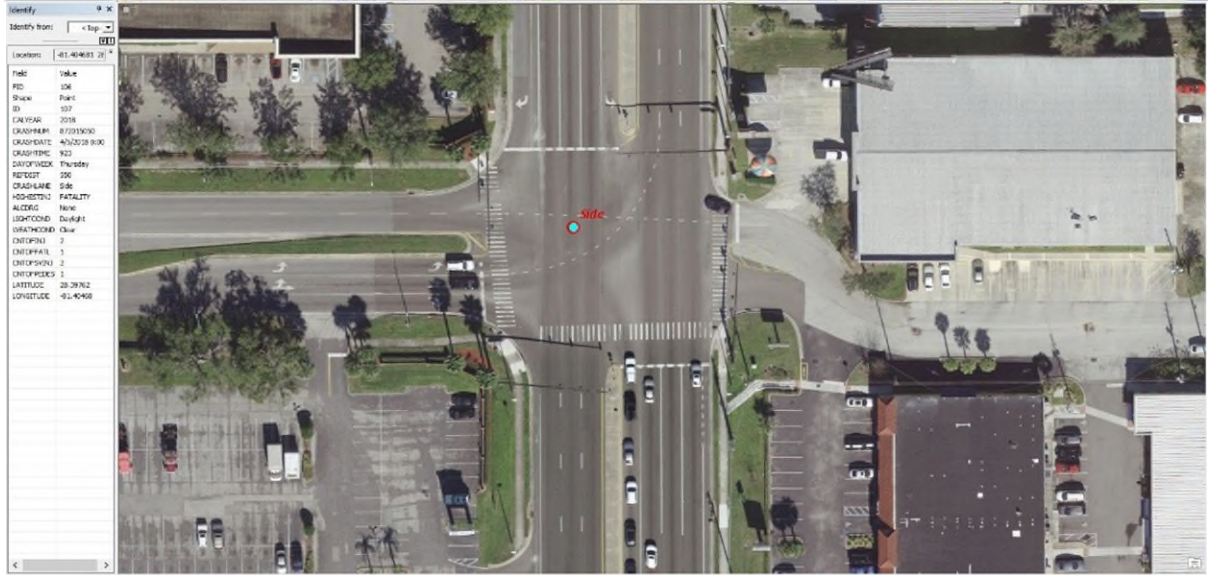
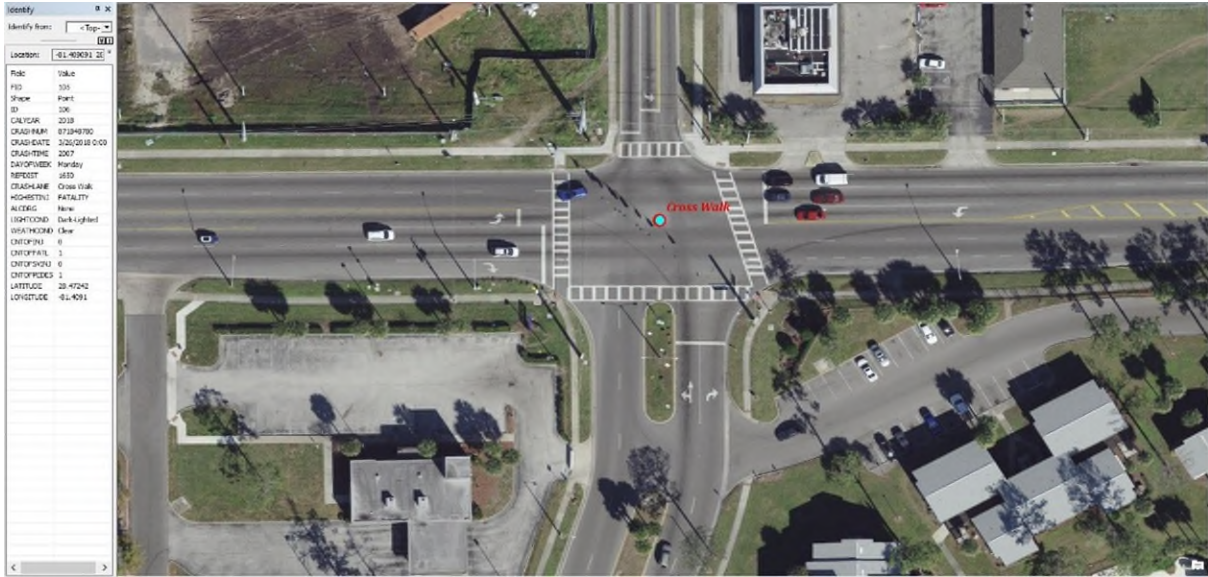
Identify

Identify from: < Top

Location: 83.332494 21

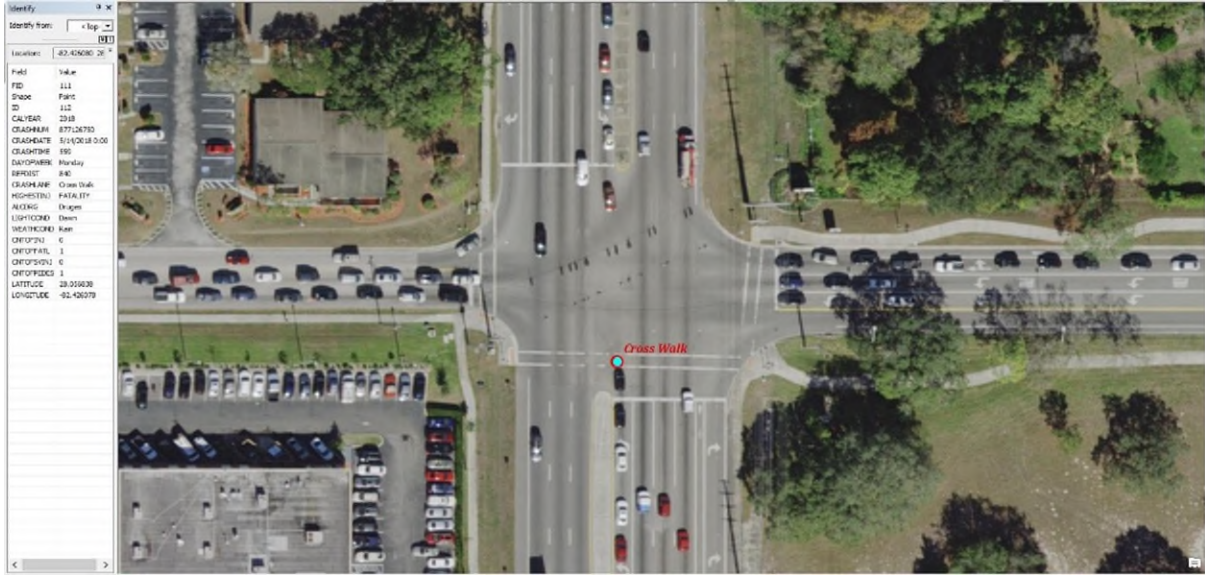
| | |
|-----------|----------------|
| Field | Value |
| FID | 102 |
| Shape | Point |
| ID | 102 |
| CALYEAR | 2018 |
| CRASHNUM | 855017206 |
| CRASHDATE | 1/22/2018 6:00 |
| CRASHTIME | 1:59 |
| DAYOFWEEK | Tuesday |
| REPORT | 1565 |
| CRASHLANE | Side |
| HIGHWAY | FATALITY |
| ALCOH | Drugs |
| WEATHCOND | Overcast |
| CYTOFNU | 0 |
| CYTOFAC1 | 1 |
| CYTOFSDNU | 0 |
| CYTOFREES | 1 |
| LATITUDE | 28.85517 |
| LONGITUDE | -83.33248 |



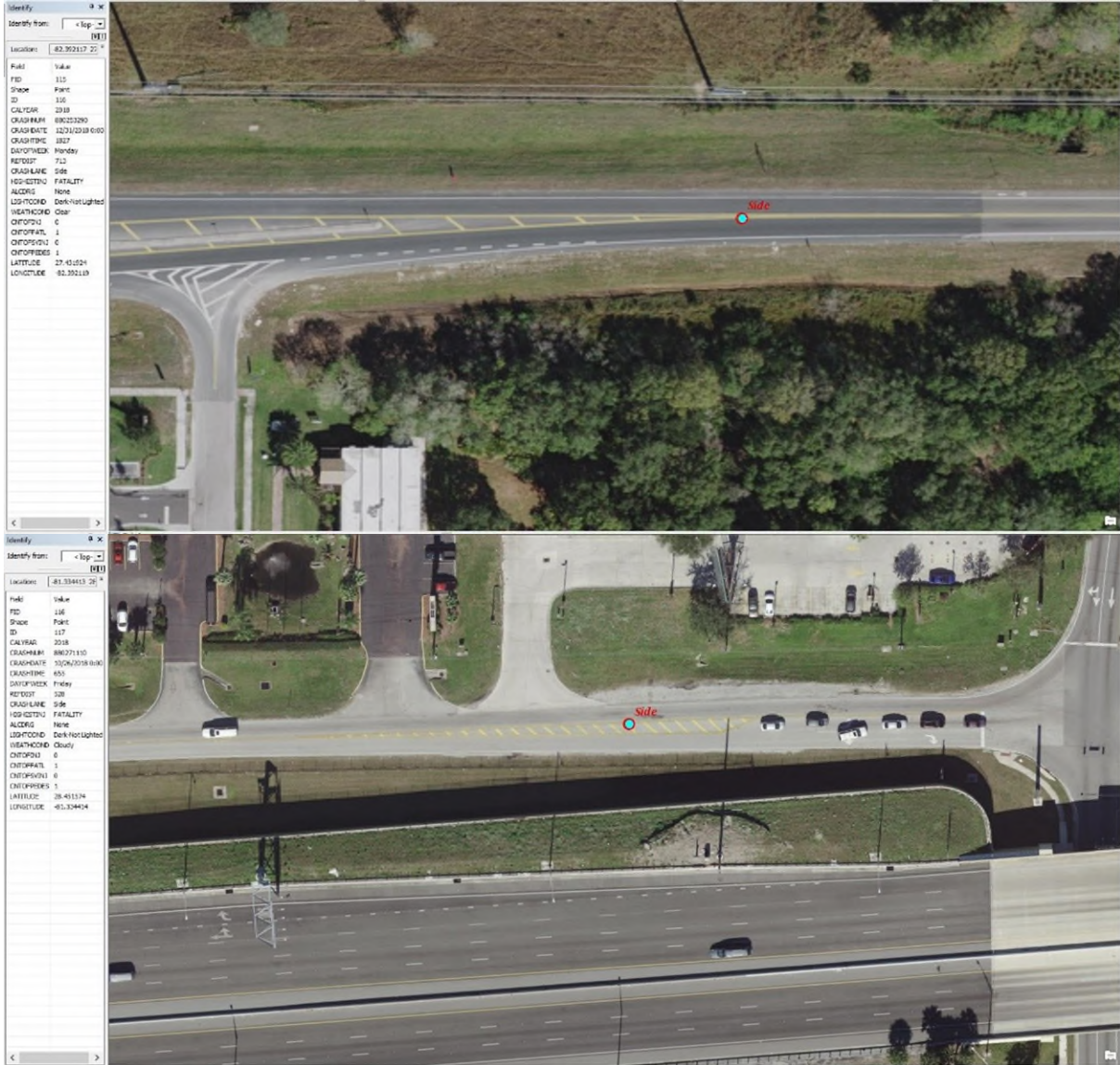


















Identify

Identify from:

Location:

| Field | Value |
|------------|----------------|
| FID | 120 |
| Shape | Point |
| ID | 121 |
| CALYEAR | 2015 |
| CRASHFID | 83864523 |
| CRASHDATE | 1/17/2015 0:00 |
| CRASHTIME | 0:03 |
| DAYOFFWEEK | Thursday |
| REPORT | 363 |
| CRASHLANE | Side |
| REG-ESTNO | FATALITY |
| AUDCIS | None |
| LSHTCOND | Dark/Not Lgt |
| WEATHCOND | Clear |
| CRFTRFID | 0 |
| CRFTRFAT | 1 |
| CRFTRFID2 | 0 |
| CRFTRFAT2 | 1 |
| LATITUDE | 28.824195 |
| LONGITUDE | -82.071403 |

Identify

Identify from:

Location:

| Field | Value |
|------------|----------------|
| FID | 121 |
| Shape | Point |
| ID | 122 |
| CALYEAR | 2019 |
| CRASHFID | 88240023 |
| CRASHDATE | 2/24/2019 0:00 |
| CRASHTIME | 0:00 |
| DAYOFFWEEK | Sunday |
| REPORT | 100 |
| CRASHLANE | Side |
| REG-ESTNO | FATALITY |
| AUDCIS | 807H |
| LSHTCOND | Dark/Lighted |
| WEATHCOND | Clear |
| CRFTRFID | 0 |
| CRFTRFAT | 1 |
| CRFTRFID2 | 0 |
| CRFTRFAT2 | 1 |
| LATITUDE | 28.5637 |
| LONGITUDE | -81.992392 |

Identify

Identify from: < Top >

Location: -81.583468 28.1

| Field | Value |
|-----------|-----------------|
| FID | 122 |
| Shape | Point |
| ID | 123 |
| CALYEAR | 2019 |
| CRASHYEAR | 88374910 |
| CRASHDATE | 5/11/2019 0:00 |
| CRASHTIME | 200 |
| SAHOPIER | Saturday |
| REPORT | 824 |
| CRASHLANE | Side |
| REQUESTED | FATALITY |
| ALDRNG | Drugs |
| LIGHTCOND | Dark-Aft Lig... |
| WEATHCOND | Clear |
| ONTRFSL | 0 |
| ONTRFSL1 | 1 |
| ONTRFSL2 | 0 |
| ONTRFSL3 | 1 |
| LATITUDE | 28.0885 |
| LONGITUDE | -81.58341 |

Identify

Identify from: < Top >

Location: -82.699147 28.1

| Field | Value |
|-----------|----------------|
| FID | 123 |
| Shape | Point |
| ID | 124 |
| CALYEAR | 2019 |
| CRASHYEAR | 88293880 |
| CRASHDATE | 2/27/2019 0:00 |
| CRASHTIME | 1405 |
| SAHOPIER | Wednesday |
| REPORT | 8001 |
| CRASHLANE | Side |
| REQUESTED | FATALITY |
| ALDRNG | None |
| LIGHTCOND | Daylight |
| WEATHCOND | Clear |
| ONTRFSL | 1 |
| ONTRFSL1 | 1 |
| ONTRFSL2 | 0 |
| ONTRFSL3 | 1 |
| LATITUDE | 28.139124 |
| LONGITUDE | -82.699196 |





Identify

Identify from:

Location:

| Field | Value |
|------------|------------|
| FID | 120 |
| Shape | Point |
| ID | 120 |
| CALYEAR | 2015 |
| CRASHNUM | 88165720 |
| CRASHDATE | 11/26/2015 |
| CRASHTIME | 1500 |
| DAYOFFWEEK | Tuesday |
| CRASHTYPE | 400 |
| CRASHLINE | Driveway |
| HIGHWAY | FATALITY |
| AIDLOC | None |
| LIGHTCOND | Dark |
| WEATHCOND | Clear |
| CRASHFID | 0 |
| CRASHFID2 | 1 |
| CRASHFID3 | 0 |
| CRASHFID4 | 0 |
| CRASHFID5 | 1 |
| LATITUDE | 26.58853 |
| LONGITUDE | -81.88221 |



Identify

Identify from:

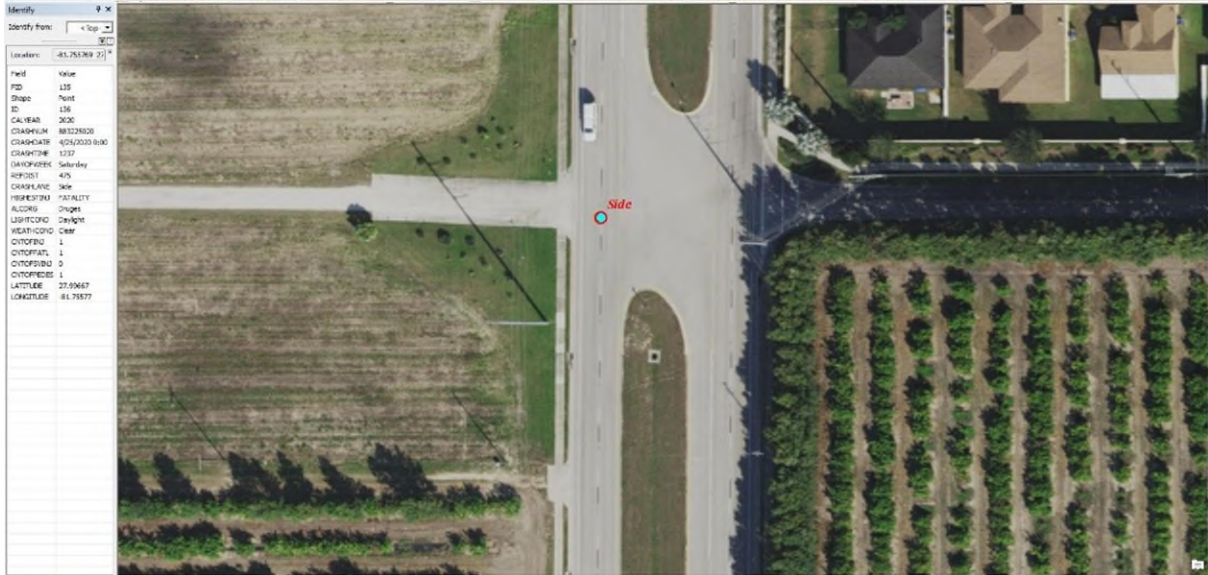
Location:

| Field | Value |
|------------|-----------------|
| FID | 126 |
| Shape | Point |
| ID | 126 |
| CALYEAR | 2019 |
| CRASHNUM | 88633970 |
| CRASHDATE | 4/3/2019 0900 |
| CRASHTIME | 624 |
| DAYOFFWEEK | Friday |
| CRASHTYPE | 200 |
| CRASHLINE | Driveway |
| HIGHWAY | FATALITY |
| AIDLOC | None |
| LIGHTCOND | Dark Not Lit Up |
| WEATHCOND | Rain |
| CRASHFID | 0 |
| CRASHFID2 | 1 |
| CRASHFID3 | 6 |
| CRASHFID4 | 1 |
| CRASHFID5 | 1 |
| LATITUDE | 26.58171 |
| LONGITUDE | -81.25000 |









Identify From: < Top >

Location: 80.859312 28.1

| Field | Value |
|-----------|------------------|
| FID | 139 |
| Shape | Point |
| ID | 137 |
| CALYEAR | 2020 |
| CRASHFLN | 80363838 |
| CRASHDATE | 05/10/2020 0:00 |
| CRASHTIME | 30 |
| DRYOFFMTR | Saturday |
| RETCOD | 309 |
| CRASHLINE | Side |
| REGESTNO | FATALITY |
| ALCKID | Crash |
| LIGHTCOND | Dark/Not Lighted |
| WEATHCOND | Cloudy |
| CHTOPSDI | 0 |
| CHTOPFAT | 1 |
| CHTOPSBI | 0 |
| CHTOPPRES | 1 |
| LATITUDE | 28.498815 |
| LONGITUDE | -80.859312 |

Identify From: < Top >

Location: -81.229251 28.1

| Field | Value |
|-----------|------------------|
| FID | 137 |
| Shape | Point |
| ID | 138 |
| CALYEAR | 2020 |
| CRASHFLN | 80364036 |
| CRASHDATE | 11/22/2020 9:00 |
| CRASHTIME | 17:30 |
| DRYOFFMTR | Sunday |
| RETCOD | 309 |
| CRASHLINE | Side |
| REGESTNO | FATALITY |
| ALCKID | Accident |
| LIGHTCOND | Dark/Not Lighted |
| WEATHCOND | Cloudy |
| CHTOPSDI | 0 |
| CHTOPFAT | 1 |
| CHTOPSBI | 0 |
| CHTOPPRES | 1 |
| LATITUDE | 28.786337 |
| LONGITUDE | -81.229251 |

Identify

Identify From: <Top>

Location: -81.809829 25

| Field | Value |
|------------|--------------------|
| FID | 138 |
| Shape | Point |
| ID | 138 |
| CALYEAR | 2020 |
| CRASHNUM | 88244238 |
| CRASHDATE | 11/12/2020 0900 |
| CRASHTIME | 2036 |
| DAYOFFWEEK | Saturday |
| REPORT | 239 |
| CRASHLANE | 306 |
| HEADSTRIKE | FATALITY |
| AUCTION | None |
| LIGHTCOND | Dark Night Lighted |
| WEATHCOND | Clear |
| CRTRFREQ | 1 |
| CRTRFREQ1 | 1 |
| CRTRFREQ2 | 0 |
| CRTRFREQ3 | 0 |
| LATITUDE | 26.71395 |
| LONGITUDE | -81.809829 |

This satellite image shows a rural landscape with a road running vertically. A red dot with a blue outline is placed on the road, labeled 'Side' in red text. The surrounding area includes trees, grass, and some buildings.

Identify

Identify From: <Top>

Location: -84.302479 35

| Field | Value |
|------------|-----------------|
| FID | 139 |
| Shape | Point |
| ID | 140 |
| CALYEAR | 2020 |
| CRASHNUM | 88147026 |
| CRASHDATE | 12/06/2020 0900 |
| CRASHTIME | 825 |
| DAYOFFWEEK | Thursday |
| REPORT | 720 |
| CRASHLANE | Cross Walk |
| HEADSTRIKE | FATALITY |
| AUCTION | None |
| LIGHTCOND | Dark Night |
| WEATHCOND | Clear |
| CRTRFREQ | 0 |
| CRTRFREQ1 | 1 |
| CRTRFREQ2 | 0 |
| CRTRFREQ3 | 1 |
| LATITUDE | 30.48261 |
| LONGITUDE | -84.302479 |

This satellite image shows a road intersection with a parking lot in the foreground. A red dot with a blue outline is placed at the intersection, labeled 'CRASH SITE' in red text. The scene includes cars on the road, trees, and a building.





Table A-1: Number of fatal pedestrian-involved crashes in Florida between 2011 and 2020

| County Name | Number of Crashes |
|----------------------|-------------------|
| Orange | 18 |
| Hillsborough | 11 |
| Pasco | 9 |
| Broward | 8 |
| Miami-Dade | 6 |
| Leon | 6 |
| Palm Beach | 5 |
| Polk | 5 |
| Collier | 5 |
| Brevard | 5 |
| Lee | 4 |
| Volusia | 4 |
| St. Johns | 4 |
| Manatee | 4 |
| Duval | 4 |
| Others Counties (<3) | 45 |

Table A-2: Attributes associated with fatal pedestrian-involved crashes in Florida between 2011 and 2020
Hillsborough; Leon; Orange; Pasco

| ID | COUNTY NAME | YEAR | CRASH NUMBER | CRASH DATE | DAY OF WEEK | DISTANCE | CRASH LANE | LATITUDE | LONGITUDE |
|----|-------------|------|--------------|----------------|-------------|----------|------------|-----------|------------|
| 1 | Escambia | 2011 | 819934570 | 3/26/2011 0:00 | Saturday | 603 | Side | 30.374286 | -87.355703 |
| 2 | Monroe | 2011 | 820535280 | 6/9/2011 0:00 | Thursday | 741 | Side | 24.661516 | -81.409844 |
| 3 | iami-Dade | 2011 | 820851010 | 5/13/2011 0:00 | Friday | 259 | Side | 25.911608 | -80.209915 |
| 4 | iami-Dade | 2011 | 823532700 | 5/5/2011 0:00 | Thursday | 600 | Side | 25.653098 | -80.329825 |
| 5 | Jackson | 2011 | 820056070 | 7/15/2011 0:00 | Friday | 441 | Side | 30.677309 | -85.080903 |
| 6 | Bay | 2011 | 820777290 | 7/12/2011 0:00 | Tuesday | 440 | Side | 30.264243 | -85.971775 |
| 7 | Brevard | 2012 | 819505460 | 2/16/2012 0:00 | Thursday | 542 | Side | 28.202851 | -80.661062 |
| 8 | iami-Dade | 2012 | 828641690 | 1/12/2012 0:00 | Thursday | 300 | Side | 25.73283 | -80.346554 |
| 9 | Orange | 2012 | 828541380 | 1/12/2012 0:00 | Thursday | 500 | Side | 28.55249 | -81.449032 |
| 10 | Marion | 2012 | 829010990 | 4/25/2012 0:00 | Wednesday | 300 | Side | 29.213898 | -82.06045 |
| 11 | iami-Dade | 2012 | 835389680 | 7/17/2012 0:00 | Tuesday | 500 | Side | 25.778012 | -80.16508 |
| 12 | Polk | 2012 | 831625860 | 2/20/2012 0:00 | Thursday | 285 | Side | 28.346991 | -81.663419 |
| 13 | Highlands | 2012 | 821239560 | 8/2/2012 0:00 | Thursday | 269 | Side | 27.299356 | -81.353653 |
| 14 | Broward | 2012 | 805222160 | 11/2/2012 0:00 | Friday | 1149 | Side | 25.975174 | -80.348209 |
| 15 | Pasco | 2012 | 832577870 | 2/18/2012 0:00 | Tuesday | 1400 | Cross Walk | 28.335006 | -82.666326 |
| 16 | Palm Beach | 2013 | 813401000 | 9/23/2013 0:00 | Monday | 300 | Side | 26.617136 | -80.105434 |
| 17 | Duval | 2013 | 836056750 | 7/19/2013 0:00 | Friday | 421 | Side | 30.277782 | -81.637204 |
| 18 | St. Johns | 2013 | 823880080 | 1/16/2013 0:00 | Saturday | 500 | Side | 29.910807 | -81.361041 |
| 19 | Broward | 2013 | 834995970 | 1/18/2013 0:00 | Monday | 1150 | Side | 26.059259 | -80.152661 |
| 20 | DeSoto | 2013 | 832455310 | 1/26/2013 0:00 | Saturday | 308 | Side | 27.171902 | -81.875534 |
| 21 | Escambia | 2013 | 829386710 | 3/22/2013 0:00 | Friday | 257 | Side | 30.499359 | -87.180042 |
| 22 | Monroe | 2013 | 832466950 | 5/26/2013 0:00 | Sunday | 2000 | Side | 24.576209 | -81.725928 |

| | | | | | | | | | |
|----|------------|------|-----------|-----------------|-----------|------|------------|-----------|------------|
| 23 | Pasco | 2013 | 833317200 | 7/21/2013 0:00 | Sunday | 336 | Side | 28.354287 | -82.698951 |
| 24 | Santa Rosa | 2013 | 833264710 | 7/16/2013 0:00 | Tuesday | 540 | Side | 30.399926 | -86.998286 |
| 25 | Volusia | 2013 | 835254720 | 8/6/2013 0:00 | Tuesday | 800 | Side | 29.013023 | -80.977086 |
| 26 | Volusia | 2013 | 834513460 | 8/27/2013 0:00 | Tuesday | 495 | Side | 28.964934 | -80.891306 |
| 27 | Orange | 2013 | 836502010 | 7/20/2013 0:00 | Saturday | 300 | Side | 28.378105 | -81.503874 |
| 28 | Highlands | 2014 | 821393790 | 3/25/2014 0:00 | Tuesday | 1000 | Side | 27.474318 | -81.443156 |
| 29 | Sarasota | 2014 | 839398140 | 4/16/2014 0:00 | Wednesday | 300 | Side | 27.325074 | -82.529757 |
| 30 | Pinellas | 2014 | 842553800 | 3/27/2014 0:00 | Thursday | 300 | Cross Walk | 27.82095 | -82.825972 |
| 31 | Orange | 2014 | 837737870 | 5/3/2014 0:00 | Saturday | 500 | Side | 28.411479 | -81.474548 |
| 32 | St. Johns | 2014 | 837654730 | 6/28/2014 0:00 | Saturday | 300 | Side | 29.987417 | -81.462466 |
| 33 | Orange | 2014 | 842874690 | 10/26/2014 0:00 | Sunday | 500 | Cross Walk | 28.672829 | -81.461176 |
| 34 | Palm Beach | 2014 | 844854970 | 10/26/2014 0:00 | Sunday | 1000 | Side | 26.347749 | -80.117968 |
| 35 | Duval | 2014 | 836035260 | 11/20/2014 0:00 | Thursday | 300 | Side | 30.282049 | -81.746558 |
| 36 | Collier | 2014 | 833359220 | 11/15/2014 0:00 | Saturday | 430 | Side | 26.019135 | -81.630128 |
| 37 | Polk | 2014 | 846237200 | 11/26/2014 0:00 | Wednesday | 1000 | Side | 28.055936 | -81.82671 |
| 38 | Sarasota | 2014 | 837227970 | 1/22/2014 0:00 | Wednesday | 792 | Side | 27.225678 | -82.518404 |
| 39 | Sarasota | 2014 | 837228030 | 1/28/2014 0:00 | Tuesday | 770 | Side | 27.080435 | -82.41215 |
| 40 | Walton | 2014 | 837941360 | 6/12/2014 0:00 | Thursday | 1584 | Side | 30.365422 | -86.22934 |
| 41 | Orange | 2014 | 838375170 | 6/28/2014 0:00 | Saturday | 740 | Driveway | 28.532092 | -81.272763 |
| 42 | Miami-Dade | 2014 | 843604230 | 4/28/2014 0:00 | Monday | 1000 | Side | 25.598607 | -80.510988 |
| 43 | Manatee | 2014 | 713847500 | 12/25/2014 0:00 | Thursday | 1100 | Driveway | 27.531638 | -82.593396 |
| 44 | Palm Beach | 2014 | 813965560 | 12/13/2014 0:00 | Saturday | 450 | Driveway | 26.615535 | -80.069852 |
| 45 | Orange | 2014 | 833584500 | 10/23/2014 0:00 | Thursday | 1584 | Cross Walk | 28.459813 | -81.468839 |
| 46 | Pasco | 2014 | 845374830 | 11/21/2014 0:00 | Friday | 350 | Driveway | 28.280578 | -82.708303 |
| 47 | Brevard | 2014 | 847982700 | 10/4/2014 0:00 | Saturday | 490 | Cross Walk | 28.121615 | -80.644702 |

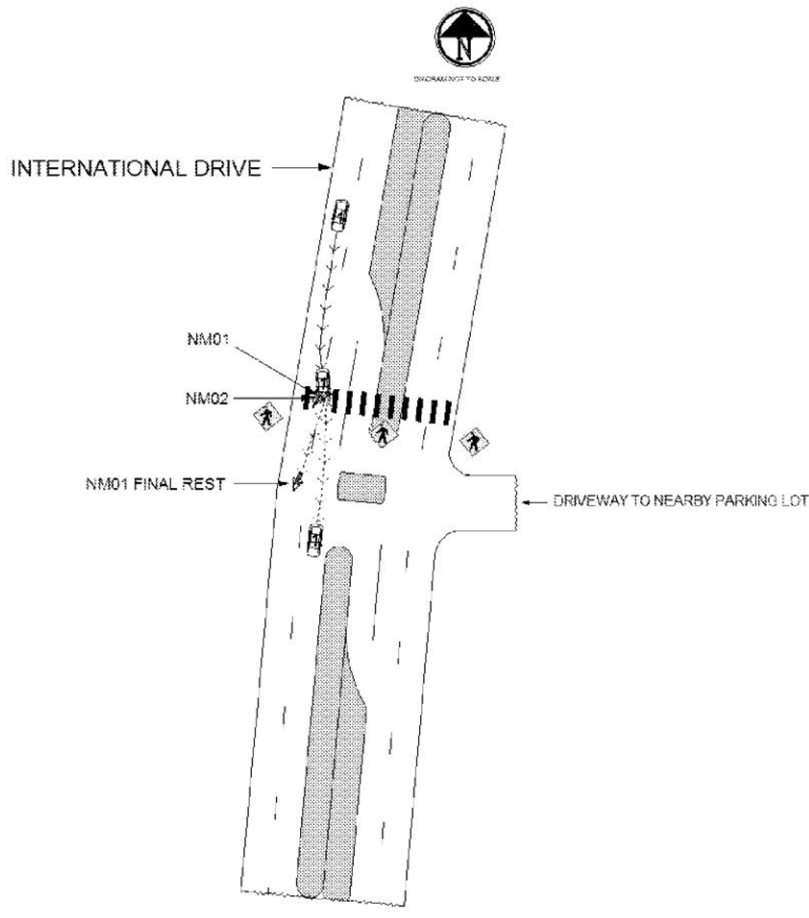
| | | | | | | | | | |
|----|--------------|------|-----------|-----------------|-----------|------|------------|-----------|------------|
| 48 | St. Johns | 2015 | 823942280 | 7/8/2015 0:00 | Wednesday | 1500 | Side | 29.936781 | -81.332803 |
| 49 | Highlands | 2015 | 837596880 | 6/2/2015 0:00 | Tuesday | 265 | Side | 27.443964 | -81.293092 |
| 50 | Collier | 2015 | 838392820 | 4/25/2015 0:00 | Saturday | 1500 | Side | 26.379237 | -81.417037 |
| 51 | Leon | 2015 | 844944380 | 12/6/2015 0:00 | Sunday | 1800 | Side | 30.456277 | -84.374872 |
| 52 | Sumter | 2015 | 845377140 | 2/8/2015 0:00 | Sunday | 550 | Side | 28.898234 | -82.095044 |
| 53 | Monroe | 2015 | 847246420 | 9/16/2015 0:00 | Wednesday | 1500 | Side | 24.552473 | -81.760688 |
| 54 | Broward | 2015 | 847631850 | 10/29/2015 0:00 | Thursday | 400 | Side | 26.164731 | -80.204477 |
| 55 | Lake | 2015 | 848646760 | 6/10/2015 0:00 | Wednesday | 500 | Side | 28.738534 | -81.87145 |
| 56 | Lee | 2015 | 848665960 | 5/4/2015 0:00 | Monday | 650 | Side | 26.705627 | -81.842494 |
| 57 | Citrus | 2015 | 848809430 | 5/11/2015 0:00 | Monday | 680 | Cross Walk | 28.950896 | -82.625855 |
| 58 | Broward | 2015 | 849072500 | 5/4/2015 0:00 | Monday | 850 | Side | 25.97745 | -80.120083 |
| 59 | Hillsborough | 2015 | 849214090 | 11/4/2015 0:00 | Wednesday | 585 | Side | 27.996465 | -82.111507 |
| 60 | Charlotte | 2015 | 851478030 | 8/18/2015 0:00 | Tuesday | 778 | Side | 26.884319 | -81.999859 |
| 61 | Brevard | 2015 | 851647250 | 9/15/2015 0:00 | Tuesday | 1056 | Side | 28.478989 | -80.780126 |
| 62 | Brevard | 2015 | 852082390 | 12/2/2015 0:00 | Wednesday | 370 | Cross Walk | 28.246599 | -80.737919 |
| 63 | Clay | 2015 | 852209840 | 11/12/2015 0:00 | Thursday | 500 | Side | 30.06289 | -81.896195 |
| 64 | Manatee | 2015 | 901933000 | 4/1/2015 0:00 | Wednesday | 376 | Side | 27.518597 | -82.563069 |
| 65 | Palm Beach | 2016 | 814557050 | 10/2/2016 0:00 | Sunday | 415 | Driveway | 26.619019 | -80.132467 |
| 66 | St. Johns | 2016 | 851688110 | 1/7/2016 0:00 | Thursday | 825 | Side | 29.965674 | -81.3504 |
| 67 | Hillsborough | 2016 | 851843570 | 11/27/2016 0:00 | Sunday | 1466 | Side | 28.050352 | -82.454776 |
| 68 | Hernando | 2016 | 852236430 | 4/1/2016 0:00 | Friday | 1584 | Side | 28.481658 | -82.319499 |
| 69 | Escambia | 2016 | 852412080 | 5/14/2016 0:00 | Saturday | 575 | Cross Walk | 30.281669 | -87.517931 |
| 70 | Citrus | 2016 | 852544650 | 2/9/2016 0:00 | Tuesday | 1056 | Side | 28.801119 | -82.508497 |
| 71 | Orange | 2016 | 852616380 | 1/14/2016 0:00 | Thursday | 469 | Cross Walk | 28.607244 | -81.294178 |
| 72 | Pasco | 2016 | 852886930 | 4/25/2016 0:00 | Monday | 1129 | Side | 28.328982 | -82.585302 |

| | | | | | | | | | |
|----|--------------|------|-----------|-----------------|-----------|------|------------|-----------|------------|
| 73 | Orange | 2016 | 852946660 | 3/27/2016 0:00 | Sunday | 330 | Cross Walk | 28.497257 | -81.396856 |
| 74 | Collier | 2016 | 853048050 | 5/16/2016 0:00 | Monday | 320 | Cross Walk | 26.269034 | -81.756409 |
| 75 | Jefferson | 2016 | 853907250 | 12/11/2016 0:00 | Sunday | 2640 | Side | 30.60471 | -83.892922 |
| 76 | Santa Rosa | 2016 | 854123590 | 11/21/2016 0:00 | Monday | 360 | Side | 30.403456 | -86.974411 |
| 77 | Miami-Dade | 2016 | 859668710 | 10/5/2016 0:00 | Wednesday | 600 | Side | 25.446129 | -80.475027 |
| 78 | Hillsborough | 2016 | 861583880 | 12/27/2016 0:00 | Tuesday | 1900 | Side | 27.977424 | -82.552766 |
| 79 | Hillsborough | 2016 | 862065590 | 3/13/2016 0:00 | Sunday | 475 | Driveway | 28.09394 | -82.580484 |
| 80 | Orange | 2016 | 864065680 | 4/21/2016 0:00 | Thursday | 300 | Cross Walk | 28.542144 | -81.376834 |
| 81 | Orange | 2016 | 864111370 | 6/23/2016 0:00 | Thursday | 615 | Side | 28.54481 | -81.311644 |
| 82 | Polk | 2016 | 864434820 | 8/22/2016 0:00 | Monday | 350 | Side | 28.17906 | -81.814112 |
| 83 | Bay | 2016 | 865489310 | 5/21/2016 0:00 | Saturday | 380 | Cross Walk | 30.2083 | -85.862727 |
| 84 | Pinellas | 2016 | 866068950 | 8/24/2016 0:00 | Wednesday | 1110 | Cross Walk | 27.94282 | -82.835991 |
| 85 | Duval | 2016 | 866454020 | 11/3/2016 0:00 | Thursday | 300 | Side | 30.402043 | -81.741799 |
| 86 | Orange | 2017 | 853448410 | 3/10/2017 0:00 | Friday | 1000 | Side | 28.365 | -81.389089 |
| 87 | Leon | 2017 | 854318530 | 5/23/2017 0:00 | Tuesday | 830 | Cross Walk | 30.320435 | -84.398095 |
| 88 | Walton | 2017 | 854356540 | 1/21/2017 0:00 | Saturday | 840 | Side | 30.740832 | -86.371844 |
| 89 | Pasco | 2017 | 854403450 | 1/12/2017 0:00 | Thursday | 700 | Side | 28.212059 | -82.181121 |
| 90 | Volusia | 2017 | 854744080 | 7/15/2017 0:00 | Saturday | 275 | Side | 29.032439 | -81.259285 |
| 91 | Orange | 2017 | 855087830 | 3/24/2017 0:00 | Friday | 880 | Cross Walk | 28.437682 | -81.472192 |
| 92 | Pasco | 2017 | 855209880 | 5/13/2017 0:00 | Saturday | 462 | Side | 28.29276 | -82.709842 |
| 93 | Orange | 2017 | 855273530 | 5/10/2017 0:00 | Wednesday | 262 | Side | 28.4022 | -81.41067 |
| 94 | Alachua | 2017 | 865955720 | 2/11/2017 0:00 | Saturday | 1156 | Side | 29.617803 | -82.377973 |
| 95 | Broward | 2017 | 866249290 | 2/27/2017 0:00 | Monday | 300 | Side | 26.108621 | -80.322172 |
| 96 | Hillsborough | 2017 | 869179310 | 6/24/2017 0:00 | Saturday | 310 | Cross Walk | 28.069197 | -82.4314 |
| 97 | Orange | 2017 | 871168860 | 12/12/2017 0:00 | Tuesday | 400 | Driveway | 28.473682 | -81.396651 |

| | | | | | | | | | |
|-----|--------------|------|-----------|-----------------|-----------|-------|------------|-----------|------------|
| 98 | Orange | 2017 | 871263310 | 12/16/2017 0:00 | Saturday | 1320 | Side | 28.55667 | -81.128602 |
| 99 | Hillsborough | 2017 | 873707410 | 10/29/2017 0:00 | Sunday | 600 | Side | 28.001668 | -82.373097 |
| 100 | Indian River | 2018 | 819920870 | 3/1/2018 0:00 | Thursday | 792 | Side | 27.658469 | -80.446487 |
| 101 | Palm Beach | 2018 | 835800800 | 2/4/2018 0:00 | Sunday | 1056 | Side | 26.81191 | -80.264141 |
| 102 | Leon | 2018 | 855433950 | 2/4/2018 0:00 | Sunday | 850 | Side | 30.50845 | -84.33731 |
| 103 | Citrus | 2018 | 855617100 | 1/23/2018 0:00 | Tuesday | 1265 | Side | 28.858017 | -82.332418 |
| 104 | St. Lucie | 2018 | 871301230 | 6/20/2018 0:00 | Wednesday | 2112 | Side | 27.392928 | -80.340203 |
| 105 | Lake | 2018 | 871818750 | 6/19/2018 0:00 | Tuesday | 300 | Side | 28.882385 | -81.72129 |
| 106 | Orange | 2018 | 871848780 | 3/26/2018 0:00 | Monday | 1650 | Cross Walk | 28.47242 | -81.4091 |
| 107 | Orange | 2018 | 872015050 | 4/5/2018 0:00 | Thursday | 550 | Side | 28.39762 | -81.40468 |
| 108 | Pasco | 2018 | 872103620 | 6/4/2018 0:00 | Monday | 950.4 | Side | 28.377003 | -82.657679 |
| 109 | Hardee | 2018 | 872892540 | 9/10/2018 0:00 | Monday | 751 | Side | 27.58209 | -81.838072 |
| 110 | Duval | 2018 | 874951520 | 10/12/2018 0:00 | Friday | 1355 | Side | 30.40426 | -81.81745 |
| 111 | Hillsborough | 2018 | 877154630 | 7/16/2018 0:00 | Monday | 300 | Side | 28.095825 | -82.50891 |
| 112 | Hillsborough | 2018 | 877126750 | 5/14/2018 0:00 | Monday | 840 | Cross Walk | 28.056838 | -82.426078 |
| 113 | Hillsborough | 2018 | 878663830 | 11/16/2018 0:00 | Friday | 1289 | Side | 28.007453 | -82.150049 |
| 114 | Walton | 2018 | 880147650 | 10/19/2018 0:00 | Friday | 300 | Cross Walk | 30.37532 | -86.35769 |
| 115 | Marion | 2018 | 880245970 | 11/13/2018 0:00 | Tuesday | 308 | Side | 29.091729 | -82.170534 |
| 116 | Manatee | 2018 | 880253290 | 12/31/2018 0:00 | Monday | 713 | Side | 27.431924 | -82.392119 |
| 117 | Orange | 2018 | 880271110 | 10/26/2018 0:00 | Friday | 528 | Side | 28.451574 | -81.334414 |
| 118 | Collier | 2018 | 880316360 | 11/13/2018 0:00 | Tuesday | 1350 | Side | 26.25622 | -81.53721 |
| 119 | Broward | 2018 | 886595450 | 10/31/2018 0:00 | Wednesday | 990 | Cross Walk | 26.064901 | -80.235285 |
| 120 | Hillsborough | 2019 | 887682620 | 5/27/2019 0:00 | Monday | 329 | Driveway | 27.95288 | -82.49636 |
| 121 | Hillsborough | 2019 | 878665620 | 1/17/2019 0:00 | Thursday | 360 | Side | 28.024195 | -82.073482 |
| 122 | Lee | 2019 | 880436280 | 2/24/2019 0:00 | Sunday | 500 | Side | 26.6607 | -81.89059 |

| | | | | | | | | | |
|-----|----------|------|-----------|-----------------|-----------|------|------------|-----------|------------|
| 123 | Putnam | 2019 | 880749910 | 5/11/2019 0:00 | Saturday | 825 | Side | 29.60853 | -81.58341 |
| 124 | Pasco | 2019 | 880985680 | 2/27/2019 0:00 | Wednesday | 1000 | Side | 28.339134 | -82.699346 |
| 125 | Lake | 2019 | 880944670 | 7/25/2019 0:00 | Thursday | 1320 | Side | 28.737608 | -81.896358 |
| 126 | Suwannee | 2019 | 881156130 | 10/10/2019 0:00 | Thursday | 450 | Side | 30.3943 | -82.945221 |
| 127 | Pasco | 2019 | 881286790 | 5/11/2019 0:00 | Saturday | 586 | Side | 28.3331 | -82.66626 |
| 128 | Manatee | 2019 | 881643760 | 8/17/2019 0:00 | Saturday | 500 | Side | 27.557678 | -82.564647 |
| 129 | Lee | 2019 | 881869720 | 11/26/2019 0:00 | Tuesday | 400 | Driveway | 26.56853 | -81.88024 |
| 130 | Volusia | 2019 | 886955970 | 4/5/2019 0:00 | Friday | 280 | Driveway | 29.263271 | -81.106599 |
| 131 | Bay | 2019 | 892800620 | 11/9/2019 0:00 | Saturday | 1220 | Cross Walk | 30.208308 | -85.862742 |
| 132 | Broward | 2019 | 894513670 | 11/26/2019 0:00 | Tuesday | 630 | Cross Walk | 26.235497 | -80.219756 |
| 133 | Marion | 2020 | 872302370 | 6/9/2020 0:00 | Tuesday | 560 | Side | 29.11962 | -82.18462 |
| 134 | Collier | 2020 | 881665440 | 5/8/2020 0:00 | Friday | 412 | Side | 26.43043 | -81.4207 |
| 135 | Leon | 2020 | 882616600 | 5/11/2020 0:00 | Monday | 450 | Side | 30.398449 | -84.315488 |
| 136 | Polk | 2020 | 883225020 | 4/25/2020 0:00 | Saturday | 475 | Side | 27.99667 | -81.75577 |
| 137 | Brevard | 2020 | 883638590 | 10/10/2020 0:00 | Saturday | 300 | Side | 28.699845 | -80.859342 |
| 138 | Seminole | 2020 | 883864230 | 11/22/2020 0:00 | Sunday | 500 | Side | 28.786327 | -81.33505 |
| 139 | Lee | 2020 | 887840510 | 1/11/2020 0:00 | Saturday | 619 | Side | 26.71105 | -81.869939 |
| 140 | Leon | 2020 | 891476250 | 1/30/2020 0:00 | Thursday | 750 | Cross Walk | 30.448261 | -84.302469 |
| 141 | Polk | 2020 | 893748810 | 2/24/2020 0:00 | Monday | 335 | Side | 27.926956 | -82.036416 |
| 142 | Broward | 2020 | 897750240 | 2/19/2020 0:00 | Wednesday | 660 | Side | 26.136951 | -80.137573 |
| 143 | Leon | 2020 | 901120060 | 11/8/2020 0:00 | Sunday | 400 | Side | 30.478015 | -84.299166 |

APPENDIX B: Crash Diagrams for the Recorded 10 Pedestrian-involved Fatalities Occurred between 2011 and 2020 in Orange County, Florida



Crash Number: 855087830 – Orange County in 2017: The vehicle was traveling south in the right lane on International Drive and two pedestrians were crossing a marked crosswalk from east to west on International Drive. The driver failed to stop for the pedestrians when another vehicle in the left lane stopped to let them cross the southbound lanes of International Drive.

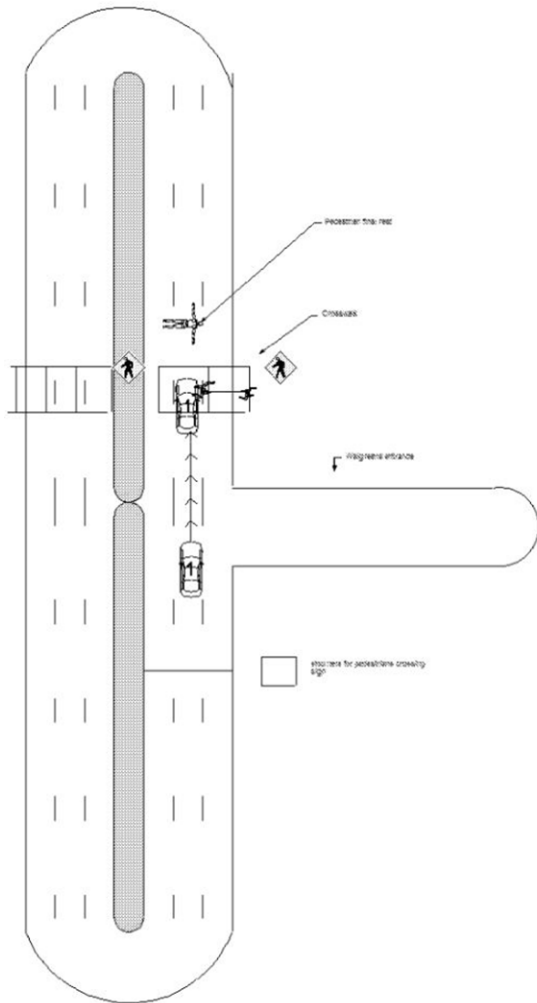
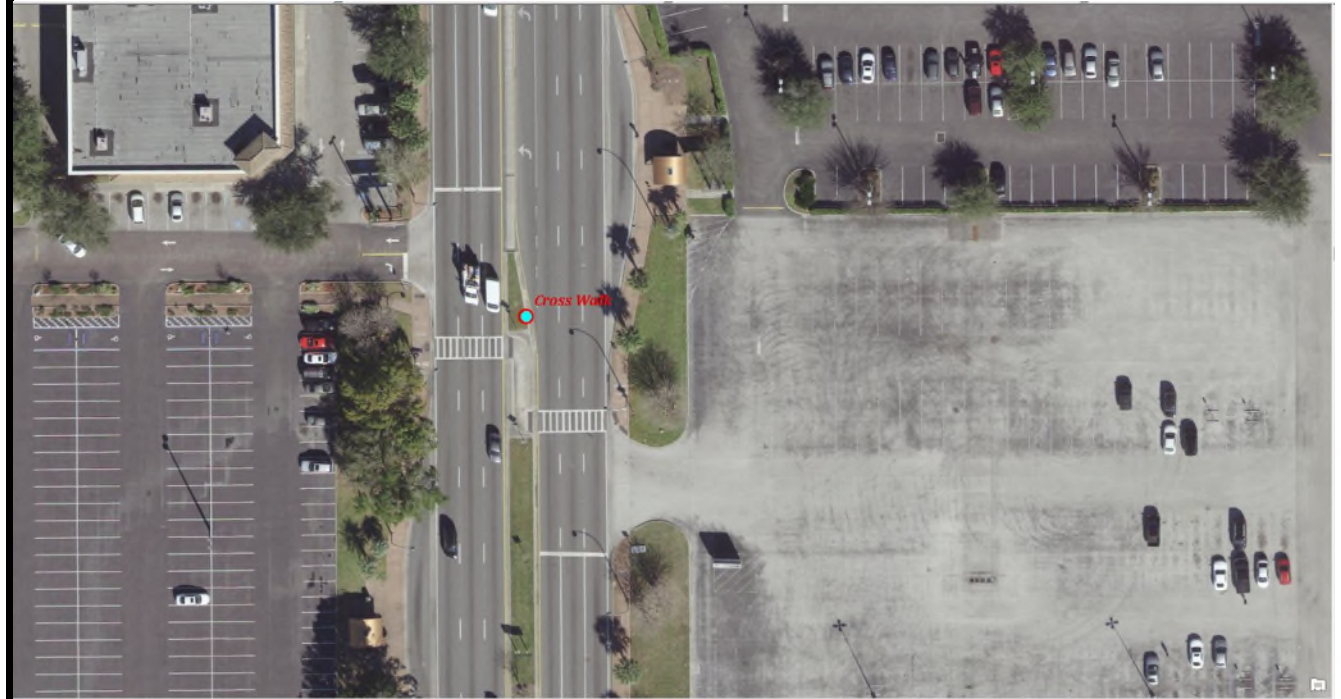
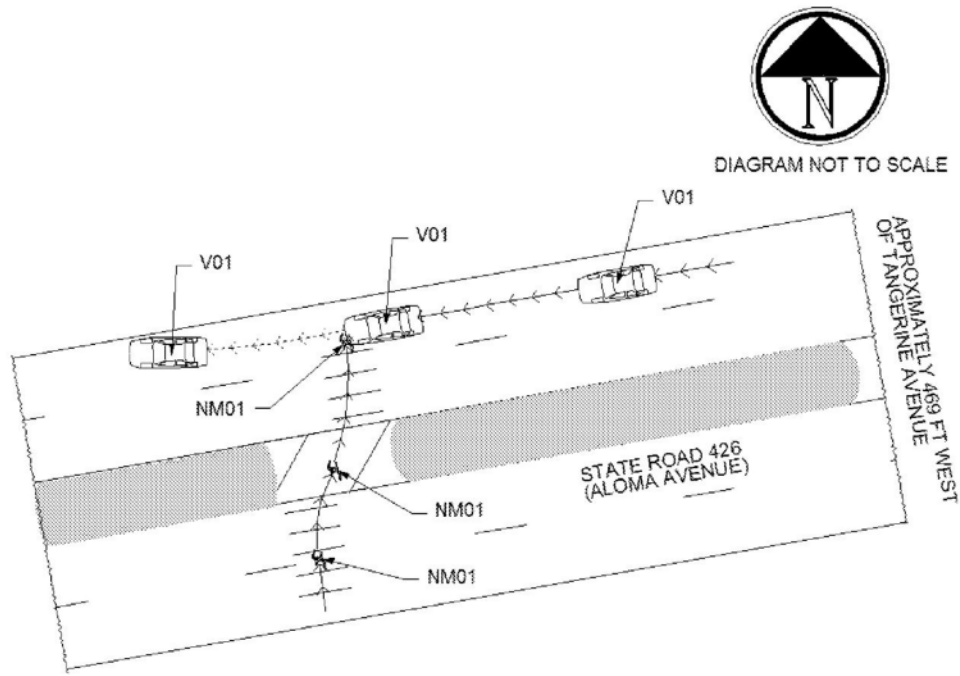


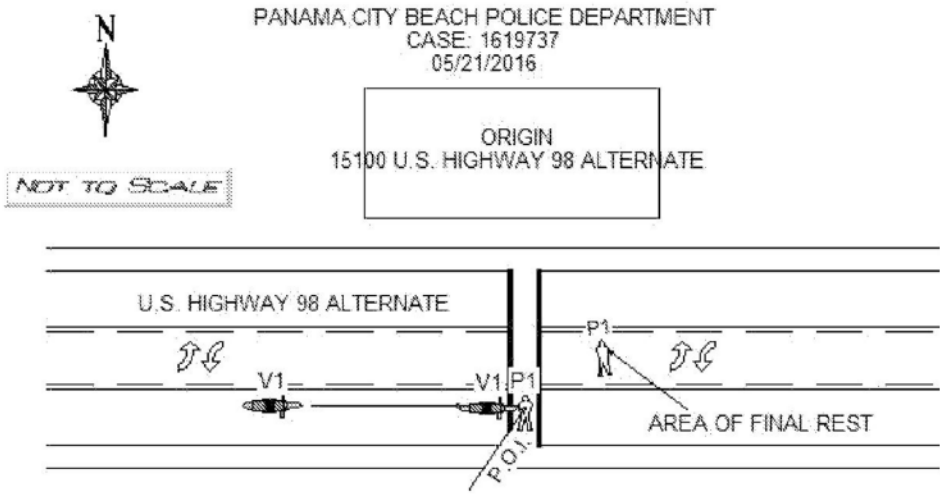
Diagram not to scale



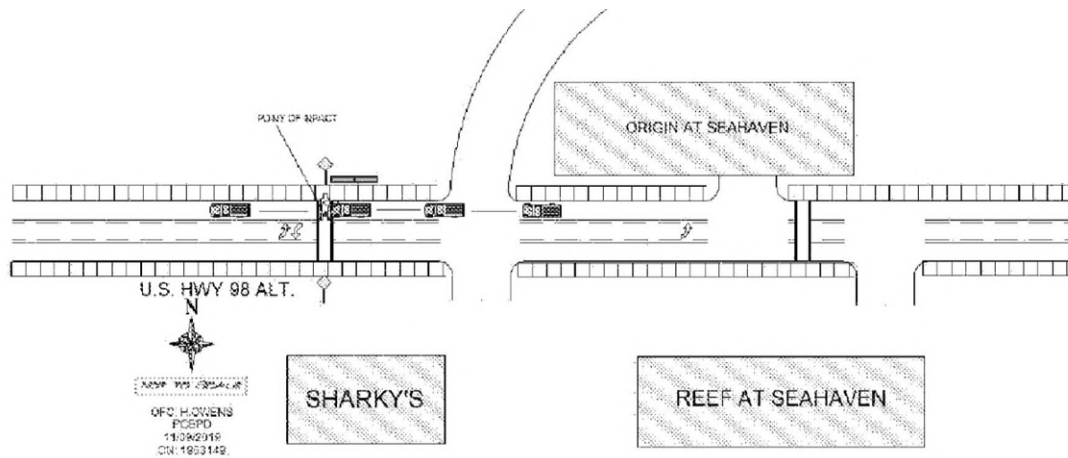
Crash Number: 852946660 – Orange County in 2016: The vehicle was traveling southbound in the center lane on US-441 (Orange Blossom Trail) and the pedestrian was walking from the west side of the road to the east side in a marked crosswalk.



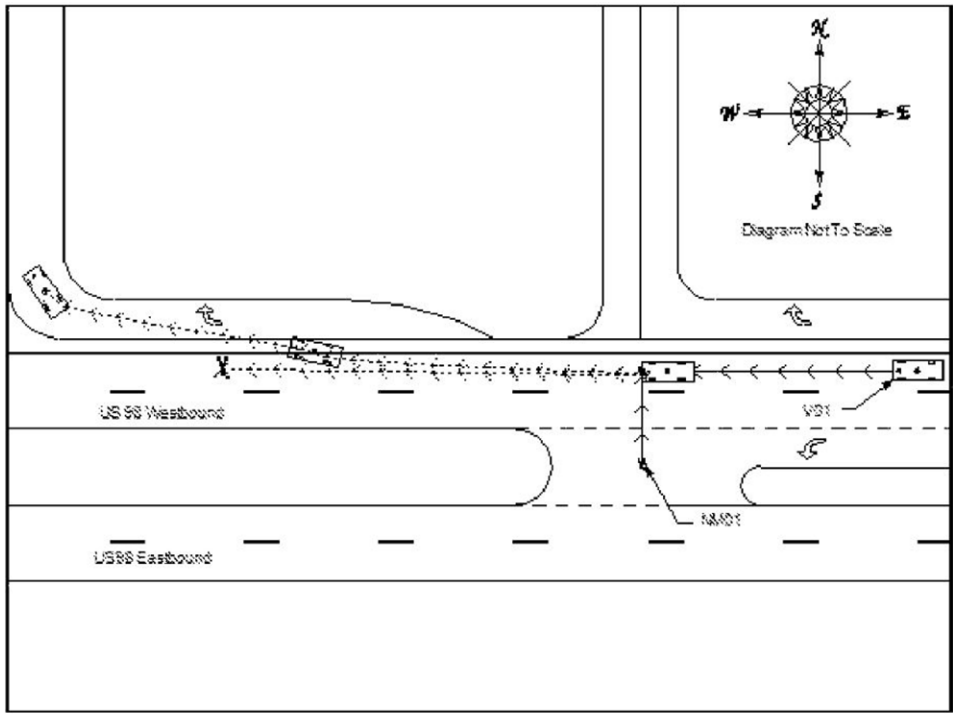
Crash Number: 852616380 – Orange County in 2016: This crash occurred during dark night time on crosswalk. The vehicle was traveling west on State Road (426), named, Aloma Avenue, in the outside lane approaching a pedestrian crosswalk just west of Tangerine Avenue. The pedestrian was walking north across the eastbound lanes of state road 426. As vehicle 1 approached the crosswalk, the pedestrian entered the crosswalk and continued traveling north. A female that was walking behind the victim stated that she told him not to cross due to the traffic, but the pedestrian stated that the cars would stop!



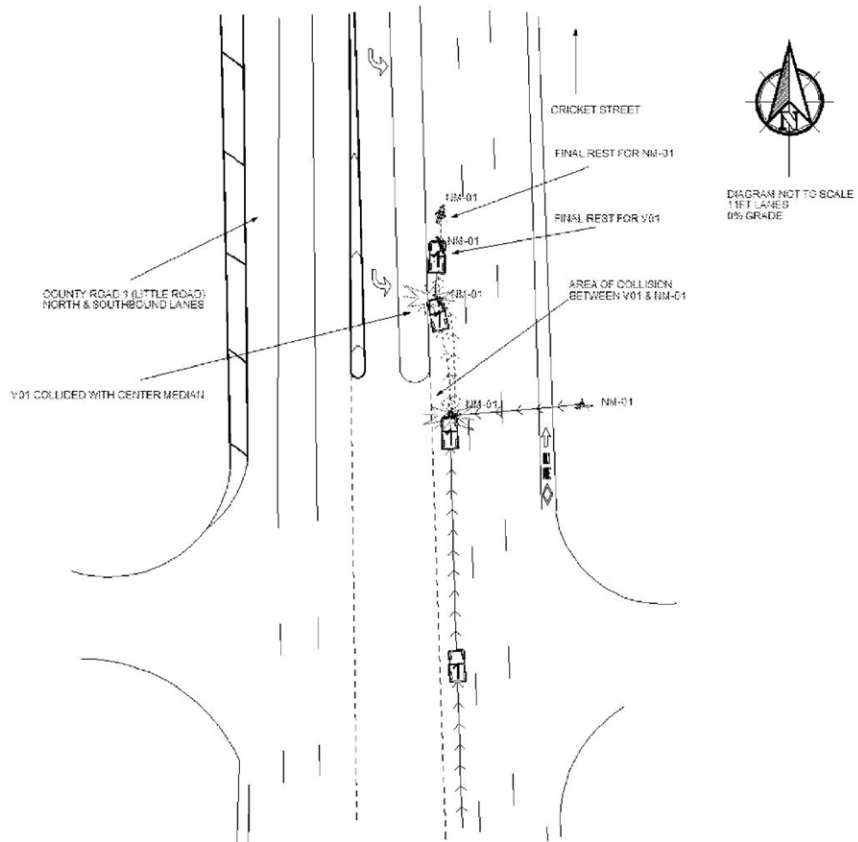
Crash Number: 865489310 – Bay County in 2016: It was a hit and run crash. The pedestrian was walking northbound across US highway 98 in the marked crosswalk and the vehicle was traveling east, struck the pedestrian and fled the scene of the crash.



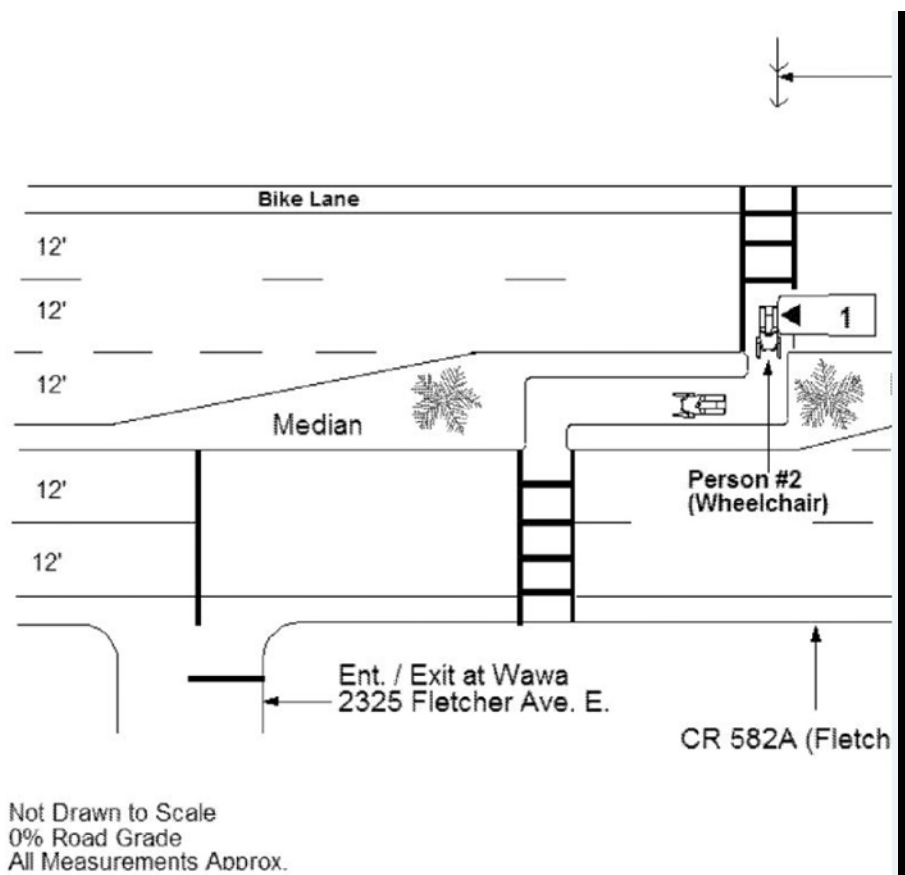
Crash Number: 892800620 – Bay County in 2019: It was a hit and run crash! The driver was traveling west on US98 and the pedestrian was crossing the crosswalk, walking north from Sharky's. The vehicle failed to yield the crosswalk to the pedestrian. The vehicle did not stop and left the scene without stopping.



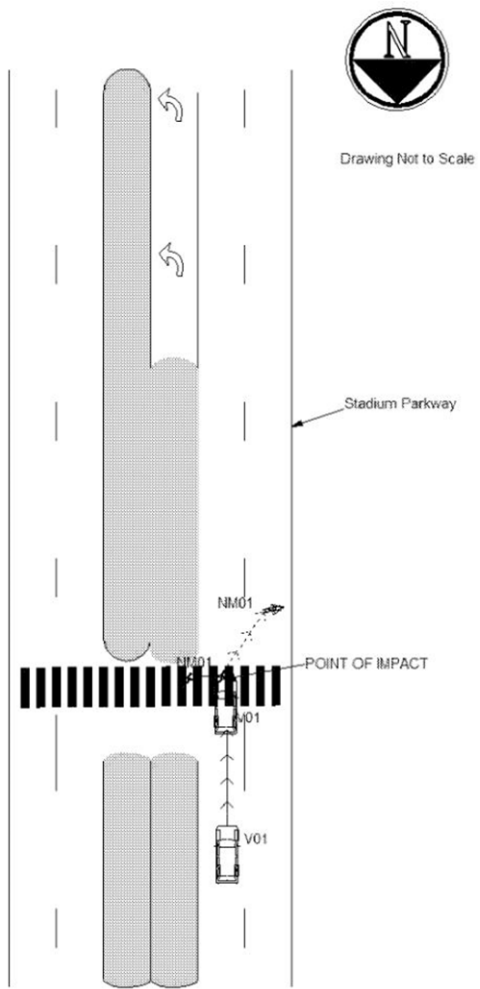
Crash Number: 820777290 – Bay County in 2011: The vehicle was traveling west on the right westbound travel lane of US98 (Panama City Beach Parkway) and the pedestrian was traveling in north direction attempting to cross US 98 from the south



Crash Number: 881286790 – Pasco County in 2019: The vehicle was traveling northbound in the inside lane on Little Road approaching the intersection with Cricket Street and the pedestrian was crossing the roadway in a westbound direction outside of the crosswalk.



Crash Number: 869179310 – Hillsborough County in 2017: The vehicle was traveling west bound within the left through lane on Fletcher Avenue and approaching a marked pedestrian crosswalk. The pedestrian was attempting to cross travel north in a wheelchair. The driver was 23 and the pedestrian was 70 years old.



Crash Number: 852082390 – Brevard County in 2015: The vehicle was traveling southbound on Stadium Parkway approaching the pedestrian crosswalk. The pedestrian was walking on the crosswalk and attempting to cross the southbound lanes.